Aus dem Institut für Virologie
Direktor: Prof. Dr. Stephan Becker
des Fachbereichs Medizin der Philipps-Universität Marburg

-Virus-host interplay-

Immediate virus recognition by RIG-I and PKR and viral counterstrategies

Inaugural-Dissertation
zur Erlangung des Doktorgrades der Naturwissenschaften
(Dr. rer. nat.)

dem Fachbereich Medizin der Philipps-Universität Marburg vorgelegt von

Michaela Gerlach, geborene Weber

aus Eisleben

Marburg, 2015

Angenommen vom Fachbereich Medizin der Philipps-Universität Marburg

Gedruckt mit Genehmigung des Fachbereichs.

Dekan: Prof. Dr. Helmut Schäfer

Referent: Prof. Dr. Friedemann Weber

Korreferent: Prof. Dr. Stefan Bauer

Table of contents

Table of contents 3

Summary 6

Zusammenfassung 7

Abbreviations 9

1. Introduction 11

1.1. Induction of antiviral defense mechanisms by RIG-I like receptors 11

1.1.1. RIG-I like receptors 11

1.1.2. RIG-I like receptor agonists 11

1.1.3. Structure-based RIG-I activation 12

1.1.4. RIG-I mediated type I interferon response 12

1.1.5. Protein kinase R 13

1.2. Viral evasion strategies to prevent immune recognition 13

1.3. Objectives of the underlying thesis 15

2. Results 16

2.1. Monitoring the activation status of RIG-I and PKR 16

2.2. Characterization of the physiological RIG-I agonist 17

2.2.1. Incoming bunyavirus nucleocapsids as RIG-I agonists 17

2.2.2. Incoming influenza virus nucleocapsids serve as RIG-I agonists 19

2.3. PKR as an immediate sensor of virus infection 20

2.4. Viral immune evasion strategies to prevent immediate recognition 22

2.4.1. Segmented negative-strand RNA viruses as strong immune stimulators 22

2.4.2. Influenza virus PB2 627K modulates nucleocapsid detection by RIG-I 23

2.4.3. Lassa virus nucleoprotein promotes proteasomal degradation of PKR 25

3. Discussion 27

3.1. RIG-I as an immune sensor of incoming viral nucleocapsids 27

3.2. PKR contributes to immediate pathogen recognition 28

3.3. Immune evasion strategies to prevent immediate recognition 29

3.4. Concluding remarks 33

4. Original publications and manuscripts 36

4.1. Monitoring activation of the antiviral pattern recognition receptors RIG-I and PKR by limited protease digestion and native PAGE 36

4.2. Incoming RNA virus nucleocapsids containing a 5'-triphosphorylated genome activate RIG-I and antiviral signaling 37

4.3. Influenza virus adaptation PB2-627K modulates nucleocapsid recognition by the pathogen sensor RIG-I 38

4.4. Intergenic region of incoming nucleocapsid activate PKR -Lassa virus nucleoprotein provides a PKR evasion strategy- 39

4.5. REVIEW: RIG-I-like receptors and negative-strand RNA viruses: RLRly bird catches some worms 40

4.6. REVIEW: Segmented negative-strand RNA viruses and RIG-I: divide (your genome) and rule 41

5. References 42

Appendix I

I. Zusätzliche Publikationen I

II. Kongressbeiträge I

III. Verzeichnis der akademischen Lehrer III

IV. Danksagung IV

This thesis is form of a cumulative dissertation.

List of publications and manuscripts:

Weber M and Weber F. Monitoring activation of the antiviral pattern recognition receptors RIG-I and PKR by limited protease digestion and native PAGE. Journal of Visual Experiments 29;(89):e51415. July, 2014.

Weber M, Gawanbacht A, Habjan M, Rang A, Borner C, Schmidt AM, Veitinger S, Jacob R, Devignot S, Kochs G, Garcia-Sastre A, Weber F. Incoming RNA virus nucleocapsids containing a 5'-triphosphorylated genome activate RIG-I and antiviral signaling. Cell host & microbe 13:336-346. March, 2013.

Weber M, Sediri H, Felgenhauer U, Binzen I, Bänfer S, Jacob R, Brunotte L, García-Sastre A, Schmid-Burgk J, Schmidt T, Hornung V, Kochs G, Schwemmle M, Klenk H-D, Weber F. Influenza virus adaptation PB2-627K modulates nucleocapsid recognition by the pathogen sensor RIG-I. Cell host & microbe. 2015.

Weber M, Fehling SK, Felgenhauer U, Kainulainen MH, Wolff S, Veitinger S, Jacob R, Becker S, Strecker T, Weber F. Intergenic region of incoming nucleocapsid activate PKR Lassa virus nucleoprotein provides a PKR evasion strategy. Manuscript in preparation.

Weber M and F Weber. RIG-I-like receptors and negative-strand RNA viruses: RLRly bird catches some worms. Cytokine Growth Factor Rev. 20. pii: S1359-6101(14)00046-X [Epub ahead of print]. May, 2014.

Weber M and F Weber. Segmented negative-strand RNA viruses and RIG-I: divide (your genome) and rule. Curr Opin Microbiol 12;20C:96-102. June, 2014.

See chapter 4 for personal contribution.

Summary

Viruses are a constant threat to mankind causing diseases ranging from mild symptoms to fatal outcome.

A rapid and efficient antiviral response is therefore crucial for the survival of the host. RIG-I-like receptors (RLR) and other immune receptors, like protein kinase R (PKR), specifically detect viral RNA species in the host cytoplasm. The sensing of virus infection triggers intracellular defense mechanisms resulting in viral alertness in the infected and surrounding cells, and forms the link to the adaptive immune system. Viruses, in turn, have evolved sophisticated countermeasures to dampen the antiviral response. The molecular mechanisms involved range from a broad shut-off of the host cell metabolism to a selective interference with key components of the immune system.

For a better understanding, which viral RNA structures are detected by immune receptors like RIG-I and PKR and what kind of viral antagonists lead to their inhibition, it is crucial to be able to determine their activation status. Hence, limited protease digestion and native polyacrylamide gel electrophoresis (PAGE) were established to directly monitor RIG-I and PKR conformational switching and oligomerization upon activation, respectively.

Various studies helped to identify RIG-I stimulating RNA features *in vitro,* but the first viral structure triggering an antiviral interferon response in the natural context of virus infection remained to be resolved. We identified 5`triphosphorylated (5`ppp) panhandle structures packaged into nucleocapsids as physiological RIG-I agonists. Independent of virus transcription and replication, the incoming encapsidated genomes of bunyaviruses (La Crosse virus; LACV and Rift Valley fever virus; RVFV) and orthomyxovirus (influenza A virus; FLUAV) were able to stimulate RIG-I activation and an antiviral signaling cascade. Surprisingly, antiviral activity of RIG-I against FLUAV was already promoted by binding to the 5`ppp panhandle and was independent of RIG-I downstream signaling ability. In addition to RIG-I, we also identified PKR as an immune sensor of incoming nucleocapsids. PKR thereby interacts with the intergenic region (IGR) of viral genome segments using ambisense coding strategy. Association of PKR with the IGR of incoming RVFV (*Bunyaviridae*) and arenavirus nucleocapsids promotes PKR phosphorylation and conformational switching and hence full PKR activation.

To antagonize immediate recognition by RIG-I and PKR, viruses need to adapt. RIG-I activation by FLUAV nucleocapsids was altered by an adaptive mutation of the polymerase complex subunit PB2. Mammalian adaptation mutation PB2 E627K stabilizes the polymerase complex association with the nucleocapsid thereby preventing RIG-I recognition of the 5`ppp panhandle. Additionally, Lassa virus (*Arenaviridae*) nucleoprotein interacts with PKR and promotes its degradation via the proteasomal pathway.

Therefore, we identified entry of viral nucleocapsids as the first time-point of immune recognition in the natural context of virus infection and give further insights how viruses have evolved to counteract immediate recognition.

Zusammenfassung

Viren stellen eine ständige Bedrohung der Menschheit dar, die Krankheiten mit milden Symptomen bis hin zu letalem Ausgang verursachen. Für das Überleben des Wirts ist daher eine schnelle und effiziente antivirale Immunantwort von entscheidender Bedeutung. Die meisten der bekannten neu auftretenden und hochpathogenen Viren besitzen ein RNA-Genom. RIG-I ähnliche Rezeptoren (RLR; RIG-I like receptors) und andere Immunrezeptoren, wie die Proteinkinase R (PKR), reagieren auf RNA-Strukturen im Zytoplasma der Wirtszelle. Die Detektion von Virusinfektionen induziert intrazelluläre Abwehrmechanismen, die einen antiviralen Zustand in der infizierten und den Nachbarzellen vermittelt und zudem das adaptive Immunsystem aktiviert. Viren wiederum haben komplexe Abwehrmaßnahmen entwickelt um die Immunreaktion zu verhindern. Die molekularen Mechanismen reichen vom unspezifischen Eingreifen in den Wirtszellmetabolismus bis hin zu einer spezifischen Inhibition von Schlüsselfaktoren der Immunantwort.

Für ein besseres Verständnis welche viralen RNA-Strukturen durch Immunrezeptoren, wie RIG-I und PKR, detektiert werden und welche Art von viralen Antagonisten zu ihrer Inhibition führen, muss man den Aktivierungszustand von Immunrezeptoren genau bestimmen können. Hierfür wurde der limitierte Proteaseverdau und die native Polyacrylamid-Gelelektrophorese (PAGE), für einen direkten Nachweis der RIG-I und PKR Konformationsänderung beziehungsweise Oligomerisierung nach Aktivierung, etabliert.

Verschiedene Studien haben geholfen, RIG-I stimulierende RNA-Strukturen *in vitro* zu identifizieren. Die erste Virusstruktur, welche die initiale antivirale Immunreaktion im natürlichen Kontext der Virusinfektion auslösen kann blieb jedoch ungeklärt. Im Rahmen dieser Studie konnten wir die 5` triphosphorylierte (5`ppp) Pfannenstielstruktur viraler Nukleokapside als physiologischen RIG-I Agonisten identifizieren. Unabhängig von viraler Transkription und Replikation konnten die eintretenden enkapsidierten Genome von Bunyaviren (La Crosse Virus; LACV und Rift Valley Fieber Virus; RVFV) und Orthomyxoviren (Influenza A Viren; FLUAV) RIG-I Aktivierung und eine antivirale Signalkaskade stimulieren. Überraschenderweise wurde die antivirale Aktivität von RIG-I gegen FLUAV bereits durch die Bindung an die 5`ppp Nukleokapside vermittelt, und war unabhängig von der RIG-I vermittelten Signalweiterleitung. Neben RIG-I konnte auch PKR als Immunsensor eintretender Nukleokapside identifiziert werden. PKR interagiert dabei mit der intergenischen Region (IGR; intergenic region) der viralen Genomsegmente mit Ambisense-Kodierungsstrategie. Die Assoziation von PKR mit der IGR eintretender RVFV (*Bunyaviridae*) und Arenavirus Nukleokapside vermittelt PKR-Phosphorylierung und Konformationsänderung und damit volle PKR Aktivierung.

Um einer unmittelbaren Detektion durch RIG-I und PKR zu entgehen, müssen sich Viren anpassen. So wird die RIG-I Aktivierung durch FLUAV Nukleokapside durch eine adaptive Mutation der PB2-Polymeraseuntereinheit verändert. Die Adaptionsmutation PB2 E627K stabilisiert die Interaktion des FLUAV Polymerasekomplexes mit dem Nukleokapsid und verhindert dadurch die RIG-I vermittelte

Detektion. Zudem interagiert das Lassa Virus (*Arenaviridae*) Nukleoprotein mit PKR und induziert dessen Abbau über das Proteasom.

Somit konnte das Eintreten der viralen Nukleokapside in die Wirtszelle als erster Zeitpunkt der Immunerkennung im natürlichen Kontext der Virusinfektion nachgewiesen werden. Des Weiteren ergeben sich aus dieser Arbeit Einblicke, wie Viren sich entwickelt haben um dieser unmittelbaren Immundetektion zu entkommen.

Abbreviations

A…	ActD	actinomycin D
	Asp	aspartic acid
B…	BDV	Borna disease virus (*Bornaviridae*)
C…	CARD	caspase activation and recruitment domains
	CHX	cycloheximide
	CL13	RVFV Cl 13
	Co-IP	co-immunoprecipitation
	CTD	carboxy-terminal domain
	CTRL	control
D…	dsRBD	dsRNA binding domain (PKR)
	dsRNA	double-stranded RNA
	D.mel-2	*Drosophila melanogaster* Schneider 2 cells
E…	E	glutamic acid
	eIF2α	eukaryotic initiation factor 2 alpha
F…	FLUAV	influenza A virus
G…	Glu	glutamic acid
	GP	glycoprotein
	GSD	ground state depletion microscopy
H…	HIV	human immunodeficiency virus (*Retroviridae*)
	His	histidine
I…	IFN	type I interferon (IFN-alpha/beta)
	IFNAR	interferon-alpha receptor
	IGR	intergenic region
	$IKK_{\varepsilon/\alpha/\beta}$	inhibitor of nuclear factor kappa-B kinase subunit ε/α/β
	IRES	internal ribosomal entry site
	IRF3/7	IFN regulatory factor 3/7
	ISG	IFN stimulated gene
	IVM	Ivermectin
J…	JAK	Janus kinase
	JUNV	Junin virus (*Arenaviridae*)
K…	K	lysin
L…	LACV	La Crosse virus (*Bunyaviridae*)
	LASV	Lassa virus (*Arenaviridae*)
	LGP2	laboratory of genetics and physiology 2
	LMB	Leptomycin B

M…	MAVS	mitochondrial antiviral signaling protein
	MAM	mitochondrial associated membrane
	MAPK	mitogen activated protein kinase
	MDA5	melanoma differentiation association factor 5
N…	N	nucleoprotein (*Bunyaviridae*)
	NF-κB	nuclear factor κ-light-chain-enhancer of activated B cells
	NP	nucleoprotein (*Arenaviridae* and *Orthomyxoviridae*)
	NS1	non-structural protein 1 (FLUAV)
	NSs	non-structural protein encoded on the S segment (RVFV)
	NSV	negative-strand RNA virus
P…	ppp	triphosphate
	PA	polymerase acidic protein
	PACT	protein activator of PKR
	PAGE	polyacrylamide gel electrophoresis
	PB1/2	polymerase basic protein 1/2
	PCR	polymerase chain reaction
	PHV	Prospect Hill virus (*Bunyaviridae*)
	PKR	protein kinase R
Q…	qRT PCR	quantitative reverse transcription polymerase chain reaction
R…	RIG-I	retinoic acid inducible gene I
	RLR	RIG-I like receptor
	RNA	ribonucleic acid
	RVFV	Rift Valley fever virus (*Bunyaviridae*)
S…	SAP	shrimp alkaline phosphatase
	siRNA	small interfering RNAs
	STAT	signal transducer and activator of transcription
T…	TAR	transactivation RNA (HIV)
	TBK1	TANK-binding kinase 1
	TCRV	tacaribe virus (*Arenaviridae*)
	TRAF 3/6	TNF receptor-associated factor 3/6
	TRIM25	tripartite motif containing 25
U…	UAP56	56 kDa U2AF65-associated protein
	URH49	UAP56-related helicase, 49 kDa
W…	wt	wildtype
Z…	Z	matrixprotein (Lassa virus)

1. Introduction

1.1. Induction of antiviral defense mechanisms by RIG-I like receptors

Viruses are a constant threat to mankind. Thereby, most of the known emerging and highly pathogenic viruses are RNA-genome based. They give rise to epidemic and rarely pandemic diseases, as often reported for influenza viruses [30]; or cause hemorrhagic fever, like members of the families *Arenaviridae* (Lassa fever virus and Junin virus) [35, 147] and *Bunyaviridae* (Rift Valley fever virus and Crimean Congo haemorrhagic fever virus) [6, 51]. Thus, to rapidly control virus infection an immediate recognition of the viral intruder is required.

1.1.1. RIG-I like receptors

The germ-line encoded RLR (RIG-I (retinoic acid inducible gene I) like receptors) represent a group of cytoplasmic sensor proteins able to detect RNA virus infection. RLR belong to the DExD/H-box helicase family (refers to Asp-Glu-x-Asp/His, where x can be any amino acid) within the helicase superfamily 2. RIG-I, the closely related MDA5 (melanoma differentiation association factor 5) and LGP2 (laboratory of genetics and physiology 2) form the family of RLR. RIG-I and MDA5 complement each other by responding to diverse virus families and initiate antiviral type I interferon (IFN-alpha/beta) responses [144]. The role of LGP2 in cytosolic virus sensing is less well characterized and currently controversially discussed. However, it is widely accepted that LGP2 represents rather a modulator of RIG-I and MDA5 activity then being involved in immune sensing or signaling [107, 109, 151].

1.1.2. RIG-I like receptor agonists

Studies have demonstrated that RIG-I and MDA5 recognize mainly distinct virus families. RIG-I is required to initiate an antiviral response against *Filoviridae* (Ebola and Marburg virus), *Paramyxoviridae* (New Castle Disease virus and respiratory syncytial virus), *Rhabdoviridae* (vesicular stomatitis virus), *Orthomyxoviridae* (Influenza virus), *Bunyaviridae* (Rift Valley Fever virus) and *Flaviviridae* (Japanese encephalitis virus). On the other hand, MDA5 responds to representatives of the *Picornaviridae* (Encephalomycarditis virus). Together, RIG-I and MDA5 react to *Reoviridae* and representatives of the *Flaviviridae* group (West Nile virus and Dengue virus) [112, 145]. An essential feature of the RLR is specificity to distinguish between host cell (self) and viral (non-self) patterns. Thereby, MDA5 is known to sense longer dsRNA (double-stranded RNA) molecules up to two kilo bases [58, 92], ideally with higher order RNA structures [92]. RIG-I mainly responds to 5′ ppp blunt-ended dsRNA of a minimal length of 10 base pairs [46, 60, 91, 111, 113]. Also dsRNA stretches bearing a 5`diphosphate were recently identified to stimulate a RIG-I dependent response [33]. Long dsRNA molecules of more than 200 base pairs (irrespective of the 5′ ends) [9], 3′-monophosphorylated cleavage products of RNase L [73], and polyuridine or polyriboadenine stretches were also decribed as

RIG-I agonists [103, 108, 112]. Importantly, these RNA structures and modalities are absent in the cytoplasm of non-infected cells, allowing the discrimination between self and non-self.

1.1.3.Structure-based RIG-I activation

All RLR share a similar structure (**manuscript 4.5, Fig. 2**). Thereby, RIG-I is composed of a CTD (carboxy-terminal domain) and a conserved RNA helicase core (formed by Hel1 and Hel2 with the insertion domain Hel2i). Both domains are required for agonist recognition in which the CTD has high affinity for the 5`ppp and the helicase domain recognizes dsRNA [128]. The helicase domain also promotes ATP hydrolysis. The CTD is connected to Hel2 via the pincer domain (also named bridging domain), which transmits the information of ligand recognition to the helicase core [57, 65, 71, 98]. Additionally, RIG-I possesses two amino-terminal CARDs (caspase activation and caspase recruitment domains) for signal transduction [64, 72, 144]. MDA5 has a similar structure whereas LGP2 lacks CARDs for downstream signaling [139, 144].

In resting state, RIG-I is present as an extended monomer in an open auto-repressed conformation [62, 71]. Thereby, the CARDs contact each other and CARD2 interacts with Hel2i, which sterically impedes ligand and coactivator engagement and initiation of downstream signaling [65, 97]. The CTD is, however, flexibly exposed and surveys the environment for 5`ppp-dsRNA. CTD binding to the 5`ppp brings the dsRNA in close proximity to the helicase domain [62]. The helicase core cooperatively binds the phosphate backbone of the dsRNA and ATP and the associated conformational switch promotes the release of CARDs [65]. CARDs are then freely accessible for polyubiquitinylation by the E3 ligase TRIM25 [29] or unanchored polyubiquitin chains [149]. Polyubiquitinylation prevents reassociation of the CARDs with the helicase domain to return into the auto-repressed state [62]. Furthermore, ubiquitinylation allows association of RIG-I molecules into a tetrameric complex [56, 89] leading to the fully signaling competent RIG-I complex.

1.1.4.RIG-I mediated type I interferon response

Activated RIG-I complexes recruit the adaptor protein MAVS (mitochondrial antiviral signaling) via CARD-CARD interaction [140]. Thereby, a transient interaction is sufficient to promote self-perpetuating MAVS filament association and thus, leading to a large-scale amplification of the antiviral signaling cascade [47]. Although the majority of MAVS is present on the mitochondria, it is also localized to peroxisomes [23]. Both organelles act sequentially as signaling platforms. Thereby, peroxisomes induce a rapid and transient IFN-independent expression of ISGs whereas mitochondrial MAVS initiates a sustained IFN-dependent response with delayed kinetics [23]. MAM (mitochondrial associated endoplasmatic reticulum membrane) directs relocalization of MAVS between the organelles, thus coordinates signaling between peroxisomes and mitochondria [45]. MAVS filament formation initiates the recruitment of several molecules to assemble a signaling platform [47, 55, 142]. Interaction of MAVS with TRAF3 and TRAF6 (TNF receptor-associated factor 3 and 6, respectively)

promotes activation of TBK1 (TANK-binding kinase 1) and IKKε (inhibitor of nuclear factor kappa-B kinase subunit ε) responsible for the phosphorylation of IRF3 and IRF7 (IFN regulatory factor 3 and 7, respectively), and IKKα and IKKβ promote NF-κB (nuclear factor κ-light-chain-enhancer of activated B cells) activation. Phosphorylated IRF3/7 forms dimers and translocates, like NF-κB, into the nucleus to initiate expression of IFN, proinflammatory cytokines and RIG-I and MDA5, providing a positive feedback mechanism for the amplification of the antiviral response [32, 103]. IFN binding to IFNAR (interferon-alpha receptor) stimulates the JAK (janus kinase)-STAT (signal transducer and activator of transcription) signaling pathway leading to selective transcriptional activation of numerous IFN-stimulated genes (ISGs) [44, 52]. ISGs represent effector proteins of the IFN response, which directly act against multiple steps of virus replication to establish an antiviral state in infected and neighboring cells [87, 116]. Furthermore, costimulatory molecules, cytokines and chemokines favor the initiation of adaptive immune responses [70, 115, 117]. The innate immune system thus controls virus infection at early phases and permits a subsequent specific adaptive immune response to clear infection and establish an immunogenic memory [41].

1.1.5. Protein kinase R

One well studied effector protein of the innate immune response is PKR (protein kinase R). PKR is expressed at a low constitutive level in the cytoplasm, but can casually be detected in the nucleus. To stimulate PKR activation there is a minimal length requirement of dsRNA of approximately 16 base pairs, but also specific structural modalities, like RNA bulges and loops, and nucleotide modifications, like a 5`ppp, support PKR stimulation [7, 25, 84]. PKR thereby contacts the dsRNA in a sequence-independent manner [7]. However, during stress PACT (protein activator of PKR) can activate PKR in absence of a stimulating dsRNA ligand [88]. Concerning PKR structure, the protein is composed of two amino-terminal dsRBD (dsRNA binding domains), a carboxy-terminal serine/threonine kinase domain, whereby both domains are linked by a flexible linker [126]. In absence of a stimulus, PKR is present as a monomer with an extended, open conformation and the dsRBDs are impeding kinase domain activity. Agonist recognition induces structural rearrangements to a closed conformation allowing dimerization and auto-phosphorylation [16-18, 67, 126]. Once activated, PKR is a multifunctional protein involved in the regulation of cap-dependent translation, it participates in the formation of virus induced stress granules required for IFN signaling and controls NF-κB, p38 MAPK and insulin pathways, among others [18, 22, 85, 148].

1.2. Viral evasion strategies to prevent immune recognition

Induction of the IFN response acts as a major barrier to virus infection, which must be circumvented to enable a productive infectious cycle. Thus, viruses have evolved multiple mechanisms to target key signaling molecules of the RLR pathway to prevent establishment of an antiviral state. A common strategy of RNA viruses comprises the modification and concealing of the viral genomes and

replicative intermediates. One mechanism presents packaging of the viral RNA with multiple copies of viral nucleoprotein and the polymerase into nucleocapsids [106]. Furthermore, some viruses possess the ability to enzymatically remove their 5`ppp in order to avoid RIG-I detection [36]. Other viruses hide their genomes by replicating in the nucleus or in inaccessible cellular compartments [152]. In course of the viral replication cycle, accumulation of erroneous, misencapsidated replication products might serve as RLR agonists. Viruses therefore mask [41, 42, 95], degrade these erroneous side products [38, 41, 63, 93] or use cellular helicases to unwind dsRNA replication intermediates [136, 137].

Overall, viruses have evolved sophisticated strategies to prevent RLR recognition and the subsequent IFN response. Further knowledge of viral evasion strategies is, however, required to comprehend the complexity of virus-host interactions to gain insights into RLR signaling and also virus pathogenesis itself.

1.3. Objectives of the underlying thesis

Despite the discoveries about stimulating RIG-I structures, the question of the physiological RIG-I agonist in the authentic infection context remained largely unresolved. Long dsRNA is not produced in a detectable amount during the course of negative-strand RNA virus (NSV) infection [131]. However, NSV possess complementary sequences at the termini of their genomes leading to the formation of the "panhandle" conformation with a short dsRNA stretch. Furthermore, because of initiation of RNA synthesis via a single nucleoside triphosphate, all NSV were believed to possess a 5`ppp at the termini of their genomes [36]. Therefore, the 5`ppp panhandle structure represents all hallmarks of a potential RIG-I agonist. Nevertheless, the genomes of NSV do not exist as free RNA, but are instead hidden in a complex with multiple copies of viral nucleoprotein and the polymerase, the so-called nucleocapsid. It has remained unclear, whether RIG-I can also recognize RNAs packaged into nucleocapsids, the main viral RNA state in the infected host cell.

First aim of this study was hence the identification of the physiological RIG-I agonist during virus infection. Thereby, we aimed to pin down the first viral structure to be detected by RIG-I and able to stimulate the host innate immune system. We focused at first on stimulating RNA structures of the cytoplasmic bunyaviruses and extended then our study towards influenza viruses, which are only briefly accessible to RIG-I during their cytoplasmic transit to the nucleus for genome replication.

Besides RIG-I, we wondered whether other immune receptors would promote an immediate antiviral response. PKR is able to respond to dsRNA, but also specific structural modalities, like bulges and loops [25]. Interestingly, intergenic regions of viral genomes using ambisense coding strategies resemble loop structures with a dsRNA stem. Thus, we hypothesized that PKR could be able to induce immediate antiviral defense mechanisms by recognizing intergenic regions of incoming viral genomes. To validate this hypothesis was the second aim of this thesis.

On the contrary, to counteract immediate recognition viruses have evolved sophisticated methods. Viral immune evasion strategies thereby range from an unspecific shut-off of the host cell metabolism to a selective interference with key components of the IFN system. In our research, we intended to assess whether NSVs have evolved so far unknown mechanisms to specifically evade immediate immune recognition.

Overall, we intend to provide further insights in immediate virus detection in the natural context of infection and how viruses, on the other hand, have adapted to evade immune recognition to allow efficient virus replication and spread.

2. Results

2.1. Monitoring the activation status of RIG-I and PKR

For a better understanding, which viral RNA structures are detected by immune receptors, like RIG-I and PKR, and what kind of viral antagonists lead to their inhibition, it is crucial to be able to determine their activation status. So far, techniques to measure downstream events like antiviral gene expression are commonly used, but since viruses interfere with RLR and IFN signaling, results might not reflect the direct activation status of RIG-I or PKR. Here, we present limited protease digestion and native polyacrylamide gel electrophoresis (PAGE) as sensitive and direct measurements of two distinct markers of RIG-I and PKR activation (**manuscript 4.1, [133]**). Upon agonist recognition RIG-I and PKR undergo conformational switching [2, 107, 121] allowing formation of oligomeric complexes [22, 56, 107]. Sensitive validation of the RIG-I and PKR activation status helps to gain further insights in physiological agonists and how viruses interfere with RIG-I and PKR activation.

In absence of a specific agonist, RIG-I has an open auto-repressed conformation [62, 71]. Agonist recognition induces conformational switching of RIG-I and formation of a much more ordered RIG-I molecule [62, 72]. PKR is also present as a monomer with an extended open conformation in the absence of a stimulus. Binding to a specific agonist leads to structural rearrangements to a closed conformation allowing dimerization and auto-phosphorylation [17, 67, 126]. Conformational rearrangements lead to alterations in protease sensitivity, which can be determined by limited protease digestion. This technique, to monitor RIG-I and PKR conformational switching, was previously described by M. Gale Jr. [107] and T. Fujita [121], and J.L. Cole [2], respectively.

To monitor RIG-I and PKR conformational switching upon virus infection, human A549 cells were either mock infected or infected with Rift Valley fever virus clone 13 (Cl 13). Cl 13 lacks a functional IFN antagonist NSs and is hence a strong activator of RIG-I and PKR [36, 37, 50]. Trypsin digestion of mock infected cell lysates results in a rapid degradation of RIG-I whereas Cl 13 infection leads to the generation of a 30 kDa protease resistant RIG-I fragment (**manuscript 4.1, Fig. 1A**). Also PKR shows partial resistance to trypsin digestion in Cl 13 infected samples, which coincides with its phosphorylation at threonine 466, a widely accepted marker of PKR activation (**manuscript 4.1, Fig. 1A**).

RIG-I and PKR conformational rearrangements form the prerequisite to associate multiple monomers into oligomeric complexes. Accumulation of RIG-I oligomers allows enhanced recruitment of downstream signaling molecules to form a platform for antiviral signal transduction [72]. In case of PKR, dimerization supports auto-phosphorylation required for its full activation [17, 22]. The formation of oligomeric complexes was assayed by native PAGE. Proteins and protein complexes are thereby not separated by their charge to mass ratio, but rather by their size [138].

By applying native PAGE, formation of RIG-I and PKR oligomeric complexes in Cl 13 infected cell lysates could be demonstrated whereas these proteins remained as monomers in mock infected

samples (**manuscript 4.1, Fig. 2, upper and middle panel**). As an additional control for the functionality of the oligomerization assay the IFN transcription factor IRF3 was included. Validation of IRF3 dimerization is widely performed to monitor activation of the IFN system [54]. Indeed, IRF3 dimerization coincides with RIG-I and PKR oligomerization in Cl 13 infected samples (**manuscript 4.1, Fig. 2, lower panel**).

Taken together, these results demonstrate limited trypsin digestion and native PAGE as useful and sensitive tools to directly monitor two distinct markers of RIG-I and PKR activation.

2.2. Characterization of the physiological RIG-I agonist

2.2.1. Incoming bunyavirus nucleocapsids as RIG-I agonists

Most studies on the identification of RIG-I agonist were performed by allowing full viral replication or by transfecting naked viral or synthetic RNA. These results helped to gain insights into RNA features required for RIG-I activation, like dsRNA and a 5`ppp, but did not answer the question about the RIG-I activating structure in the natural virus infection. Therefore, the first objective of this thesis was the identification of the earliest infection step exposing a viral RNA pattern able to activate RIG-I and stimulate an antiviral IFN response in an authentic virus infection (**manuscript 4.2, [132]**).

The infection cycle of NSV starts with particle attachment to the host cell, followed by entry of the viral genome into the cytoplasm, mRNA (messenger RNA) synthesis during primary transcription via the viral polymerase, genome replication via a positive-sense template, assembly and finally release of progeny viruses. It has been demonstrated that full-length and defective RNAs produced during viral replication serve as RIG-I stimulators [5, 101]. However, whether these RNA structures represent naked erroneous side products of viral replication was not addressed. During virus infection, the viral genomic and intermediate RNA products never exist as free RNA, but are instead hidden within the nucleocapsid [131]. So far, it has remained unresolved whether RIG-I can also recognize RNAs packaged into nucleocapsids, the main viral RNA state in the infected host cell.

Nucleocapsids of NSVs represent hallmarks of a potential RIG-I agonist. Terminal complementary sequences of the viral genomes allow hybridization into a short dsRNA stretch, classified as the “panhandle” conformation. Moreover, the 5`ppp is generated during initiation of RNA synthesis via a single nucleoside triphosphate [110]. To study whether the incoming 5`ppp nucleocapsids would suffice to trigger an IFN response the peculiar characteristics of the bunyaviruses were exploited. Bunyavirus transcription is dependent on on-going translation [94]. Hence, treatment with the translation inhibitor CHX (cycloheximide) aborts primary transcription and allows validation of incoming nucleocapsids as IFN stimulators. Infections were performed with two representatives of the *Bunyaviridae*, RVFV (Rift valley fever virus) and LACV (La Crosse virus). To test induction of an IFN response, IFN-beta and ISG56 mRNA upregulation were measured by qRT PCR (quantitative reverse transcription PCR). Results indicate that independent of primary transcription or genome replication, already the incoming LACV and RVFV nucleocapsids stimulate an IFN response

(**manuscript 4.2, Fig. 1B**). To validate the influence of the 5`ppp, PHV (Prospect Hill virus), another bunyavirus, which processes its 5`terminus to a 5`p (monophosphate) [31, 36] was included into the study. This allows a direct comparison of the antiviral response by nucleocapsids with (LACV and RVFV) or without (PHV) the 5`ppp. By performing the experiment with PHV no upregulation of IFN-beta and ISG56 was detected (**manuscript 4.2, Fig. 2A**). This indicates that the induction of the IFN response by nucleocapsids seems to be dependent on the presence of a 5`ppp.

To further validate induction of the IFN response by 5`ppp nucleocapsids, the activation status of the IFN transcription factor IRF3 was analyzed. Thereby, phosphorylation, dimerization and translocation of IRF3 into the nucleus represent central features of its activation [143]. Indeed, LACV and RVFV nucleocapsids promote phosphorylation, dimerization (**manuscript 4.2, Fig. S3D and S4D, respectively**) and translocation of IRF3 (**manuscript 4.2, Fig. S3E**) whereas PHV 5`p nucleocapsids do not stimulate a detectable IRF3 activation (**manuscript 4.2, Fig. S3F**). This data supports the previous result that triggering an antiviral IFN response requires 5`ppp nucleocapsids.

To test which RLR is responsible for the induction of the immune response, knockdown cells were generated by transfecting siRNA (small interfering RNAs) against non-specific target (CTRL), MDA5 or RIG-I. Knockdown of MDA5 did not affect the ability of incoming LACV nucleocapsids to stimulate IFN-beta and ISG56 expression (**manuscript 4.2, Fig. 2B**). However, absence of RIG-I resulted in an impaired IFN response. This indicates that RIG-I is required to sense nucleocapsids. Taken together, incoming 5`ppp nucleocapsids promote a RIG-I dependent antiviral IFN response.

To analyze whether RIG-I is able to interact with the incoming nucleocapsids, confocal immunofluorescence microscopy and co-IP (co-immunoprecipitation) assay were performed. Detection of the nucleoprotein N served thereby as a marker for the viral nucleocapsids. Confocal immunofluorescence microscopy revealed that RIG-I colocalized with LACV and RVFV nucleocapsids (**manuscript 4.2, Fig. 4A and S4E**). Incoming nucleocapsids also showed a colocalization with peroxisomes (**manuscript 4.2, Fig. S4B**), which are known organelles for induction of an immediate antiviral response [23]. This interaction between RIG-I and incoming nucleocapsids was further validated by co-IP. With a RIG-I specific co-IP, also LACV nucleocapsids could be precipitated (**manuscript 4.2, Fig. 4B**). This demonstrates that RIG-I is able to interact with incoming nucleocapsids. Whether RIG-I interaction with the incoming nucleocapsids would promote RIG-I activation was validated by the previously described assays (**manuscript 4.1, [133]**). Therefore, we performed limited protease digestion and native PAGE to monitor RIG-I conformational switching and oligomerization, respectively. Full viral replication and incoming LACV and RVFV nucleocapsids induced trypsin resistant RIG-I fragments as a marker of conformational switching (**manuscript 4.2, Fig. 3G and S4D**). However, PHV full replication cycle and PHV incoming 5`p nucleocapsids only poorly stimulated RIG-I conformational changes. Also RIG-I oligomerization increased upon full LACV and RVFV replication and remained at a constant, but clearly detectable level if replication cycle was aborted after entry of the viral nucleocapsids (**manuscript 4.2, Fig. 3F**

and S4D). In contrast, PHV infection and incoming 5`p nucleocapsids failed to promote accumulation of RIG-I oligomeric complexes (**manuscript 4.2, Fig. 3H**).

An insect cell system was additionally employed to investigate whether RIG-I activation by viral nucleocapsids is direct or mediated by one of the abundant cellular cofactors of RIG-I [61, 81, 87, 146]. Therefore, isolated nucleocapsids from purified RVFV or LACV virions were used to stimulate human RIG-I expressed from D.mel-2 (*Drosophila melanogaster* Schneider 2) cells. In absence of mammalian cofactors, purified nucleocapsids promote RIG-I conformational switching (**manuscript 4.2, Fig. 6C**). Thus, mammalian cofactors are not required for nucleocapsid-stimulated RIG-I activation. To test the requirement of the 5`ppp and dsRNA for RIG-I activation by incoming nucleocapsids, purified nucleocapsids were either treated with a ssRNA-specific RNase A, a dsRNA-specific RNase III or SAP (shrimp alkaline phosphatase). By destroying the dsRNA stretch (RNase III) or removal of the 5`ppp (SAP), the nucleocapsids lost their ability to promote RIG-I conformational switching, whereas RNase A treatment did not have an effect (**manuscript 4.2, Fig. 6E**). This indicates that the 5`ppp dsRNA panhandle is required for RIG-I activation. Furthermore, by employing super-resolution GSD (ground state depletion) microscopy we were able to display the pseudocircular structure of LACV nucleocapsids and that accumulations of RIG-I contact the nucleocapsids via a single contact site, most likely the 5`ppp dsRNA panhandle (**manuscript 4.2, Fig. 7**).

In summary, RIG-I interacts with incoming nucleocapsids comprising a 5`ppp dsRNA panhandle. This interaction leads to RIG-I conformational switching and oligomerization independent of other mammalian cofactors. Once activated, RIG-I promotes, partially via the peroxisomal signaling platform, activation of the IFN transcription factor IRF3 and the antiviral type I IFN response. This defines nucleocapsid entry as the first time-point when the host immune system encounters the viral intruder to promote an immediate antiviral response.

2.2.2. Incoming influenza virus nucleocapsids serve as RIG-I agonists

Influenza A viruses (FLUAV) belong to the family *Orthomyxoviridae* containing a segmented, single-stranded RNA genome with negative-strand polarity. Each FLUAV particle comprises eight genome segments encapsidated by the viral nucleoprotein NP and the polymerase complex subunits PB1, PB2 and PA. The 5` and 3` ends of each viral RNA contain partially complementary sequences forming, as described for other NSVs, a panhandle conformation with a short dsRNA [48, 90]. Since incoming 5`ppp nucleocapsids of the bunyaviruses could be identified as physiological RIG-I agonists (**manuscript 4.2, [132]**), we wondered if also FLUAV nucleocapsids would serve as RIG-I stimulators. However, FLUAV transcription and replication occur in the nucleus. Due to the viral replication cycle, the incoming FLUAV nucleocapsids are only shortly exposed to cytoplasmic immune receptors. Here, we addressed the question if the short cytoplasmic exposure of FLUAV

nucleocapsids during their transit to the nucleus is sufficient to activate RIG-I (**manuscript 4.3, (Weber et al., in press)**).

To study, whether RIG-I is able to recognize incoming FLUAV nucleocapsids, diverse inhibitors were used to restrict virus infection. CHX (cycloheximide) blocks protein synthesis and therefore viral genome replication, LMB (Leptomycin B) inhibits nuclear export of nucleocapsids, ActD (actinomycin D) is an inhibitor of viral transcription, and IVM (Ivermectin) is known to block nuclear import of viral nucleocapsids [130]. Furthermore, to ensure analysis of an immediate response infection was stopped one hour post infection. Indeed, independent of the applied inhibitor, incoming A/PR/8/34 (H1N1) nucleocapsids promote RIG-I conformational switching and oligomerization and thus its full activation (**manuscript 4.3, Fig. 1A and B**).

To verify an interaction between RIG-I and the incoming FLUAV nucleocapsids various approaches were applied. Super-resolution GSD microscopy revealed that RIG-I is attached to the rod-like FLUAV nucleocapsids via a single contact site (**manuscript 4.3, Fig. 2A**). Association of RIG-I with FLUAV nucleocapsids was further confirmed by co-IP and co-sedimentation assays. Thereby, FLUAV nucleocapsids could be coprecipitated with a RIG-I specific IP (**manuscript 4.3, Fig. 2B**). Likewise, by performing co-sedimentation assay, RIG-I and FLUAV nucleocapsids partially shifted together into the same fractions (**manuscript 4.3, Fig. 2C**). This indicates that RIG-I is indeed able to interact with incoming FLUAV nucleocapsids.

To test the influence of mammalian RIG-I cofactors the D-mel.2 *in vitro* system was applied. Also in absence of any mammalian factors, purified FLUAV nucleocapsids induced RIG-I conformational switching (**manuscript 4.3, Fig. S2F**), oligomerization (**manuscript 4.3, Fig. S2G**) and a RIG-I shift in a co-sedimentation assay (**manuscript 4.3, Fig. S2H**). Therefore, also in absence of other mammalian factors RIG-I interacts and gets activated by FLUAV nucleocapsids. RIG-I activation is, however, dependent on the presence of a 5`ppp and a dsRNA structure since the FLUAV nucleocapsids lose their RIG-I activating potential after treatment with a dsRNA-specific RNase III or the phosphatase SAP, respectively (**manuscript 4.3, Fig. 2D**).

To validate whether FLUAV nucleocapsids can promote an IFN response, the activation status of IRF3 was validated. IRF3 phosphorylation, one marker of its activation, was induced upon presence of FLUAV nucleocapsids (**manuscript 4.3, Fig. 1D**).

As a conclusion, incoming FLUAV nucleocapsids serve as natural RIG-I agonist independent of RNA synthesis or presence of mammalian cofactors, triggering a signaling cascade that culminates in the activation of the IFN transcription factor IRF3.

2.3. PKR as an immediate sensor of virus infection

As previous results indicate, incoming RVFV and LACV (*Bunyaviridae*) and FLUAV (*Orthomyxoviridae*) nucleocapsids serve as physiological RIG-I agonists enabling an immediate antiviral type I IFN response (**manuscript 4.2, [132] and manuscript 4.3, (Weber et al., in press)**).

However, whether other host immune receptors would likewise contribute to immediate virus recognition remained unresolved.

One well-characterized cytoplasmic immune sensor is PKR. With its ability to recognize dsRNA stretches or specific structural RNA modalities, like bulges and loops [18], PKR comprises the potential to recognize dsRNA replicative intermediates of NSVs [20]. However, whether PKR can be activated by incoming viral RNA structures packaged within the nucleocapsids was not addressed so far (**manuscript 4.4, (Weber et al., manuscript in preparation)**).

Upon agonist recognition, conformational rearrangements of PKR lead to partial protease resistance allowing dimerization and auto-phosphorylation (**manuscript 4.1, [133]**). By comparing the potential of the two closely related LACV and RVFV to promote PKR conformational switching and phosphorylation, interesting differences were observed. LACV full infectious cycle and incoming LACV nucleocapsids stimulate only weakly these two markers of PKR activation (**manuscript 4.4, Fig. 1B**). On the contrary, full RVFV replication and incoming nucleocapsids of RVFV lead to a robust detection of PKR conformational switching and phosphorylation. Interaction of PKR with bunyavirus nucleocapsids was validated by co-sedimentation assay and co-IP. By performing co-sedimentation assay, PKR shifted to similar fractions as RVFV nucleocapsids whereas upon stimulation with LACV nucleocapsids PKR showed a similar distribution in the gradient as upon mock infection (**manuscript 4.4, Fig. 1C**). Co-IPs confirmed PKR interaction with RVFV, but not LACV, nucleocapsids (**manuscript 4.4, Fig. 1D**). This indicates that incoming RVFV nucleocapsids can be recognized by PKR and stimulate its activation. Hence, incoming RVFV nucleocapsids serve as natural PKR agonists.

To identify the PKR stimulating structure present within RVFV, but absent in LACV nucleocapsids, the coding strategies of these two viruses were analyzed. Bunyaviruses divide their genome into three segments, which are named L (large), M (middle) and S (small) according to their size [11]. RVFV L and M segment and all segments of LACV are present in negative polarity with one transcriptional unit coding for one or more proteins. RVFV S segment, however, uses ambisense coding strategy (**manuscript 4.4, Fig. 2B**). Thereby, two open reading frames in opposite directions are separated by a non-coding intergenic region (IGR). RVFV IGR resembles a hairpin structure with a central dsRNA stem disordered by internal loops (**manuscript 4.4, Fig. 2A**). To test whether this peculiar structure is responsible for PKR activation, RVF VLP (RVF virus like particles) containing either M (no IGR) or S (with IGR) segmented nucleocapsids were generated. Due to the same 5`ppp dsRNA panhandle of M and S segments the nucleocapsids promote RIG-I conformational switching to the same extent (**manuscript 4.4, Fig. 2C**). However, only S segmented nucleocapsids possessing the IGR are able to stimulate PKR conformational switching. As detected by super-resolution GSD microscopy, RIG-I colocalized with both M and S segmented nucleocapsids whereas PKR only showed interaction with S segmented nucleocapsids (**manuscript 4.4, Fig. 2D**). Taken together, PKR activation by incoming nucleocapsids requires the presence of a structured IGR.

To further support this result, arenavirus nucleocapsids were validated based on their potential to promote PKR activation. According to antigenicity, phylogeny and geographical distribution, arenaviruses are classified into Old World and New World viruses [63]. Arenavirus particles comprise two genome segments both using ambisense coding strategy with an IGR for transcriptional control. Compared to RVFV IGR, representatives of the arenaviruses, like the Old World LASV (Lassa virus) and New World JUNV (Junin virus) and TCRV (Tacaribe virus) possess also a highly structured IGR with a central dsRNA stem (**manuscript 4.4, Fig. 3A**). By validating PKR activation, TCRV, JUNV and LASV nucleocapsids induce PKR phosphorylation and conformational rearrangements (**manuscript 4.4, Fig. 3B, right panel**). Thus, incoming arenavirus nucleocapsids serve, like RVFV nucleocapsids, as natural PKR agonists.

This data demonstrate that PKR is able to recognize IGRs exposed from the incoming nucleocapsid complex. IGR engagement promotes PKR conformational switching and phosphorylation identifying IGRs of RVFV S segment, New World arenavirus TCRV and JUNV and Old World arenavirus LASV nucleocapsids as natural PKR activators. This emphasizes PKR as an immune sensor of immediate virus infection.

2.4. Viral immune evasion strategies to prevent immediate recognition

2.4.1. Segmented negative-strand RNA viruses as strong immune stimulators

The reviews included in this cumulative doctoral thesis briefly summarize the current understanding of immune evasion strategies of segmented and non-segmented NSVs (**manuscript 4.5, [135]** and **manuscript 4.6, [134]**). However, in our research, we focused on the molecular mechanisms of NSVs with a segmented genome to evade immediate immune recognition.

Besides *Orthomyxoviridae* with up to eight genome segments, members of the *Arenaviridae* and *Bunyaviridae* have two and three genome segments, respectively. Viruses with a segmented genome possess complementary sequences at the termini of their genomes leading to the formation of the panhandle conformation [26, 27, 76]. As outlined above, 5`ppp dsRNA panhandle structures of incoming bunyavirus (**manuscript 4.2, [132]**) and influenza virus (**manuscript 4.3, (Weber et al., in press)**); and arenavirus nucleocapsids (**manuscript 4.4, (Weber et al., manuscript in preparation)**) serve as natural RIG-I and PKR agonists, respectively. Hence, NSVs with segmented genomes immediately present an increased number of potential immune receptor agonists leading to an early activation of antiviral defense mechanisms (**manuscript 4.5, Fig. 3**). To evade early immune recognition and the subsequent antiviral IFN response sophisticated countermeasures are thus required. Here, we address the question how influenza viruses and arenaviruses prevent immediate nucleocapsid detection by the host immune receptors RIG-I and PKR, respectively.

2.4.2. Influenza virus PB2 627K modulates nucleocapsid detection by RIG-I

Adaptation of FLUAV to humans is required for establishment of an efficient virus infection. The influenza virus polymerase subunit PB2 has been described as a major determinant of host switching [74]. In particular, amino acid substitution at PB2 residue 627 from an avian E (glutamic acid) signature to mammalian adapted K (lysin) has been extensively characterized [120]. It was described that mammalian adaptation mutation PB2 627K results in an increased replication in mammalian cells whereas in chicken cells no major replication differences between avian PB2 627E and mammalian PB2 627K were detectable. Furthermore, different groups observed reduced interaction of avian PB2 627E with the viral nucleocapsid and this failure in nucleocapsid assembly was absent in chicken cells [66, 80, 96]. The molecular background for replication advantages of mammalian PB2 627K remained elusive [15, 74, 118]. Interestingly, chicken cells, where no major differences between avian PB2 627E and mammalian PB2 627K could be observed, lack RIG-I [4]. This raises the question whether adaptation mutation PB2 627K might be an influenza virus evasion strategy to avoid immediate RIG-I recognition in mammalian cells to enhance virus replication (**manuscript 4.3, (Weber et al., in press)**).

To address this question, the potential of the incoming nucleocapsids of four diverse influenza virus strains (A/quail/Shantou/2061/00 (H9N2), A/Thai/KAN-1/04 (H5N1), pandemic A/Hamburg/05/2009 (pH1N1), or A/WSN/33 (H1N1)) with either the avian PB2 627E or mammalian PB2 627K to promote RIG-I conformational switching was compared. Strikingly, nucleocapsids with the avian PB2 627E induced a robust RIG-I activation, which was strongly reduced in the presence of the mammalian signature PB2 627K (**manuscript 4.3, Fig. 3A**). Also by performing co-sedimentation assay, avian PB2 627E induced a more robust shift of RIG-I, TRIM25 and MAVS containing fractions in the gradient indicating an enhanced activation of the RIG-I signaling pathway in comparison to nucleocapsids bearing mammalian PB2 627K (**manuscript 4.3, Fig. 3C**).

Despite the clear effect on RIG-I activation, no significant differences between induction of the IFN response by an aborted replication cycle of avian PB2 627E or mammalian PB2 627K containing FLUAV were observed (**manuscript 4.3, Fig. 3D**). Likewise, the activation of the IFN transcription factor IRF3 by FLUAV nucleocapsids bearing either PB2 627E or PB2 627K did not differ. This indicates that mammalian adaptation mutation PB2 627K prevents RIG-I activation without major effects on IFN induction.

To test the influence of RIG-I on virus replication, wt (wildtype) or ΔRIG-I (RIG-I deficient) HEK293 cells were infected with A/Thai/KAN-1/04 (H5N1) with avian PB2 627E or mammalian PB2 627K signature. Allowing multi-cycle growth for 24 hours, titer differences between viruses with avian and mammalian polymerase complex were reduced from 50.000 fold in wt cells to 400 fold in ΔRIG-I cells (**manuscript 4.3, Fig. 4D**). These results could be further supported by monitoring the expression of viral nucleoprotein NP. Compared to wt cells, in ΔRIG-I cells viruses with the avian PB2 627E show an earlier NP synthesis, whereas viruses with the mammalian PB2 627K are not

strongly affected by the presence or absence of RIG-I (**manuscript 4.3, Fig. 4E, S4C and S4D**). Likewise, in chicken DF-1 cells, naturally lacking RIG-I [4], FLUAV bearing the avian PB2 627E or mammalian PB2 627K express NP to a similar extent (**manuscript 4.3, Fig. 4C, upper panel)**. However, overexpression of human RIG-I severely reduces NP expression of the avian PB2 627E virus, whereas replication efficiency of FLUAV with the mammalian PB2 627K is not strongly influenced (**manuscript 4.3, Fig. 4C, middle panel)**.

As mentioned above, no striking differences in IFN induction stimulated by nucleocapsids bearing avian or mammalian polymerase complex could be observed (**manuscript 4.3, Fig. 3D**). Therefore, we wondered whether the IFN response has an influence on the different replication efficiencies of FLUAV with either avian PB2 627E or mammalian PB2 627K. Curiously, by using ΔMAVS (MAVS depleted) HEK293 cells incapable to transmit RIG-I signaling for IFN induction, no rescue of NP expression of FLUAV with avian PB2 627E could be detected (**manuscript 4.3, Fig. 5A**). This indicates that inhibition of RIG-I signaling seems to be not sufficient to regain replication potential of avian viruses. To support this hypothesis, ΔRIG-I cells or chicken DF-1 cells were transcomplementated with either RIG-I wt or signaling incompetent RIG-I K270A mutant. Strikingly, RIG-I K270A did impair PB2 627E virus as much as RIG-I wt (**manuscript 4.3, Fig. 5B and Fig. 5C**). Antiviral activity of RIG-I against nucleocapsids bearing the avian PB2 627E is consequently independent of RIG-I downstream signaling function. Thus, RIG-I binding to the avian nucleocapsids seems to be sufficient to impair virus replication suggesting a novel direct antiviral RIG-I activity.

Mammalian PB2 627K adaptation was described to enhance association of the polymerase complex with the nucleocapsid [66]. To test whether RIG-I affects association of the avian polymerase complex with the nucleocapsids in mammalian cells, co-IPs were performed. In wt cells the avian polymerase complex was less efficiently coprecipitated with the nucleocapsids whereas the PB2 627E-nucleocapsid interaction was slightly increased in ΔRIG-I cells (**manuscript 4.3, Fig. 6A**). By performing a RIG-I specific co-IP, more nucleocapsids with the avian PB2 627E could be coprecipitated in comparison to nucleocapsids bearing PB2 627K (**manuscript 4.3, Fig. 6B**). Although less nucleocapsids of a mammalian adopted strain could be precipitated, more PB2 627K was associated. This indicates that stronger binding of the mammalian polymerase complex to the 5`ppp panhandle prevents RIG-I recognition and hence displacement of the polymerase complex. To test this, a polymerase complex disassembling compound (PB1-T6Y) was applied [141]. Destabilization of the viral polymerase complex converts nucleocapsids with the mammalian PB2 627K to strong RIG-I activators (**manuscript 4.3, Fig. 6D**). However, the potential of PB2 627E bearing nucleocapsids to promote RIG-I conformational switching is more modestly affected. This implies that the strength of the polymerase complex-nucleocapsid interaction influences RIG-I activation.

In summary, we found that RIG-I acts as an influenza virus restriction factor by promoting the dissociation of the weakly interacting avian polymerase complex, thus impairing virus replication. The

inhibitory effect of RIG-I represents moreover a so far undescribed direct, signaling independent antiviral activity. On the other hand, influenza viruses have adapted to allow efficient replication in mammalian cells. Mammalian adaptation mutation PB2 627K enhances binding to the nucleocapsid, thereby preventing RIG-I recognition.

2.4.3.Lassa virus nucleoprotein promotes proteasomal degradation of PKR

Also arenaviruses need to adapt to evade immune recognition for a productive infection. It is known that arenaviruses have evolved diverse strategies to simultaneously attack diverse steps of RIG-I signaling [134, 135]. However, it remained elusive how arenaviruses prevent immediate detection by PKR. Interestingly, we observed that arenavirus nucleocapsids stimulated PKR phosphorylation and conformational switching only if the translation inhibitor CHX was applied (**manuscript 4.4, Fig. 3B**). This raises the question whether arenaviruses encode for a yet unidentified PKR antagonist. To investigate this hypothesis, we focused on LASV. By performing co-IP, an interaction of PKR with incoming (**manuscript 4.4, Fig. 4A, right panel**) and newly synthesized LASV nucleocapsids could be observed (**manuscript 4.4, Fig. 4A, left panel**). However, phosphorylated PKR could only be detected if protein synthesis was inhibited. As a control, a RIG-I specific co-IP was included. RIG-I does not interact with incoming LASV nucleocapsids (**manuscript 4.4, Fig. 4A, left panel**), which is in agreement with the results of Marq *et al.* that 5`overhang structures impair RIG-I recognition [75, 76]. A weak interaction of RIG-I with LASV nucleocapsids could only be observed if full replication cycle was allowed, which might reflect erroneous replication intermediates (**manuscript 4.4, Fig. 4A, right panel**). To identify the protein responsible for PKR inhibition, LASV NP (nucleoprotein), GP (glycoprotein) and Z (matrixprotein) were transfected with increasing concentrations together with PKR at a constant plasmid amount. Thereby, overexpression of PKR alone resulted in PKR activation due to proximity of the single PKR molecules allowing auto-phosphorylation. LASV GP and Z further increased the phosphorylation status of PKR whereas increasing amounts of LASV NP dramatically reduced PKR activation (**manuscript 4.4, Fig. 4B**). By performing co-IP, an interaction of LASV NP, but not GP or Z, with PKR was identified (**manuscript 4.4, Fig. 4C**). Thus, LASV NP is able to interact with PKR and impair PKR phosphorylation. To validate the involvement of the proteasome, the proteasomal inhibitor MG132 was tested. In absence of MG132, LASV NP overexpression results in decreased PKR phosphorylation as expected (**manuscript 4.4, Fig. 4D, left panel)**. However, PKR activation in LASV NP-overexpressing cells can be rescued if the proteasomal degradation pathway is blocked (**manuscript 4.4, Fig. 4D, right panel)**. Also during LASV infection MG132 application can prevent NP promoted PKR inhibition (**manuscript 4.4, Fig. 4E**). Surprisingly, MG132 treatment likewise rescued PKR activation in TCRV and JUNV infected cells.

In summary, we discovered that LASV NP interacts with PKR and promotes the proteasomal degradation of activated PKR. This seems to be a conserved mechanism within the arenavirus family

since MG132 treatment rescues PKR activation during Old World LASV infection, but also in New World TCRV and JUNV infected cells.

3. Discussion

3.1. RIG-I as an immune sensor of incoming viral nucleocapsids

A rapid immune response to virus infection is crucial to ensure survival of the host. *In vitro* studies helped to identify major determinants triggering a RIG-I dependent antiviral IFN response, like dsRNA and a 5`ppp [46, 91, 111, 113]. However, in the natural context of infection the first viral structure able to stimulate RIG-I activation still needed to be resolved.

Here, RIG-I is presented as an immune sensor of incoming bunyavirus and influenza virus nucleocapsids enabling an immediate antiviral response. RIG-I directly interacts with the incoming nucleocapsids independent of viral or cellular RNA synthesis or mammalian cofactors. RIG-I contacts the nucleocapsids via a single site, most likely via the 5`ppp dsRNA panhandle. Thereby, interaction is dependent on the presence of a 5`ppp and a dsRNA, since viral nucleocapsids lacking these features failed to mediate RIG-I activation. This is in contrast to the observation that 3` untranslated regions of the influenza virus genome induce RIG-I activation independent of a 5`ppp [21]. However, these data are based on *in vitro* assays transfecting unpackaged viral or synthetic RNA into cells. During infection, RIG-I activation seems to be dependent on a 5`ppp. This was also proposed by the A.M. Pyle group, who likewise detected RIG-I activation in absence of a 5`ppp in *in vitro* experiments, but postulated that during virus infection the 5`ppp would be required for robust RIG-I binding and activation in presence of a less abundant agonist [60]. Indeed, our results demonstrate that during virus infection, an interaction of RIG-I with 5`ppp nucleocapsids stimulates conformational switching and oligomerization, two hallmarks of RIG-I activation. Activated RIG-I promotes then a signaling cascade that stimulates the activation of the IFN transcription factor IRF3 and eventually culminates in the induction of the antiviral IFN response. This defines the release of viral nucleocapsids as the first time-point of a RIG-I-dependent immune recognition in the natural context of virus infection.

In former studies, transfected measles and vesicular stomatitis virus nucleocapsids could already be identified as immune stimulators [124, 125]. However, during transfection the correct assembly of the viral nucleocapsids cannot be ensured and furthermore, the immune response was not associated with RIG-I. Immune recognition of incoming nucleocapsids is, however, in contrast to previous reports suggesting that replication intermediates occurring later during viral infection cycle would trigger RIG-I-dependent immune responses [5, 101]. Especially for FLUAV, in a recent paper it was argued that the IFN induction is dependent on RNA synthesis [59, 86]. Killip *et al.* observed an activation of the IFN transcription factor IRF3 only if RNA synthesis and nuclear export of the progeny nucleocapsids was permitted [59]. However, we detected IRF3 activation even if the transcription inhibitor ActD was applied or nuclear export was blocked by LMB treatment. The discrepancy could be due to the chosen time-point of analysis. In case of Killip *et al.*, IRF3 translocation was validated eight hours post infection, a time-point where IRF3 might have already disappeared from the nucleus [59]. In our study, IRF3 activation was observed as early as one hour post-infection. This indicates

that also incoming FLUAV nucleocapsids serve as stimulators of the antiviral IFN response, as previously demonstrated for influenza B viruses [86].

It is somewhat intriguing how RIG-I gains access to the 5`ppp panhandle, which is covered by the viral polymerase. Recent structural data of the bat influenza virus panhandle further complicates the view of the accessibility of the 5`terminus [90]. The 5`terminus folds by intrastrand base-pairing into a hook-like structure followed by a dsRNA stretch of 14 base pairs. Moreover, the whole structure is deeply covered within the polymerase complex. It can be hypothesized that during the transit to the nucleus the association of the polymerase complex with the panhandle is dynamic and to some extend flexible. This is in agreement with the observation that that the polymerase complex, especially PB2, is mobile within the structure [102]. A partial release of the 5`terminal hook may enable RIG-I binding to the 5'ppp. Because of the four base-paired nucleotides forming the hook structure, the nucleotide bearing the 5`ppp is base-paired enabling a robust interaction of the RIG-I CTD domain. Additionally, dsRNA stretches are associated with a stabilization of the RNA helix in a fixed conformation supporting engagement of the RIG-I helicase domain [62]. Due to the high affinity of RIG-I for the 5`ppp [128], RIG-I can rapidly entrap its agonist, even if it is only shortly exposed. RIG-I interaction with the 5`ppp may allow first structural rearrangements of RIG-I thereby triggering a disposition of the polymerase complex. This is supported by the hypothesis of Schmidt *et al.*, who argue that RIG-I can drive an ATP-dependent removal of proteins [114]. It seems also plausible, that the panhandle is briefly exposed allowing RIG-I to rapidly interact. Both hypotheses, however, require further investigation.

In summary, RIG-I is in a yet to be identified mechanism able to engage the 5`ppp dsRNA panhandle of incoming nucleocapsids. This interaction induces RIG-I activation, enabling downstream signaling for induction of an immediate antiviral response.

3.2.PKR contributes to immediate pathogen recognition

Immune recognition of incoming nucleocapsids allows an immediate antiviral response. However, viruses have evolved to evade RIG-I recognition. Therefore, alternative immune receptors are required to ensure immediate induction of antiviral defense mechanisms or to support RIG-I immune recognition for a sustained response.

In the present thesis, we identified PKR involvement in immediate virus recognition. PKR interacts with the IGR of incoming bunyavirus RVFV S segmented nucleocapsids and incoming New World arenavirus TCRV and JUNV and Old World arenavirus LASV nucleocapsids. Like RIG-I, PKR interacts with the nucleocapsids only via a single contact site. By analyzing the predicted RVFV and arenavirus IGR, a hairpin structure can be observed with a central dsRNA stem with internal loops and sporadic mismatches. A 16 base pair dsRNA stem with additional 10 to 15 nucleotides of single-stranded tails was previously described as the minimal requirement for PKR activation [150]. Thereby, the dsRNA does not have to possess perfect base pairing since PKR can tolerate non-Watson-Crick

structures and also internal loops as long as the overall A-form geometry of the RNA is retained [7, 8]. Hence, the IGR of the RVFV small genome segment and all genome segments of TCRV, JUNV and LASV present all criteria of a potential PKR agonist. Previous studies demonstrated an interaction of PKR with structured elements of viral RNA, like Hepatitis C virus IRES (internal ribosomal entry site) [119] or dimerized stem-loop structures of TAR (transactivation RNA) of HIV [43].

In vitro experiments by Dauber *et al.* suggest that 5`ppp panhandle structures also serve as PKR agonists [19]. Our data indicates, however, that RIG-I, but not PKR, interacts with the 5`ppp dsRNA panhandle structure in the natural context of infection. Thereby, RVFV M segmented nucleocapsids presenting a 5`ppp dsRNA panhandle, but lacking the IGR promoted RIG-I conformational switching and failed to stimulate PKR activation. It can be postulated that RIG-I outcompetes PKR for 5`ppp panhandle interaction. Another plausible explanation could be that engagement of the 5`ppp terminus by PKR plays a role only during later time-points of infection, when misencapsidated side products of viral replication occur. So far, PKR was not associated with the ability to remove proteins from RNA as it was postulated for RIG-I [114]. Thus, PKR might not gain access to the panhandle of incoming nucleocapsids covered by the viral polymerase.

However, the question about the accessibility of the IGR within the nucleocapsid complex remains elusive. In case of orthobunyaviruses, like LACV, the RNA is deeply buried within the nucleocapsids [3] hindering PKR association. However, RVFV and arenavirus nucleocapsids are less tightly packaged leaving the viral genome partially accessible [40, 99, 100]. Exposure of the viral RNA alone is nevertheless not sufficient for PKR activation since RVF VLPs containing either M or S segment, with the same packaging grade of the viral RNA within the nucleocapsid, do only activate PKR if the IGR is present. Moreover, data by Moy *et al.* indicates that the IGR is exposed for host protein interaction [83]. The group thereby identified an interaction of human DDX17 or *Drosophila* Rm62 with the IGR of RVFV S segment indicating that also PKR could gain access to the IGR. Indeed, our data demonstrates that PKR is able to engage the IGR within the viral nucleocapsid in the natural context of virus infection. Protein interaction with the IGR was proposed to have a negative impact on virus replication [83]. It can therefore be hypothesized that PKR association with the RVFV and arenavirus IGR could also impair virus replication independent of its downstream signaling activity. This represents an exciting assumption, but still requires further investigation.

Taken together, PKR contributes to immediate virus recognition by interacting with the IGR of incoming viral nucleocapsids.

3.3. Immune evasion strategies to prevent immediate recognition

Antiviral immunity acts as a major barrier to virus infection, which must be circumvented to enable a productive infection. Viruses have therefore evolved to prevent immediate recognition and activation of antiviral defense mechanisms.

As presented above, incoming FLUAV nucleocapsids serve as immediate triggers of a RIG-I-dependent IFN response. To ensure an efficient replication cycle, influenza viruses have evolved multiple strategies to circumvent immune recognition by RIG-I, downstream signaling and activation of an antiviral response. On one hand, during evolution *Orthomyxoviridae* have located viral transcription and replication to the nucleus thereby limiting exposure of potential agonist to cytoplasmic immune sensors. Furthermore, immune recognition is actively impaired by sequestering dsRNA by viral NS1 [42] or dsRNA unwinding via the cellular helicases UAP56 and URH49 [136, 137]. Also FLUAV polymerase complex interferes with the host immune system. Thereby, MAVS downstream signaling ability is impaired by influenza virus polymerase subunits PB1, PB2 and PA [34, 53] and a variant of PB1-F2 [24, 127]. Like NS1 protein [49], the polymerase complex is already present within the virion allowing a rapid interference with immune recognition.

Here, we present a single substitution at position 627 of PB2 from avian adapted glutamic acid (E) signature to mammalian lysin (K) as a novel FLUAV strategy to impair immediate immune recognition by RIG-I. A change from avian PB2 627E to mammalian PB2 627K has been extensively characterized in the context of host adaptation [74]. Also adaptation to the host immune system is required to ensure efficient replication in a new host. Previous data suggested that adaptation mutation PB2 627K positively affects viral replication in mammalian cells, which was accompanied with increased nucleocapsid stability [66, 80, 96]. The PB2 627 position is in close proximity to the NP binding site and hence an unstable binding between PB2 627E and NP might lead to a failure in nucleocapsid assembly [80, 82].

Our data indicates that RIG-I specifically recognized and got activated by nucleocapsids with avian polymerase complex whereas nucleocapsids bearing mammalian PB2 627K failed to promote RIG-I activation. Furthermore, RIG-I specifically interfered with the association of the avian polymerase complex with the nucleocapsids. This is in agreement with previous reports describing a disturbed interaction of PB2 627E with the viral nucleocapsids in mammalian cells, but the responsible host factor or mechanisms was not identified [66, 80, 96]. In contrast, Cauldwell *et al.* argued that mammalian adaptation mutation PB2 627K does not enhance stability of the polymerase complex, but rather increases the amount of replicated RNA [14]. This would consequently lead to the false interpretation of co-IP data that more mammalian polymerase complex associated to the nucleocapsids excluding the fact that less avian nucleocapsids are present. However, in our case cells were treated with CHX and LMB to block viral replication and still, in presence of RIG-I, more mammalian PB2 627K was associated to the incoming nucleocapsids in comparison to avian PB2 627E. In RIG-I depleted cells, interaction of the avian PB2 627E bearing polymerase complex with the nucleocapsids was partially rescued. This implicates that RIG-I specifically affects the association of a destabilized avian polymerase complex. PB2 627K, however, enhances interaction of the polymerase complex with the nucleocapsid thus limiting RIG-I recognition of the incoming nucleocapsids. This is also supported

by the observation that disturbance of the polymerase complex assembly through applying competing peptides reverts PB2 627K nucleocapsids to a RIG-I stimulating agonist.

It was furthermore described that the mutation at position 627 of influenza virus PB2 does not alter the structure of the polymerase subunit, but rather disrupts a basic patch on the surface of the protein [122]. The change of surface charge might alter the association of the polymerase complex with host factors. Interaction with either enhancing or suppressing cellular proteins might therefore be responsible for the diverse polymerase activity between PB2 627E and 627K [96]. Indeed, the García-Sastre group described several proteins differentially regulating polymerase activity depending if there is an E or K at position 627 of PB2. Interestingly, DDX17, a DEAD box RNA helicase like RIG-I, was among the identified proteins [10]. In our hands, an interaction of RIG-I specifically with avian PB2 627E or the mammalian PB2 627K could not be detected. However, others did identify an association of FLUAV polymerase complex subunits with RIG-I [69]. Due to sensitivity problems, our experiments might have failed to detect this interaction. The biological significance of polymerase-RIG-I interaction still needs to be resolved. It was, however, demonstrated that the interaction does not affect RIG-I mediated IFN signaling [69]. It can be postulated that RIG-I entraps the viral polymerase complex to the panhandle promoter region and blocks polymerase processivity by interaction, since the RIG-I CTD is anchored via association to the 5`ppp. This might promote an IFN signaling-independent block of viral replication. Our data likewise indicate an IFN-independent mechanism of inhibiting virus replication of FLUAV with the avian signature. Firstly, by validating the ability of incoming nucleocapsids bearing either avian PB2 627E or mammalian PB2 627K to stimulate IFN induction no striking differences were observed. Furthermore, depletion of cells of the signaling molecule MAVS did not rescue replication of the FLUAV with avian PB2 627E. Likewise, a signaling-incompetent mutant RIG-I with an active binding capacity inhibited replication of FLUAV with avian PB2 627E as much as RIG-I wt did. Taken together, not the downstream IFN signaling ability of RIG-I promotes the antiviral effect against FLUAV with the avianized polymerase complex, but rather already the association with the panhandle promoter. This indicates a novel direct antiviral activity of RIG-I independent of its signaling ability.

In conclusion, RIG-I detects incoming influenza virus nucleocapsids. Activation of RIG-I is thereby enhanced in presence of an avian PB2 627E. Poor association of the polymerase complex with the nucleocapsid might allow full engagement of RIG-I with the 5`ppp panhandle promoting its activation. RIG-I interaction with the panhandle alone dislocates the avian polymerase and impairs virus replication independent of RIG-I mediated IFN signaling. However, a polymerase complex with the mammalian signature PB2 627K shows enhanced interaction with the nucleocapsid impairing RIG-I recognition. This suggests that also for recognizing other viral nucleocapsids the polymerase needs to be disposed for enabling RIG-I binding and activation. It would be hence interesting to investigate whether other viruses possess similar adaptation mutations to avoid immediate RIG-I recognition.

Despite RIG-I, also PKR contributes to immediate recognition of virus infection. PKR, however, detects the IGR of incoming nucleocapsids presented by viruses using ambisense coding strategy, like RVFV S and arenavirus genome segments. RVFV NSs promotes the proteasomal degradation of PKR thereby limiting PKR recognition and its antiviral activity [37]. An evasion strategy by arenavirus able to inhibit PKR activation was not identified so far.

Here, we present that arenaviruses promote, like RVFV, the proteasomal degradation of PKR. Specifically, LASV NP could be identified as the responsible PKR antagonist. LASV NP interacts with PKR and promotes PKR degradation via the proteasomal pathway in a dose dependent manner. However, NP encapsidating the viral genome did not affect the activation status of PKR indicating that only free LASV NP was comprising PKR antagonistic properties. LASV NP possesses the ability to bind dsRNA [39], which could serve as a scaffold for PKR interaction. Co-IP data of LASV proteins expressed in absence of viral RNA indicates, however, that the interaction of LASV NP with PKR is rather independent of viral RNA. Nevertheless, a complex formation of LASV NP with cellular RNA cannot be excluded. It was reported in this regard that recombinant nucleoproteins of NSV can associate with cellular RNA into nucleocapsid like structures [106]. Moreover, LASV NP comprises the ability to oligomerize [68]. Whether NP monomers or LASV oligomeric complexes promote PKR antagonism still needs to be clarified. It was, however, previously described that the NP oligomerization is no strict requirement for impairing the IFN response [68]. Hastie *et al.* reported that the dsRNA specific 3` to 5` exonuclease activity of LASV NP is essential for inhibiting IFN signaling [39]. Since incoming nucleocapsids do not present long dsRNA stretches to the host immune system, degradation of dsRNA might play a distinct immune evasion strategy during later infectious stages.

Arenavirus NP is well conserved among Old and New World arenaviruses, suggesting that an IFN antagonistic activity may be a shared feature [39, 40]. Indeed, lymphocytic choriomeningitis virus (Old World arenavirus) and Whitewater Arroyo virus, Pichinde virus, JUNV, Machupo virus and Latino virus, but not TCRV, (New World arenaviruses) were able to impair the IFN and proinflammatory response [77, 78, 104]. Likewise, arenaviruses use proteasomal degradation as a common PKR antagonism, but the responsible TCRV and JUNV protein inducing PKR inhibition remains elusive. TCRV, incapable to impair IFN signaling [78], inhibited PKR activation. This highlights the requirement to prevent early recognition by PKR to ensure efficient virus propagation, even in the case of apathogenic viruses like TCRV.

Despite of proteasomal degradation of PKR by arenaviruses, other viruses have also evolved strategies to prevent antiviral activity of PKR. Thereby, Kaposi-sarcoma herpesvirus vIRF2 and vaccinia virus K3L block PKR auto-phosphorylation [13, 105]. Hepatitis C virus E2 protein presents homologies with PKR and eIF2α and can serve as a pseudosubstrate [123]. This broad spectrum of viruses ranging from DNA to RNA viruses antagonizing PKR indicates the relevance of PKR inhibition for efficient virus replication.

In summary, we found that LASV NP and a yet to be identified TCRV and JUNV protein promote the proteasomal degradation of PKR. Thereby, LASV NP interacts with PKR most likely independent of viral RNA and induces PKR degradation via the proteasomal pathway. Therefore, arenavirus have evolved an efficient strategy to counteract immediate recognition and activation of antiviral defense mechanisms.

3.4. Concluding remarks

The presented data provides evidence that incoming bunyavirus, FLUAV and arenavirus nucleocapsids are rapidly recognized by RIG-I and PKR. RIG-I recognition is dependent on the presence of a 5`ppp dsRNA panhandle, whereas PKR detects the IGR of genome segments using ambisense coding strategy. Hence, the first host response to virus infection already occurs immediately after virus entry. Furthermore, we describe a novel antiviral activity of RIG-I that is independent of its signaling ability. In this regard, already binding of RIG-I to the 5`ppp panhandle limits FLUAV replication.

Viruses evade immune recognition by various mechanisms. Here, we present two diverse strategies of FLUAV and arenaviruses to prevent immediate detection by the host immune system. For FLUAV, the mammalian adaptation PB2 627K stabilizes the polymerase complex association with the nucleocapsids, thus preventing RIG-I recognition of the 5`ppp dsRNA panhandle. In case of arenaviruses, we show that LASV NP prevents PKR sensing of the incoming nucleocapsids via induction of the proteasomal degradation of PKR. This later seems to be common within the arenavirus family since not only Old World arenavirus LASV, but also New World TCRV and JUNV induce PKR degradation via the proteasomal pathway.

It is known that the constant immune pressure leads to positive selection of viruses combining potent immune evasion with efficient replication strategies within the host cell. FLUAV bearing PB2 627K is associated with enhanced pathogenicity [120], like LASV being the causative agent of fatal human hemorrhagic fever [79]. This supports the idea that viral proteins involved in circumventing RLR and IFN signaling represent also determinants of virulence and pathogenesis [12, 129].

In conclusion, we pin down entry of viral nucleocapsids as the first time-point of immune recognition in the natural context of virus infection and give further insights how viruses have evolved to counteract immediate detection.

Despite these achievements, future studies are required to comprehend the complexity of virus-host interactions. It remains to be clarified how RIG-I gains access to the 5`ppp dsRNA panhandle covered by the viral polymerase and nucleoproteins. Furthermore, the direct antiviral activity of RIG-I combined with the fact that cofactors are not essential for RIG-I activation raises the question whether RIG-I would also perform an antiviral activity in the nucleus. Indeed, RIG-I was previously observed in the nucleus [69], however, no antiviral activity was associated. Interestingly, it was hypothesized

that an unknown factor interacts with avian PB2 627E in the nucleus, thereby limiting mobility and disturbing nucleocapsid assembly [28]. Whether RIG-I represents this factor is a tempting assumption. For FLUAV, several adaptation mutations associated with increased pathogenesis were described [15]. The effect of these mutations on cellular defense mechanisms was not addressed so far. It would be thus of interest to validate the influence of other adaptive mutations, despite PB2 627K, on the host immune response.

To effectively control virus infections, the generation of new therapeutically tools is required. Interestingly, peculiar poly-C (viral sense) and poly-G (viral anti-sense) repeats within the IGR were previously described as essential transcription termination signals [1]. These structures are therefore less likely to be altered by the virus despite the existing immune pressure. Moreover, interaction of a protein with the IGR of viral genomes was associated with reduced viral replication [83]. Thus, targeting of this conserved region, by for instance aptamers, might be a promising therapeutic approach to limit virus replication and ensure survival of the host.

Conclusively, detailed knowledge how viruses interfere with the RLR detection and signaling system may provide not only new insights into RLR signaling, but also virus pathogenesis itself. A better understanding of the pathogenic potential of viruses would thereby allow to rapidly react and provide preparedness for future epidemics or even pandemics.

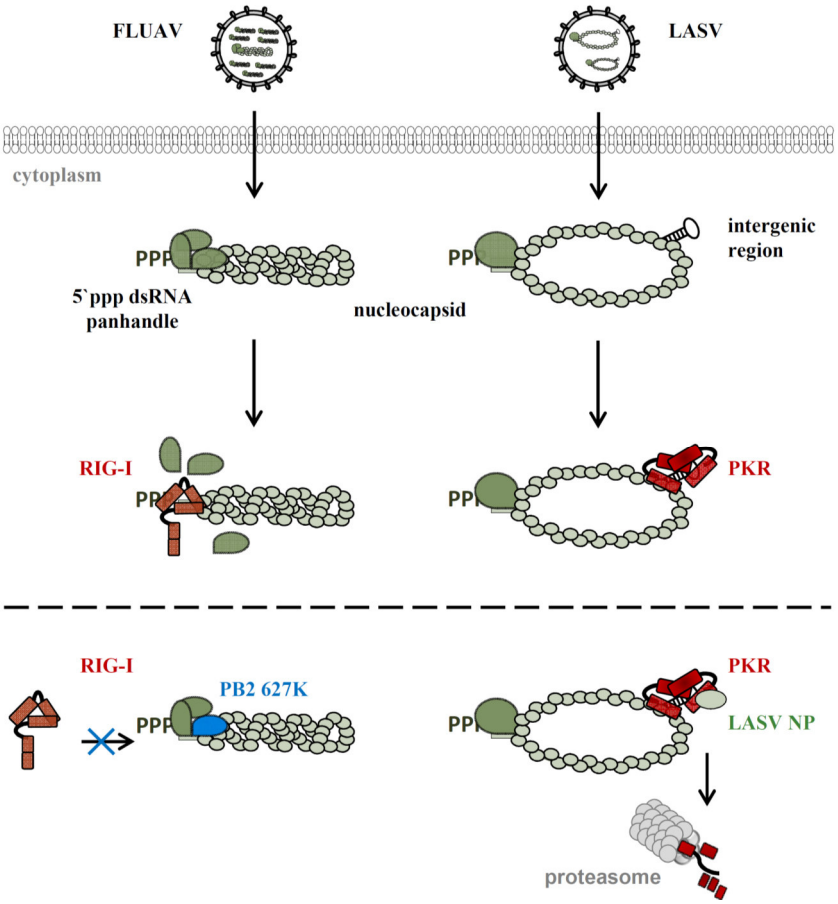

Immediate virus recognition by RIG-I and PKR and viral counterstrategies.

Exemplarily, immune recognition of incoming influenza A virus (FLUAV) and Lassa virus (LASV) nucleocapsids by RIG-I and PKR is shown, respectively. RIG-I rapidly detects the 5`ppp dsRNA panhandle upon release of FLUAV nucleocapsids

into the host cytoplasm. PKR, however, reacts to the intergenic region of incoming nucleocapsids. To antagonize immediate immune recognition, FLUAV mammalian adaptation mutation PB2 627K stabilizes association of the polymerase complex with the nucleocapsids, thereby preventing RIG-I recognition. For PKR evasion, LASV nucleoprotein (NP) interacts with PKR and promotes its degradation via the proteasome.

4. Original publications and manuscripts

4.1. Monitoring activation of the antiviral pattern recognition receptors RIG-I and PKR by limited protease digestion and native PAGE

Own contribution:

I established the techniques in our lab and performed all experiments shown in Fig. 1 and 2. I contributed to writing of the manuscript.

Michaela Gerlach

Video Article

Monitoring Activation of the Antiviral Pattern Recognition Receptors RIG-I And PKR By Limited Protease Digestion and Native PAGE

Michaela Weber[1], Friedemann Weber[1]

[1]Institute for Virology, Philipps-University Marburg

Correspondence to: Friedemann Weber at friedemann.weber@staff.uni-marburg.de

URL: http://www.jove.com/video/51415
DOI: doi:10.3791/51415

Keywords: Infectious Diseases, Issue 89, innate immune response, virus infection, pathogen recognition receptor, RIG-I, PKR, IRF-3, limited protease digestion, conformational switch, native PAGE, oligomerization

Date Published: 7/29/2014

Citation: Weber, M., Weber, F. Monitoring Activation of the Antiviral Pattern Recognition Receptors RIG-I And PKR By Limited Protease Digestion and Native PAGE. *J. Vis. Exp.* (89), e51415, doi:10.3791/51415 (2014).

Abstract

Host defenses to virus infection are dependent on a rapid detection by pattern recognition receptors (PRRs) of the innate immune system. In the cytoplasm, the PRRs RIG-I and PKR bind to specific viral RNA ligands. This first mediates conformational switching and oligomerization, and then enables activation of an antiviral interferon response. While methods to measure antiviral host gene expression are well established, methods to directly monitor the activation states of RIG-I and PKR are only partially and less well established.

Here, we describe two methods to monitor RIG-I and PKR stimulation upon infection with an established interferon inducer, the Rift Valley fever virus mutant clone 13 (Cl 13). Limited trypsin digestion allows to analyze alterations in protease sensitivity, indicating conformational changes of the PRRs. Trypsin digestion of lysates from mock infected cells results in a rapid degradation of RIG-I and PKR, whereas Cl 13 infection leads to the emergence of a protease-resistant RIG-I fragment. Also PKR shows a virus-induced partial resistance to trypsin digestion, which coincides with its hallmark phosphorylation at Thr 446. The formation of RIG-I and PKR oligomers was validated by native polyacrylamide gel electrophoresis (PAGE). Upon infection, there is a strong accumulation of RIG-I and PKR oligomeric complexes, whereas these proteins remained as monomers in mock infected samples.

Limited protease digestion and native PAGE, both coupled to western blot analysis, allow a sensitive and direct measurement of two diverse steps of RIG-I and PKR activation. These techniques are relatively easy and quick to perform and do not require expensive equipment.

Video Link

The video component of this article can be found at http://www.jove.com/video/51415/

Introduction

A crucial event in antiviral host defense is the rapid detection of the pathogen by the so-called pattern recognition receptors (PRRs)[1,2]. Intracellular detection of RNA virus infection is dependent on two cytoplasmic RNA helicases, RIG-I (retinoic acid inducible gene I) and MDA5 (melanoma differentiation associated protein 5)[3-5]. RIG-I is composed of two N-terminal caspase recruitment domains (CARDs), a central DECH-box type RNA helicase domain, and a C-terminal domain (CTD)[4,6]. Whereas the CTD and the helicase domain are required for recognition of non-self (viral) RNAs, the CARDs mediate downstream signaling leading to establishment of an antiviral host status.

If RIG-I is in the silent state, *i.e.* in the absence of a specific RNA ligand, the second CARD interacts with the central helicase domain and keeps RIG-I in an auto-inhibitory conformation[7-11]. RIG-I binds to short double-strand (ds) RNA bearing a 5'-triphosphate (5'PPP), long dsRNA, and polyU/UC-rich RNA, classic signature structures which are present on the genomes of many RNA viruses[12-16]. Two major characteristics of RIG-I activation are a switch to a closed conformation[6,17] and the homo-oligomerization[6,18,19]. The conformational switch enhances RNA binding, exposes the CARDs for downstream signaling, and reconstitutes an active ATPase site[8,9,11,20]. The formation of oligomeric RIG-I complexes leads to enhanced recruitment of downstream signaling adaptor molecules to form a platform for antiviral signal transduction[11]. The RIG-I-regulated signaling chain eventually activates the transcription factor IRF-3 for up-regulation of interferon (IFN-alpha/beta) genes and hence the gene expression of interferon stimulated genes (ISGs) for a full antiviral response[21,22]. One of the best characterized ISGs is the RNA-activated protein kinase (PKR) [23]. PKR belongs to the family of eukaryotic translation initiation factor 2 alpha (eIF2α) kinases and is composed of an N-terminal double-stranded RNA binding domain and a C-terminal kinase domain. The kinase domain constitutes the dimerization interface crucial for PKR activation and carries out the catalytic functions of the protein. Binding of PKR to viral dsRNA leads to its conformational change permitting dimerization and auto-phosphorylation at Thr 446 among other residues. PKR then mediates phosphorylation of eIF2α, thereby blocking the translation of viral mRNAs[23-27].

Both RIG-I and PKR undergo major structural rearrangements, form oligomeric complexes and are post-translationally modified by phosphorylation/dephosphorylation and ubiquitination[10,11,19,23,24,26-29]. For a better understanding of which viral RNA structures are activating RIG-I and PKR (and at what stage viral antagonists could be interfering), it is important to precisely determine the activation status. For both PRRs it was previously described that activation leads to the emergence of trypsin-resistant protein fragments[6,17,30] and higher-order

oligomers[6,18,19]. However, given the wealth of literature on these key factors of the antiviral host response[1,2,24], application of direct methods seems comparatively rare. In the hope of stimulating broader usage, we provide convenient and sensitive protocols to robustly analyze the activation states of RIG-I and PKR. The IFN competent human cell line A549 is infected with an established activator of RIG-I and PKR, the attenuated Rift Valley fever virus mutant clone 13 (Cl 13)[31,32]. After a simple lysing procedure, the extracts of infected cells are tested by limited trypsin digestion/western blot analysis to evaluate conformational switching, and by blue native polyacrylamide gel electrophoresis (PAGE) / Western blot analysis to measure formation of oligomers.

Protocol

1. Seeding of A549 Cells for Infection

1. Cultivate a T75 flask of A549 cells at 37 °C and 5% CO_2 in cell culture medium (DMEM supplemented with 10% FCS, 526.6 mg/l L-glutamine, 50.000 U/l penicillin, and 50 mg/l streptomycin).
2. Before starting to harvest the cells, warm up cell culture medium, PBS and 0.05% trypsin-EDTA in a waterbath heated to 37 °C.
3. Remove the medium and wash the cells with 10 ml PBS. Remove the PBS again.
4. Add 3 ml of trypsin-EDTA and distribute equally in the flask. Transfer the flask in an incubator with 37 °C and 5% CO_2.
5. When all cells are detached, add 7 ml of cell culture medium, resuspend the cells, and transfer the cell suspension into a 15 ml Falcon tube.
6. Centrifuge the cells at 800 x g for 5 min at RT, remove the supernatant and resuspend the pellet in 10 ml fresh cell culture medium.
7. Count the cells with a counting chamber.
8. Add 2.5 x 10^6 cells in 5 ml of cell culture medium in two T25 flasks each. Incubate for 16 hr at 37 °C and 5% CO_2. One flask serves for the mock control and one for Cl 13 infection.

2. Infection with Rift Valley Fever Virus Clone 13 (Cl 13)

1. NOTE: Cl 13 is an attenuated virus mutant which in Germany can be handled under BSL-2 conditions. Please refer to relevant national guidelines. Other typical IFN inducers would be Sendai virus (strain Cantell) or Newcastle disease virus.
2. Pre-warm PBS, serum-free medium, and cell culture medium containing 5% FCS.
3. Prepare 1.25 x 10^7 PFU/ml of Cl 13 in serum-free medium to infect 2.5 x 10^6 A549 cells with a multiplicity of infection (MOI) of 5. Prepare a slightly (roughly 10%) greater amount than needed to account for pipette errors.
4. Wash the cells with PBS as described under 1.3.
5. Add 1 ml of the Cl 13 dilution or of serum-free medium (uninfected control, mock) to the cells, and incubate for 1 hr at 37 °C and 5% CO_2. Move the flask carefully every 15 min to ensure equal distribution of Cl 13 dilution and serum-free medium, respectively.
6. After 1 hr of infection, remove the inocula, add 5 ml of pre-warmed cell culture medium with 5% FCS, and incubate for 5 hr at 37 °C and 5% CO_2.

3. Preparation of Cell Lysates

1. Prepare PBS / 0.5% Triton X-100 at 4 °C. Do not add serine protease inhibitors.
2. Wash the cells with cold PBS and add 10 ml of fresh PBS.
3. Scrape the cells off, transfer the cell suspension in a falcon tube, and centrifuge at 800 x g for 5 min at RT.
4. Remove the supernatant and resuspend the cell pellet in 30 µl PBS / 0.5% Triton X-100. Transfer the lysate into a fresh 1.5 ml tube and incubate for at least 10 min at 4 °C.
5. Centrifuge the lysate at 10.000 x g for 10 min at 4 °C and transfer the clarified cell lysate (supernatant) into a fresh tube.
6. Determine the protein concentration by Bradford assay as described elsewhere[33].
7. Store at -20 °C or proceed to trypsin digestion (4.1) or native PAGE (5.1).

4. Determination of Conformational Changes of Pattern Recognition Receptors

1. TPCK-trypsin Treatment of Cell Lysates
    1. Dilute L-1-tosylamido-2-phenylethyl chloromethyl ketone-treated (TPCK) trypsin in PBS to a final working concentration of 2 µg/µl.
    2. Adjust in two new tubes a final protein concentration of 25 µg of each protein lysate (mock or Cl 13) in a final volume of 9 µl with PBS. Hence, it should be four tubes with 25 µg lysate each, two times mock and two times Cl 13 infection. One set as input control (untreated) and one set for treatment with TPCK-trypsin.
    3. Add 1 µl of PBS (untreated) or 1 µl of 2 µg/µl TPCK-trypsin (final concentration: 0.2 µg/µl) to the cell lysates and mix the reactions by pipetting. DO NOT freeze and thaw TPCK-trypsin aliquots, because it will compromise the efficiency of digestion.
    4. Incubate the lysates at 37 °C for 25 min. Stop the reaction by adding 5x denaturing sample buffer (250 mM Tris-HCl pH 6.8, 10% SDS, 50% glycerol, 25% β-mercaptoethanol, 0.5% bromphenol blue) and by boiling for 5 min at 95 °C. It is important to NOT extend the trypsin incubation time. In case no protease-resistant fragments are detectable, the time of trypsin digestion must be shortened.
    5. After boiling, the samples can be stored at -20 °C.

2. SDS Polyacrylamide Gel Electrophoresis (PAGE) and Western Blotting
    1. Load the samples on a sodium dodecyl sulfate (SDS) polyacrylamide gel containing a 5% stacking over a 12% resolving gel. Separate the proteins at 25 mA per gel until the bromphenol blue runs out.
    2. Activate a polyvinylidene fluoride (PVDF) membrane for 30 sec with methanol and put it into transfer buffer (48 mM Tris, 39 mM glycin, 1.3 mM SDS, 20% methanol).

3. Prepare the blotting with a semidry blotting system and allow the transfer of the proteins at 10 V for 1 hr. Take the membrane out, rinse it briefly with water, and let it dry.
4. Reactivate the membrane by shortly transferring into methanol. Wash for 5 min with TBS. Block with 10% skim milk in TBS for 1 hr at RT or at 4 °C O/N. Wash the membrane 3x for 5 min each with TBS.
5. Prepare antibody dilution as recommended in table 1 and incubate the membrane for 1 hr at RT or at 4 °C O/N.
6. Wash the membrane 3x for 10 min each with TBS-T. Add the appropriate secondary antibody coupled with horseradish peroxidase at a 1:20,000 dilution in 1% skim milk in TBS. Incubate 45 min at RT.
7. Wash the membrane 3x for 10 min each with TBS-T, and one additional time with TBS.
8. For signal detection use a commercial chemiluminescense kit and a digital gel imaging system.

3. Coomassie Brilliant Blue G-250 Staining
   1. Perform SDS-PAGE as described in 4.2.1. Load samples on an SDS polyacrylamide gel and run the gel at 25 mA per gel until bromphenol blue runs out.
   2. Perform Coomassie Brilliant Blue G-250 staining at RT. Do all incubations under constant shaking.
   3. Transfer the gel to the fixation solution containing 40% methanol and 10% acetic acid for 30 min.
   4. Exchange the buffer to destaining solution (25% ethanol and 8% acetic acid) and incubate for 5 min.
   5. Stain the gel with 0.2% Coomassie Brillant Blue G-250 in 40% methanol and 10% acetic acid for 1 hr.
   6. Destain the gel with the destaining solution and exchange the buffer after 10 min, 30 min, and 60 min.
   7. Store the gel in 25% ethanol, 8% acetic acid, and 4% glycerol at 4 °C.
   8. Perform imaging and analysis as described under 4.2.8.

5. Analysis of Oligomeric States of Pattern Recognition Receptors

1. Native PAGE
   1. Prepare 50 µg of cell lysate in a final volume of 10 µl with PBS and add 5× native sample buffer (250 mM Tris-HCl pH 6.8, 1% sodium deoxycholate, 50% glycerol, 0.5% bromphenol blue) to a final concentration of 1x.
   2. Load the samples IMMEDIATELY on a native polyacrylamide gel with 5% as stacking and 8% as resolving gel. Any delay will result in a loss of native complexes[34].
   3. Run the gel at 20 mA per gel at 4 °C with 50 mM Tris-NaOH pH 9.0, 384 mM glycin as as anode and 50 mM Tris pH 8.3, 384 mM glycin, 1% sodium deoxycholate as cathode buffer. After 1.5-2 hr (bromphenol blue band has left the gel approximately 45 min earlier) the electrophoresis is finished.

2. Western Blotting
   1. Activate a polyvinylidene fluoride (PVDF) membrane for 30 sec with methanol and put it into Towbin buffer (25 mM Tris, 192 mM glycin, 0.1% SDS, 20% methanol).
   2. Assemble a wet blot chamber according to the manufacturer's instructions and fill the tank with Towin buffer.
   3. Perform the blotting with 250 mA for 1.5 hr at 4 °C.
   4. When blotting is finished proceed as described from 4.2.3 on.

Representative Results

Recognition of a viral agonist by RIG-I or PKR triggers conformational switching[6,17,30] and oligomerization[6,18,27]. We assayed these two activation markers by limited protease digestion and native polyacrylamide gel electrophoresis (PAGE), respectively.

Human A549 cells were infected with Rift Valley fever virus clone 13 (Cl 13), which is characterized by a mutation of the IFN antagonist NSs[35,36]. Due to the absence of functional NSs, Clone 13 strongly induces RIG-I and PKR, leading to the establishment of a robust antiviral state in the cells[12,31,32,37].

Trypsin digestion of mock infected cell lysates results in a rapid degradation of RIG-I, whereas Cl 13 infection leads to the generation of a 30 kDa resistant RIG-I fragment **Figure 1A**. Also PKR shows partial resistance to trypsin digestion in infected samples, which coincides with its phosphorylation **Figure 1A**. To monitor efficiency and specificity of trypsin digestion, gels were stained with Coomassie Brilliant Blue G-250. Untreated samples show equal amounts of loaded proteins **Figure 1B**. Subjecting mock and Cl 13 cell lysates to trypsin digestion leads to a comparable decrease of global protein amounts. This demonstrates that trypsin treatment has the same efficiency for mock and Cl 13-infected samples.

The formation of oligomeric complexes was assayed by native PAGE. In uninfected cells, only monomers of RIG-I and PKR were detected **Figure 2**. As additional control we included the transcription factor IRF-3, which is present as a monomer but known to dimerize upon activation via *e.g.*, RIG-I[38]. Cl 13 infection leads to a strong accumulation of RIG-I oligomeric complexes in form of a smear and of PKR and IRF-3 dimers/oligomers as a defined protein band.

These results demonstrate that limited trypsin digestion and native PAGE are useful tools to monitor conformational changes and oligomer formation of RIG-I and PKR upon infection.

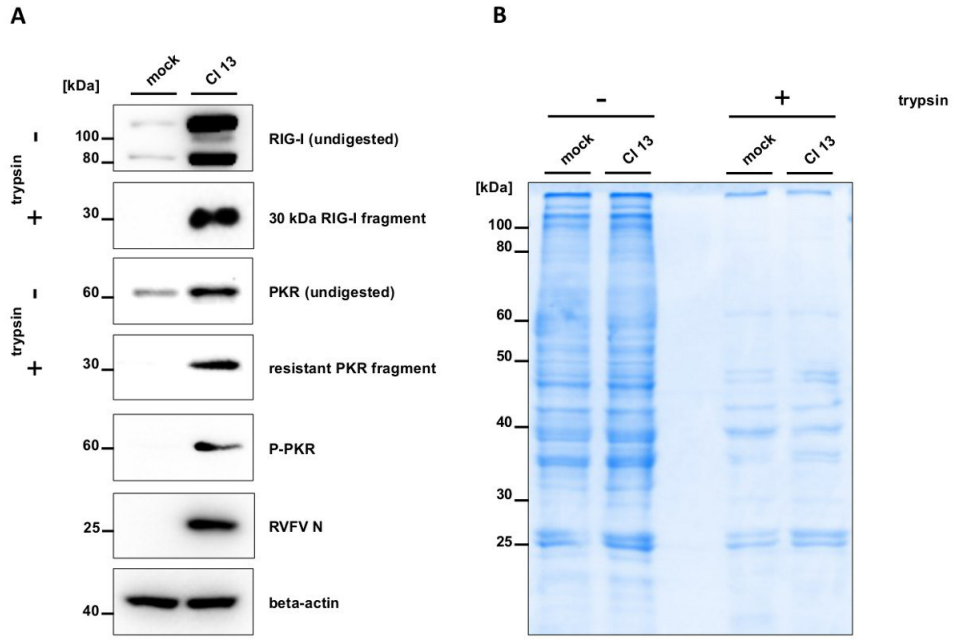

Figure 1. Conformational switch of RIG-I and PKR. A549 cells were mock infected or infected with Cl 13 at an MOI of 5. After 5 hr, cells were lysed in PBS supplemented with 0.5% Triton X-100 and cleared cell lysates were either left untreated or treated with trypsin. Samples were subjected to SDS PAGE followed by Western blotting **(A)** or Coomassie staining **(B)**. Blots were stained against RIG-I, PKR, phosphorylated PKR (Thr 446) and against RVFV nucleoprotein (RVFV N) and beta-actin as infection and loading control, respectively. Please click here to view a larger version of this figure.

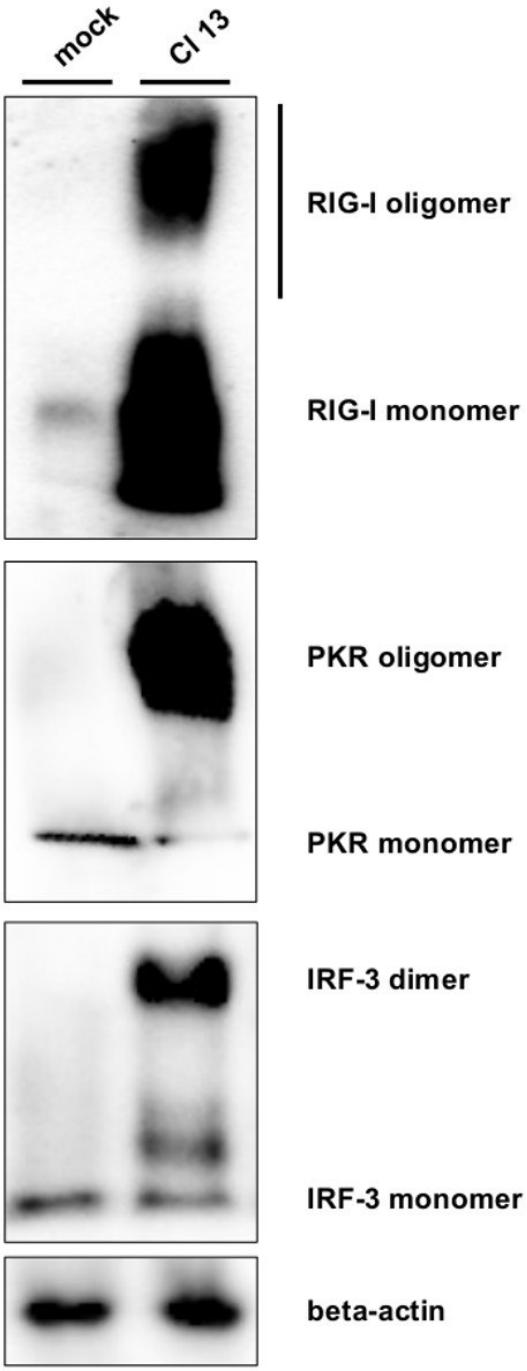

Figure 2. Oligomerization of RIG-I, PKR, and IRF-3. Cell lysates of mock and CI 13-infected cell lysates were subjected to native PAGE followed by Western blot analysis. Staining was performed with antibodies against RIG-I, PKR, IRF-3, and beta-actin as loading control. PKR oligomers most likely represent dimers[27]. Please click here to view a larger version of this figure.

Discussion

Sensing the presence of viruses and activation of the antiviral type I IFN system are crucial for successful innate immune responses[22]. Virus detection is thereby mediated by pathogen recognition receptors (PRRs) like RIG-I and PKR, enabling a rapid response and activation of antiviral defense mechanisms. Here, we describe two methods to directly evaluate the activation status of RIG-I and PKR.

Limited protease digestion as a tool to monitor conformational changes of RIG-I and PKR was first described by the groups of M. Gale Jr. and T. Fujita[6,17], and J. L. Cole[30], respectively. It represents a sensitive method to evaluate sensitivity alterations to trypsin treatment caused by conformational changes. Applying trypsin digestion, we detected rapid degradation of RIG-I and PKR in mock infected samples, whereas trypsin treatment of virus-infected cell lysates led to trypsin resistant RIG-I fragments. Similarly, a trypsin resistant PKR fragment was detected upon CI 13 infection. This was accompanied by PKR phosphorylation at Thr 446, a widely used marker of PKR activation. Comparing trypsin digestion of

mock and Cl 13 cell lysates by Coomassie staining demonstrates a comparable decrease of global protein levels. This indicates that formation of resistant fragments is specific for proteins like RIG-I and PKR.

The formation of oligomeric complexes of RIG-I, PKR and IRF-3 was monitored by native PAGE. Subjecting Cl 13-infected cell lysates to native PAGE, we detected RIG-I, PKR and IRF-3 oligomers, whereas these proteins remained as monomers in mock infected samples. RIG-I needs to form oligomers to activate downstream pathways. It was hypothesized that RIG-I oligomerization supports recruitment of cofactors to form a signaling platform for antiviral response mechanisms[11]. The function of PKR dimerization is not entirely understood. Most likely, the PKR subunits in the dimer phosphorylate each other[25]. The type I IFN system is tightly regulated on a transcriptional level, and IRF-3 represents one central transcription factor for the induction of IFN and ISGs[38]. Central hallmarks of activation are phosphorylation, dimerization, and translocation to the nucleus, where it recruits the transcriptional co-activators p300 and CREB-binding protein (CBP) to initiate IFN mRNA synthesis[21,39]. Analysis of IRF-3 dimerization is a widely used tool to monitor activation of the type I IFN response[38]. Therefore, we used the detection of IRF-3 oligomeric complexes as a proof of principle for the oligomerization assays of RIG-I and PKR oligomerization. Indeed, allowing separation of protein lysates under non-denaturing conditions, we were able to detect IRF-3 dimerization in Cl 13 infected samples.

Undoubtedly, each lab will need to optimize the protocols of limited protease digestion and native PAGE. If confronted with no detection of any resistant proteins or too many resistant fragments, one might shorten or prolong the time of digestion, respectively. Differences can also be due to the specific TPCK-trypsin stock, as preparations slightly differ. Therefore, various TPCK-trypsin concentrations should be tested for optimization. Cell lysates can be prepared from other cell lines than A549, but adaptations of the protocol might be required. It is recommended to adjust the amount of total proteins for trypsin digestion and native PAGE according to the expression level of the protein of interest in this specific cell type. Moreover, limited detection or weak separation of oligomeric complexes by native PAGE can have several reasons and can be addressed as followed: make sure that the equipment is cleaned to remove remaining denaturing agents, keep all samples and the gel during the PAGE at 4 °C, and do not extend the time between sample preparation and loading onto the gel. Limited protease digestion and native PAGE have also been employed to monitor the activation of another important, closely related PRR, MDA5[40-42]. Monitoring of MDA5 activation required different experimental conditions compared to RIG-I and PKR, and was therefore not included here.

In summary, point-by-point protocols for two useful and sensitive methods to measure activation of RIG-I and PKR are presented. Limited protease digestion and native PAGE, both coupled to Western blot analysis, permit monitoring of conformational changes and oligomerization, respectively. Using these methods, we had previously shown that RIG-I can be activated by nucleocapsids of various viruses directly after their entry into the cells[32].

The exact nature and origin of the RNA species relevant for RIG-I and PKR activation in infected cells are still not entirely solved. Furthermore, many viruses interfere with the functions of PRRs by a wide variety of strategies[12,43-46]. The presented techniques enlarge the spectrum of methods by allowing an easy and direct measurement of RIG-I and PKR activation, are quick to perform, and do not require expensive equipment.

Disclosures

No conflicts of interest declared.

Acknowledgements

We thank Alejandro Brun from CISA-INIA for providing anti-Rift Valley fever Virus sera. Work in our laboratories is supported by Forschungsförderung gem. §2 Abs. 3 Kooperationsvertrag Universitätsklinikum Giessen und Marburg, the Leibniz Graduate School for Emerging viral diseases (EIDIS), the DFG Sonderforschungsbereich (SFB) 1021, and the DFG Schwerpunktprogramm (SPP) 1596.

References

1. Gurtler, C., & Bowie, A. G. Innate immune detection of microbial nucleic acids. *Trends in Microbiology.* **21**, 413-420, doi:10.1016/j.tim.2013.04.004 (2013).
2. Jensen, S., & Thomsen, A. R. Sensing of RNA viruses: a review of innate immune receptors involved in recognizing RNA virus invasion. *Journal of Virology.* **86**, 2900-2910, doi:10.1128/jvi.05738-11 (2012).
3. Kato, H., Takahasi, K., & Fujita, T. RIG-I-like receptors: cytoplasmic sensors for non-self RNA. *Immunological Reviews.* **243**, 91-98, doi:10.1111/j.1600-065X.2011.01052.x (2011).
4. Yoneyama, M. *et al.* The RNA helicase RIG-I has an essential function in double-stranded RNA-induced innate antiviral responses. *Nature Immunology.* **5**, 730-737, doi:10.1038/ni1087 (2004).
5. Andrejeva, J. *et al.* The V proteins of paramyxoviruses bind the IFN-inducible RNA helicase, mda-5, and inhibit its activation of the IFN-beta promoter. *Proceedings of the National Academy of Sciences of the United States of America.* **101**, 17264-17269, doi:10.1073/pnas.0407639101 (2004).
6. Saito, T. *et al.* Regulation of innate antiviral defenses through a shared repressor domain in RIG-I and LGP2. *Proc Natl Acad Sci U S A.* **104**, 582-587 (2007).
7. Ferrage, F. *et al.* Structure and dynamics of the second CARD of human RIG-I provide mechanistic insights into regulation of RIG-I activation. *Structure (London, England : 1993).* **20**, 2048-2061, doi:10.1016/j.str.2012.09.003 (2012).
8. Kolakofsky, D., Kowalinski, E., & Cusack, S. A structure-based model of RIG-I activation. *RNA (New York, N.Y.).* **18**, 2118-2127, doi:10.1261/rna.035949.112 (2012).
9. Luo, D., Kohlway, A., Vela, A., & Pyle, A. M. Visualizing the determinants of viral RNA recognition by innate immune sensor RIG-I. *Structure (London, England : 1993).* **20**, 1983-1988, doi:10.1016/j.str.2012.08.029 (2012).
10. Kowalinski, E. *et al.* Structural basis for the activation of innate immune pattern-recognition receptor RIG-I by viral RNA. *Cell.* **147**, 423-435, doi:10.1016/j.cell.2011.09.039 (2011).

11. Luo, D. *et al.* Structural insights into RNA recognition by RIG-I. *Cell.* **147**, 409-422, doi:10.1016/j.cell.2011.09.023 (2011).
12. Habjan, M. *et al.* Processing of genome 5" termini as a strategy of negative-strand RNA viruses to avoid RIG-I-dependent interferon induction. *PloS One.* **3**, e2032, doi:10.1371/journal.pone.0002032 (2008).
13. Rehwinkel, J., & Reis, E. S. C. Targeting the viral Achilles' heel: recognition of 5'-triphosphate RNA in innate anti-viral defence. *Current Opinion in Microbiology.* **16**, 485-492, doi:10.1016/j.mib.2013.04.009 (2013).
14. Pichlmair, A. *et al.* RIG-I-mediated antiviral responses to single-stranded RNA bearing 5'-phosphates. *Science (New York, N.Y.)* **314**, 997-1001, doi:10.1126/science.1132998 (2006).
15. Hornung, V. *et al.* 5'-Triphosphate RNA is the ligand for RIG-I. *Science (New York, N.Y.)* **314**, 994-997, doi:10.1126/science.1132505 (2006).
16. Saito, T., & Gale, M., Jr. Differential recognition of double-stranded RNA by RIG-I-like receptors in antiviral immunity. *The Journal of Experimental Medicine.* **205**, 1523-1527, doi:10.1084/jem.20081210 (2008).
17. Takahasi, K. *et al.* Nonself RNA-sensing mechanism of RIG-I helicase and activation of antiviral immune responses. *Mol Cell.* **29**, 428-440 (2008).
18. Binder, M. *et al.* Molecular mechanism of signal perception and integration by the innate immune sensor retinoic acid-inducible gene-I (RIG-I). *J Biol Chem.* **286**, 27278-27287, doi:10.1074/jbc.M111.256974 (2011).
19. Jiang, X. *et al.* Ubiquitin-induced oligomerization of the RNA sensors RIG-I and MDA5 activates antiviral innate immune response. *Immunity.* **36**, 959-973, doi:10.1016/j.immuni.2012.03.022 (2012).
20. Civril, F. *et al.* The RIG-I ATPase domain structure reveals insights into ATP-dependent antiviral signalling. *EMBO reports.* **12**, 1127-1134, doi:10.1038/embor.2011.190 (2011).
21. Hiscott, J. Triggering the innate antiviral response through IRF-3 activation. *The Journal of Biological Chemistry.* **282**, 15325-15329, doi:10.1074/jbc.R700002200 (2007).
22. Hertzog, P. J., & Williams, B. R. Fine tuning type I interferon responses. *Cytokin., & Growth Factor Reviews.* **24**, 217-225, doi:10.1016/j.cytogfr.2013.04.002 (2013).
23. Pindel, A., & Sadler, A. The role of protein kinase R in the interferon response. *Journal of Interfero., & Cytokine Research : the Official Journal of the International Society for Interferon and Cytokine Research.* **31**, 59-70, doi:10.1089/jir.2010.0099 (2011).
24. Donnelly, N., Gorman, A. M., Gupta, S., & Samali, A. The eIF2alpha kinases: their structures and functions. *Cellular and Molecular Life Sciences : CMLS.* **70**, 3493-3511, doi:10.1007/s00018-012-1252-6 (2013).
25. Cole, J. L. Activation of PKR: an open and shut case? *Trends in Biochemical Sciences.* **32**, 57-62, doi:10.1016/j.tibs.2006.12.003 (2007).
26. Dauber, B., & Wolff, T. Activation of the Antiviral Kinase PKR and Viral Countermeasures. *Viruses.* **1**, 523-544, doi:10.3390/v1030523 (2009).
27. Dey, M. *et al.* Mechanistic link between PKR dimerization, autophosphorylation, and eIF2alpha substrate recognition. *Cell.* **122**, 901-913, doi:10.1016/j.cell.2005.06.041 (2005).
28. Gack, M. U. *et al.* TRIM25 RING-finger E3 ubiquitin ligase is essential for RIG-I-mediated antiviral activity. *Nature.* **446**, 916-920, doi:10.1038/nature05732 (2007).
29. Zeng, W. *et al.* Reconstitution of the RIG-I pathway reveals a signaling role of unanchored polyubiquitin chains in innate immunity. *Cell.* **141**, 315-330, doi:10.1016/j.cell.2010.03.029 (2010).
30. Anderson, E., & Cole, J. L. Domain stabilities in protein kinase R (PKR): evidence for weak interdomain interactions. *Biochemistry.* **47**, 4887-4897, doi:10.1021/bi702211j (2008).
31. Habjan, M. *et al.* NSs protein of rift valley fever virus induces the specific degradation of the double-stranded RNA-dependent protein kinase. *Journal of Virology.* **83**, 4365-4375, doi:10.1128/jvi.02148-08 (2009).
32. Weber, M. *et al.* Incoming RNA virus nucleocapsids containing a 5'-triphosphorylated genome activate RIG-I and antiviral signaling. *Cell Hos., & Microbe.* **13**, 336-346, doi:10.1016/j.chom.2013.01.012 (2013).
33. Bradford, M. M. A rapid and sensitive method for the quantitation of microgram quantities of protein utilizing the principle of protein-dye binding. *Analytical Biochemistry.* **72**, 248-254 (1976).
34. Wittig, I., & Schagger, H. Advantages and limitations of clear-native PAGE. *Proteomics.* **5**, 4338-4346, doi:10.1002/pmic.200500081 (2005).
35. Muller, R. *et al.* Characterization of clone 13, a naturally attenuated avirulent isolate of Rift Valley fever virus, which is altered in the small segment. *Am J Trop Med Hyg.* **53**, 405-411 (1995).
36. Bouloy, M. *et al.* Genetic evidence for an interferon-antagonistic function of rift valley fever virus nonstructural protein NSs. *Journal of Virology.* **75**, 1371-1377, doi:10.1128/jvi.75.3.1371-1377.2001 (2001).
37. Ikegami, T. *et al.* Rift Valley fever virus NSs protein promotes post-transcriptional downregulation of protein kinase PKR and inhibits eIF2alpha phosphorylation. *PLoS Pathogens.* **5**, e1000287, doi:10.1371/journal.ppat.1000287 (2009).
38. Iwamura, T. *et al.* Induction of IRF-3/-7 kinase and NF-kappaB in response to double-stranded RNA and virus infection: common and unique pathways. *Genes to Cells : Devoted to Molecula., & Cellular Mechanisms.* **6**, 375-388 (2001).
39. Yoneyama, M., Suhara, W., & Fujita, T. Control of IRF-3 activation by phosphorylation. *Journal of Interfero., & Cytokine Research : the Official Journal of the International Society for Interferon and Cytokine Research.* **22**, 73-76, doi:10.1089/107999002753452674 (2002).
40. Bamming, D., & Horvath, C. M. Regulation of signal transduction by enzymatically inactive antiviral RNA helicase proteins MDA5, RIG-I, and LGP2. *The Journal of Biological Chemistry.* **284**, 9700-9712, doi:10.1074/jbc.M807365200 (2009).
41. Wu, B. *et al.* Structural basis for dsRNA recognition, filament formation, and antiviral signal activation by MDA5. *Cell.* **152**, 276-289, doi:10.1016/j.cell.2012.11.048 (2013).
42. Berke, I. C., & Modis, Y. MDA5 cooperatively forms dimers and ATP-sensitive filaments upon binding double-stranded RNA. *The EMBO Journal.* **31**, 1714-1726, doi:10.1038/emboj.2012.19 (2012).
43. Garcia-Sastre, A. Induction and evasion of type I interferon responses by influenza viruses. *Virus Research.* **162**, 12-18, doi:10.1016/j.virusres.2011.10.017 (2011).
44. Taylor, K. E., & Mossman, K. L. Recent advances in understanding viral evasion of type I interferon. *Immunology.* **138**, 190-197, doi:10.1111/imm.12038 (2013).
45. Goodbourn, S., & Randall, R. E. The regulation of type I interferon production by paramyxoviruses. *Journal of Interfero., & Cytokine Research : the Official Journal of the International Society for Interferon and Cytokine Research.* **29**, 539-547, doi:10.1089/jir.2009.0071 (2009).
46. Versteeg, G. A., & Garcia-Sastre, A. Viral tricks to grid-lock the type I interferon system. *Current Opinion in Microbiology.* **13**, 508-516, doi:10.1016/j.mib.2010.05.009 (2010).

4.2. Incoming RNA virus nucleocapsids containing a 5'-triphosphorylated genome activate RIG-I and antiviral signaling

Own contribution:

I performed experiments of Fig. 2B, Fig. 3, Fig. 4, Fig. 5 (whereas RIG-I constructs were cloned by Anna Mareike Schmidt), Fig. 6 and Fig. 7 and Suppl. Fig. 1, Suppl. Fig. 2H, Suppl. Fig. 3A-G, Suppl. Fig. 4, Suppl. Fig. 5 and Suppl. Fig. 6. I contributed to writing of the manuscript.

Michaela Gerlach

Cell Host & Microbe
Article

Incoming RNA Virus Nucleocapsids Containing a 5′-Triphosphorylated Genome Activate RIG-I and Antiviral Signaling

Michaela Weber,[1] Ali Gawanbacht,[3] Matthias Habjan,[3] Andreas Rang,[4] Christoph Borner,[5,6] Anna Mareike Schmidt,[3,6,10] Sophie Veitinger,[2] Ralf Jacob,[2] Stéphanie Devignot,[1] Georg Kochs,[3] Adolfo García-Sastre,[7,8,9] and Friedemann Weber[1,3,6,*]

[1]Institute for Virology
[2]Department of Cell Biology and Cell Pathology
Philipps-University Marburg, 35043 Marburg, Germany
[3]Department of Virology, University Freiburg, Hermann-Herder-Strasse 11, 79008 Freiburg, Germany
[4]Institute of Virology, Helmut-Ruska-Haus, University Hospital Charité, Charité Campus Mitte, 10117 Berlin, Germany
[5]Institute of Molecular Medicine, Stefan-Meier-Strasse 17, 79104 Freiburg, Germany
[6]Centre for Biological Signalling Studies (BIOSS), Albert-Ludwigs University, 79104 Freiburg, Germany
[7]Department of Microbiology
[8]Department of Medicine, Division of Infectious Diseases
[9]Global Health and Emerging Pathogens Institute
Mount Sinai School of Medicine, New York, NY 10029, USA
[10]Present address: Institute of Molecular Systems Biology, ETH Zurich, 8093 Zurich, Switzerland
*Correspondence: friedemann.weber@staff.uni-marburg.de
http://dx.doi.org/10.1016/j.chom.2013.01.012

SUMMARY

Host defense to RNA viruses depends on rapid intracellular recognition of viral RNA by two cytoplasmic RNA helicases: RIG-I and MDA5. RNA transfection experiments indicate that RIG-I responds to naked double-stranded RNAs (dsRNAs) with a triphosphorylated 5′ (5′ppp) terminus. However, the identity of the RIG-I stimulating viral structures in an authentic infection context remains unresolved. We show that incoming viral nucleocapsids containing a 5′ppp dsRNA "panhandle" structure trigger antiviral signaling that commences with RIG-I, is mediated through the adaptor protein MAVS, and terminates with transcription factor IRF-3. Independent of mammalian cofactors or viral polymerase activity, RIG-I bound to viral nucleocapsids, underwent a conformational switch, and homo-oligomerized. Enzymatic probing and superresolution microscopy suggest that RIG-I interacts with the panhandle structure of the viral nucleocapsids. These results define cytoplasmic entry of nucleocapsids as the proximal RIG-I-sensitive step during infection and establish viral nucleocapsids with a 5′ppp dsRNA panhandle as a RIG-I activator.

INTRODUCTION

Host defenses to RNA viruses are dependent on rapid detection by pathogen recognition receptors (PRRs). Intracellular recognition of virus infection is mediated by two cytoplasmic RNA helicases: RIG-I and MDA5 (termed RIG-like receptors, RLRs) (Kato et al., 2011). The binding of an RNA ligand to these PRRs leads to phosphorylation and dimerization of interferon regulated factor 3 (IRF-3), which subsequently activates genes for type I interferons (IFN-α/β) (Hiscott, 2007). These cytokines trigger the expression of IFN-stimulated gene (ISG) products that have antiviral and immunomodulatory activities (Randall and Goodbourn, 2008).

The infection cycle of RNA viruses consists of the phases attachment, entry, messenger RNA (mRNA) transcription, genome replication, assembly, and exit. Negative-strand RNA viruses carry an RNA-dependent RNA polymerase (RdRp) within their particles and immediately start transcribing their genome after entering the cell. The protein products of this so-called primary transcription then drive the replication of the genome via a positive-sense intermediate. Positive-strand RNA viruses do not carry an RdRp in their particles and directly translate their genome after entry. The newly synthesized RdRp then produces a negative-sense intermediate, mRNA, and progeny genome. Usually, the genome of both negative- and positive-strand RNA viruses is packaged by a viral nucleocapsid protein (often called N).

Most studies on activation of RLRs were based either on infection with RNA viruses undergoing a full replication cycle or on transfection of cells with naked viral or synthetic RNAs. The infection experiments established that RIG-I and MDA5 recognize mostly nonoverlapping subsets of viruses (McCartney and Colonna, 2009). The RNA transfection experiments revealed that RIG-I responds to long double-stranded RNA (dsRNA) molecules, short dsRNAs with a triphosphorylated 5′ (5′ppp) terminus, and poly-U/UC-rich sequences, whereas MDA5 activation is more dependent on branched dsRNA structures (Binder et al., 2011; Hornung et al., 2006; Kato et al., 2008; Pichlmair et al., 2006, 2009; Saito et al., 2008; Schlee et al., 2009; Schmidt et al., 2009). Despite these achievements, the question

of the natural RLR ligands (i.e., which viral structures are stimulating the RLRs in the authentic infection context) is largely unsolved. Two recent RNA fractionation studies showed that full-length and shortened RNAs arising during genome replication of 5′ppp-RNA viruses are natural stimulators of RIG-I (Baum et al., 2010; Rehwinkel et al., 2010). However, it remained open whether these RIG-I ligands were naked RNA side products of viral genome replication or whether RIG-I could also recognize nucleoprotein-encapsidated RNA, the main viral structure in the infected cell. Our study presented here addresses this problem and indicates that RIG-I is capable of reacting to incoming, encapsidated RNA virus genomes. This immediate early IFN response requires the viral 5′ppp dsRNA "panhandle" structure but is independent of viral RNA synthesis. RIG-I thereby directly interacts with the panhandle on the viral nucleocapsids, switches conformation, oligomerizes, and triggers the activation of IRF-3.

RESULTS

Our first aim was to identify the earliest infection step that triggers IFN induction. In the hope of drawing conclusions on the responsible viral determinant, we employed a set of RNA viruses with different genomic features. Dependent on the particular virus, a block of viral mRNA translation by cycloheximide (CHX) has different effects on primary transcription and genome replication (Table S1 available online).

Entry of Negative-Sense RNA Viruses Can Activate IFN Induction in the Absence of Replication

Influenza A virus (FLUAV) and vesicular stomatitis virus (VSV) are negative-strand RNA viruses. Application of CHX allows particle attachment, entry of nucleocapsids, and primary transcription, but not genome replication (Figure S1). We measured the virus-inducible genes for IFN-β and ISG56 in human A549 cells by real-time RT-PCR. Figure 1A shows that both FLUAV and VSV are strongly activating these genes, even when CHX was applied. Thus, an IFN response can occur before the viruses start replicating their genome.

To narrow down the IFN-relevant infection step, we repeated the experiment using Rift Valley fever virus (RVFV) and La Crosse virus (LACV). These bunyaviruses are peculiar in that their transcription depends on concurrent translation (Raju et al., 1989). CHX treatment arrests viral primary transcription at a very early step, but had only a minor influence on *IFN-β* and *ISG56* induction (Figure 1B). Apparently, not even a fully operating primary transcription is required for triggering an IFN response.

Recent reports suggested that particle attachment or membrane fusion can activate an antiviral response (Holm et al., 2012; Noyce et al., 2011), although other groups did not observe this in their systems (Handke et al., 2009; Spiropoulou et al., 2007; Stoltz and Klingström, 2010). We employed several methods to study the involvement of particle attachment. First, we pretreated cells with NH_4Cl, an agent that inhibits bunyaviral entry into the cytoplasm (Filone et al., 2006) but does not impede the IFN response (Figure S2A). As shown in Figure 1C, NH_4Cl almost entirely abrogated the host response to RVFV. Similarly, three other bunyavirus entry inhibitors (de Boer et al., 2012) (Figure S2B–S2D), as well as virus inactivation by β-propiolactone

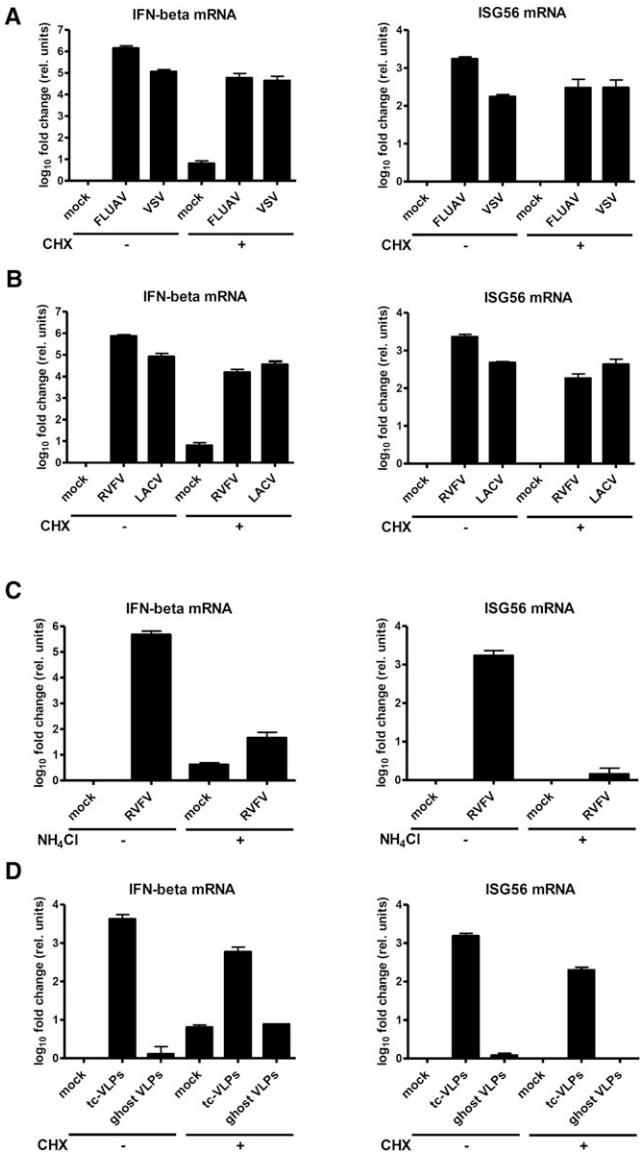

Figure 1. IFN Response to Incoming Negative-Strand RNA Viruses

(A–D) Cells were treated with inhibitors, infected, incubated for 24 hr, and then assayed for mRNA levels of IFN-β (left panels) and ISG56 (right panels) using real-time RT-PCR. Here and in all following figures, mean values and SDs from three independent experiments are shown. (A and B) IFN response in the absence of viral genome replication. Cells were treated for 1 hr with 0 or 50 μg/ml CHX and then infected either with FLUAVΔNS1 (FLUAV) and VSV (A) or with RVFVΔNSs::GFP (RVFV) and LACVdelNSs (LACV) (B). (C and D) Requirement for virus entry. (C) Cells were treated for 1 hr with 0 or 50 mM NH_4Cl and then infected with RVFVΔNSs::GFP. (D) Infection with different types of VLPs. Cells were CHX treated and infected with tc-VLPs or the equivalent amount of ghost VLPs. See also Figures S1–S2H.

(Figure S2E) or UV irradiation (Figure S2F), all led to a reduction of IFN induction. In a complementary approach, we employed two types of virus-like particles (VLPs) of RVFV. Complete VLPs contain nucleocapsids with a reporter minigenome, whereas "ghost" VLPs have just the N protein inside (Figure S2G). The complete VLPs, also called transcriptionally competent (tc-) VLPs (Hoenen et al., 2011), are capable of

primary transcription, but not of replication (Habjan et al., 2009a). tc-VLPs triggered *IFN-β* and *ISG56* expression, even under CHX (Figure 1D). Ghost VLPs, however, did not elicit any IFN response, although they bind equally well to the cells (Figure S2H). These data indicate that, in our system, virus entry or primary transcription is necessary and sufficient for IFN induction.

The Immediate Early IFN Response Requires Viral 5′Triphosphate RNA and RIG-I

All viruses used so far contained the RIG-I-activating 5′ppp group on their RNA genome (Habjan et al., 2008a; Hornung et al., 2006; Pichlmair et al., 2006). To clarify the contribution of the genome end, we employed two RNA viruses that lack this feature (see Table S1). Prospect Hill virus (PHV; family *Bunyaviridae*) has a monophosphate at the 5′ end (Garcin et al., 1995; Habjan et al., 2008a). Semliki Forest virus (SFV; family *Togaviridae*) has a 5′ cap structure (McInerney et al., 2005). CHX inhibits PHV in the same way as the related RVFV or LACV (Figure S1). SFV is a positive-strand RNA virus (i.e., its genome is directly translated after entry). In the absence of CHX, PHV minimally activated the *IFN-β* promoter and moderately activated *ISG56* transcription, as expected (Prescott et al., 2005), whereas the IFN response to SFV was similar to LACV (Figure 2A). Strikingly, application of CHX completely abrogated the IFN response to both PHV and SFV. In line with this, the transcription factor IRF-3 was activated under CHX-restricted infection with VSV or LACV, but not PHV or SFV (Figure S3A–S3F). Thus, IFN responses to incoming RNA virus nucleocapsids occur only if the genome contains a 5′ppp.

To pin down the responsible RLR, we evaluated the influence of specific knockdowns. Cells were transfected with small interfering RNAs (siRNAs) for *MDA5*, *RIG-I*, or a control (Figure S3G), treated with CHX, and infected with VSV or LACV. Knockdown of *RIG-I*, but not of *MDA5*, impaired IFN induction by VSV and LACV nucleocapsids (Figure 2B). To bolster these findings, we utilized mouse embryo fibroblasts (MEFs) deficient in *RIG-I* or *MDA5*. Because these cells were extremely sensitive to CHX (data not shown), we employed tc-VLPs as a virus system halted at the stage of primary transcription. MEFs lacking *MDA5* displayed similar host responses to tc-VLPs as WT MEFs (Figure 2C). MEFs lacking *RIG-I*, by contrast, completely lost their ability to respond (Figure 2D). Knockout of *MAVS* (Seth et al., 2005), the adaptor common to MDA5 and RIG-I, had a similar impact (Figure S3H). Taken together, these data suggest that nucleocapsids of 5′ppp RNA viruses activate an IFN response via the RIG-I-MAVS signaling cascade.

Activation of RIG-I

Binding of a target RNA to RIG-I triggers a conformational switch (Saito et al., 2007; Takahasi et al., 2008) and oligomerization (Binder et al., 2011; Saito et al., 2007). The conformational switch is indicated by partial resistance to trypsin digestion. We observed that the full infection cycle of SFV, VSV, and LACV leads to the emergence of trypsin-resistant fragments of RIG-I (Figure 3A). When cells had been pretreated with CHX, VSV and LACV still triggered the conformational switch of RIG-I, whereas SFV infection had no effect (Figure 3B). The oligomerization of RIG-I was assayed by native PAGE. In uninfected cells,

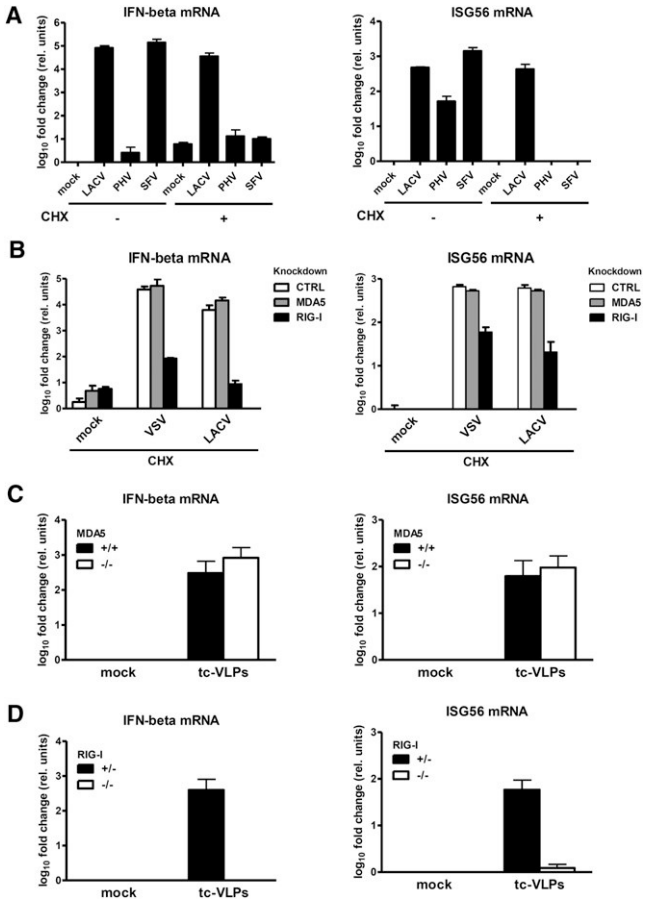

Figure 2. Influence of the Viral 5′ppp Group and of RIG-I

(A) Cells were CHX treated; infected with LACVdelNSs, PHV, or SFV; and assayed as described in Figure 1.

(B) Innate response to VSV or LACVdelNSs by cells treated with CHX and with siRNAs targeting MDA5 or RIG-I.

(C and D) MEFs lacking MDA5 (C) or RIG-I (D), and the corresponding WT MEFs, were tested for their innate response to tc-VLPs. See also Figures S3A–S3H.

only monomers of RIG-I were detected (Figure 3C). Curiously, also in SFV-infected cells only monomeric RIG-I is present (Figure 3D), although RIG-I switches conformation (see Figure 3A). For the 5′ppp RNA viruses VSV and LACV, both the full and the CHX-aborted replication cycle resulted in RIG-I oligomerization (Figures 3E and 3F). The 5′-monophosphorylated PHV, by contrast, only weakly activated the conformational switch (Figure 3G) and not the oligomerization (Figure 3H). Taken together, these results suggest that RIG-I is rapidly and strongly activated by viral nucleocapsids in the absence of genome replication, provided the genome is carrying a 5′ppp group.

Interaction between RIG-I and Incoming Nucleocapsids

We wondered whether RIG-I could form a complex with viral 5′ppp RNA nucleocapsids. As an experimental system, we chose the setup closest to the immediate early phase (arrested primary transcription), namely infection with bunyaviruses such as LACV under CHX treatment. The N protein thereby served as a marker for viral nucleocapsids. Using confocal immunofluorescence

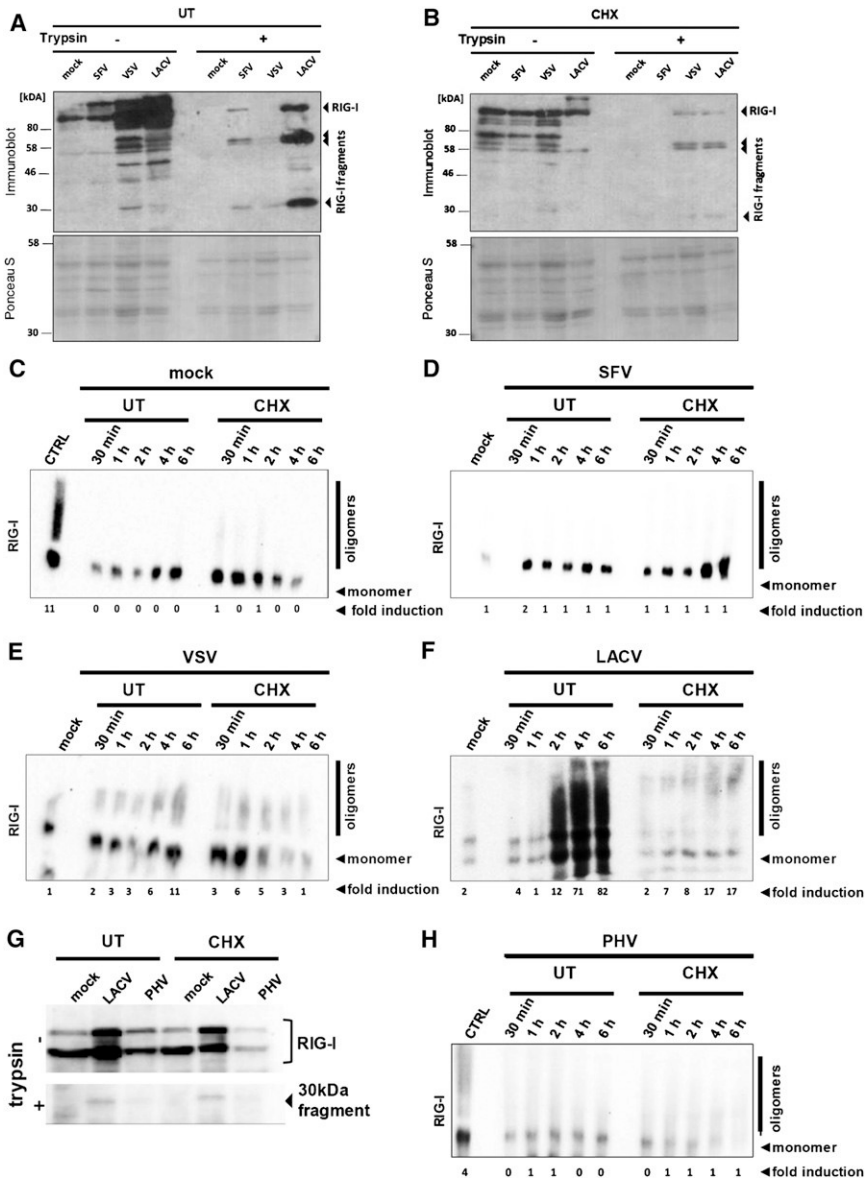

Figure 3. Activation of RIG-I

(A and B) Conformational switch. A549 cells were treated with 0 (A) or 50 μg/ml CHX (B), infected with the indicated viruses, and lysed 6 hr later. Cell extracts were subjected to limited trypsin digestion (right panels) or left untreated (left panels). Upper panels show western blot analysis with an anti-RIG-I antibody, and lower panels show Ponceau S staining as loading control.

(C–F) Oligomerization. A549 cells were left untreated (UT) or treated with 50 μg/ml CHX. Then, cells were either mock infected (C) or infected with SFV (D), VSV (E), or LACVdelNSs (F). At the indicated time points, RIG-I was analyzed by native PAGE and western blotting. As positive and negative controls, VSV-infected cells at 6 hr postinfection (CTRL) and mock-infected cells, respectively, were used.

(G and H) PHV and RIG-I. A549 cells infected with LACVdelNSs or PHV were monitored for the RIG-I conformation at 6 hr postinfection (G) or for RIG-I oligomerization over a time course (H). The ratio of oligomers to monomers (normalized to the actin signal and in relation to mock cells) is indicated below the blots (fold induction).

microscopy, we detected the nucleocapsids of incoming LACV particles as individual dots in the cytoplasm (Figure 4A). These LACV N dots colocalize with RIG-I (Figure S4A), as indicated by overlay pictures and intensity profiles of the fluorescence signals. Quantitative analysis revealed that LACV nucleocapsids colocalize with RIG-I in 51% of the cases but with the cytoplasmic control protein glyceraldehyde-3-phosphate dehydrogenase (GAPDH) in 33% of the cases (data not shown). N/RIG-I colocalization was also observed in cells undergoing a full replication cycle (data not shown), in agreement with observations on FLUAV (Onomoto et al., 2012). The incoming LACV nucleocapsids also colocalized with peroxisomes (Figure S4B), cytoplasmic organelles involved in immediate early activation of RIG-I (Dixit et al., 2010). Coimmunoprecipitation demonstrated that RIG-I was capable of binding the incoming LACV nucleocapsids (Figure 4B). The same RIG-I/LACV nucleocapsid interaction was observed when a full replication cycle was allowed, whereas MDA5 did not interact under any condition (data not shown). Overexpressed N protein, by contrast, could not be precipitated via RIG-I (Figure S4C). We performed similar experiments with RVFV. Again, incoming nucleocapsids triggered the conformational switch and oligomerization of RIG-I and activated IRF-3 (Figure S4D). Moreover, the nucleocapsids of RVFV colocalized (Figure S4E) and coprecipitated with RIG-I (Figure S4F). Strikingly, incoming nucleocapsids could be forced into a high-molecular-weight RIG-I complex. The ATP analog ADP•AlF_3 traps RIG-I in an RNA-bound closed conformation unable to cycle between the different states (Kowalinski et al., 2011). When CHX-treated and infected cells were incubated with ADP•AlF_3, the oligomers of RIG-I shifted from a smear into a single high-molecular-weight band (Figure 4C, upper panels). Probing of the lysates for the viral N protein revealed a similar shift from an oligomeric state to a high-molecular-weight complex (Figure 4C, lower panels). This was true for LACV as well as for RVFV, indicating a general phenomenon. Together, these findings demonstrate that RIG-I is able to associate with nucleocapsids of 5′ppp RNA viruses directly after entry into the cell, leading to RIG-I activation and innate immune signaling.

Nucleocapsid Binding and Activation of RIG-I Are Independent of Mammalian Cofactors

The RIG-I/nucleocapsid interaction could either be direct or mediated by one of the cellular cofactors of RIG-I (Kato et al., 2011; Kok et al., 2011; Miyashita et al., 2011). To distinguish between these possibilities, we employed an insect cell system.

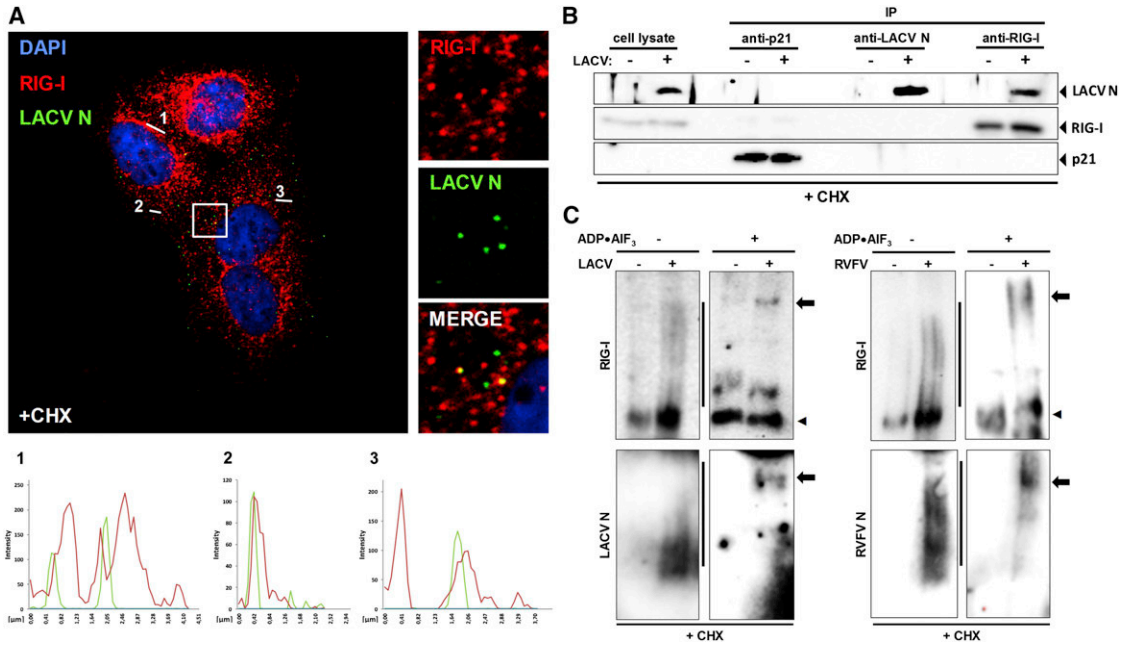

Figure 4. Interaction of RIG-I with LACV Nucleocapsids

(A) Colocalization analysis. CHX-treated A549 cells were infected with LACVdelNSs and analyzed 5 hr later by double immunofluorescence using antisera against LACV N (green channel) or RIG-I (red channel). Cell nuclei were counterstained with DAPI (blue channel). The square area of the inset is digitally magnified on the right hand side. Three fluorescence intensity profiles are shown on the bottom.

(B) Coimmunoprecipitation. CHX-treated A549 cells were infected with LACVdelNSs (moi 10), lysed 5 hr later, and subjected to IP and western blot analysis using antibodies against p21 (negative control), LACV N, and RIG-I. As input control, 10% of the cell lysate were analyzed in parallel (left lanes).

(C) ADP-aluminum fluoride trapping. CHX-treated A549 cells were infected with LACVdelNSs (left panels) or RVFVΔNSs::REN (right panels). At 5 hr postinfection, lysates were incubated with ADP•AlF_3 and analyzed by native PAGE and western blot using antibodies against RIG-I (upper panels) or viral N (lower panels). Lines indicate oligomers, arrowheads monomers, and arrows point toward high-molecular-weight complexes. See also Figures S4A–S4F.

Drosophila melanogaster cells are a useful tool to reconstitute mammalian signaling complexes in a background-free setting (Yang and Reth, 2012) and are infectable with RVFV (Kortekaas et al., 2011). When human *RIG-I* was expressed in *Drosophila* D.mel-2 cells, conformational switching and oligomerization were observed after infection with RVFV (Figures 5A and 5B). RIG-I was also activated in vitro by mixing of lysates from RIG-I-transfected D.mel-2 cells with lysates of infected D.mel-2 cells (Figure 5C). Coimmunoprecipitation experiments demonstrated binding of RIG-I to viral nucleocapsids in the *Drosophila* system (Figure 5D). Again, this nucleocapsid interaction was independent of whether RIG-I contacted RVFV during authentic virus infection or whether lysates containing either RIG-I or RVFV nucleocapsids were mixed in vitro. Thus, activation and nucleocapsid interaction of RIG-I occur in a direct manner and without the contribution of a mammalian cofactor.

Nucleocapsid-Borne 5′ppp-dsRNA Is Necessary and Sufficient for RIG-I Activation

Our experiments with bunyaviruses and CHX implicated that the transcriptional activity of nucleocapsids may not be relevant for RIG-I activation. However, CHX still allows some abortive transcription (Raju et al., 1989). To clarify whether RIG-I requires this residual RNA synthesis, we performed several experiments. First, we depleted the cellular NTP pool with the compounds Brequinar (BRQ; inhibits pyrimidine synthesis), mycophenolic acid (MA; reduces GTP levels), pyrazofurin (PYF; reduces CTP and UTP levels), or cyclopentenylcytosine (CPEC; depletes the CTP pool) (Linke et al., 1996; Qing et al., 2010). Each of these inhibitors affected viral RNA synthesis (Figure S5A). Nonetheless, even when combined with CHX, neither inhibitor diminished RIG-I activation by LACV (Figure 6A). In fact, some of the compounds slightly increased RIG-I activation and enhanced the activation of IRF-3 (Figure 6A). Second, we depleted *Drosophila* D.Mel-2 cell lysates containing either RIG-I or nucleocapsids from NTPs by dialysis. When these dialyzed lysates were mixed with each other, the conformational switch of RIG-I still occurred and was enhanced by adding back ATP (Figure 6B). Third, we employed nucleocapsids that had been isolated from purified virus particles. Dialyzed RIG-I-containing D.Mel-2 extracts were incubated with nucleocapsids of RVFV or LACV. The nucleocapsids clearly induced the conformational switch of RIG-I in vitro (Figure 6C). We conclude from these experiments that viral transcription is not necessary for triggering RIG-I. As outlined above, the genomic RNA of bunyaviruses forms a panhandle structure that has remarkable similarity with the optimal 5′ppp dsRNA ligand identified by transfection and in vitro binding experiments (Figure S5B). Indeed, destroying the dsRNA structures with RNase III or cleaving the triphosphates with a phosphatase abolished the ability of viral nucleocapsids to activate RIG-I (Figures 6D and 6E). Treatment with the single-stranded RNA-specific RNase A, by contrast, had no effect. Thus, a 5′ppp dsRNA structure is indeed necessary for the activation of RIG-I by nucleocapsids.

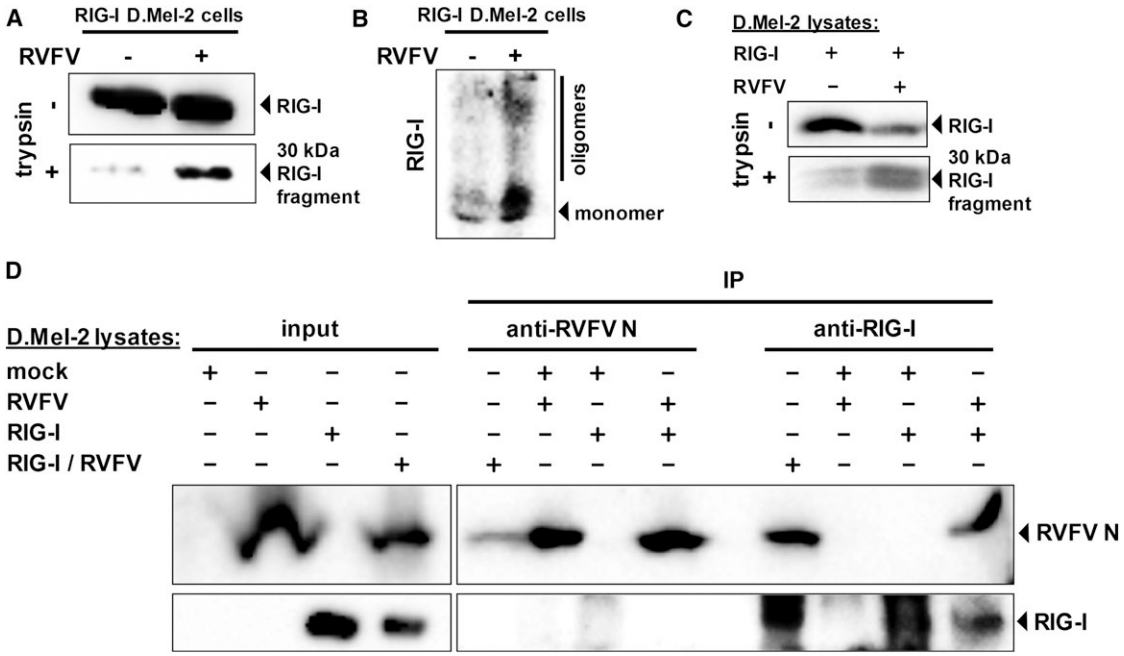

Figure 5. Activation of RIG-I and Binding to Viral Nucleocapsids in Insect Cells

(A and B) D.Mel-2 cells expressing human *RIG-I* were infected for 72 hr with RVFVΔNSs::REN (RVFV) and then tested for RIG-I conformation (A) and oligomerization (B).

(C) In vitro activation of RIG-I. Lysates of RIG-I-expressing D.Mel-2 cells were mixed with lysates of naive or RVFVΔNSs::REN-infected D.Mel-2 cells and assayed for RIG-I conformation.

(D) Coimmunoprecipitation. D.Mel-2 cells were either left naive (mock), or only infected with RVFVΔNSs::REN (RVFV), only expressing *RIG-I* (RIG-I), or were both expressing *RIG-I* and superinfected with RVFVΔNSs::REN (RIG-I / RVFV). Combinations of lysates were subjected to IP and western blot analysis using antibodies against RVFV N or RIG-I. As input control, 10% of the cell lysate were analyzed in parallel (left lanes).

A Single Site on the Nucleocapsids Is Contacted by RIG-I

We employed ground state depletion (GSD) microscopy to visualize the RIG-I/LACV nucleocapsid complex at 20 nm resolution. This technique allows the display of individual nucleocapsids in their characteristic pseudocircular shape (Figure 7, green channel), which is caused by the dsRNA panhandle formation between the 5′ and 3′ genome ends (Obijeski et al., 1976). Strikingly, accumulations of RIG-I are contacting nucleocapsids at a single site, lending the cocomplexes a "diamond ring"-like appearance (Figure 7, red channel). The negative control GAPDH, by contrast, appeared to be more distant and not accumulated at the nucleocapsids (Figure S6). These observations add additional weight to our hypothesis that RIG-I binds the nucleocapsids via the terminal 5′ppp dsRNA panhandle.

DISCUSSION

The aim of our study was to clarify whether RIG-I is capable of recognizing the RNA contained within incoming viral nucleocapsids. Our results indicate that this is indeed the case. RIG-I was rapidly activated by viruses with the prototypical 5′ppp dsRNA panhandle structure, even when viral RNA synthesis was abolished. Moreover, we detected a direct, single-site interaction between RIG-I and nucleocapsids that was dependent on 5′ppp dsRNA. Thus, viral nucleocapsids containing a 5′ppp panhandle represent a pathogen-associated molecular pattern (PAMP) for RIG-I. These findings advance the proximal RIG-I-sensitive step of the viral infection cycle from the late stage of genome replication (Baum et al., 2010; Rehwinkel et al., 2010) to the immediate early step of nucleocapsids entering the cytoplasm.

Erroneous, nonencapsidated replication products appear during infection with FLUAV (Vreede et al., 2004). It is quite likely that such naked replication products (Rehwinkel et al., 2010; Vreede et al., 2004), along with defective interfering RNAs (Baum et al., 2010; Killip et al., 2011; Strahle et al., 2006) and newly formed nucleocapsids (this study), are responsible for RIG-I induction under a full viral multiplication cycle. Previous reports already demonstrated that genome replication is not an absolute requirement for IFN induction (Killip et al., 2012; Marcus and Sekellick, 1980) and that transfected nucleocapsids of the 5′ppp viruses measles and VSV can activate IRF-3 even if they are transcriptionally inactive (tenOever et al., 2002, 2004). None of these studies, however, had addressed the involvement of RIG-I or the requirement for a specific 5′ genome end. Our work extends their conclusions by showing that incoming viral nucleocapsids can directly activate RIG-I, thus triggering a rapid innate immune response.

It remains to be shown how RIG-I manages to access the encapsidated viral RNA. Although the dsRNA-panhandle structure is covered by the viral polymerase (Resa-Infante et al., 2011), some cytoplasmic exposure is necessary (e.g., to initiate mRNA transcription). The global presence of RIG-I in the

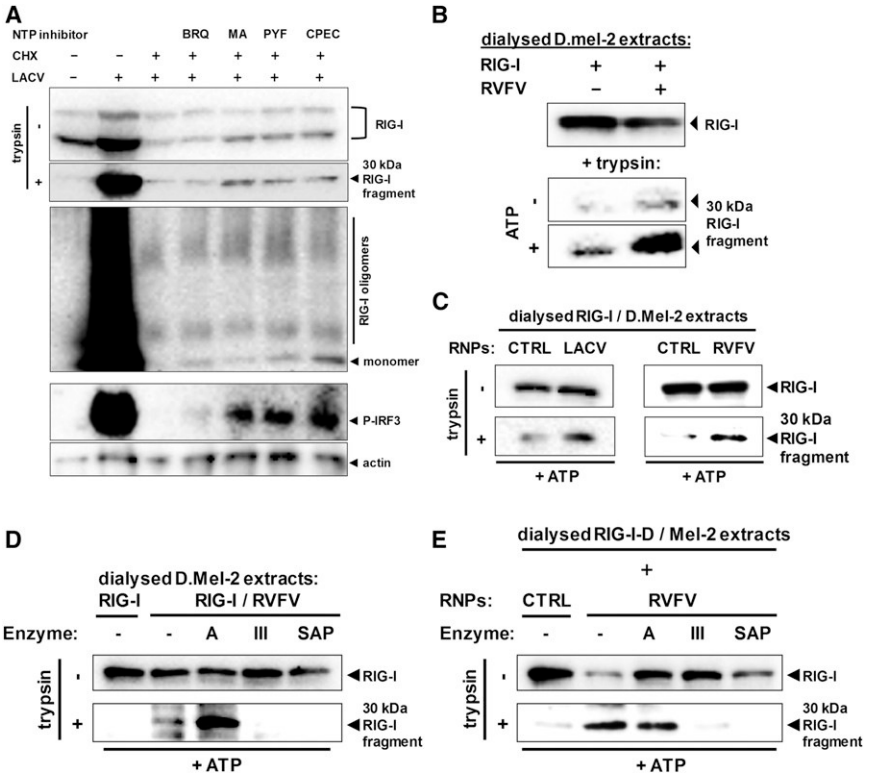

Figure 6. Activation of RIG-I Solely Depends on the Nucleocapsid-Borne Panhandle Structure

(A) Effect of NTP withdrawal on activation of RIG-I and IRF-3. Pretreated A549 cells were infected with LACVdelNSs for 5 hr. Pretreatment with CHX (50 μg/ml) was for 1 hr and with BRQ (10 μM, stocks dissolved in DMSO), MA (10 μM, stocks dissolved in methanol), PYF (10 μM, stocks dissolved in DMSO), or CPEC (5 μM, stocks dissolved in DMSO) for 24 hr. RIG-I conformation (upper two panels), RIG-I oligomerization (upper middle panel), and IRF-3 phosphorylation (lower middle panel) were monitored. Immunoblot for actin served as loading control.

(B) RIG-I activation in dialyzed samples. Lysates from D.Mel-2 cells expressing *RIG-I* (RIG-I) or infected with RVFVΔNSs::REN (RVFV) were dialyzed against PBS, mixed with each other, and incubated with or without ATP. After 1 hr incubation, mixes were subjected to the RIG-I conformational switch assay.

(C) RIG-I activation by purified viral nucleocapsids (RNPs). Lysates from D.Mel-2 cells expressing *RIG-I* were dialyzed against PBS and mixed with purified nucleocapsids from particles of LACV (left panels) or RVFV (right panels). Incubation with ATP and conformational switch assay were performed as described for (B). Equivalent fractions of gradient-purified supernatants from mock-infected cells were used as negative control (CTRL).

(D and E) Structural requirements for viral nucleocapsids to activate RIG-I. Lysates from RVFV-infected D.Mel-2 cells (D) or purified RVFV nucleocapsids (E) were incubated with ATP and one of the indicated enzymes, namely RNase A (A), RNase III (III), or SAP. After mixing and incubation with dialyzed lysates from RIG-I-expressing D.Mel-2 cells, the RIG-I conformational switch assay was performed. Negative controls (CTRL) were performed as described for (C). See also Figures S5A and S5B.

cytoplasm and its high affinity for 5′ppp dsRNA may allow to rapidly entrap a panhandle, even if it is only briefly exposed. Our observation of an early and substantial formation of RIG-I oligomers in response to incoming nucleocapsids supports this hypothesis.

The standard model of RIG-I activation implies that ligand binding induces a conformational change followed by oligomerization (Kowalinski et al., 2011; Saito et al., 2007; Takahasi et al., 2008). Interestingly, oligomerization seems not to be a strict consequence of the conformational switch. While infection with the negative-stranded 5′ppp-RNA viruses VSV, LACV, and RVFV triggers both the conformational switch and the oligomerization, infection with the positive-strand 5′capped RNA virus SFV triggers only the conformational switch. It is known that innate immune recognition of SFV occurs mainly through MDA5 with a modest contribution from RIG-I (Schulz et al., 2010). VSV, LACV, and RVFV are mainly recognized by RIG-I (Habjan et al., 2008a; Kato et al., 2006; Verbruggen et al., 2011). Thus, a weak RIG-I trigger like SFV may only cause the conformational switch, whereas stronger RIG-I triggers continue to the subsequent oligomerization.

We have introduced *Drosophila* cells as a tool to establish that RIG-I activation occurs independent of mammalian cofactors. In mammalian cells, RIG-I is fine-tuned by inhibitors and cofactors. The *Drosophila* cells, which can coexpress up to 12 different recombinant proteins (Yang and Reth, 2012), hold promise as a system to reconstitute the RIG-I signaling complex for studying the details of its regulation.

The classical studies on PRRs and PAMPs involved the usage of purified RNA ligands. However, as we and others (Baum and García-Sastre, 2011; Kato et al., 2011) have pointed out, viral RNAs in their physiological context are complexed with host cell or viral proteins. Recent reports on the PRRs PKR and TLR3 provide increasing evidence that protein-bound RNA ligands are comparable or even more powerful PRR ligands than naked RNAs (Dauber et al., 2009; Lai et al., 2011). It would be interesting to test other PRRs for activation by physiological nucleic acid-protein complexes.

In summary, our results indicate that RIG-I, the major intracellular PRR for viral pathogens, is capable of recognizing the 5′ppp-dsRNA of viral nucleocapsids. This enables a cytoplasmic response to incoming negative-strand RNA viruses at the earliest possible time point of infection.

EXPERIMENTAL PROCEDURES

Cells, Viruses, Plasmids, and Reagents

A549, 293T, and MEFs deficient in *RIG-I*, *MDA5* (Kato et al., 2006), or *MAVS* (Seth et al., 2005) were cultivated in Dulbecco's modified Eagle's medium (DMEM) supplemented with 10% fetal calf serum (FCS) at 37°C and 5% CO_2. D.Mel-2 cells (GIBCO) were cultivated in Spodopan (Pan Biotech) at 28°C with no additional CO_2. VSV, SFV, FLUAVΔNS1 (García-Sastre et al., 1998), RVFVΔNSs::GFP (Habjan et al., 2008b; Kuri et al., 2010),

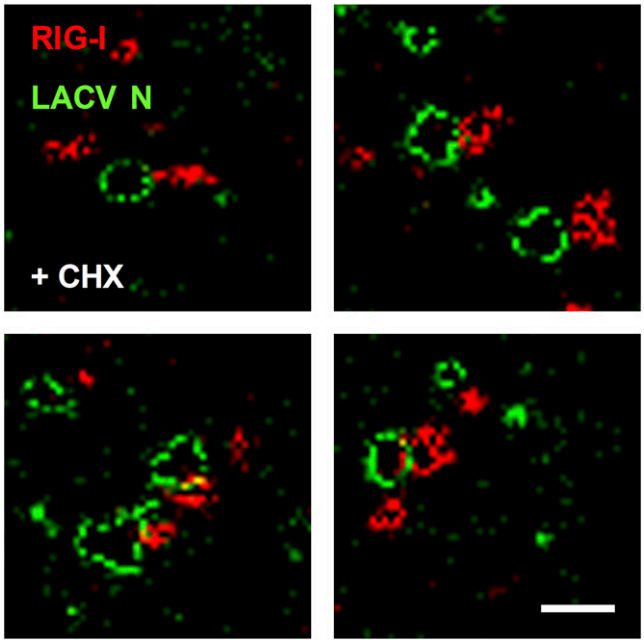

Figure 7. Superresolution Immunofluorescence Microscopy of RIG-I/LACV Nucleocapsid Complexes

CHX-treated A549 cells were infected with LACVdelNSs and analyzed 5 hr later by GSD double immunofluorescence using antisera against LACV N (green channel) or RIG-I (red channel). Four example areas with nucleocapsids are shown. Scale bar represents 200 nm. See also Figure S6.

RVFVΔNSs::REN (Habjan et al., 2008b; Kuri et al., 2010), and LACVdelNSs (Blakqori et al., 2007) were propagated on Vero cells. Plasmids pI.18_RVFV_N, pI.18_RVFV_L, pI.18_RVFV_M, and pHH21_RVFV_vMGFP were described previously (Habjan et al., 2008b, 2009a). Plasmid pRmHA3-RIG-I was constructed by cloning a PCR-generated RIG-I complementary DNA (cDNA) fragment into pRmHA3 (Bunch et al., 1988) using engineered 5′ KpnI and 3′ SalI restriction sites. Primer sequences are available upon request. CHX, NH_4Cl, $CuSO_4$, BRQ, and MA were from Sigma. PYF (NSC-143095) and CPEC (NSC-375575) were kindly obtained from the Drug Synthesis and Chemistry Branch of the National Cancer Institute.

Production of VLPs

RVFV VLPs were generated as described previously (Habjan et al., 2009a). Briefly, subconfluent monolayers of 293T cells in 90 mm dishes were transfected with 3 μg each of pI.18_RVFV_N, pI.18_RVFV_L, pI.18_RVFV_M, and pHH21_RVFV_vMGFP (tc-VLPs), or pI.18_RVFV_N and pI.18_RVFV_M only (ghost VLPs) using Nanofectin (PAA Laboratories). At 5 hr posttransfection, medium was changed and 48 hr later supernatants collected and clarified from cell debris by centrifugation (6,000 × *g*, 10 min at 4°C). VLPs were concentrated with Amicon Ultra-15 (Millipore) Ultracel-100 kDa filter devices.

Infection of Cells

Cells grown to 90% confluency were inoculated for 1 hr with viruses or VLPs dissolved in 200 μl OptiMEM (Invitrogen; for mammalian cells) or Spodopan (for insect cells) at a multiplicity of infection (moi) of 5. FLUAVΔNS1 was washed off with PBS, whereas for all other infections the inoculum was directly replaced with DMEM 5% FCS (mammalian cells) or Spodopan (insect cells). If required, cells were pretreated with inhibitors dissolved in complete medium for 1 hr (CHX, NH_4Cl) or 24 hr (BRQ, MA, PYF, CPEC). The inhibitors were also added to the virus inoculum and the incubation medium.

Real-Time RT-PCR

Cellular RNA was isolated with the NucleoSpin RNA II kit (Macherey-Nagel). A total of 600 ng was used for cDNA synthesis and PCR employing the QuantiTect SYBR Green RT-PCR Kit (QIAGEN) and a LightCycler II (Roche). mRNAs of human and murine *IFN-β* and *ISG56* were detected with specific QuantiTect primers (see Supplemental Information) and normalized against γ-actin (human cells) or GAPDH (murine cells) using the ddCT method (Livak and Schmittgen, 2001). Upregulation of inducible genes is depicted in relation to nonstimulated, noninfected (mock) cells.

siRNA Knockdown

Knockdown of gene expression was achieved by 2-fold reverse transfection of siRNAs. siRNAs (25 nM each; see Supplemental Information) were diluted in 100 μl DMEM, mixed with 3 μl HiPerFect (QIAGEN), incubated for 10 min at room temperature, and dropped onto a 12-well plate. Then, 1.5 × 10^5 cells in DMEM 10% FCS were seeded on top. After 48 hr at 37°C, cells were harvested, counted, and 1.5 × 10^5 cells were again reverse transfected as described.

Activation State of RIG-I

To assay the conformation of RIG-I, cells were lysed in PBS/0.5% Triton X-100 and incubated on ice for 10 min. Then, samples were sonified in a Branson 3200 Ultrasonic cleaner at 4°C for 10 min and centrifuged at 4°C for 10 min at 10,000 × *g*. An aliquot of 25 μg of total protein in 10 μl PBS was digested for 25 min with 0.2 μg/μl L-1-tosylamido-2-phenylethyl chloromethyl ketone-treated trypsin (Sigma-Aldrich) at 37°C. Reaction was stopped by adding 5× sample buffer (250 mM Tris-HCl [pH 6.8], 10% SDS, 50% glycerol, 25% β- mercaptoethanol [β-ME], 0.5% bromphenol blue) and heating at 95°C for 5 min. Samples were subjected to 12% SDS-PAGE and western blot analysis using mouse monoclonal anti-RIG-I antibody (ALME-1; Enzo Life Sciences) at 1:1,000. Staining of the blot with 0.1% Ponceau S in 5% acetic acid served as a loading control.

To investigate the oligomerization of RIG-I, 50 μg of sonified cell lysate in native loading buffer (50 mM Tris-HCl [pH 6.8], 10% glycerol, 0.1% bromphenol blue) was loaded onto a nondenaturing 8% polyacrylamide gel. Proteins were separated by electrophoresis with 50 mM Tris-NaOH (pH 9.0), 384 mM glycin as anode buffer and 50 mM Tris (pH 8.3), 384 mM glycin, 1% sodium deoxycholate as cathode buffer. Western blot analysis was performed as outlined above.

Immunofluorescence Assays

Cells were grown on coverslips to 30%–50% confluency, infected, and incubated for the indicated time. Cells were fixed with 3% paraformaldehyde, permeabilized with 0.5% Triton X-100 in PBS, and washed three times with PBS. Primary antibodies were diluted in PBS/1% FCS. Primary antibodies were either rabbit polyclonal anti-LACV N (1:1,000) (Blakqori et al., 2007) or rabbit polyclonal anti-RVFV N (1:1,000) (Lorenzo et al., 2008) combined with mouse polyclonal anti-human RIG-I (1:200) (Baum et al., 2010). After 1 hr incubation at room temperature, coverslips were washed three times in PBS then treated with goat anti-rabbit Cy2 and goat anti-mouse Cy3 at a dilution of 1:200. After washing three times in PBS, coverslips were mounted with Fluorsave solution (Calbiochem) and examined using a Leica SP5 confocal microscope.

For the superresolution microscopy, a Leica SR GSD microscope was used. Samples were prepared as described for confocal microscopy except that goat anti-rabbit Alexa Fluor 488 (LACV N) and goat anti-mouse Alexa Fluor 647 (RIG-I) were employed as secondary antibody antibodies. Samples were embedded in freshly prepared 100 mM β-mercaptoethylamine in PBS (pH 7.4) directly before imaging.

Coimmunoprecipitation Assays

Cells grown in two T175 flasks were scraped off in 10 ml PBS, centrifuged at low speed, and the pellets lysed in 1,050 μl RIPA buffer (prepared with DEPC-treated H_2O) containing protease inhibitors, incubated on ice for 30 min and centrifuged at 4°C for 10 min at 10,000 × *g*. Supernatants were transferred to fresh tubes and 10% kept as input control. The remaining 90% of the lysates were subjected to immunoprecipitation (IP) using Dynabeads (Invitrogen). In parallel, 1.5 mg beads per IP were coupled with the appropriate antibodies using the Dynabeads antibody coupling kit (Invitrogen). For the anti-p21 and anti-RIG-I IPs, beads were coupled with rabbit polyclonal anti-mouse antibody (DAKO); for the anti-LACV N IP, beads were coupled with rabbit polyclonal anti-LACV N (each at a 1:200 dilution per IP); and for

the anti-RVFV N IP, beads were coupled with mouse polyclonal anti-N serum (Habjan et al., 2009b) for 20 hr at 37°C. After antibody coupling, beads were washed two times with RIPA buffer, and the anti-mouse antibody beads were further incubated with mouse monoclonal anti-p21 (Santa Cruz Biotechnology) or mouse monoclonal anti-RIG-I antibody ALME-1 at a 1:200 dilution in RIPA buffer for 2 hr at 4°C. The beads were then incubated with the lysates for 2 hr at 4°C and the immunoprecipitates washed three times with RIPA buffer and then eluted with sample buffer (50 mM Tris-HCl [pH 6.8], 2% SDS, 10% glycerol, 5% β-ME, 0.1% bromphenol blue) for 5 min at 95°C. Eluates were analyzed by western blotting using rabbit polyclonal anti-LACV N or anti-RVFV N antisera (1:1,000), mouse monoclonal anti-RIG-I antibody ALME-1 (1:1,000), or mouse monoclonal anti-p21 (1:500). Protein A horseradish peroxidase conjugate (Millipore; 1:10,000) was used for detection.

ADP-Aluminum Fluoride Trapping

ADP•AlF_3 trapping was performed essentially as described elsewhere (Chaney et al., 2001). Briefly, 50 μg cell protein was prepared in STA buffer (25 mM Tris-acetate [pH 8.0], 8 mM Mg-acetate, 10 mM KCl, 3.5% w/v PEG 6000, 1 mM DTT) with 0.2 mM ADP and 10 mM NaF and incubated at 37°C for 5 min. After addition of 0.4 mM $AlCl_3$, the reactions were incubated for further 10 min and then supplemented with native loading buffer (50 mM Tris-HCl [pH 6.8], 10% glycerol, 0.1% bromophenol blue). Native gel electrophoresis and western blot analysis were performed as described above.

Expression of *RIG-I* in *Drosophila* Cells

D.Mel-2 cells (1×10^7) resuspended in 10 ml Spodopan were transfected with 16 μg pRmHa3-RIG-I plasmid mixed with 48 μl Cellfectin (Invitrogen) and incubated at 28°C in T75 flasks. RIG-I expression was induced 48 hr later with 1 mM $CuSO_4$, and 24 hr later cells were scraped off in 10 ml PBS. Cells were pelleted by 5 min centrifugation at 100 × *g* and resuspended in 800 μl RIPA buffer (for IPs) or in 150 μl 0.5% Triton X-100 in PBS (for RIG-I assays). The suspensions were incubated for 10 min at 4°C and centrifuged at 10,000 × *g*, and the supernatants were kept at 4°C.

Dialysis and ATP Supplementation of Cell Lysates

Visking dialysis tubing 27/32 with a diameter of 21 mm (Serva Electrophoresis) was used to deplete cell lysates from low-molecular-weight compounds. The membrane tubes were activated by submerging in H_2O and boiling for 1 min in the microwave oven, followed by a transfer into H_2O at room temperature. For cell lysates, 100 μl was dialyzed at 4°C against PBS in 1 ml Eppendorf tubes covered with the dialysis membrane. For nucleocapsids, 10 μl was dialyzed using 200 μl PCR tubes. The buffer was exchanged after 1 hr, 12 hr, and then again 1 hr later. To test the contribution of ATP, lysates or nucleocapsids were first mixed and then incubated with or without 1 mM ATP for 1 hr at 37°C. The RIG-I conformational switch assay was performed as indicated above.

Purification of Viral Nucleocapsids

BHK cells seeded in ten T175 flasks were infected with virus at an moi of 0.01. Cell supernatants were harvested at 3 days later and virions purified by centrifugation through a 30% glycerol cushion at 25,000 rpm for 1.5 hr at 4°C in a SW-32 rotor. Pellets were resuspended in hypotonic lysis buffer (10 mM Tris/HCl [pH 7.8], 150 mM NaCl, 1 mM EDTA, 1% NP40) in the presence of complete protease inhibitors (Roche). Nucleocapsids were purified in a CsCl gradient as described elsewhere (Mavrakis et al., 2002), with minor modifications. Briefly, the cleared lysate was loaded on top of a continuous 20%–40% CsCl gradient in 20 mM Tris/HCl (pH 7.9), 200 mM NaCl, centrifuged at 52,000 rpm for 2 hr at 12°C in a SW60 rotor, and the recovered fraction pelleted at 45,000 rpm for 1 hr at 4°C in a TLA45 rotor. Nucleocapsids were resuspended in PBS and dialyzed against PBS to remove residual CsCl. Nucleocapsid-containing fractions were identified by SDS-PAGE with Coomassie blue staining and western blot analysis.

Enzymatic Treatment of Lysates

Dialyzed lysates of RVFV-infected D.Mel-2 cells (50 μg protein in 10 μl) or nucleocapsids were supplemented with 1 mM ATP and incubated either with 5 μg RNase A, 1 U RNase III, or 2 U shrimp alkaline phosphatase (SAP) for 1 hr at 37°C. Samples were then mixed 1:1 with dialyzed lysates from RIG-I-expressing D.Mel-2 cells (50 μg protein in 10 μl) and incubated for 1 hr at 37°C. The RIG-I conformation assay was performed with half of the sample, whereas the other half was kept as input control.

SUPPLEMENTAL INFORMATION

Supplemental Information includes six figures, one table, and Supplemental Experimental Procedures and can be found with this article online at http://dx.doi.org/10.1016/j.chom.2013.01.012.

ACKNOWLEDGMENTS

We thank Valentina Wagner and Jörg Schmidt for excellent technical assistance, Michael Reth for drawing our attention to *Drosophila* cells, and Stefan Bauer and Marco Binder for critically reading the manuscript. We also thank the antibody facility at MSSM NY and Shizuo Akira, Zhijian J. Chen, Gema Lorenzo, Alejandro Brun, Markus Schnare, and the National Cancer Institute for reagents. F.W. is supported by the DFG grants We2616/2-3 and We2616/5-2, SFB 593, grant 47/2012MR from the Forschungsförderung (§2 Abs. 3) Kooperationsvertrag UKGM, and the Leibniz Graduate School for Emerging viral diseases (EIDIS). G.K. is supported by DFG grant Ko1579/52. S.V. and R.J. are supported by SFB 593. A.G.-S. is supported by National Institute of Allergy and Infectious Diseases (NIAID) grants R01AI046954 and U19AI083025 and by the CEIRS program of NIAID under contract HHSN266200700010C.

Received: March 27, 2012
Revised: October 12, 2012
Accepted: January 25, 2013
Published: March 13, 2013

REFERENCES

Baum, A., and García-Sastre, A. (2011). Differential recognition of viral RNA by RIG-I. Virulence *2*, 166–169.

Baum, A., Sachidanandam, R., and García-Sastre, A. (2010). Preference of RIG-I for short viral RNA molecules in infected cells revealed by next-generation sequencing. Proc. Natl. Acad. Sci. USA *107*, 16303–16308.

Binder, M., Eberle, F., Seitz, S., Mücke, N., Hüber, C.M., Kiani, N., Kaderali, L., Lohmann, V., Dalpke, A., and Bartenschlager, R. (2011). Molecular mechanism of signal perception and integration by the innate immune sensor retinoic acid-inducible gene-I (RIG-I). J. Biol. Chem. *286*, 27278–27287.

Blakqori, G., Delhaye, S., Habjan, M., Blair, C.D., Sánchez-Vargas, I., Olson, K.E., Attarzadeh-Yazdi, G., Fragkoudis, R., Kohl, A., Kalinke, U., et al. (2007). La Crosse bunyavirus nonstructural protein NSs serves to suppress the type I interferon system of mammalian hosts. J. Virol. *81*, 4991–4999.

Bunch, T.A., Grinblat, Y., and Goldstein, L.S. (1988). Characterization and use of the Drosophila metallothionein promoter in cultured Drosophila melanogaster cells. Nucleic Acids Res. *16*, 1043–1061.

Chaney, M., Grande, R., Wigneshweraraj, S.R., Cannon, W., Casaz, P., Gallegos, M.T., Schumacher, J., Jones, S., Elderkin, S., Dago, A.E., et al. (2001). Binding of transcriptional activators to sigma 54 in the presence of the transition state analog ADP-aluminum fluoride: insights into activator mechanochemical action. Genes Dev. *15*, 2282–2294.

Dauber, B., Martínez-Sobrido, L., Schneider, J., Hai, R., Waibler, Z., Kalinke, U., García-Sastre, A., and Wolff, T. (2009). Influenza B virus ribonucleoprotein is a potent activator of the antiviral kinase PKR. PLoS Pathog. *5*, e1000473.

de Boer, S.M., Kortekaas, J., Spel, L., Rottier, P.J., Moormann, R.J., and Bosch, B.J. (2012). Acid-activated structural reorganization of the Rift Valley fever virus Gc fusion protein. J. Virol. *86*, 13642–13652.

Dixit, E., Boulant, S., Zhang, Y., Lee, A.S., Odendall, C., Shum, B., Hacohen, N., Chen, Z.J., Whelan, S.P., Fransen, M., et al. (2010). Peroxisomes are signaling platforms for antiviral innate immunity. Cell *141*, 668–681.

Filone, C.M., Heise, M., Doms, R.W., and Bertolotti-Ciarlet, A. (2006). Development and characterization of a Rift Valley fever virus cell-cell fusion assay using alphavirus replicon vectors. Virology *356*, 155–164.

García-Sastre, A., Egorov, A., Matassov, D., Brandt, S., Levy, D.E., Durbin, J.E., Palese, P., and Muster, T. (1998). Influenza A virus lacking the NS1 gene replicates in interferon-deficient systems. Virology *252*, 324–330.

Garcin, D., Lezzi, M., Dobbs, M., Elliott, R.M., Schmaljohn, C., Kang, C.Y., and Kolakofsky, D. (1995). The 5′ ends of Hantaan virus (Bunyaviridae) RNAs suggest a prime-and-realign mechanism for the initiation of RNA synthesis. J. Virol. *69*, 5754–5762.

Habjan, M., Andersson, I., Klingström, J., Schümann, M., Martin, A., Zimmermann, P., Wagner, V., Pichlmair, A., Schneider, U., Mühlberger, E., et al. (2008a). Processing of genome 5′ termini as a strategy of negative-strand RNA viruses to avoid RIG-I-dependent interferon induction. PLoS ONE *3*, e2032.

Habjan, M., Penski, N., Spiegel, M., and Weber, F. (2008b). T7 RNA polymerase-dependent and -independent systems for cDNA-based rescue of Rift Valley fever virus. J. Gen. Virol. *89*, 2157–2166.

Habjan, M., Penski, N., Wagner, V., Spiegel, M., Overby, A.K., Kochs, G., Huiskonen, J.T., and Weber, F. (2009a). Efficient production of Rift Valley fever virus-like particles: The antiviral protein MxA can inhibit primary transcription of bunyaviruses. Virology *385*, 400–408.

Habjan, M., Pichlmair, A., Elliott, R.M., Overby, A.K., Glatter, T., Gstaiger, M., Superti-Furga, G., Unger, H., and Weber, F. (2009b). NSs protein of rift valley fever virus induces the specific degradation of the double-stranded RNA-dependent protein kinase. J. Virol. *83*, 4365–4375.

Handke, W., Oelschlegel, R., Franke, R., Krüger, D.H., and Rang, A. (2009). Hantaan virus triggers TLR3-dependent innate immune responses. J. Immunol. *182*, 2849–2858.

Hiscott, J. (2007). Triggering the innate antiviral response through IRF-3 activation. J. Biol. Chem. *282*, 15325–15329.

Hoenen, T., Groseth, A., de Kok-Mercado, F., Kuhn, J.H., and Wahl-Jensen, V. (2011). Minigenomes, transcription and replication competent virus-like particles and beyond: reverse genetics systems for filoviruses and other negative stranded hemorrhagic fever viruses. Antiviral Res. *91*, 195–208.

Holm, C.K., Jensen, S.B., Jakobsen, M.R., Cheshenko, N., Horan, K.A., Moeller, H.B., Gonzalez-Dosal, R., Rasmussen, S.B., Christensen, M.H., Yarovinsky, T.O., et al. (2012). Virus-cell fusion as a trigger of innate immunity dependent on the adaptor STING. Nat. Immunol. *13*, 737–743.

Hornung, V., Ellegast, J., Kim, S., Brzózka, K., Jung, A., Kato, H., Poeck, H., Akira, S., Conzelmann, K.K., Schlee, M., et al. (2006). 5′-Triphosphate RNA is the ligand for RIG-I. Science *314*, 994–997.

Kato, H., Takeuchi, O., Sato, S., Yoneyama, M., Yamamoto, M., Matsui, K., Uematsu, S., Jung, A., Kawai, T., Ishii, K.J., et al. (2006). Differential roles of MDA5 and RIG-I helicases in the recognition of RNA viruses. Nature *441*, 101–105.

Kato, H., Takeuchi, O., Mikamo-Satoh, E., Hirai, R., Kawai, T., Matsushita, K., Hiiragi, A., Dermody, T.S., Fujita, T., and Akira, S. (2008). Length-dependent recognition of double-stranded ribonucleic acids by retinoic acid-inducible gene-I and melanoma differentiation-associated gene 5. J. Exp. Med. *205*, 1601–1610.

Kato, H., Takahasi, K., and Fujita, T. (2011). RIG-I-like receptors: cytoplasmic sensors for non-self RNA. Immunol. Rev. *243*, 91–98.

Killip, M.J., Young, D.F., Ross, C.S., Chen, S., Goodbourn, S., and Randall, R.E. (2011). Failure to activate the IFN-β promoter by a paramyxovirus lacking an interferon antagonist. Virology *415*, 39–46.

Killip, M.J., Young, D.F., Precious, B.L., Goodbourn, S., and Randall, R.E. (2012). Activation of the beta interferon promoter by paramyxoviruses in the absence of virus protein synthesis. J. Gen. Virol. *93*, 299–307.

Kok, K.H., Lui, P.Y., Ng, M.H., Siu, K.L., Au, S.W., and Jin, D.Y. (2011). The double-stranded RNA-binding protein PACT functions as a cellular activator of RIG-I to facilitate innate antiviral response. Cell Host Microbe *9*, 299–309.

Kortekaas, J., Oreshkova, N., Cobos-Jiménez, V., Vloet, R.P., Potgieter, C.A., and Moormann, R.J. (2011). Creation of a nonspreading Rift Valley fever virus. J. Virol. *85*, 12622–12630.

Kowalinski, E., Lunardi, T., McCarthy, A.A., Louber, J., Brunel, J., Grigorov, B., Gerlier, D., and Cusack, S. (2011). Structural basis for the activation of innate immune pattern-recognition receptor RIG-I by viral RNA. Cell *147*, 423–435.

Kuri, T., Habjan, M., Penski, N., and Weber, F. (2010). Species-independent bioassay for sensitive quantification of antiviral type I interferons. Virol. J. *7*, 50.

Lai, Y., Yi, G., Chen, A., Bhardwaj, K., Tragesser, B.J., Rodrigo A Valverde, Zlotnick, A., Mukhopadhyay, S., Ranjith-Kumar, C.T., and Kao, C.C. (2011). Viral double-strand RNA-binding proteins can enhance innate immune signaling by toll-like Receptor 3. PLoS ONE *6*, e25837.

Linke, S.P., Clarkin, K.C., Di Leonardo, A., Tsou, A., and Wahl, G.M. (1996). A reversible, p53-dependent G0/G1 cell cycle arrest induced by ribonucleotide depletion in the absence of detectable DNA damage. Genes Dev. *10*, 934–947.

Livak, K.J., and Schmittgen, T.D. (2001). Analysis of relative gene expression data using real-time quantitative PCR and the 2(-Delta Delta C(T)) Method. Methods *25*, 402–408.

Lorenzo, G., Martín-Folgar, R., Rodríguez, F., and Brun, A. (2008). Priming with DNA plasmids encoding the nucleocapsid protein and glycoprotein precursors from Rift Valley fever virus accelerates the immune responses induced by an attenuated vaccine in sheep. Vaccine *26*, 5255–5262.

Marcus, P.I., and Sekellick, M.J. (1980). Interferon induction by viruses. III. Vesicular stomatitis virus: interferon-inducing particle activity requires partial transcription of gene N. J. Gen. Virol. *47*, 89–96.

Mavrakis, M., Kolesnikova, L., Schoehn, G., Becker, S., and Ruigrok, R.W. (2002). Morphology of Marburg virus NP-RNA. Virology *296*, 300–307.

McCartney, S.A., and Colonna, M. (2009). Viral sensors: diversity in pathogen recognition. Immunol. Rev. *227*, 87–94.

McInerney, G.M., Kedersha, N.L., Kaufman, R.J., Anderson, P., and Liljeström, P. (2005). Importance of eIF2alpha phosphorylation and stress granule assembly in alphavirus translation regulation. Mol. Biol. Cell *16*, 3753–3763.

Miyashita, M., Oshiumi, H., Matsumoto, M., and Seya, T. (2011). DDX60, a DEXD/H box helicase, is a novel antiviral factor promoting RIG-I-like receptor-mediated signaling. Mol. Cell. Biol. *31*, 3802–3819.

Noyce, R.S., Taylor, K., Ciechonska, M., Collins, S.E., Duncan, R., and Mossman, K.L. (2011). Membrane perturbation elicits an IRF3-dependent, interferon-independent antiviral response. J. Virol. *85*, 10926–10931.

Obijeski, J.F., Bishop, D.H., Palmer, E.L., and Murphy, F.A. (1976). Segmented genome and nucleocapsid of La Crosse virus. J. Virol. *20*, 664–675.

Onomoto, K., Jogi, M., Yoo, J.S., Narita, R., Morimoto, S., Takemura, A., Sambhara, S., Kawaguchi, A., Osari, S., Nagata, K., et al. (2012). Critical role of an antiviral stress granule containing RIG-I and PKR in viral detection and innate immunity. PLoS ONE *7*, e43031.

Pichlmair, A., Schulz, O., Tan, C.P., Näslund, T.I., Liljeström, P., Weber, F., and Reis e Sousa, C. (2006). RIG-I-mediated antiviral responses to single-stranded RNA bearing 5′-phosphates. Science *314*, 997–1001.

Pichlmair, A., Schulz, O., Tan, C.P., Rehwinkel, J., Kato, H., Takeuchi, O., Akira, S., Way, M., Schiavo, G., and Reis e Sousa, C. (2009). Activation of MDA5 requires higher-order RNA structures generated during virus infection. J. Virol. *83*, 10761–10769.

Prescott, J., Ye, C., Sen, G., and Hjelle, B. (2005). Induction of innate immune response genes by Sin Nombre hantavirus does not require viral replication. J. Virol. *79*, 15007–15015.

Qing, M., Zou, G., Wang, Q.Y., Xu, H.Y., Dong, H., Yuan, Z., and Shi, P.Y. (2010). Characterization of dengue virus resistance to brequinar in cell culture. Antimicrob. Agents Chemother. *54*, 3686–3695.

Raju, R., Raju, L., and Kolakofsky, D. (1989). The translational requirement for complete La Crosse virus mRNA synthesis is cell-type dependent. J. Virol. *63*, 5159–5165.

Randall, R.E., and Goodbourn, S. (2008). Interferons and viruses: an interplay between induction, signalling, antiviral responses and virus countermeasures. J. Gen. Virol. *89*, 1–47.

Rehwinkel, J., Tan, C.P., Goubau, D., Schulz, O., Pichlmair, A., Bier, K., Robb, N., Vreede, F., Barclay, W., Fodor, E., and Reis e Sousa, C. (2010). RIG-I detects viral genomic RNA during negative-strand RNA virus infection. Cell *140*, 397–408.

Resa-Infante, P., Jorba, N., Coloma, R., and Ortin, J. (2011). The influenza virus RNA synthesis machine: advances in its structure and function. RNA Biol. *8*, 207–215.

Saito, T., Hirai, R., Loo, Y.M., Owen, D., Johnson, C.L., Sinha, S.C., Akira, S., Fujita, T., and Gale, M., Jr. (2007). Regulation of innate antiviral defenses through a shared repressor domain in RIG-I and LGP2. Proc. Natl. Acad. Sci. USA *104*, 582–587.

Saito, T., Owen, D.M., Jiang, F., Marcotrigiano, J., and Gale, M., Jr. (2008). Innate immunity induced by composition-dependent RIG-I recognition of hepatitis C virus RNA. Nature *454*, 523–527.

Schlee, M., Roth, A., Hornung, V., Hagmann, C.A., Wimmenauer, V., Barchet, W., Coch, C., Janke, M., Mihailovic, A., Wardle, G., et al. (2009). Recognition of 5′ triphosphate by RIG-I helicase requires short blunt double-stranded RNA as contained in panhandle of negative-strand virus. Immunity *31*, 25–34.

Schmidt, A., Schwerd, T., Hamm, W., Hellmuth, J.C., Cui, S., Wenzel, M., Hoffmann, F.S., Michallet, M.C., Besch, R., Hopfner, K.P., et al. (2009). 5′-triphosphate RNA requires base-paired structures to activate antiviral signaling via RIG-I. Proc. Natl. Acad. Sci. USA *106*, 12067–12072.

Schulz, O., Pichlmair, A., Rehwinkel, J., Rogers, N.C., Scheuner, D., Kato, H., Takeuchi, O., Akira, S., Kaufman, R.J., and Reis e Sousa, C. (2010). Protein kinase R contributes to immunity against specific viruses by regulating interferon mRNA integrity. Cell Host Microbe *7*, 354–361.

Seth, R.B., Sun, L., Ea, C.K., and Chen, Z.J. (2005). Identification and characterization of MAVS, a mitochondrial antiviral signaling protein that activates NF-kappaB and IRF 3. Cell *122*, 669–682.

Spiropoulou, C.F., Albariño, C.G., Ksiazek, T.G., and Rollin, P.E. (2007). Andes and Prospect Hill hantaviruses differ in early induction of interferon although both can downregulate interferon signaling. J. Virol. *81*, 2769–2776.

Stoltz, M., and Klingström, J. (2010). Alpha/beta interferon (IFN-alpha/beta)-independent induction of IFN-lambda1 (interleukin-29) in response to Hantaan virus infection. J. Virol. *84*, 9140–9148.

Strahle, L., Garcin, D., and Kolakofsky, D. (2006). Sendai virus defective-interfering genomes and the activation of interferon-beta. Virology *351*, 101–111.

Takahasi, K., Yoneyama, M., Nishihori, T., Hirai, R., Kumeta, H., Narita, R., Gale, M., Jr., Inagaki, F., and Fujita, T. (2008). Nonself RNA-sensing mechanism of RIG-I helicase and activation of antiviral immune responses. Mol. Cell *29*, 428–440.

tenOever, B.R., Servant, M.J., Grandvaux, N., Lin, R., and Hiscott, J. (2002). Recognition of the measles virus nucleocapsid as a mechanism of IRF-3 activation. J. Virol. *76*, 3659–3669.

tenOever, B.R., Sharma, S., Zou, W., Sun, Q., Grandvaux, N., Julkunen, I., Hemmi, H., Yamamoto, M., Akira, S., Yeh, W.C., et al. (2004). Activation of TBK1 and IKKvarepsilon kinases by vesicular stomatitis virus infection and the role of viral ribonucleoprotein in the development of interferon antiviral immunity. J. Virol. *78*, 10636–10649.

Verbruggen, P., Ruf, M., Blakqori, G., Överby, A.K., Heidemann, M., Eick, D., and Weber, F. (2011). Interferon antagonist NSs of La Crosse virus triggers a DNA damage response-like degradation of transcribing RNA polymerase II. J. Biol. Chem. *286*, 3681–3692.

Vreede, F.T., Jung, T.E., and Brownlee, G.G. (2004). Model suggesting that replication of influenza virus is regulated by stabilization of replicative intermediates. J. Virol. *78*, 9568–9572.

Yang, J., and Reth, M. (2012). Drosophila S2 Schneider cells: a useful tool for rebuilding and redesigning approaches in synthetic biology. Methods Mol. Biol. *813*, 331–341.

Cell Host & Microbe, Volume *13*

Supplemental Information

Incoming RNA Virus Nucleocapsids Containing a 5′-Triphosphorylated Genome Activate RIG-I and Antiviral Signaling

Michaela Weber, Ali Gawanbacht, Matthias Habjan, Andreas Rang, Christoph Borner, Anna Mareike Schmidt, Sophie Veitinger, Ralf Jacob, Stéphanie Devignot, Georg Kochs, Adolfo García-Sastre, and Friedemann Weber

Table S1

Viral system[1]	Genome polarity[2]	Genome 5'end	Attachment	Primary transcription	Genome replication / secondary transcription	Earliest step affected by CHX[3]
FLUAV	(-)	**ppp**AGCGAAAGCA... (Segment 1 of 8)	yes	yes	yes	Genome replication
VSV	(-)	**ppp**ACGAAGACAA...	yes	yes	yes	Genome replication
RVFV	(-)	**ppp**ACACAAAGAC... (3 segments)	yes	yes	yes	Primary transcription
RVFV tc-VLPs	(-)	**ppp**ACACAAAGAC... (M segment ends)	yes	yes	no	Primary transcription
ghost VLPs	none	**None**	yes	no	no	none
LACV	(-)	**ppp**ACACAAAGAC... (3 segments)	yes	yes	yes	Primary transcription
PHV	(-)	**p**UAGUAGUAGU... (3 segments)	yes	yes	yes	Primary transcription
SFV	(+)	**m7G**ATGGCGGATG...	yes	n.a.[4]	n.a.	Genome replication

[1]Virus abbreviations: FLUAV, influenza A virus; LACV, La Crosse virus; PHV, Prospect Hill virus; RVFV, Rift Valley fever virus; SFV, Semliki Forest virus; VLPs, virus-like particles; VSV, Vesicular stomatitis virus. [2](-): negative-strand RNA virus, (+): positive-strand RNA virus. [3]CHX, Cycloheximide. [4]n.a., not applicable

Figure S1

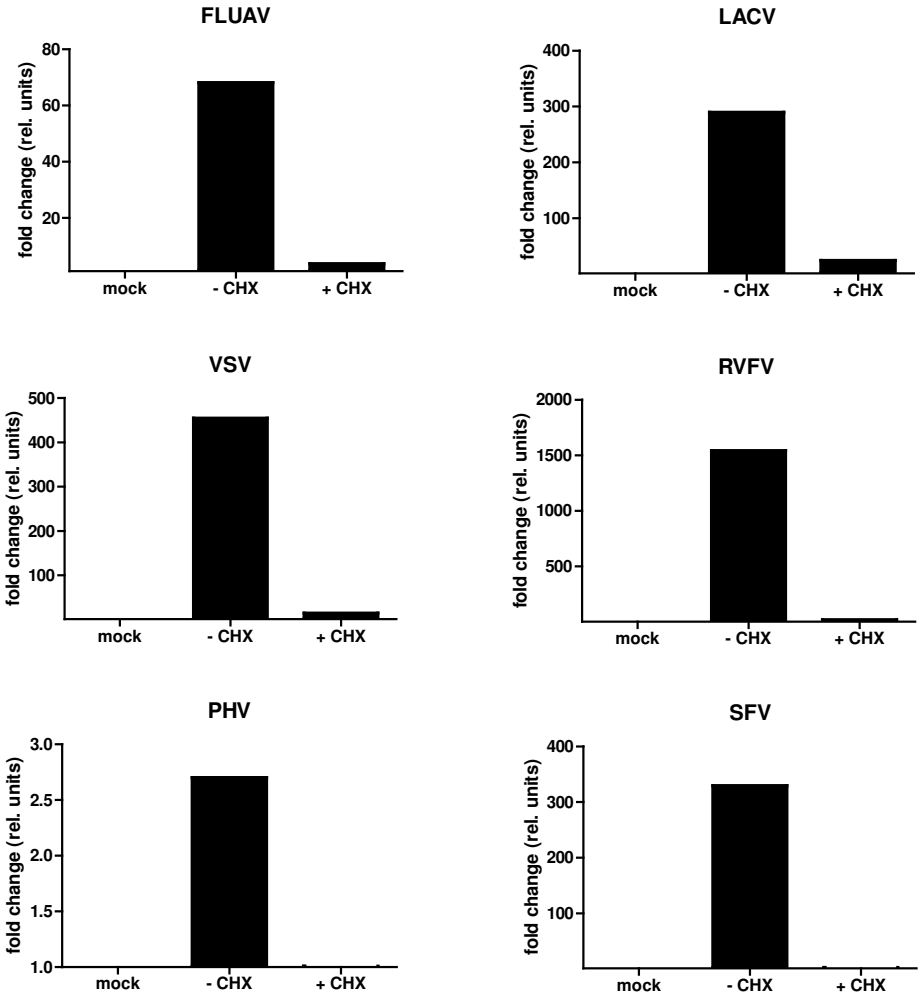

Figure S1. Effect of CHX Treatment on Viral RNA Synthesis (related to all figures)

A549 cells were either left untreated, or pretreated with CHX (50 µg/ml) for 1 h at 37°C, and infected with viruses at an MOI of 1. Seven hours (RVFV) or twelve hours (all other viruses) post-infection, cells were lysed and the total cell RNA was extracted. Viral RNA levels were measured by real-time RT-PCR as indicated in Supplemental Experimental Procedures.

Figure S2

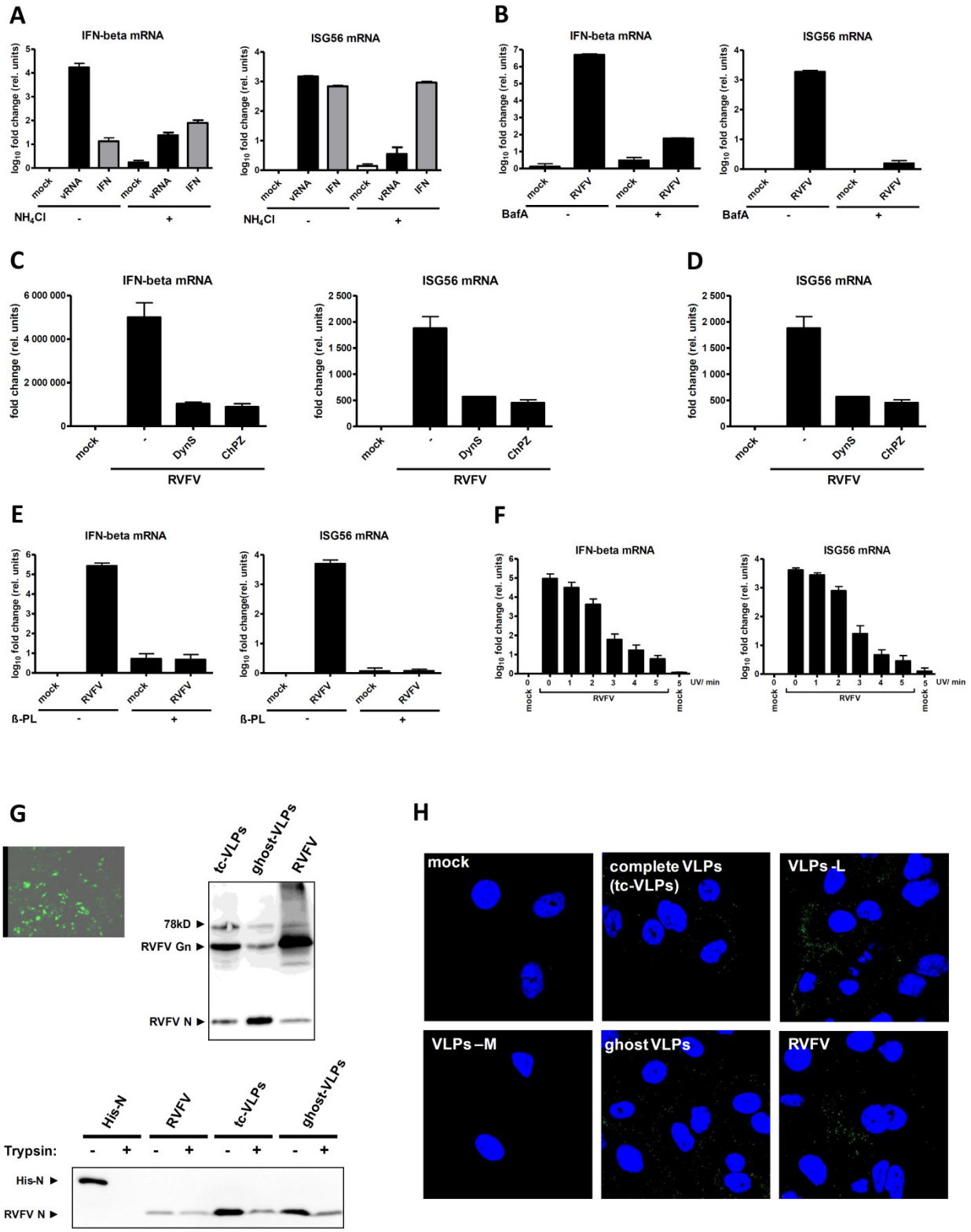
A
IFN-beta mRNA
ISG56 mRNA
log10 fold change (rel. units)
mock
vRNA
IFN
NH4Cl
-
+
B
IFN-beta mRNA
ISG56 mRNA
RVFV
BafA
C
IFN-beta mRNA
ISG56 mRNA
fold change (rel. units)
DynS
ChPZ
RVFV
D
ISG56 mRNA
E
IFN-beta mRNA
ISG56 mRNA
ß-PL
F
IFN-beta mRNA
ISG56 mRNA
UV/ min
G
tc-VLPs
ghost-VLPs
RVFV
78kD
RVFV Gn
RVFV N
His-N
Trypsin:
H
mock
complete VLPs (tc-VLPs)
VLPs -L
VLPs –M
ghost VLPs
RVFV

Figure S2. Control Experiments, Methods, and Tools for Investigating IFN Induction by Incoming Virus Particles (related to Figure 1)

(A) ISG response to IFN is unaffected by NH4Cl. A549 cells were treated for 1 h with 0 or 50 mM NH_4Cl, and then either transfected with 500 ng RNA of RVFVΔNSs::GFP particles (vRNA), or treated with 1000 U/ml IFN-α (IFN). IFN-β and ISG56 mRNA levels were analyzed 24 h later by real-time RT-PCR. **(B, C, and D) RVFV entry inhibitors and the IFN response**. (B) A549 cells were treated for 1 h either with 8 µl DMSO, or with 100 nM of Bafilomycin A (BafA) in DMSO, and infected and analysed as described for Figure 1C. (C) A parallel experiment employing 160 µM of Dynasore (DynS), or 40 µM of Chlorpromazine (ChPZ), each dissolved in DMSO. (D) Real-time RT-PCR analysis for the RVFV L gene as described (Bird et al., 2007). **(E and F) IFN response to inactivated virus particles.** A549 cells were infected with RVFVΔNSs::GFP particles inactivated with ß-propiolactone (ß-PL) (E) or irradiated with UV (λ=311 nm) for the indicated period of time (F). **(G) Production of RVFV VLPs.** (Upper left panel) Biological activity of GFP-expressing tc-VLPs. BSR-T7/5 cells were transfected with plasmids for RVFV N and L and 24 h later infected with tc-VLPs. At 24 h post infection, GFP-positive cells were observed by fluorescence microscopy. (Upper right panel) Concentrated tc-VLPs or ghost VLPs, or cell lysate of RVFV-infected Vero cells were loaded on a 12% polyacrylamide gel and tested by immunoblot using pan-specific anti-RVFV mouse antiserum. (Lower panel) Ghost VLP preparations contain intact particles which protect the N from trypsin digestion. Recombinant RVFV nucleoprotein rN (0.2µg) containing a His-tag (His-N), as well as RVFVΔNSs::GFP, tc-VLPs, and ghost VLPs purified by ultracentrifugation were exposed to trypsin (100 µg/ml), and incubated for 30 min at 37° C. Samples were immunoblotted using an anti-RVFV N antibody. Fractions of trypsin-sensitive N indicate the presence of free N secreted by infected and transfected cells, as observed earlier (Kortekaas et al., 2011). **(H) Attachment of VLPs.** A549 cells were incubated with RVFV VLPs that are either complete (tc-VLPs), or for which either the polymerase (-L), the glycoproteins (-M), or the polymerase and the minireplicon (ghost VLPs) were omitted. RVFVΔNSs::REN infection served as positive control (RVFV). Cells were infected for 1 h at 4°C, fixed with 3% paraformaldehyde and analyzed by immunofluorescense using rabbit anti-RVFV N antiserum (1:200, green channel) and Hoechst 33342 (blue channel) as nuclear counterstain. Note that cells were not permeabilized prior to analysis. Therefore only particles attached to the cells are detected. Figures S2A to F show mean values and standard deviations from three independent experiments.

Figure S3

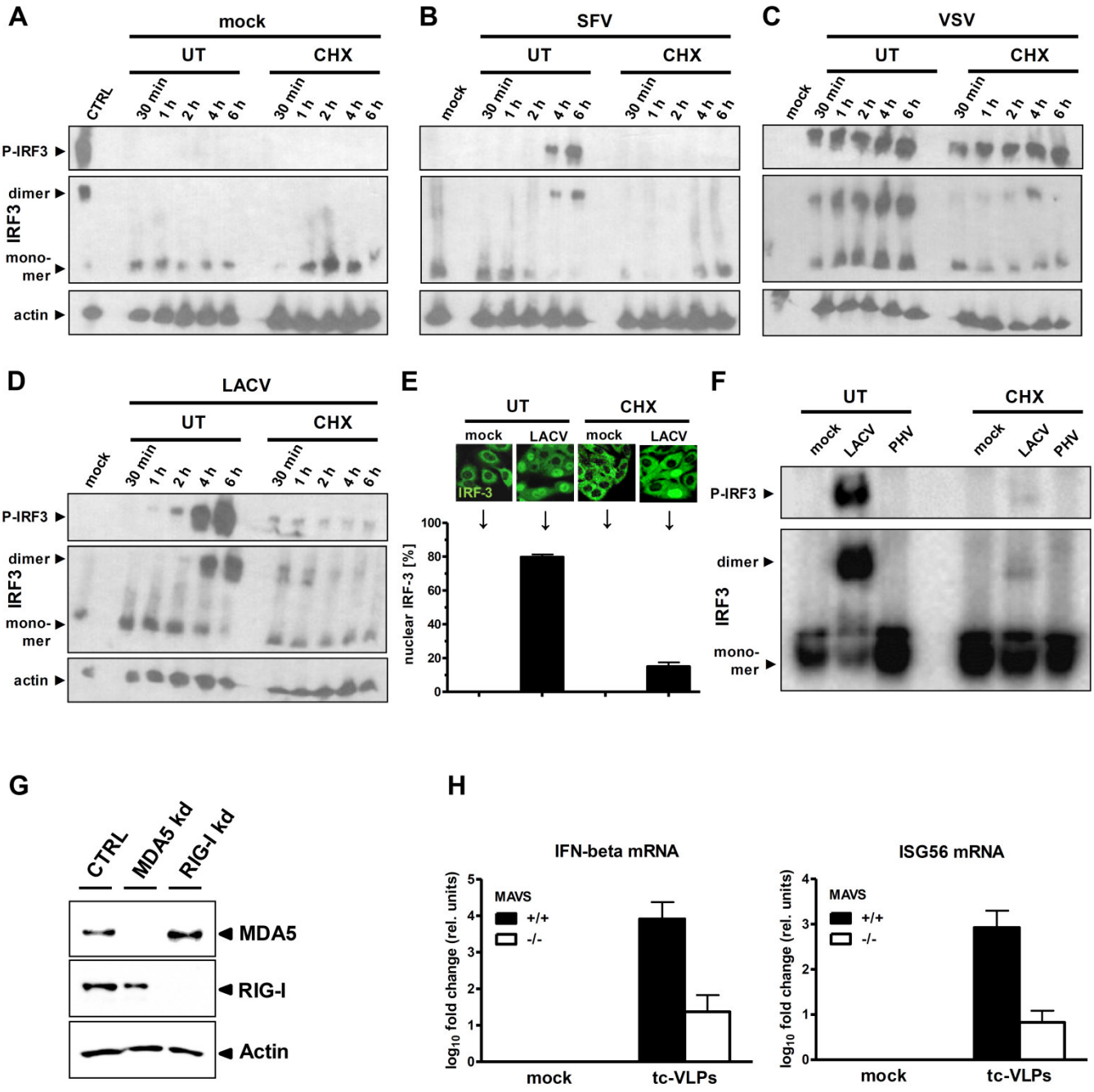
A
mock
UT
CHX
CTRL
30 min
1 h
2 h
4 h
6 h
P-IRF3
dimer
IRF3
mono-
mer
actin
B
SFV
C
VSV
D
LACV
E
IRF-3
nuclear IRF-3 [%]
F
PHV
G
CTRL
MDA5 kd
RIG-I kd
MDA5
RIG-I
Actin
H
IFN-beta mRNA
ISG56 mRNA
MAVS
+/+
-/-
log10 fold change (rel. units)
mock
tc-VLPs

Figure S3. Companion Experiments and Controls for the Influence of the 5'ppp Group and RIG-I / MAVS Signaling on IFN Induction (related to Figure 2)

(A to F) Activation of IRF-3 in dependence of viral 5' genome ends. A549 cells were left untreated (UT) or treated with 50 µg/ml CHX. Then, cells were either mock infected (A) or infected with SFV (B), VSV (C), or LACVdelNSs (D) as described for Figure 1. At the indicated time points post-infection, cells were lysed with RIPA buffer and protein extracts cleared from cell debris separated by native PAGE. The presence of phospho-IRF-3 (P-IRF-3) and actin, and the oligomerization state of total IRF-3 were analyzed by Western blot using specific antisera. As internal controls, lysate from VSV-infected cells at 6 h post-infection was used as positive control for the mock infected cells (CTRL), and lysates from mock infected cells were used as negative control for the virus-infected cells. (E) Subcellular localization of IRF-3 in LACV-infected cells. A549 cells were treated with CHX or left untreated, and then mock infected or infected with LACVdelNSs. Upper panel shows representative examples of immunofluorescence analyses for IRF-3 (green). Graph shows statistics (mean and standard deviations) of the IRF-3 subcellular localization from a total of 4 independent experiments, in each of which 100 cells were randomly chosen. (F) PHV and IRF-3 activation. A549 cells were mock infected or infected with LACVdelNSs or PHV, and 6 h later monitored for IRF-3 phosphorylation and dimerisation as described for panels A to D. **(G) Knockdown of intracellular PRRs.** A549 cells were transfected with a negative control siRNA (CTRL), or with siRNAs directed against MDA5 or RIG-I. After two rounds of transfection, cells were either infected as indicated for Figure 2B, or lysed and tested for the presence of the siRNA targets by western blot analysis. MDA5 was immunodetected using rabbit polyclonal antiserum NBP1-03299 (1:500; Novus Biologicals), actin and RIG-I were immunodetected as indicated for A–D and Figure 3, respectively. **(H) Host response to RVFV primary transcription in MAVS knockout cells.** wt MEFs or MEFs lacking the MAVS gene were infected with transcriptionally competent RVFV VLPs expressing a GFP reporter minireplicon (tc-VLPs). After 24 h of infection, mRNA levels of IFN-β and ISG56 were determined by real-time RT-PCR. Mean values and standard deviations from three independent experiments are shown.

Figure S4

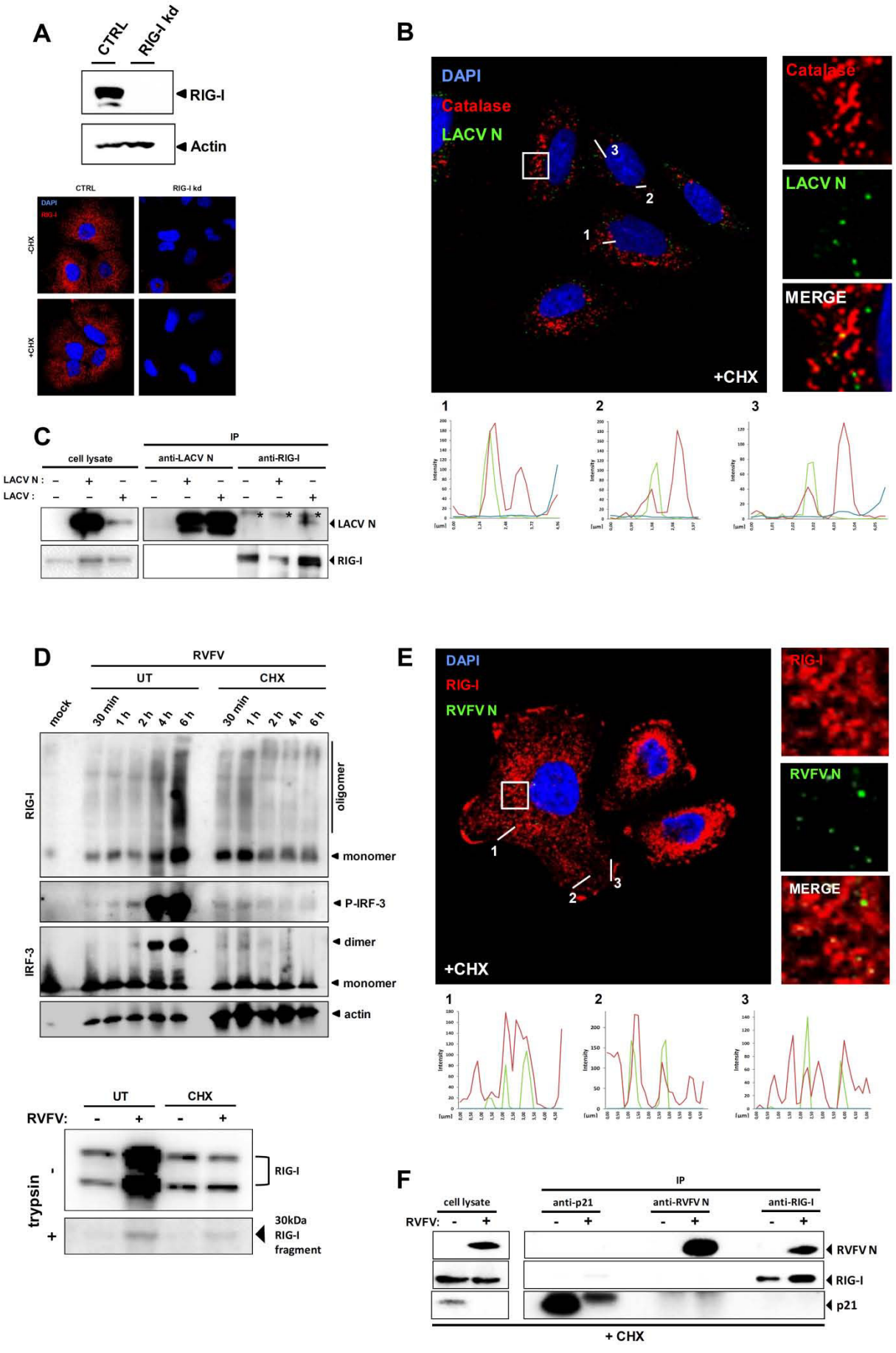
A
CTRL
RIG-I kd
RIG-I
Actin
CTRL
RIG-I kd
-CHX
+CHX
B
DAPI
Catalase
LACV N
MERGE
+CHX
1
2
3
C
IP
cell lysate
anti-LACV N
anti-RIG-I
LACV N :
LACV :
LACV N
RIG-I
D
RVFV
UT
CHX
mock
30 min
1 h
2 h
4 h
6 h
RIG-I
oligomer
monomer
P-IRF-3
IRF-3
dimer
monomer
actin
UT
CHX
RVFV:
trypsin
RIG-I
30kDa
RIG-I
fragment
E
DAPI
RIG-I
RVFV N
MERGE
+CHX
1
2
3
F
IP
cell lysate
anti-p21
anti-RVFV N
anti-RIG-I
RVFV:
RVFV N
RIG-I
p21
+ CHX

Figure S4. Companion Experiments and Controls for the Interaction of RIG-I with Viral Nucleocapsids (related to Figure 4)

(A) RIG-I signal in knock-down cells. A549 cells were transfected with a negative control siRNA (CTRL), or with an siRNA against RIG-I. After two rounds of transfection, cells were tested for the presence of RIG-I by Western blot (upper panel) and immunofluorescence analysis (lower panel). **(B) Co-localization of LACV nucleocapsids with peroxisomes.** CHX-treated A549 cells were infected with LACVdelNSs (MOI 5) and 5 h later analyzed by immunofluorescence using rabbit and mouse antisera directed against LACV N (green channel) or catalase as a marker for peroxisomes (red channel), respectively. Cell nuclei were counterstained with DAPI (blue channel). The square area of the inset is digitally magnified on the right hand side. Three fluorescence intensity profiles (numbered 1 to 3) are shown on the bottom. **(C) Only viral nucleocapsids, but not the nucleocapsid protein alone, interact with RIG-I.** A549 cells were either untreated, transfected for 24 h with plasmid pI.18-LACV N, or infected for 5 h with LACVdelNSs (MOI of 5). Cells were lysed in RIPA buffer and subjected to immunoprecipitation (IP) for LACV N or RIG-I and analyzed by Western blot. As input control, 10% of the cell lysate were analyzed in parallel (left lanes). * indicate unspecific bands. **(D) Activation of RIG-I and IRF-3 by RVFV.** (Upper panel) A549 cells were treated with 0 or 50 µg/ml CHX and then infected with RVFVΔNSs::REN at an MOI of 5. After the indicated incubation periods, cells were lysed in PBS / 0.5% Triton X-100 and analysed for oligomerization of RIG-I and IRF-3, and for phosphorylation of IRF-3. (Lower panel) RIG-I conformational switch assay of A549 cells treated with CHX and infected for 5 h with RVFVΔNSs:REN. **(E) Co-localization of RIG-I with RVFV nucleocapsids.** CHX-treated A549 cells were infected with RVFVΔNSs::GFP (MOI 5) for 5 h and analyzed by immunofluorescence using a rabbit antiserum against RVFV N (1:5000; green channel) and mouse polyclonal antiserum against RIG-I (1:200; red channel), respectively. Cell nuclei were counterstained with DAPI (blue channel). The square area of the inset is digitally magnified on the right hand side. Three fluorescence intensity profiles (numbered 1 to 3) are shown on the bottom. **(F) Co-immunoprecipitation of RIG-I and RVFV nucleocapsids.** CHX-treated A549 cells were infected with RVFVΔNSs::GFP (MOI 5) and 5 h later lysed in RIPA buffer. Lysates were subjected to immunoprecipitation (IP) using rabbit antiserum against RVFV N (1:1000), mouse monoclonal anti-RIG-I antibody ALME-1 (1:1000), or mouse monoclonal anti-p21 (1:500). As input control, 10% of the cell lysate were analyzed in parallel (left lanes).

Figure S5

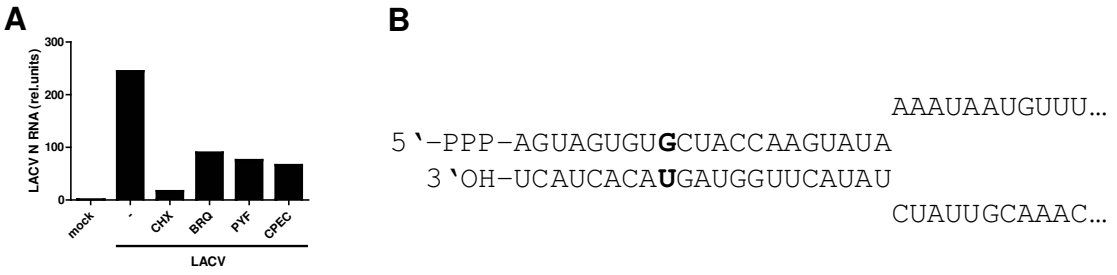

Figure S5. Control Experiment and Illustration for the Activation of RIG-I by the Viral Panhandle (related to Figure 6).

(A) Effect of NTP withdrawal on LACV RNA synthesis. A549 cells pretreated with different inhibitors were infected with LACVdelNSs for 5 h at an MOI of 5. Before and during the infection period, the cell culture medium contained either no additive (-), CHX (50 µg/ml) added 1 h before infection, or BRQ (10 µM, stocks dissolved in DMSO), MA (10 µM, stocks dissolved in methanol), PYF (10 µM, stocks dissolved in DMSO), or CPEC (5 µM, stocks dissolved in DMSO) added 24 h before infection. Total cellular RNA was isolated and analyzed by real-time RT-PCR using primers specific for the LACV N RNA (Verbruggen et al., 2011). **(B) LACV panhandle structure.** The first 32 nucleotides of the 5' and 3' LACV M genome segment (Genbank acc # NC_004109) are depicted as an example. Note that the non-Watson–Crick base pair G-U (bold face characters) does not disturb the dsRNA structure (Holbrook et al., 1991).

Figure S6

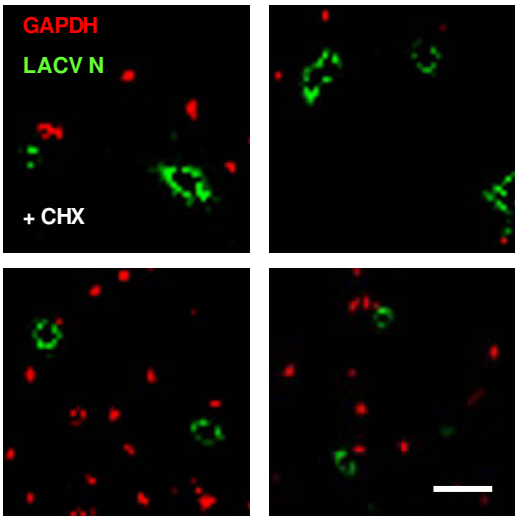

Figure S6. Super-Resolution Immunofluorescence Microscopy of GAPDH and LACV Nucleocapsids (related to Figure 7). A549 cells were treated with 50 µg/ml CHX and infected with LACVdelNSs (MOI 5). Cells were analyzed 5 h later by GSD double immunofluorescence using antisera against LACV N (green channel) or glyceraldehyde-3-phosphate dehydrogenase (GAPDH, red channel). The primary antibody anti-GAPDH mouse monoclonal 9B3 (HyTest) was diluted 1:100. Four example areas with nucleocapsids are shown. Scale bar 200 nm.

Supplemental Experimental Procedures

Primers for real-time RT-PCR

mRNAs of human IFN-β, ISG56, and γ-actin were measured with QuantiTect primers QT00203763, QT00201012, and QT00996415, respectively. mRNAs of murine IFN-β, ISG56, and GAPDH were measured with QuantiTect primers QT00249662, QT01161286, and QT01658692, respectively.

Short interfering RNAs

AllStar Negative Control siRNA and validated FlexiTube siRNAs (Qiagen) against RIG-I mRNA (SI03649037) and MDA5 mRNA (GS23586) were used.

Chemical inactivation of virus particles

Virus stocks containing 0.05% β-propiolactone (Acros Organics) were incubated at 4° C for 16 h. β-propiolactone was subsequently hydrolyzed by incubating samples at 37° C for 2 h.

Homodimerisation and phosphorylation of IRF-3

A549 cells were grown to 80% confluency in T25 flasks. Cell lysis and native-polyacrylamide gel electrophoresis (PAGE) were performed as described (Iwamura et al., 2001), with minor modifications. Briefly, cells were lysed in 0.5% Triton X-100 dissolved in PBS supplemented with protease inhibitor cocktail (Roche) and incubated on ice for 10 min. Lysates were sonified in a Branson 3200 Ultrasonic cleaner for 10 min at 4°C and then centrifuged at 4°C for 10 min at 10,000×g. Protein concentration was determined by Bradford assay (BioRad) and 50 μg of total protein lysate were separated by electrophoresis in a nondenaturing 8% polyacrylamide gel, with 1% sodiumdeoxycholate in the cathode buffer. Total IRF-3 and phosphorylated IRF-3 monomers and oligomers were detected by Western blot analysis with rabbit polyclonal anti-IRF-3 antibody FL-425 (1:500, Santa Cruz Biotechnology) or rabbit monoclonal anti-P386-IRF-3 (1:100, IBL), respectively. β-actin, detected by mouse monoclonal antibody 8H10D10 (1:1000, Cell signaling) served as a loading control.

Subcellular localization of IRF-3

Cells were analyzed by immunofluorescence (see Experimental Procedures) using the FL-425 rabbit polyclonal anti-IRF-3 as primary antibody (1:500, Santa Cruz Biotechnology). And goat anti-rabbit Cy2 conjugated as secondary antibody.

Real-time RT-PCR for detection of viral sequences

Total cellular RNA was isolated with the NucleoSpin RNA II kit (Macherey-Nagel) and eluted in 30 µl of ddH_2O. An aliquot of 600 ng RNA was then used as a template for cDNA synthesis. For detection of FLUAV and VSV sequences, reverse transcription was performed using the Qiagen QuantiTect Reverse Transcription Kit using the (-) strand specific forward primers 5'-GAT AGT ACC GGA GGA TTG ACG ACT A-3' (VSV) and 5'-GGA CTG CAG CGT AGA CGC TT-3' (FLUAV). PCR was performed using QuantiTect SYBR Green PCR Kit and the respective forward primers, combined with the reverse primers 5'- TCA AAC CAT CCG AGC CAT TC-3' (VSV) and 5'- CAT CCT GTT GTA TAT GAG GCC CAT-3' (FLUAV). For detection of LACV, PHV and SFV sequences, the one-step QuantiTect SYBR Green RT-PCR Kit was used. Primer sequences were 5'-GGG TAT ATG GAC TTC TGT G-3' and 5'-GCC TTC CTC TCT GGC TTA-3' (LACV S segment forward and reverse (Verbruggen et al., 2011)), 5'-CTC AAA ATT GGC AGC TAC A-3' and 5'-CTT CAC CGG CAG GCT G-3' (PHV S segment forward and reverse, and 5'-GCA AGA GGC AAA CGA ACA GA-3' and 5'-GGG AAA AGA TGA GCA AAC CA-3' (SFV nsp3 forward and reverse (Fragkoudis et al., 2008)). mRNA levels of human γ-actin were detected with QuantiTect primers QT00996415. All virus-specific values were normalized against the γ-actin mRNA signal using the ddCT method. Up-regulation of viral sequences is depicted in relation to non-stimulated, non-infected (mock) cells.

Supplemental References

Bird, B.H., Bawiec, D.A., Ksiazek, T.G., Shoemaker, T.R., and Nichol, S.T. (2007). Highly sensitive and broadly reactive quantitative reverse transcription-PCR assay for high-throughput detection of Rift Valley fever virus. J Clin Microbiol *45*, 3506-3513.

Fragkoudis, R., Chi, Y., Siu, R.W., Barry, G., Attarzadeh-Yazdi, G., Merits, A., Nash, A.A., Fazakerley, J.K., and Kohl, A. (2008). Semliki Forest virus strongly reduces mosquito host defence signaling. Insect Mol Biol *17*, 647-656.

Holbrook, S.R., Cheong, C., Tinoco, I., Jr., and Kim, S.H. (1991). Crystal structure of an RNA double helix incorporating a track of non-Watson-Crick base pairs. Nature *353*, 579-581.

Iwamura, T., Yoneyama, M., Yamaguchi, K., Suhara, W., Mori, W., Shiota, K., Okabe, Y., Namiki, H., and Fujita, T. (2001). Induction of IRF-3/-7 kinase and NF-kappaB in response to double- stranded RNA and virus infection: common and unique pathways. Genes Cells *6*, 375-388.

Kortekaas, J., Oreshkova, N., Cobos-Jimenez, V., Vloet, R.P., Potgieter, C.A., and Moormann, R.J. (2011). Creation of a nonspreading Rift Valley fever virus. J Virol *85*, 12622-12630.

Verbruggen, P., Ruf, M., Blakqori, G., Overby, A.K., Heidemann, M., Eick, D., and Weber, F. (2011). Interferon antagonist NSs of La Crosse virus triggers a DNA damage response-like degradation of transcribing RNA polymerase II. J Biol Chem *286*, 3681-3692.

4.3. Influenza virus adaptation PB2-627K modulates nucleocapsid recognition by the pathogen sensor RIG-I

Own contribution:

I performed or contributed to all experiments. Work in biosafety level 3 was performed by Hanna Sediri (group of Prof. Dr. Klenk, Institute for Virology, Marburg) while I performed analysis of the samples. I contributed to writing of the manuscript.

Michaela Gerlach

Influenza virus adaptation PB2-627K modulates nucleocapsid inhibition by the pathogen sensor RIG-I

Michaela Weber[1], Hanna Sediri[1], Ulrike Felgenhauer[1], Ina Binzen[1], Sebastian Bänfer[2], Ralf Jacob[2], Linda Brunotte[3], Adolfo García-Sastre[4,5,6], Jonathan L. Schmid-Burgk[7], Tobias Schmidt[7], Veit Hornung[7], Georg Kochs[3], Martin Schwemmle[3], Hans-Dieter Klenk[1], and Friedemann Weber[1*]

[1]Institute for Virology, Philipps-University Marburg, D-35043 Marburg, Germany.

[2]Department of Cell Biology and Cell Pathology, Philipps-University Marburg, D-35043 Marburg, Germany.

[3]Institute for Virology, University Medical Center, D-79008 Freiburg, Germany.

[4]Department of Microbiology,

[5]Department of Medicine, Division of Infectious Diseases, and

[6]Global Health and Emerging Pathogens Institute, Icahn School of Medicine at Mount Sinai, New York, New York 10029, USA.

[7]Institute of Molecular Medicine, University Hospital, University of Bonn, D-53127 Bonn, Germany.

*corresponding author: Tel.: +49-6421 2864525

Fax: +49-6421 2868962

E-mail: friedemann.weber@staff.uni-marburg.de

Running title: Influenza virus PB2-627K counteracts RIG-I

Key words: influenza virus; nucleocapsids; 5' triphosphate dsRNA; panhandle; RIG-I; signaling-independent virus inhibition; PB2-627K; PB2-627E

Summary

The cytoplasmic RNA helicase RIG-I plays a key role in innate immune-sensing of RNA viruses and antiviral signaling. We show that RIG-I recognizes incoming nucleocapsids of influenza A virus (FLUAV) during their short cytoplasmic transit to the nucleus. RIG-I activation was mediated by 5'-triphosphorylated dsRNA on nucleocapsids and modulated by polymorphisms at position 627 of polymerase subunit PB2. Avian FLUAV nucleocapsids possessing PB2-627E were prone to an increased RIG-I recognition as compared to those with mammalian-adapted PB2-627K. Previously known phenotypes of PB2-627E in mammals such as delayed onset of infection and reduced nucleocapsid stability were partially restored in RIG-I-defective cells. The inhibitory effect of RIG-I on PB2-627E nucleocapsids was independent of antiviral signaling. These results identify RIG-I as a directly acting mammalian restriction factor for avian FLUAV and highlight nucleocapsid disruption as a promising target for antiviral therapy.

Highlights

- ► 5’ppp dsRNA panhandle of incoming influenza virus nucleocapsids activates RIG-I
- ► Human-adaptive mutation PB2-627K counteracts activation of RIG-I
- ► RIG-I directly inhibits incoming nucleocapsids with the avian PB2-627E signature
- ► Strength of polymerase binding to NP determines the sensitivity to RIG-I

Introduction

Influenza A viruses (FLUAV; family *Orthomyxoviridae*) are a significant health threat. Regular, global outbreaks are occuring due to replenishment from a seemingly unlimited reservoir of strains in birds (Cauldwell et al., 2014; Klenk, 2014; Manz et al., 2013). FLUAV virions consist of a lipid envelope with the glycoproteins HA and NA, that also provide the basis for taxonomic classification, as well as the proton channel M2. The inner leaflet of the viral envelope is covered by the M1 protein. Inside the particles are eight nucleocapsids containing the negative-strand RNA genome encapsidated by the nucleoprotein (NP) and associated with the RNA polymerase complex with subunits PB1, PB2, and PA. The eight genome segments encode the main structural proteins, auxiliary proteins (NS1, NEP), and sometimes other, strain-dependent, factors. Gene expression is regulated by partially complementary 5` and 3` end sequences (the "panhandle") that pseudo-circularize the single-stranded RNA genome and serve as promoter for transcription and replication. An outstanding feature of FLUAV is that most parts of the replication cycle occur in the nucleus.

RIG-I (Retinoic acid-inducible gene I) is an RNA helicase that acts as a major host sensor for virus infections in the cytoplasm (Yoo et al., 2014). RIG-I recognizes non-self RNA structures and activates a signaling cascade leading to phosphorylation of transcription factor IRF3 and induction of the antiviral type I interferons (IFN-α/β).

RIG-I contains a central multipartite helicase/ATPase domain flanked by N-terminal caspase recruitment domains (CARDs) and a C-terminal domain (CTD) (Yoo et al., 2014). Unstimulated RIG-I is in an auto-repressed, monomeric conformation with the CARDs confined and the CTD exposed. When the CTD binds a ligand RNA, RIG-I undergoes a conformational switch enabling it expose the CARDs for interaction with TRIM25 and MAVS to initiate antiviral signaling (Gack, 2014; Kowalinski et al., 2011; Rawling and Pyle, 2014).

Synthetic short 5'ppp-dsRNA represents the optimal RIG-I ligand (Schlee et al., 2009; Schmidt et al., 2009), a structure with remarkable similarity to the panhandle formed by the annealed 5' and 3' genome ends of segmented negative-strand RNA viruses (Schlee, 2013; Weber and Weber, 2014b). Accordingly, naked genomic RNA of FLUAV and other negative-strand RNA viruses is an excellent activator of RIG-I (Habjan et al., 2008; Hornung et al., 2006; Pichlmair et al., 2006). We recently reported that RIG-I is capable of recognizing 5'ppp-dsRNA panhandles also in the physiological context, when packaged by viral nucleoprotein and polymerase into nucleocapsids (Weber et al., 2013). That study, however, had focused on the cytoplasmically replicating bunyaviruses. Therefore, it remained open whether the panhandles of FLUAV nucleocapsids could also be sensed by the cytoplasmic RIG-I, and whether this occurs during the passage of the incoming nucleocapsids from the endosome to the nucleus early in infection. Here, we report that the transiting FLUAV nucleocapsids are indeed recognized and directly impaired by RIG-I, and that the degree of RIG-I sensitivity varies depending on adaptive mutations in the polymerase subunit PB2.

Results

Activation of RIG-I by incoming FLUAV nucleocapsids

At the onset of infection, the nucleocapsids of FLUAV are released from endosomes to be transported through the cytoplasm and into the nucleus. Only there they start primary transcription, followed by translation and genome replication. To investigate the interaction between incoming nucleocapsids (and not their RNA products arising later on) and RIG-I in the cytoplasm, we (i) synchronized infection by incubating the virus inoculum at 4°C for 1 h, (ii) allowed the subsequent infection at 37°C to proceed for only 1 h, and (iii) added various inhibitors to ensure restriction to the immediate early infection phase. The inhibitors were Cycloheximide (CHX; blocks protein synthesis and therefore viral genome replication), leptomycin B (LMB; inhibits nuclear export of nucleocapsids), and actinomycin D (ActD; inhibits viral transcription) (Figure S1A). In addition, we tested Ivermectin (IVM) which is known to block the nuclear import machinery (Wagstaff et al., 2012). Human A549 cells were pretreated with one or several of the inhibitors, and 1 h-infected with strain A/PR8/34 (H1N1) at a multiplicity of infection (MOI) of 1 as outlined above. Irrespective of the inhibitor, incoming FLUAV nucleocapsids triggered two markers of RIG-I activation: the formation of homo-oligomers (Figure 1A), and the conformational switch reflected by a partial trypsin resistance (Figure 1B). RIG-I activation by incoming nucleocapsids was comparable to levels obtained by 1 h-transfection of naked virus particle RNA (vRNA). Quantification by RT-qPCR demonstrated the expected absence of viral RNA synthesis (Figures 1C and S1B). In line with this, transcription inhibition by various NTP depleting agents also had no influence on RIG-I activation by FLUAV (Figure S1C). Nonetheless, not only RIG-I, but also its downstream target IRF3 were activated by the incoming nucleocapsids (Figure 1D). It must be remarked that in all our experiments, virus stocks were used which were free of defective interfering particles (data not shown), a known activator of RIG-I (Baum et al., 2010).

Moreover, in agreement with a previous study (Killip et al., 2014) we noted that addition of ActD to the mix containing CHX and LMB results in occasional background activation of antiviral signaling in uninfected cells (data not shown). We therefore conducted the majority of subsequent experiments with CHX/LMB treatment and within the short, 1 h-period of synchronized infection, conditions that were optimal for robustly studying interactions of RIG-I with incoming nucleocapsids.

RIG-I binds to the panhandle on FLUAV nucleocapsids

Confocal microscopy revealed that the incoming nucleocapsids are co-localizing with RIG-I, but not with the related helicase MDA5 (Figure S2A and data not shown). Superresolution microscopy suggests that RIG-I directly attaches on one side of the rod-like nucleocapsids (Figure 2A). The stability of these co-complexes was tested by pull-down experiments. Although the viral input was barely detectable as expected for a 1 h infection, the RIG-I immunoprecipitates contained enriched amounts of NP (Figure 2B), indicating interaction of RIG-I with incoming nucleocapsids. Again, this was not dependent on viral RNA synthesis (Figure S2B). When cell lysates were separated in a CsCl gradient, we observed a partial, virus-induced shift of RIG-I from higher density fractions towards the lower density fractions which also contained the nucleocapsids (Figure 2C; fractions 7,8,9 in uninfected cells vs fractions 3,4 and 6 in infected cells). RIG-I was also activated and shifted towards lower density CsCl fractions when its ATPase activity was inhibited with ADP●AlF_3, suggesting that complex formation is independent of downstream events (Figures S2C-S2E). We also used our insect cell / *in vitro* system (Weber et al., 2013). Extracts of *Drosophila* S2 cells expressing human RIG-I were dialyzed and supplemented with ATP (to support RIG-I activation). The recombinant RIG-I reacted to purified and dialyzed FLUAV nucleocapsids by conformational switching, oligomerization, and a shift of RIG-I fractions in the CsCl gradient (Figure S2F-S2H). To test the structural determinants of RIG-I activation, purified

FLUAV nucleocapsids were pretreated *in vitro* with enzymes. Both destruction of dsRNA by RNase III as well as cleavage of the 5'ppp by a phosphatase aborted RIG-I stimulation, whereas the ssRNA-specific RNase A had no such effect (Figure 2D). Importantly, RIG-I activation did not depend on the specific nucleocapsid preparation method, and was also observed for nucleocapsids that were affinity-purified via a Strep-tagged PB2 subunit (Figure S2I-S2K). Also cotransfection experiments demonstrated that the pull-down of NP by RIG-I is dependent on the genomic RNA, and not on protein-protein interactions (see below). Together, these data suggest that RIG-I directly interacts with the 5'ppp dsRNA panhandle on intact FLUAV nucleocapsids and in a manner that is independent of mammalian cofactors or viral RNA synthesis.

PB2 is a RIG-I antagonist

Avian FLUAV strains need to acquire adaptive mutations to establish infection in mammals. A major determinant of host switching and virulence is the polymerase subunit PB2 (Hatta et al., 2001). PB2 position 627, in particular, carries in avian strains a glutamic acid (E), but in most mammalian-adapted strains a lysine (K) (Subbarao et al., 1993). The reason for the mammalian selection pressure towards PB2-627K is not fully understood (Cauldwell et al., 2014; Manz et al., 2013). Interestingly, however, chicken are known to be deficient in RIG-I (Barber et al., 2010). Using the conformational switch assay, we investigated whether RIG-I might be involved in the mammalian-specific effects on avian-signature PB2 polymerases. Human A549 cells were exposed to the immediate early infection phase of variants of four FLUAV strains, A/quail/Shantou/2061/00 (H9N2), A/Thai/KAN-1/04 (H5N1), pandemic A/Hamburg/05/2009 (pH1N1), or A/WSN/33 (H1N1). In all cases, those viruses with the avian signature PB2-627E activated RIG-I much stronger than those with the mammalian signature PB2-627K (Figure 3A and S3A). These differences were not due to variations in input RNA or RNA synthesis, as viral RNA levels were comparable and did not increase

during the 1 h-experiment (Figure 3B and S3B-S3D). Also in CsCl gradient assays, we observed a more pronounced shift of RIG-I fractions in response to a PB2-627E virus (Fig. 3C, left panels). The PB2-627E virus also relocalized the RIG-I interactors MAVS and TRIM25 (Fig. 3C, right panels), further supporting the notion of a stronger RIG-I activation by the avian-signature nucleocapsids.

The A/PR/8/34 strain used for the initial RIG-I activation experiments (see Figures 1 and 2) contains PB2-627K (Foeglein et al., 2011). A comparison of A/PR/8/34 with PB2-627K and -627E variants of A/WSN/33 (H1N1) demonstrates its relatively weak RIG-I activation potential (Figure S3E), thus being in line with the correlation between reduced RIG-I activation and the PB2-627K signature. Virus-like particles containing a A/WSN/33 (H1N1) reporter minigenome (VLPs) showed the same PB2-627-dependent phenotype, independent of the particular envelope protein (Figure S3F). This confirms that nucleocapsids are the critical component. As expected, RIG-I activation by PB2-627E virus was independent of any viral RNA synthesis (Figure S3G). We also measured IFN induction obtained after overnight infection by the different FLUAV strains, again under CHX and LMB. Surprisingly, despite the clear effects on RIG-I activation described above, there were no consistent PB2-627-dependent differences in IFN induction, both in wt and in RIG-I- depleted knockdown cells (Figure 3D and S3H). Of note, human-adapted PB2-627K has a higher polymerase activity in mammalian cells (Naffakh et al., 2000), but nonetheless activated RIG-I much weaker than PB2-627E. This again argues against RNA synthesis as a trigger of RIG-I. Collectively, our data indicate that the adaptive mutation PB2-E627K represents a viral countermechanism to RIG-I recognition, even if it has no significant effect on IFN induction.

158 **RIG-I influences infection by incoming PB2-627E nucleocapsids**

159 PB2-627E confers reduced polymerase activity in mammalian cells, whereas in avian cells the
160 activity is similar to PB2-627K (Massin et al., 2001; Paterson et al., 2014). The species-
161 specific differences were attributed to a mammalian restriction factor acting on PB2-627E
162 only (Mehle and Doudna, 2008). We wondered whether RIG-I could be contributing to PB2-
163 627E suppression in mammalian cells. The classic assay for measuring FLUAV polymerase
164 activity is the minireplicon reporter system, consisting of plasmid-expressed polymerase
165 subunits and NP that encapsidate, transcribe and replicate a reporter minigenome bearing
166 panhandle sequences. Minireplicon activity in human 293 wt cells confirmed the difference
167 between the two PB2 variants (Figure 4A). We generated knockout 293 cells (Figure S4A) to
168 test the effect of RIG-I on minireplicon activity, but could not detect major differences to wt
169 cells or *MDA5* knockout cells (see Figure 4A). It needs to be noted, however, that here the
170 recombinant nucleocapsids are not entering the cytoplasm like in infection, but are artificially
171 assembled in the nucleus by the plasmid-encoded proteins. Thus, as an alternative closer to
172 the immediate early infection situation, we employed VLPs containing recombinant FLUAV
173 nucleocapsids. Reporter activity in the 293 wt cells used to produce VLPs for strain
174 A/WSN/33 (H1N1) differed between the two PB2 variants, as expected (Figure 4B and S4B).
175 However, VLPs with PB2-627E re-gained considerable activity upon infection of Δ*RIG-I*
176 cells, but not in wt cells or Δ*MDA5* cells (Figure 4C). Curiously, in cells that lacked the RIG-I
177 adaptor MAVS, PB2-627E could also not be rescued, suggesting that signaling may not be
178 necessary (see below). We also tested the influence of RIG-I on viral multiplication. To
179 obtain multicycle growth, we infected 293 wt or Δ*RIG-I* cells for 24 h with MOI 0.0001 of
180 PB2 variants of strain A/Thai/KAN-1/04 (H5N1). The absence of RIG-I rescued the low
181 yields of the PB2-627E virus by one order of magnitude, whereas the PB2-627K virus was
182 slightly reduced (Figure 4D). Overall, the approximately 50.000 fold growth difference
183 between the PB2 signature viruses in wt cells decreased to 400 fold in Δ*RIG-I* cells. Since

RIG-I is activated by nucleocapsid entry, we also monitored the initial establishment of infection. Wt or Δ*RIG-I* cells were infected with MOI 1, and the synthesis of NP assayed for 8 h. For PB2-627K viruses, NP was detected from 4 h p.i. on in both cell types (Figures 4E, S4C and S4D). For the PB2-627E virus, by contrast, NP was detected at 8 h p.i. in wt cells, but from 6 h on in Δ*RIG-I* cells. Since viral entry is neither affected by the PB2 signature nor by the cell genotype (Figure S4E), we conclude that RIG-I targets PB2-627E-type nucleocapsids during the onset of infection.

Species- and signaling-independent antiviral effect of RIG-I

An unexpected result of our VLP infection experiments (see figure 4C) was that the attenuated phenotype of incoming PB2-627E nucleocapsids was not rescued by deleting the signaling adaptor *MAVS*. Similarly, also virus with PB2-627E was delayed in Δ*MAVS* cells (Figure 5A). To investigate this further, we transcomplemented Δ*RIG-I* cells with an ATPase-negative RIG-I mutant (K270A) that is unable to signal but still able to bind RNA (Takahasi et al., 2008). Strikingly, the RIG-I K270A mutant was as potent as wt RIG-I in delaying the onset of PB2-627E virus and VLP infection (Figures 5B and S5). This is in line with our observation that chemical ATPase inhibition of RIG-I does not impede activation and nucleocapsid binding (see Figures S2C to S2E). Transcomplementation with human RIG-I also endowed chicken cells with the ability to slow down PB2-627E virus infection (Figure 5C). Again, this was independent of antiviral signaling. These data suggest that the binding of RIG-I to incoming nucleocapsids (see Figs. 2 and S2) is sufficient to delay infection by FLUAV strains with the avian PB2-627E signature. Thus, RIG-I signaling may not be required for the restriction of avian strains early in infection.

Nucleocapsid stability influences RIG-I binding and sensitivity

209 The 627K adaptation is known to increase the binding of PB2 to NP (Labadie et al., 2007).
210 Although this had been disputed as an artefact of the stronger polymerase activity (and hence
211 nucleocapsid formation) by PB2-627K (Cauldwell et al., 2013), others had shown stronger
212 NP binding by PB2-627K also in a nucleocapsid-free *in vitro* system (Ng et al., 2012). In our
213 immediate-early infection setup, infection occured for 1 h and the formation of daughter
214 nucleocapsids was impossible due to CHX treatment. Nonetheless, also under these
215 conditions NP co-precipitated more PB2-627K than PB2-627E, confirming the adaptation-
216 specific differences in binding affinity (Figure 6A). Moreover, NP / PB2-627E interactions
217 slightly increased in Δ*RIG-I* cells that were infected (see Figure 6A) or are harbouring
218 minireplicon systems (Figures S6A and S6B).
219 RIG-I directly interacts with the panhandles of FLUAV nucleocapsids (see Figures 2D and
220 S2K). Interestingly, RIG-I pulled down more incoming nucleocapsids of the PB2-627E type
221 than of the PB2-627K type (Figure 6B). Moreover, the PB2 protein of the 627K type was
222 found to be co-precipitated, but not PB2 of the 627E type. Similar results were obtained with
223 recombinant nucleocapids of the minireplicon system, an experimental set-up that also
224 allowed to demonstrate that RIG-I-NP interactions are depending on the encapsidated genome
225 RNA (Figure 6C). Thus, nucleocapsids of the PB2-627E type are more efficiently bound by
226 RIG-I.
227 The lower affinity of PB2-627E to NP may enable RIG-I to better access the nucleocapsid-
228 borne panhandle RNA. This would implicate that the strength of the polymerase -
229 nucleocapsid interaction influences RIG-I activity. To directly test this hypothesis, we
230 disrupted the polymerase complex with a PB1-derived peptide (PB1-T6Y) (Wunderlich et al.,
231 2011). The inhibitor peptide massively increased RIG-I activation by incoming nucleocapsids,
232 and independent of the PB2-627 signature (Figures 6D and S6C). Thus, the strength of
233 polymerase binding, modulated either naturally (by PB2 mutation) or artificially (by
234 disrupting PB1-PA interactions), sensitizes nucleocapsids to RIG-I.

In summary, our results indicate that FLUAV nucleocapids are prone to signaling-independent RIG-I inhibition during their passage through the cytoplasm early in infection. RIG-I recognizes the panhandle structure on the viral genome RNA, which is normally bound by the polymerase complex. The sensitivity to RIG-I is determined by the well known host adaptation at PB2-627, which affects the binding affinity of PB2 to nucleocapsids. Thus, RIG-I apparently represents one of the mammalian restriction factors driving adaption of avian FLUAV strains towards tighter polymerase binding.

Discussion

An outstanding feature of influenza viruses is the replication in the nucleus. This allows access to the cellular transcription and splicing machineries, and - as our results suggest - the hiding from cytoplasmic RIG-I during most phases of the infection cycle. In fact, since orthomyxoviruses are also unique with respect to the unusually high number of genome segments (and hence RIG-I ligands), it is possible that moving into the nucleus initially evolved as a RIG-I counterstrategy. In line with this, efficient interaction with the nuclear import machinery was shown to be a determinant of host adaptation (Gabriel et al., 2011; Hudjetz and Gabriel, 2012; Resa-Infante et al., 2008). However, the virus remains vulnerable during the transit to the nucleus, since at this stage of infection neither the classic IFN antagonist NS1 (Hale, 2014) nor the host response suppressors PA-X (Jagger et al., 2012) or PB1-F2 (Varga et al., 2011) would be expressed. Therefore, it appears plausible that the nucleocapsids themselfes have to cope with the pathogen recognition system, an assumption that is in agreement with our data and also with previous reports that FLUAV polymerase subunits can prevent IFN induction (Marcus et al., 2005; Perez-Cidoncha et al., 2014) and interact with RIG-I and MAVS (Graef et al., 2010; Iwai et al., 2010; Li et al., 2014; Liedmann et al., 2014). Moreover, for influenza B virus it was demonstrated that nucleocapsids were sufficient to induce IFN, whereas for FLUAV RNA synthesis was required (Osterlund et al., 2012). These comparative data again point towards nucleocapsids being able to both induce or suppress innate immunity, dependent on the genetic background.

The connection between RIG-I activation and IFN induction is not straightforward. Avian FLUAV strains that strongly activated RIG-I were in fact weaker or equal IFN inducers than the mammalian strains whose nucleocapsids had inhibited RIG-I. Most likely, the underlying reason is found in the differences in RNA polymerase activities, which are inseparable from the RIG-I inhibition capacity. While PB2-627E nucleocapsids have low RNA synthesis rates but are strong activators of RIG-I, PB2-627K nucleocapsids have a highly active polymerase

but inhibit RIG-I. Thus, the RIG-I inhibition by PB2-627K might be overwhelmed by the higher RNA synthesis rate.

It was previously stated that IFN induction by FLUAV occurs exclusively through RNA synthesis products (Killip et al., 2014; Osterlund et al., 2012). However, we observed IRF3 activation by incoming nucleocapsids even when viral transcription was shut off by ActD treatment. This appears to contradict the results by Killip *et al.*, who had not seen any such IRF3 activation (Killip et al., 2014). However, in that study IRF3 was assayed at 8 h post-infection, a time point at which IRF3 activity may have waned, as IRF3 returns to the inactive state in case of low inducers (Long et al., 2014). We therefore propose that incoming FLUAV nucleocapsids can activate RIG-I and antiviral signaling, similar to those of influenza B virus (Osterlund et al., 2012) and the cytoplasmic RNA viruses (Weber et al., 2013). IFN induction by nucleocapsids is however comparatively weak and the subsequent RNA synthesis becomes the dominant IFN elicitor once the nucleocapsids have reached the nucleus.

Although PB2-627K had no apparent bearing on IFN induction, for PB2-627E viruses and VLPs the establishment of infection was slowed down by RIG-I. Strikingly, while deletion of *RIG-I* accelerated infection by avian strains, deletion of the downstream adaptor *MAVS* did not. Moreover, a signaling-inactive mutant of RIG-I was as potent as wt RIG-I itself in slowing down PB2-627E viruses. It is therefore likely that the binding of RIG-I to the panhandle RNA results in a direct (although transient) antiviral effect against avian strains. The mammalian-adapted nucleocapsids are more efficient in hiding their panhandle, and it could be speculated this to be due to the stronger binding of the PB2 to the NP. The signaling-independent antiviral effect may also explain why RIG-I follows the nucleocapsids into the nucleus at the late stage of infection (Li et al., 2014).

Besides PB2-627K, there might be more factors influencing the RIG-I sensitivity of nucleocapsids. The circulating 2009 pandemic pH1N1 strains have retained the PB2-627E signature, but acquired compensating second-site mutations (Mehle and Doudna, 2009;

296 Yamada et al., 2010). Nonetheless, our direct comparisons between variants of four FLUAV
297 strains that differed only in position PB2-627 strongly indicate that this major adaptation is in
298 fact a RIG-I escape mechanism. It will be interesting to see whether other adaptive mutations
299 in the polymerase or the NP also affect RIG-I.
300 FLUAV epidemics feed from avian reservoirs. Wild bird species, e.g. ducks, express
301 functional *RIG-I*, but domestic chicken do not (Barber et al., 2010; Kowalinski et al., 2011).
302 Many avian FLUAV strains cause asymptomatic infection e.g. in ducks, but an acute systemic
303 disease in chicken (Kim et al., 2009). Populations of wild birds are comparatively disperse,
304 i.e. overt disease would reduce the chance of viral spread. Chicken, by contrast, are held
305 under crowded conditions and with a constant, non-natural replenishment of susceptible
306 individuals. A certain RIG-I sensitivity may allow FLUAV to persist in the wild bird
307 reservoir. In domestic chicken, there is no selection pressure on sparing the host, and the
308 absence of RIG-I could enable rapid viral spread. In humans, the viral transmission mode
309 requires replication to levels causing respiratory symptoms. Hence, it could be speculated that
310 mutations suppressing RIG-I activation are needed for efficient and sustainable infection of
311 humans, but not in chicken (no RIG-I) or wild birds (RIG-I enables asymptomatic infection).
312 While RIG-I appears to be acting on incoming nucleocapsids of avian-adapted viruses, other
313 host cell factors are likely to contribute to the PB2-directed host restriction during later stages
314 of infection.
315 Applying a polymerase-disrupting peptide massively increased RIG-I activation by
316 nucleocapsids. This uncovers the full potential of RIG-I and implies that even for avian-
317 adapted strains only a fraction of the nucleocapsids is actually recognized. Therefore, drugs
318 targeting the FLUAV polymerase complex will have the secondary benefit of boosting
319 antiviral host responses.

In sum, our data implicate that incoming FLUAV nucleocapsids are prone to a direct antiviral inhibition by RIG-I, and that the degree of RIG-I sensitivity is dependent on nucleocapsid stability.

Experimental Procedures

Cells and viruses

A549, HEK 293, DF-1, MDCK II, and *Drosophila* S2 cells were cultivated as described (Weber et al., 2013). FLUAV A/PR/8/34, the recombinant strains of A/quail/Shantou/2061/2000 (H9N2) (Baron et al., 2013), A/Hamburg/05/2009 (pH1N1), A/WSN/33 (H1N1), and A/WSN/33 with Strep-tagged PB2 (Rameix-Welti et al., 2009) were grown on MDCK II cells. A/Thai/KAN-1/04 (H5N1) was grown on chicken DF-1 cells (Manz et al., 2012). All viruses were entirely sequenced and confirmed to harbor only the intended mutations.

Infections

Cells were washed once with phosphate-buffered saline (PBS) and inoculated for 1 h at 4°C with virus dissolved in OptiMEM (Invitrogen) or 250 µl cell supernatant containing VLPs. The inoculum was replaced with DMEM containing 0,2% BSA and (except for VSV-G VLP infections) 1 µg/ml L-1-tosylamido-2-phenylethyl chloromethyl ketone (TPCK)-treated trypsin (Sigma-Aldrich), and cells were further incubated at 37°C.

RIG-I activation assays

Analyses of RIG-I conformation and oligomerization were described elsewhere (Weber et al., 2013; Weber and Weber, 2014a). For co-sedimentation assays from mammalian cells, cell

lysates were prepared as for co-immunoprecipitation (see below). The cleared lysates were loaded on a discontinuous 5% to 15% CsCl gradient in 20 mM Tris/HCl pH 7.9, 200 mM NaCl and centrifuged at 52,000 rpm for 2 h at 12°C in a SW60 rotor (Beckman). Altogether 12 fractions were recovered from top to bottom and pelleted at 45,000 rpm for 1 h at 4°C in a TLA45 rotor (Beckman). Pellets were dissolved in sample buffer, boiled for 5 min and analyzed by immunoblotting. Proteins were detected with rabbit polyclonal anti-A/quail/Shantou/2061/00 (H9N2) (Baron et al., 2013) at 1:8000, and the mouse monoclonals anti-RIG-I ALME-1 (Enzo Life Sciences; 1:1000), anti-MAVS (Abcam; 1:500), and anti-human TRIM25 (BD Transduction laboratories, 1:5000).

Co-sedimentation assays with S2 cell samples were performed by a similar procedure. Briefly, 50 µl dialyzed lysates (containing 100 µg protein) were mixed with 50 µl of dialyzed PR/8/34 nucleocapsids and supplemented with 1 mM ATP. After 1 h at 37°C the samples were analyzed using a discontinuous 10% to 30% CsCl gradient.

Inhibitor treatments

CHX, $CuSO_4$, ActD and IVM were purchased from Sigma Aldrich, and LMB from Biomol. Cells were pretreated with CHX (50 µg/ml, stocks dissolved in DMSO), LMB (16 nM, stocks dissolved in ethanol), ActD (1µg/ml, stocks dissolved in DMSO), or IVM (50 µM, stocks dissolved in DMSO) for 1 h before infection. Inhibitors were also included in the virus inoculum and the incubation medium. ADP●AlF_3 treatment was performed as described (Weber et al., 2013).

Immunofluorescence microscopy

For superresolution immunfluorescence by ground state depletion (GSD) microscopy, samples were prepared as described for confocal microscopy (see supplemental information) with minor modifications. As secondary antibodies donkey anti-rabbit Alexa Fluor 555

(FLUAV) and goat anti-mouse Alexa Fluor 647 (RIG-I) were used and samples were embedded in 50 mM Tris-HCl pH 8.0 dissolved in 10% Vectashield mounting medium (VectorLabs) and 90% glycerol. Analysis was performed with the Leica SR GSD microscope.

Purification of native viral nucleocapsids

MDCK II cells were seeded in 9 T175 cell culture flasks at a confluency of 40% and infected with FLUAV strain PR/8/34 at an MOI of 0.01 or left uninfected (control). Supernatants were harvested at 48 h p.i. and nucleocapsids were purified as described (Weber et al., 2013).

Co-immunoprecipitation assay

Immunoprecipitations using mouse monoclonals anti-p21 (Santa Cruz Biotechnology) and anti-RIG-I (ALME-1) were performed as described (Weber et al., 2013). Mouse monoclonal anti-NP (HB65) (Wisskirchen et al., 2011) was used at a 1:200 dilution in RIPA buffer. Mouse monoclonals anti-p21 (1:500), anti-RIG-I ALME-1 (1:1000), and rabbit polyclonal H9N2 (1:8.000) were used for immunoblotting.

Enzymatic treatment of nucleocapsids

Dialyzed nucleocapsids were treated with RNase A, RNase III, or SAP and incubated with dialyzed lysates from RIG-I-expressing S2 cells (supplemented with 1 mM ATP) as described (Weber et al., 2013).

Real-time RT-PCR

RNA was isolated from cells using the RNeasy Mini Kit (Qiagen), and 10 ng were analyzed with the one-step QuantiTect SYBR Green RT PCR kit (Qiagen) in a StepOne Real-Time-PCR-Cycler (Applied Biosystems). Cellular RNA was quantified with specific QuantiTect primers against IFN-β (QT00203763) and γ-actin (QT00996415). For detection of FLUAV

segment 7 sequences, reverse transcription was performed using the QiagenQuantiTect® Reverse Transcription Kit with the (-) strand specific forward (5'-GGA CTG CAG CGT AGA CGC TT-3') and (+) strand specific reverse primer (5'- CAT CCT GTT GTA TAT GAG GCC CAT-3'). PCR was performed using QuantiTect® SYBR® Green PCR. Values were normalized against γ-actin using the ΔΔCT method (Livak and Schmittgen, 2001). Up-regulation of inducible genes is depicted in relation to non-stimulated, non-infected (mock) cells.

siRNA knockdown

A549 cells were twice reverse-transfected with predesigned siRNAs from Qiagen (AllStar Negative Control siRNA and FlexiTube siRNAs against RIG-I (SI03649037) and MDA5 mRNA (GS23586)). For each siRNA, 25 nM were diluted in 100 µl DMEM, supplemented with 1 µl Lipofectamine RNAiMAX Reagent (Invitrogen) and incubated for 15 min at room temperature. The siRNA transfection mixes were transferred into a 24 well plate, and 1×10E5 cells dissolved in 900µl DMEM 10% FCS were seeded on top. After 48 h of incubation at 37°C with 5% CO_2, cells were harvested, and 1×10E5 cells were again reverse transfected as described above and incubated for additional 24 h at 37°C with 5% CO_2.

Generation of knockout cell lines

Using GeneJuice reagent (Merck), 2.5×10E4 HEK 293T cells were transfected with plasmids for either a Zinc finger nuclease targeting the *RIG-I* gene or for a pair of Transcription Activator-Like Effectors to Nucleases targeting the genes for *MDA5* or *MAVS*. Two days later, 0.5 cells per well were seeded into 6 96-well plates. After two weeks, colonies were trypsinized and seeded into two replica plates. The next day, one of the replicates was lysed (0.2 mg/ml proteinase K, 1 mM $CaCl_2$, 3 mM $MgCl_2$, 1 mM EDTA, 1% Triton-X-100, 10 mM Tris pH 7.5). Genotypes were obtained by sequencing PCR amplicons covering the target

site of interest (target sequences and primer sequences available upon request). For each target gene, a clone was selected that had all alleles disrupted.

VLP system

HEK293 cells were transiently transfected with plasmids in 2 µl GeneJammer (Agilent) per 1 µg DNA, and medium was changed after 4 h. VLPs for strain A/WSN/33 were generated as described (Neumann et al., 2000). HEK293 wt cells were transfected with plasmids for VSV-G oder FLUAV HA (1 µg), as well as M1 (2 µg), M2 (100 ng), NEP (1 µg), PB2-627E or PB2-627K (1 µg), PB1 (1 µg), PA (100 ng), NP (1 µg), a firefly luciferase minigenome construct (1 µg), and a Renilla luciferase construct (pRL-SV40; 75 ng). As negative control, PB2 was replaced by additional PB1 plasmid. Two days later supernatants were collected and treated with 25 U/ml Benzonase (Novagen) for 3 h at 37°C. Cleared cell supernatants were used for VLP infections of HEK293 cells (pretransfected with NP, PA, PB1 and the matching PB2) as described above. Luciferase activities were measured 48 h post transfection (VLP-producing cells) or infection (VLP-infected cells). Firefly luciferase activity was normalized against Renilla activity. Relative polymerase activity is depicted as fold induction with respect to mock control.

Peptide inhibitor treatment

A549 cells seeded at 80% confluency in T25 flasks were washed once with PBS and infected with A/Thai/KAN-1/04 (MOI 1) for 1 h at 4°C. Then, cells were treated with 10 ng/ml Borna-X-Tat or $PB1_{1\text{-}15}$ T6Y-Tat (Wunderlich et al., 2011) dissolved in medium with 0,2% BSA. At 1 h post-treatment, cells were lysed and subjected to the RIG-I conformational switch assay.

Acknowledgements

We thank Silke Stertz and Jovan Pavlovic for the kind gift of anti-PB2 and anti-NP antibodies. We are indebted to the Drug Synthesis and Chemistry Branch of the National Cancer Institute for donating NTP-depleting agents. Work in the FW laboratory is supported by the DFG grants We 2616/7-1 of SPP 1596, SFB 593 and SFB 1021, by the Forschungsförderung gem. §2 Abs. 3 Kooperationsvertrag UKGM, and by the Leibniz Graduate School EIDIS. H-DK is supported by the European Commission (FP7 project FLUPHARM), and MS by the Bundesministerium für Bildung und Forschung (FluResearchNet). Work in AG-S laboratories is partly supported by CRIP (Center for Research on Influenza Pathogenesis), an NIAID funded Center of Excellence for Influenza Research and Surveillance (CEIRS, contract # HHSN272201400008C), and by NIAD HHSN 272201000054C contract and U19AI083025 grant. The authors declare that there is no conflict of interest.

References

Barber, M.R., Aldridge, J.R., Jr., Webster, R.G., and Magor, K.E. (2010). Association of RIG-I with innate immunity of ducks to influenza. Proceedings of the National Academy of Sciences of the United States of America *107*, 5913-5918.

Baron, J., Tarnow, C., Mayoli-Nussle, D., Schilling, E., Meyer, D., Hammami, M., Schwalm, F., Steinmetzer, T., Guan, Y., Garten, W.*, et al.* (2013). Matriptase, HAT, and TMPRSS2 activate the hemagglutinin of H9N2 influenza A viruses. Journal of virology *87*, 1811-1820.

Baum, A., Sachidanandam, R., and Garcia-Sastre, A. (2010). Preference of RIG-I for short viral RNA molecules in infected cells revealed by next-generation sequencing. Proceedings of the National Academy of Sciences of the United States of America *107*, 16303-16308.

Cauldwell, A.V., Long, J.S., Moncorge, O., and Barclay, W.S. (2014). Viral determinants of influenza A virus host range. The Journal of general virology *95*, 1193-1210.

Cauldwell, A.V., Moncorge, O., and Barclay, W.S. (2013). Unstable polymerase-nucleoprotein interaction is not responsible for avian influenza virus polymerase restriction in human cells. Journal of virology *87*, 1278-1284.

Foeglein, A., Loucaides, E.M., Mura, M., Wise, H.M., Barclay, W.S., and Digard, P. (2011). Influence of PB2 host-range determinants on the intranuclear mobility of the influenza A virus polymerase. The Journal of general virology *92*, 1650-1661.

Gabriel, G., Klingel, K., Otte, A., Thiele, S., Hudjetz, B., Arman-Kalcek, G., Sauter, M., Shmidt, T., Rother, F., Baumgarte, S.*, et al.* (2011). Differential use of importin-alpha isoforms governs cell tropism and host adaptation of influenza virus. Nature communications *2*, 156.

Gack, M.U. (2014). Mechanisms of RIG-I-like receptor activation and manipulation by viral pathogens. Journal of virology *88*, 5213-5216.

Graef, K.M., Vreede, F.T., Lau, Y.F., McCall, A.W., Carr, S.M., Subbarao, K., and Fodor, E. (2010). The PB2 subunit of the influenza virus RNA polymerase affects virulence by interacting with the mitochondrial antiviral signaling protein and inhibiting expression of beta interferon. Journal of virology *84*, 8433-8445.

Habjan, M., Andersson, I., Klingstrom, J., Schumann, M., Martin, A., Zimmermann, P., Wagner, V., Pichlmair, A., Schneider, U., Muhlberger, E.*, et al.* (2008). Processing of genome 5' termini as a strategy of negative-strand RNA viruses to avoid RIG-I-dependent interferon induction. PloS one *3*, e2032.

Hale, B.G. (2014). Conformational plasticity of the influenza A virus NS1 protein. The Journal of general virology.

Hatta, M., Gao, P., Halfmann, P., and Kawaoka, Y. (2001). Molecular basis for high virulence of Hong Kong H5N1 influenza A viruses. Science *293*, 1840-1842.

Hornung, V., Ellegast, J., Kim, S., Brzozka, K., Jung, A., Kato, H., Poeck, H., Akira, S., Conzelmann, K.K., Schlee, M.*, et al.* (2006). 5'-Triphosphate RNA is the ligand for RIG-I. Science *314*, 994-997.

Hudjetz, B., and Gabriel, G. (2012). Human-like PB2 627K influenza virus polymerase activity is regulated by importin-alpha1 and -alpha7. PLoS pathogens *8*, e1002488.

Iwai, A., Shiozaki, T., Kawai, T., Akira, S., Kawaoka, Y., Takada, A., Kida, H., and Miyazaki, T. (2010). Influenza A virus polymerase inhibits type I interferon induction by binding to interferon beta promoter stimulator 1. The Journal of biological chemistry *285*, 32064-32074.

Jagger, B.W., Wise, H.M., Kash, J.C., Walters, K.A., Wills, N.M., Xiao, Y.L., Dunfee, R.L., Schwartzman, L.M., Ozinsky, A., Bell, G.L.*, et al.* (2012). An overlapping protein-coding region in influenza A virus segment 3 modulates the host response. Science *337*, 199-204.

Killip, M.J., Smith, M., Jackson, D., and Randall, R.E. (2014). Activation of the interferon induction cascade by influenza A viruses requires viral RNA synthesis and nuclear export. Journal of virology *88*, 3942-3952.
Kim, J.K., Negovetich, N.J., Forrest, H.L., and Webster, R.G. (2009). Ducks: the "Trojan horses" of H5N1 influenza. Influenza and other respiratory viruses *3*, 121-128.
Klenk, H.D. (2014). Influenza viruses en route from birds to man. Cell host & microbe *15*, 653-654.
Kowalinski, E., Lunardi, T., McCarthy, A.A., Louber, J., Brunel, J., Grigorov, B., Gerlier, D., and Cusack, S. (2011). Structural Basis for the Activation of Innate Immune Pattern-Recognition Receptor RIG-I by Viral RNA. Cell *147*, 423-435.
Labadie, K., Dos Santos Afonso, E., Rameix-Welti, M.A., van der Werf, S., and Naffakh, N. (2007). Host-range determinants on the PB2 protein of influenza A viruses control the interaction between the viral polymerase and nucleoprotein in human cells. Virology *362*, 271-282.
Li, W., Chen, H., Sutton, T., Obadan, A., and Perez, D.R. (2014). Interactions between the Influenza A Virus RNA Polymerase Components and Retinoic Acid-Inducible Gene I. Journal of virology.
Liedmann, S., Hrincius, E.R., Guy, C., Anhlan, D., Dierkes, R., Carter, R., Wu, G., Staeheli, P., Green, D.R., Wolff, T.*, et al.* (2014). Viral suppressors of the RIG-I-mediated interferon response are pre-packaged in influenza virions. Nature communications *5*, 5645.
Livak, K.J., and Schmittgen, T.D. (2001). Analysis of relative gene expression data using real-time quantitative PCR and the 2(-Delta Delta C(T)) Method. Methods (San Diego, Calif *25*, 402-408.
Long, L., Deng, Y., Yao, F., Guan, D., Feng, Y., Jiang, H., Li, X., Hu, P., Lu, X., Wang, H.*, et al.* (2014). Recruitment of phosphatase PP2A by RACK1 adaptor protein deactivates transcription factor IRF3 and limits type I interferon signaling. Immunity *40*, 515-529.
Manz, B., Brunotte, L., Reuther, P., and Schwemmle, M. (2012). Adaptive mutations in NEP compensate for defective H5N1 RNA replication in cultured human cells. Nature communications *3*, 802.
Manz, B., Schwemmle, M., and Brunotte, L. (2013). Adaptation of avian influenza A virus polymerase in mammals to overcome the host species barrier. Journal of virology *87*, 7200-7209.
Marcus, P.I., Rojek, J.M., and Sekellick, M.J. (2005). Interferon induction and/or production and its suppression by influenza A viruses. Journal of virology *79*, 2880-2890.
Massin, P., van der Werf, S., and Naffakh, N. (2001). Residue 627 of PB2 is a determinant of cold sensitivity in RNA replication of avian influenza viruses. Journal of virology *75*, 5398-5404.
Mehle, A., and Doudna, J.A. (2008). An inhibitory activity in human cells restricts the function of an avian-like influenza virus polymerase. Cell host & microbe *4*, 111-122.
Mehle, A., and Doudna, J.A. (2009). Adaptive strategies of the influenza virus polymerase for replication in humans. Proceedings of the National Academy of Sciences of the United States of America *106*, 21312-21316.
Naffakh, N., Massin, P., Escriou, N., Crescenzo-Chaigne, B., and van der Werf, S. (2000). Genetic analysis of the compatibility between polymerase proteins from human and avian strains of influenza A viruses. The Journal of general virology *81*, 1283-1291.
Neumann, G., Watanabe, T., and Kawaoka, Y. (2000). Plasmid-driven formation of influenza virus-like particles. Journal of virology *74*, 547-551.
Ng, A.K., Chan, W.H., Choi, S.T., Lam, M.K., Lau, K.F., Chan, P.K., Au, S.W., Fodor, E., and Shaw, P.C. (2012). Influenza polymerase activity correlates with the strength of interaction between nucleoprotein and PB2 through the host-specific residue K/E627. PloS one *7*, e36415.

562 Osterlund, P., Strengell, M., Sarin, L.P., Poranen, M.M., Fagerlund, R., Melen, K., and
563 Julkunen, I. (2012). Incoming influenza A virus evades early host recognition, while influenza
564 B virus induces interferon expression directly upon entry. Journal of virology *86*, 11183-
565 11193.
566 Paterson, D., te Velthuis, A.J., Vreede, F.T., and Fodor, E. (2014). Host restriction of
567 influenza virus polymerase activity by PB2 627E is diminished on short viral templates in a
568 nucleoprotein-independent manner. Journal of virology *88*, 339-344.
569 Perez-Cidoncha, M., Killip, M.J., Oliveros, J.C., Asensio, V.J., Fernandez, Y., Bengoechea,
570 J.A., Randall, R.E., and Ortin, J. (2014). An unbiased genetic screen reveals the polygenic
571 nature of the influenza virus anti-interferon response. Journal of virology *88*, 4632-4646.
572 Pichlmair, A., Schulz, O., Tan, C.P., Naslund, T.I., Liljestrom, P., Weber, F., and Reis, E.S.C.
573 (2006). RIG-I-Mediated Antiviral Responses to Single-Stranded RNA Bearing 5' Phosphates.
574 Science *314*, 997-1001.
575 Rameix-Welti, M.A., Tomoiu, A., Dos Santos Afonso, E., van der Werf, S., and Naffakh, N.
576 (2009). Avian Influenza A virus polymerase association with nucleoprotein, but not
577 polymerase assembly, is impaired in human cells during the course of infection. Journal of
578 virology *83*, 1320-1331.
579 Rawling, D.C., and Pyle, A.M. (2014). Parts, assembly and operation of the RIG-I family of
580 motors. Current opinion in structural biology *25*, 25-33.
581 Resa-Infante, P., Jorba, N., Zamarreno, N., Fernandez, Y., Juarez, S., and Ortin, J. (2008).
582 The host-dependent interaction of alpha-importins with influenza PB2 polymerase subunit is
583 required for virus RNA replication. PloS one *3*, e3904.
584 Schlee, M. (2013). Master sensors of pathogenic RNA - RIG-I like receptors. Immunobiology
585 *218*, 1322-1335.
586 Schlee, M., Roth, A., Hornung, V., Hagmann, C.A., Wimmenauer, V., Barchet, W., Coch, C.,
587 Janke, M., Mihailovic, A., Wardle, G.*, et al.* (2009). Recognition of 5' triphosphate by RIG-I
588 helicase requires short blunt double-stranded RNA as contained in panhandle of negative-
589 strand virus. Immunity *31*, 25-34.
590 Schmidt, A., Schwerd, T., Hamm, W., Hellmuth, J.C., Cui, S., Wenzel, M., Hoffmann, F.S.,
591 Michallet, M.C., Besch, R., Hopfner, K.P.*, et al.* (2009). 5'-triphosphate RNA requires base-
592 paired structures to activate antiviral signaling via RIG-I. Proceedings of the National
593 Academy of Sciences of the United States of America *106*, 12067-12072.
594 Subbarao, E.K., London, W., and Murphy, B.R. (1993). A single amino acid in the PB2 gene
595 of influenza A virus is a determinant of host range. Journal of virology *67*, 1761-1764.
596 Takahasi, K., Yoneyama, M., Nishihori, T., Hirai, R., Kumeta, H., Narita, R., Gale, M., Jr.,
597 Inagaki, F., and Fujita, T. (2008). Nonself RNA-sensing mechanism of RIG-I helicase and
598 activation of antiviral immune responses. Molecular cell *29*, 428-440.
599 Varga, Z.T., Ramos, I., Hai, R., Schmolke, M., Garcia-Sastre, A., Fernandez-Sesma, A., and
600 Palese, P. (2011). The influenza virus protein PB1-F2 inhibits the induction of type I
601 interferon at the level of the MAVS adaptor protein. PLoS pathogens *7*, e1002067.
602 Wagstaff, K.M., Sivakumaran, H., Heaton, S.M., Harrich, D., and Jans, D.A. (2012).
603 Ivermectin is a specific inhibitor of importin alpha/beta-mediated nuclear import able to
604 inhibit replication of HIV-1 and dengue virus. The Biochemical journal *443*, 851-856.
605 Weber, M., Gawanbacht, A., Habjan, M., Rang, A., Borner, C., Schmidt, A.M., Veitinger, S.,
606 Jacob, R., Devignot, S., Kochs, G.*, et al.* (2013). Incoming RNA virus nucleocapsids
607 containing a 5'-triphosphorylated genome activate RIG-I and antiviral signaling. Cell host &
608 microbe *13*, 336-346.
609 Weber, M., and Weber, F. (2014a). Monitoring activation of the antiviral pattern recognition
610 receptors RIG-I and PKR by limited protease digestion and native PAGE. Journal of
611 visualized experiments : JoVE, e51415.

612 Weber, M., and Weber, F. (2014b). Segmented negative-strand RNA viruses and RIG-I:
613 divide (your genome) and rule. Curr Opin Microbiol *20C*, 96-102.
614 Wisskirchen, C., Ludersdorfer, T.H., Muller, D.A., Moritz, E., and Pavlovic, J. (2011). The
615 cellular RNA helicase UAP56 is required for prevention of double-stranded RNA formation
616 during influenza A virus infection. Journal of virology *85*, 8646-8655.
617 Wunderlich, K., Juozapaitis, M., Ranadheera, C., Kessler, U., Martin, A., Eisel, J., Beutling,
618 U., Frank, R., and Schwemmle, M. (2011). Identification of high-affinity PB1-derived
619 peptides with enhanced affinity to the PA protein of influenza A virus polymerase.
620 Antimicrobial agents and chemotherapy *55*, 696-702.
621 Yamada, S., Hatta, M., Staker, B.L., Watanabe, S., Imai, M., Shinya, K., Sakai-Tagawa, Y.,
622 Ito, M., Ozawa, M., Watanabe, T.*, et al.* (2010). Biological and structural characterization of a
623 host-adapting amino acid in influenza virus. PLoS pathogens *6*, e1001034.
624 Yoo, J.S., Kato, H., and Fujita, T. (2014). Sensing viral invasion by RIG-I like receptors. Curr
625 Opin Microbiol *20C*, 131-138.
626
627

Figure legends

Fig. 1. Activation of RIG-I signaling by incoming influenza virus nucleocapsids.

(A and B) RIG-I activity assays. A549 cells were pre-incubated for 1 h with inhibitors, inoculated with strain A/PR/8/34 (MOI 1) or left uninfected (mock) for 1 h at 4°C, incubated 1 h at 37°C, and analyzed. (A) Oligomerization assay. Lysates of cells treated with CHX (50 µg/ml), LMB (16 nM), ActD (1 µg/ml), or IVM (50 µM) were separated by native PAGE and immunostained for RIG-I. Actin served as loading control. (B) Conformational switch. Lysates as in (A) were subjected to limited trypsin digest and analyzed by RIG-I immunoblot. The Ponceau S protein stain (representative section shown) serves as loading control for the digested samples. (C) Quantification of total FLUAV segment 7 RNA by RT-qPCR. Input represents RNA amounts harvested after the 1 h inoculation period at 4°C. (D) IRF3 activation. A549 cells were pretreated with inhibitors, inoculated with strain A/PR/8/34 (MOI 1) or left uninfected (mock) for 1 h at 4°C, and incubated for 1 h under inhibitor treatment. Lysates from cells were separated by native PAGE and analyzed by immunoblotting for phosphorylated IRF3 (P-IRF3) and actin as described (Weber et al., 2013). See also Figures S1A-S1C.

Fig. 2. RIG-I interacts with incoming influenza virus nucleocapsids and is activated in a 5'ppp-dsRNA-dependent manner.

(A to C) CHX / LMB-treated A549 cells were infected with A/PR/8/34 (MOI 1) for 1 h. (A) Cells analyzed for RIG-I and FLUAV by 3D GSD superresolution immunofluorescence microscopy. Scale bar, 1 µm. Insets are digitally magnified and shown below the main image (taken from one individual cell). (B) Co-immunoprecipitation. Cell lysates were subjected to immunoprecipitation (IP) using antibodies against p21 (negative control), RIG-I, or FLUAV NP, and analyzed by immunoblot. Input control: 2% of the lysate. Asterisks (*) indicate

unspecific bands. (C) Co-sedimentation assay. Cell lysates were separated by a discontinuous CsCl gradient (2% lysate as input control), and fractions analyzed by immunoblotting. (D) Conditions for activation of RIG-I by nucleocapsids *in vitro*. Dialyzed lysate of RIG-I-expressing S2 cells was mixed with nucleocapsids of strain A/PR/8/34 (RNPs) or a control preparation (CTRL) and supplemented with 1 mM ATP. The nucleocapsids had either been pretreated with 5 µg RNase A (A), 1 U RNase III (III), or 2 U Shrimp Alkaline Phosphatase (SAP), or left untreated (-), for 1 h at 37°C. RIG-I conformational switch was assayed after 1 h of nucleocapsid co-incubation at 37°C. See also Figures S2A-S2K.

Fig. 3. Adaptive mutations in PB2 influence the activation of RIG-I by FLUAV nucleocapsids.

(A) RIG-I activation by viruses with different PB2-627 signatures. Cells were infected with strains of A/quail/Shantou/2061/00 (H9N2), A/Thai/KAN-1/04 (H5N1), A/Hamburg/05/2009 (pH1N1), or A/WSN/33 (H1N1) containing avian-signature E or mammalian-signature K at PB2-627. Infections, CHX/LMB treatment and RIG-I conformational switch testing were performed as described for 1 and 2. (B) Quantification of virus RNAs by RT-qPCR for genomic segment 7. Input represents RNA amounts harvested after the 1-h infection period. (C) Co-sedimentation assay. Lysates of cells infected with PB2 variants of A/WSN/33 (H1N1) using our standard 1 h-protocol were separated by a CsCl gradient and analyzed by immunoblotting. (D) RIG-I-dependent IFN induction by incoming nucleocapsids. A549 cells were transfected with the indicated siRNAs or a negative control siRNA (CTRL). A549 cells siRNA-depleted of RIG-I or MDA5 were pretreated with CHX and LMB, and infected with FLUAV strains (MOI 1) for 16 h. IFN-β mRNA levels were determined by real-time RT-PCR. See also Figures S3A-S3H.

Fig. 4. RIG-I evasion by PB2-E627K.

(A) Activity of A/WSN/33-based minireplicon systems containing PB2-627K, -627E, or no PB2 (-) in HEK293 wt, *ΔRIG-I* or *ΔMDA5* cells. (B) Reporter activities in HEK293 cells producing VLPs containing nucleocapsids with the indicated PB2 signatures. (C) Reporter activities in wt and deletion cells infected with VLPs. Cells had been pretransfected with PB1, PA, NP, and matching PB2. (D) Multicycle virus kinetics. 293 wt or *ΔRIG-I* cells were infected with the indicated PB2 variants of strain A/Thai/KAN-1/04 (H5N1) at an MOI 0.0001. Virus yields were determined 24 h later by plaque assay. In all cases, mean and SDs from 3 independent experiments are shown. (E) Single-cycle virus kinetics. Cells were infected at an MOI of 1 and monitored for NP expression over time. See also Figures S4A-S4D.

Fig. 5. Signaling-independent RIG-I effect on early infection

Single-cycle infection kinetics of A/WSN/33 on human cells lacking *MAVS* (A) or *RIG-I* (B), or on chicken DF-1 cells that naturally lack RIG-I (C). The *ΔRIG-I* and the DF-1 cells were transiently transfected with plasmids encoding GFP (negative control), FLAG-RIG-I wt, or FLAG-RIG-I K270A, as indicated. Overexpression was controlled using antibodies against GFP or the N-terminal Flag tag of the RIG-I constructs. See also Figure S5.

Fig. 6. Effect of the PB2 627 signature on protein-protein interactions.

(A) NP immunoprecipitation. Cells were CHX / LMB treated and infected with A/WSN/33 strains carrying PB2-627K or 627E as described for 1A. Lysates were immunoprecipitated 1 h later with anti-NP and immunoblotted as indicated. Normalized quantifications of the immunoprecipitated proteins are shown below. Note that amounts of viral input proteins are too low to be detected in the total extracts. (B) RIG-I immunoprecipitations from infected cells. HEK293 cells were infected with A/WSN/33 PB2 variants as described for 1A. Immunoprecipations with anti-RIG-I and immunoblotting were performed as indicated for

706 2B. (C) RIG-I immunoprecipitations of recombinant nucleocapsids. HEK293 cells were
707 transfected with A/WSN/33 NP combined with GFP or the PB2 variants (left panel), or with
708 all A/WSN/33 minireplicon plasmids (right panel). Immunoprecipations with anti-RIG-I were
709 performed as indicated for (B). (D) Polymerase destabilization. A549 cells were infected with
710 PB2 variants of strain A/WSN/33 (MOI 1), treated with peptides Borna-X-Tat (CTRL) or
711 $PB1_{1\text{-}15}$ T6Y-Tat (PB1-T6Y), and tested for RIG-I conformational switch 1 h post-infection.
712 See also Figures S6A-S6C.
713

Figure 1

Click here to download high resolution image

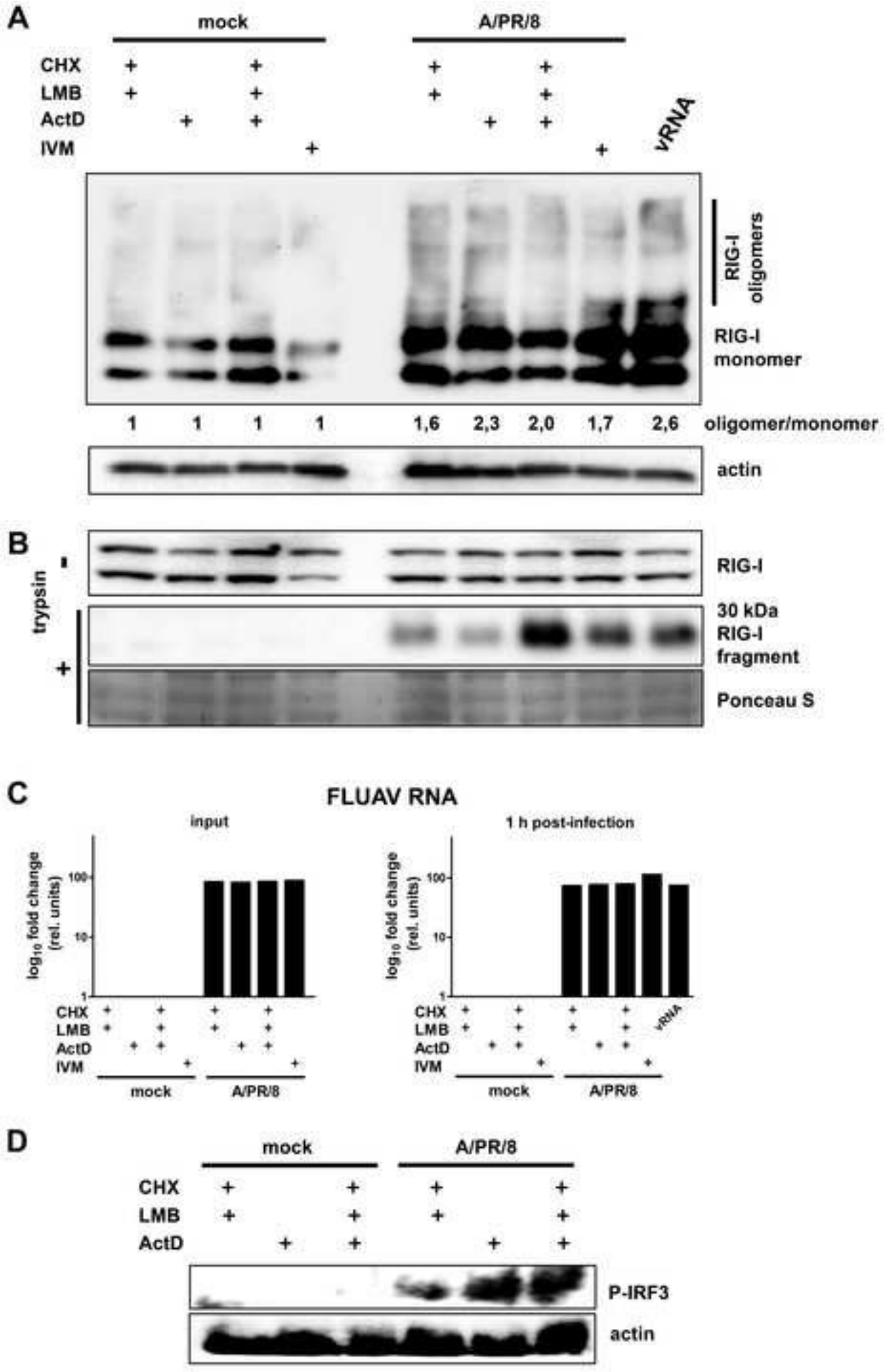

Figure 2
Click here to download high resolution image

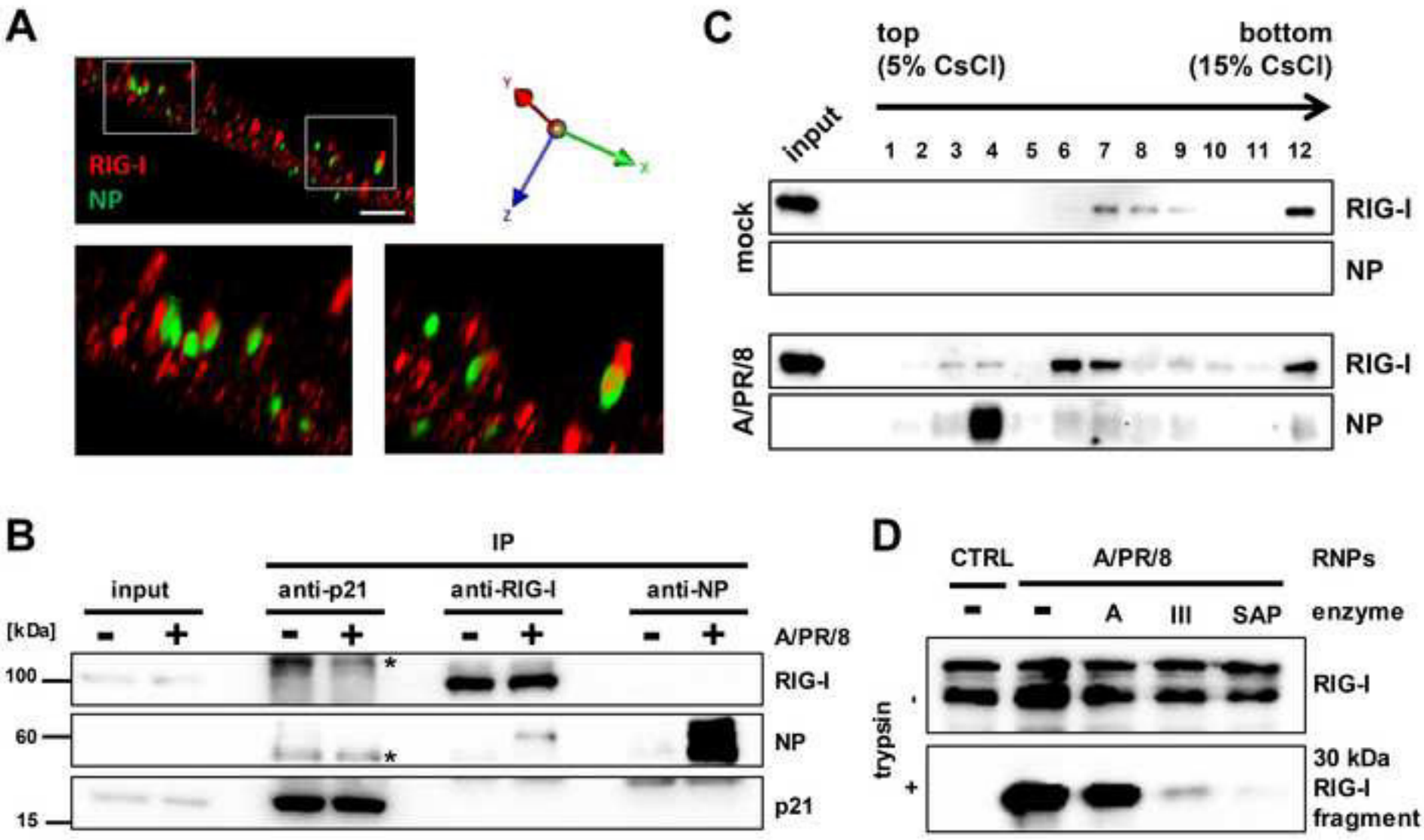

Figure 3
Click here to download high resolution image

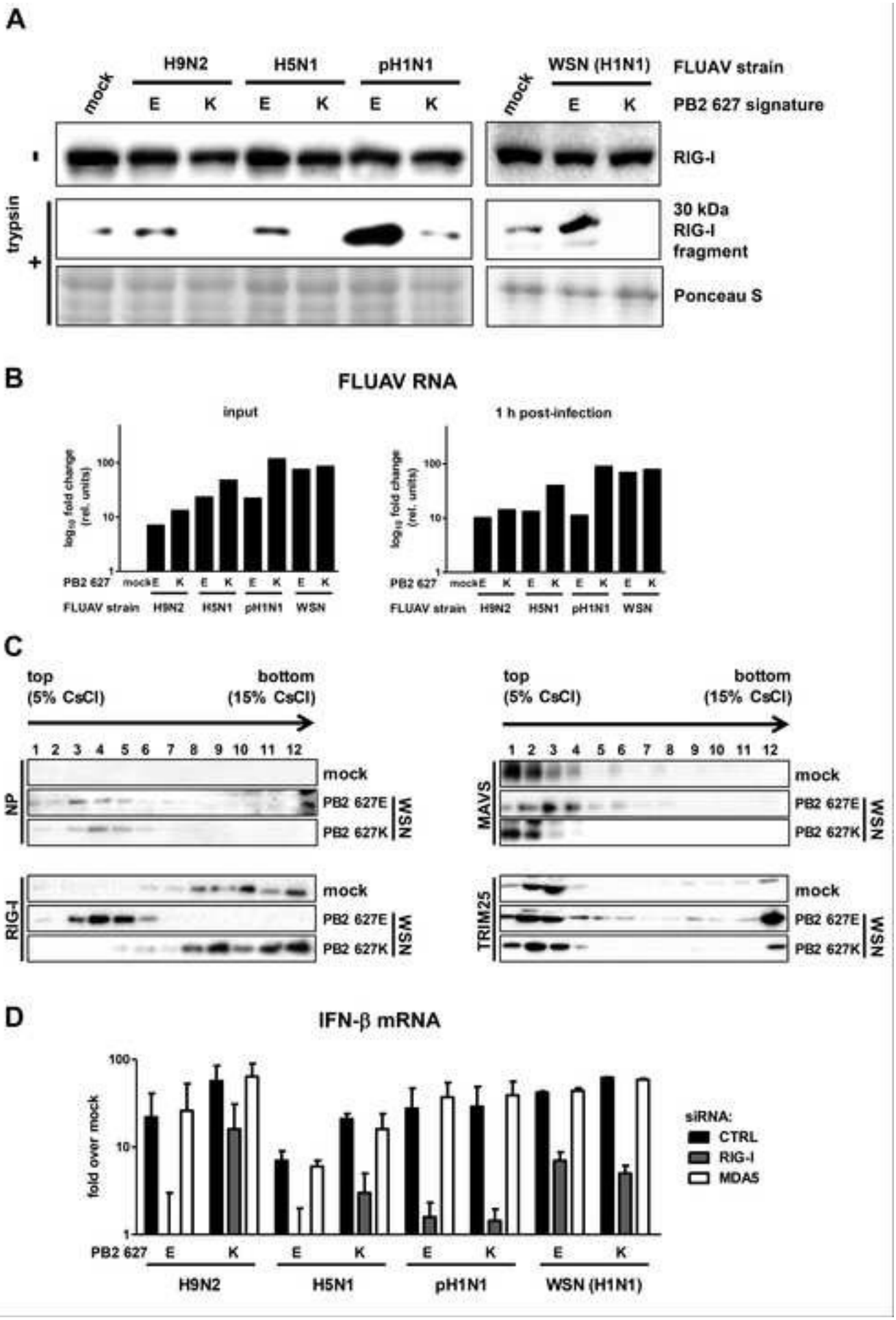

Figure 4

Click here to download high resolution image

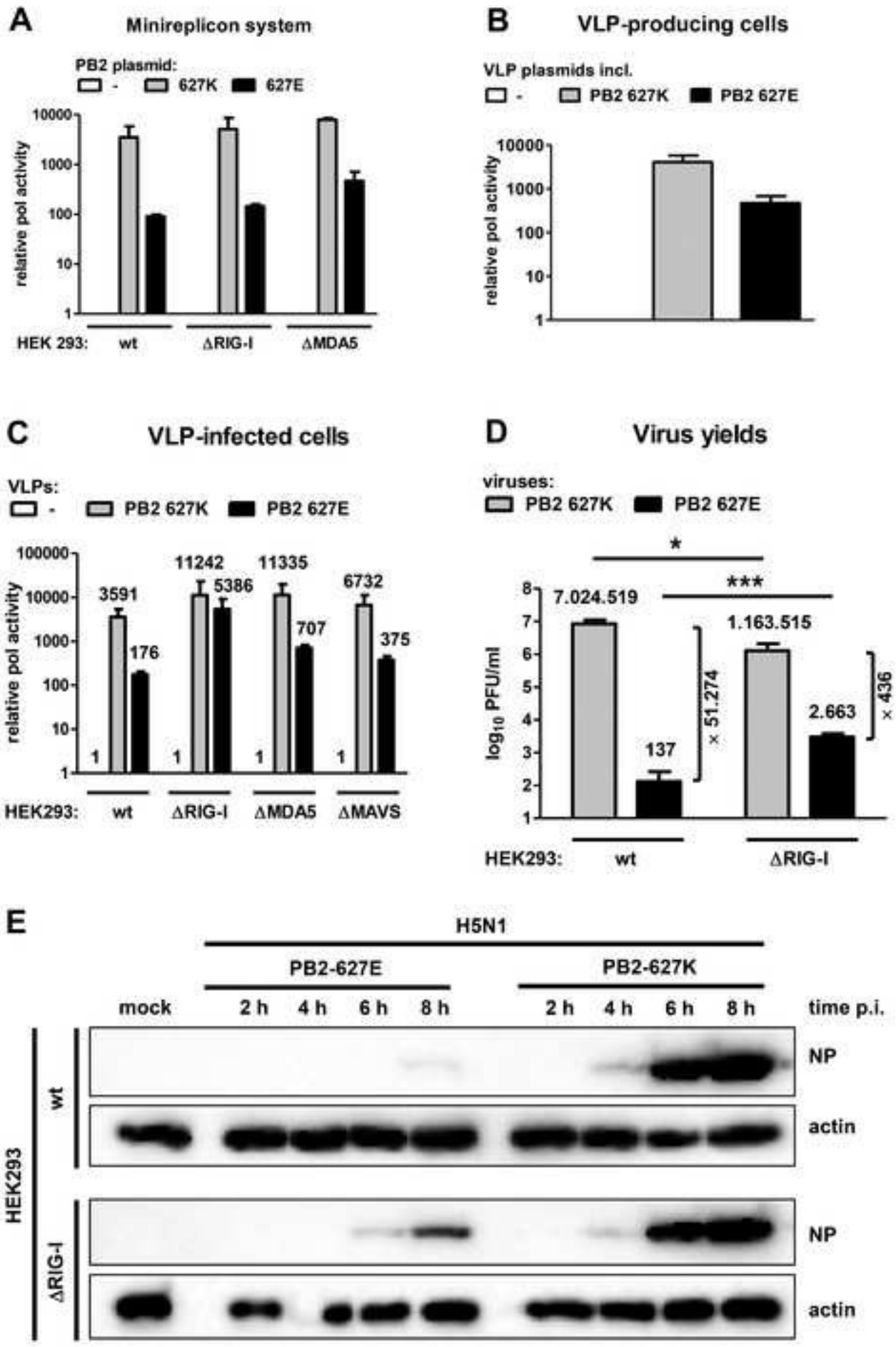

Figure 5
Click here to download high resolution image

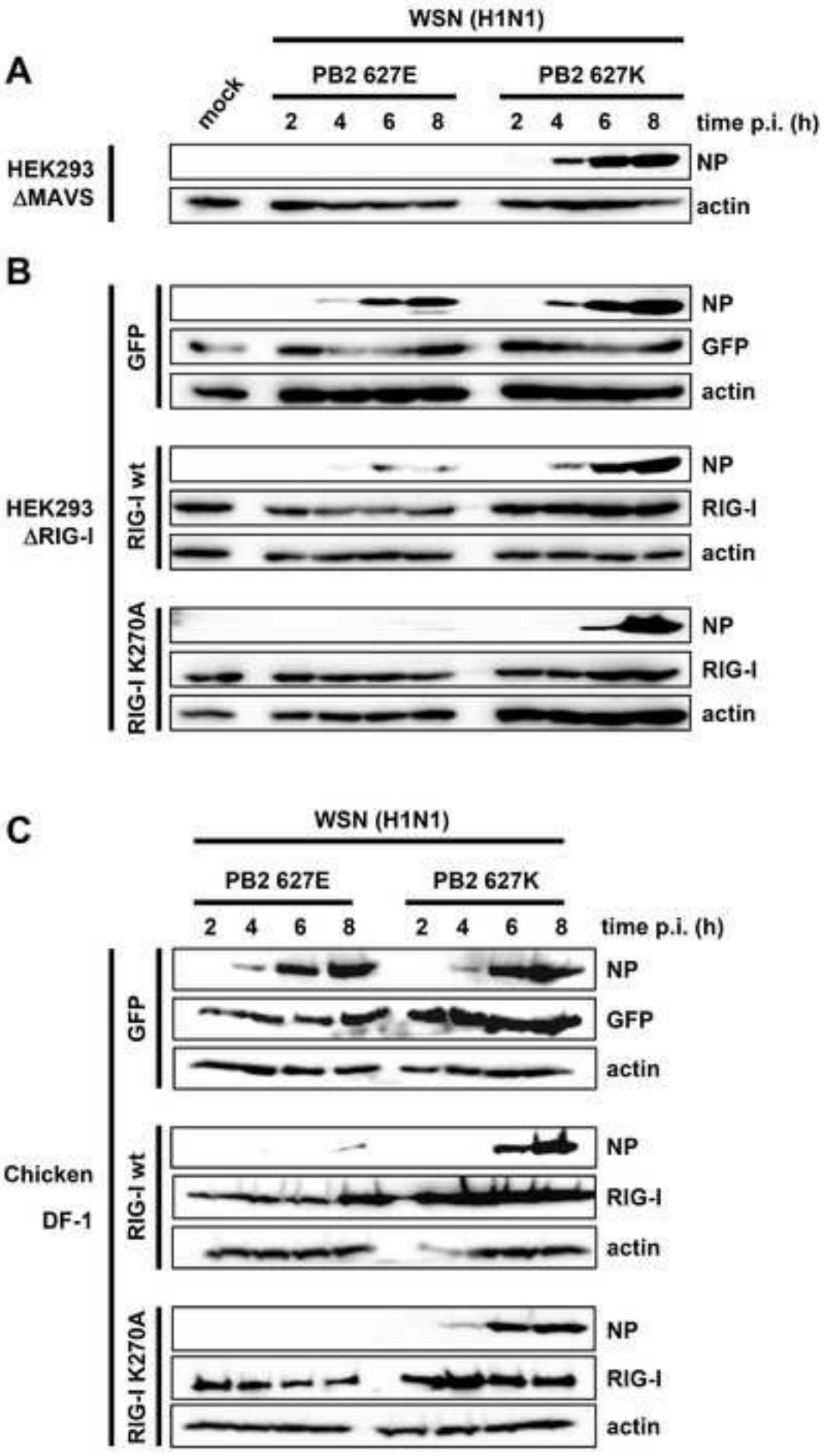

Figure 6

Click here to download high resolution image

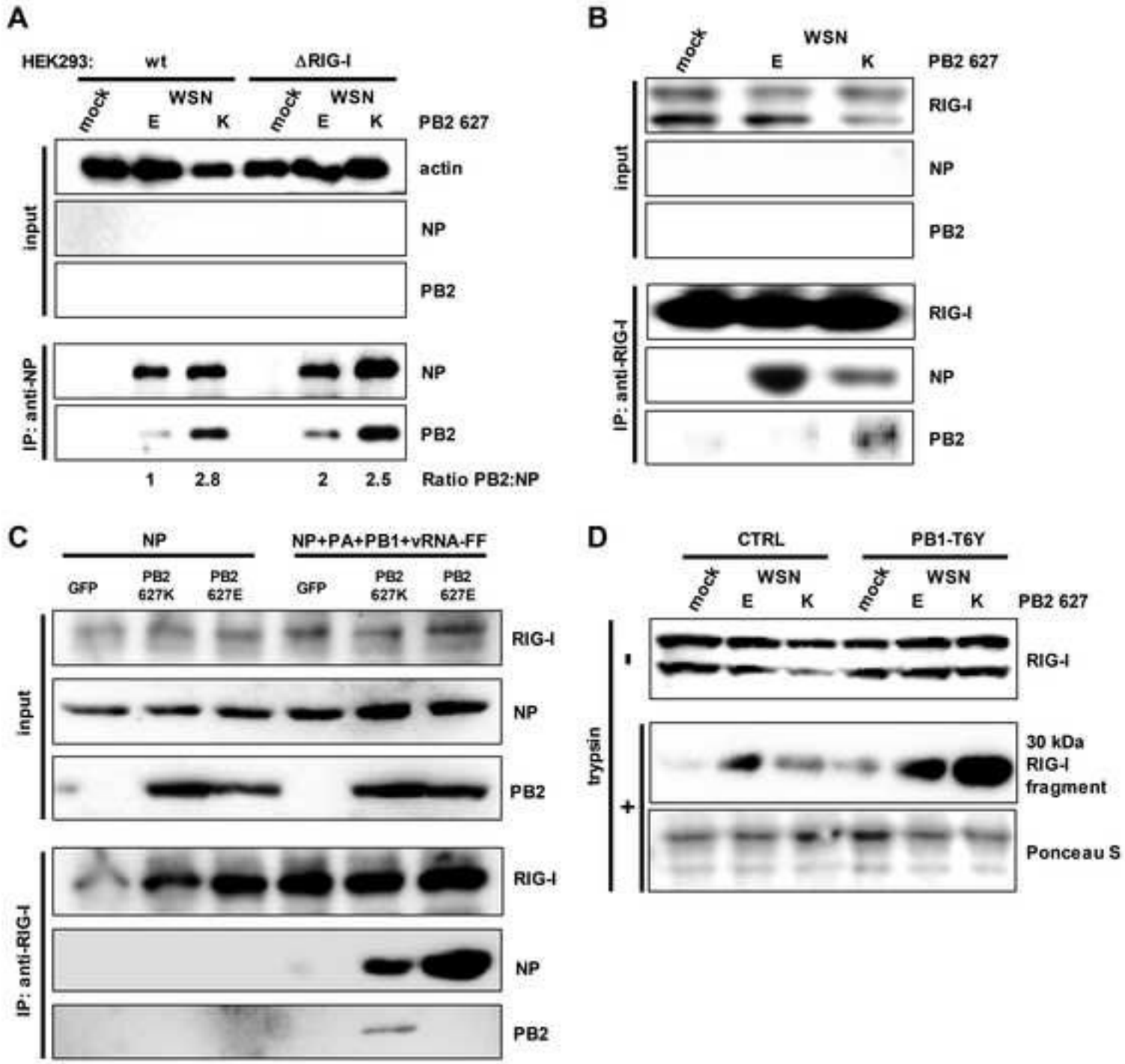

Figure S1

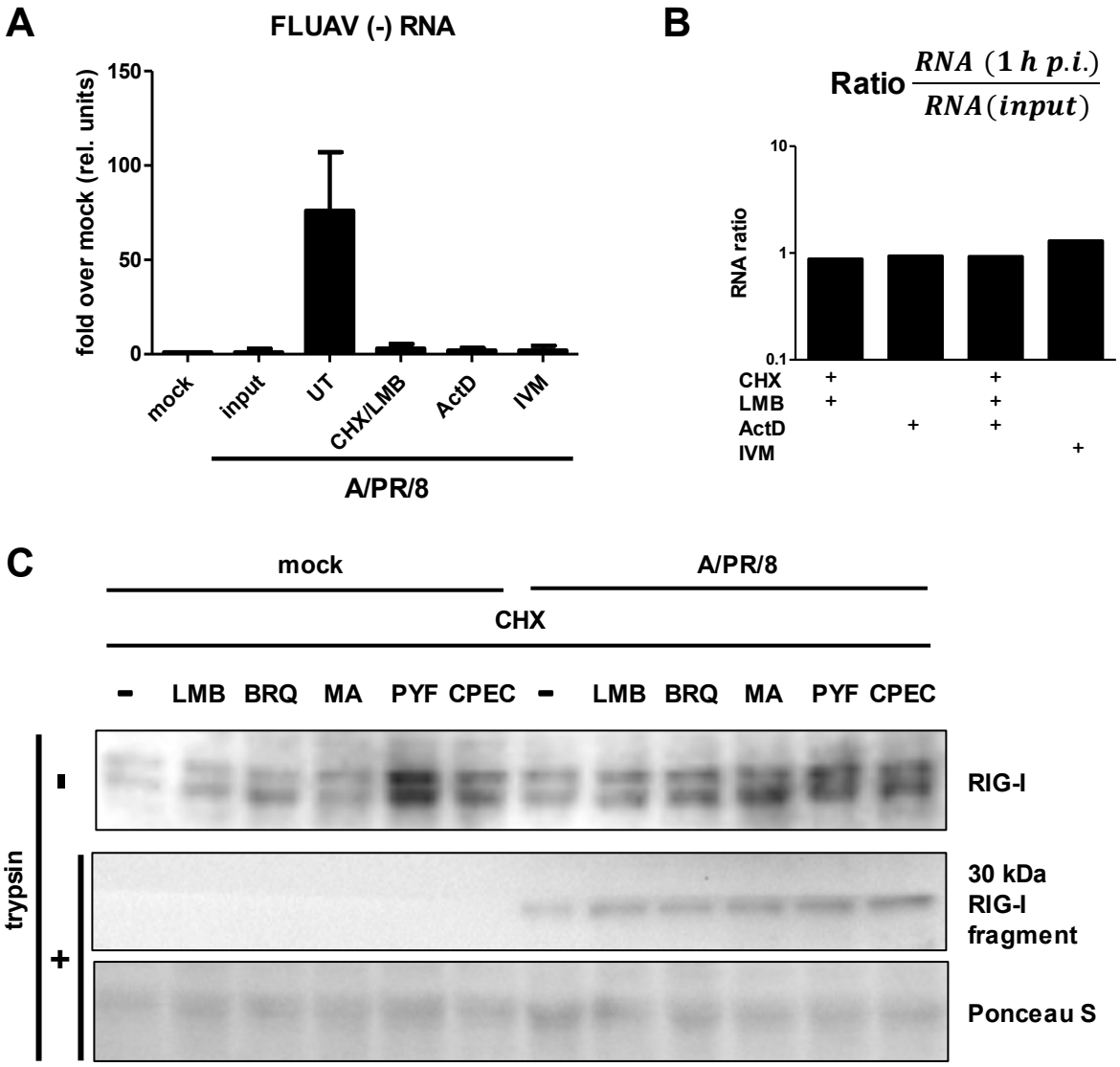

Figure S1. Immediate-early activation of RIG-I is independent of viral RNA synthesis (related to Figure 1).

(A) Effect of inhibitors on viral RNA synthesis. Cells pretreated with the inhibitors used for the experiment in figure 1 were infected with FLUAV strain A/PR/8 for 8 h. The amounts of viral (-) sense RNA (segment 7) were then measured by RT-qPCR. **(B) Normalization of the RNA values shown in Fig.1A.** The graph illustrates the absence of RNA synthesis during the 1 h-infection period. **(C) Inhibitors of translation and viral RNA synthesis do not influence immediate early activation of RIG-I.** Conformational switch assay of infected A549 cells pretreated with CHX (50 µg/ml) in combination with either 16 nM LMB, 10 µM Brequinar (BRQ; depletes pyrimidine synthesis), 10 µM mycophenolic acid (MA; depletes GTP), 10 µM Pyrazofurin (PYF; depletes CTP and UTP), or 5 µM cyclopentenylcytosine (CPEC; depletes CTP).

Figure S2

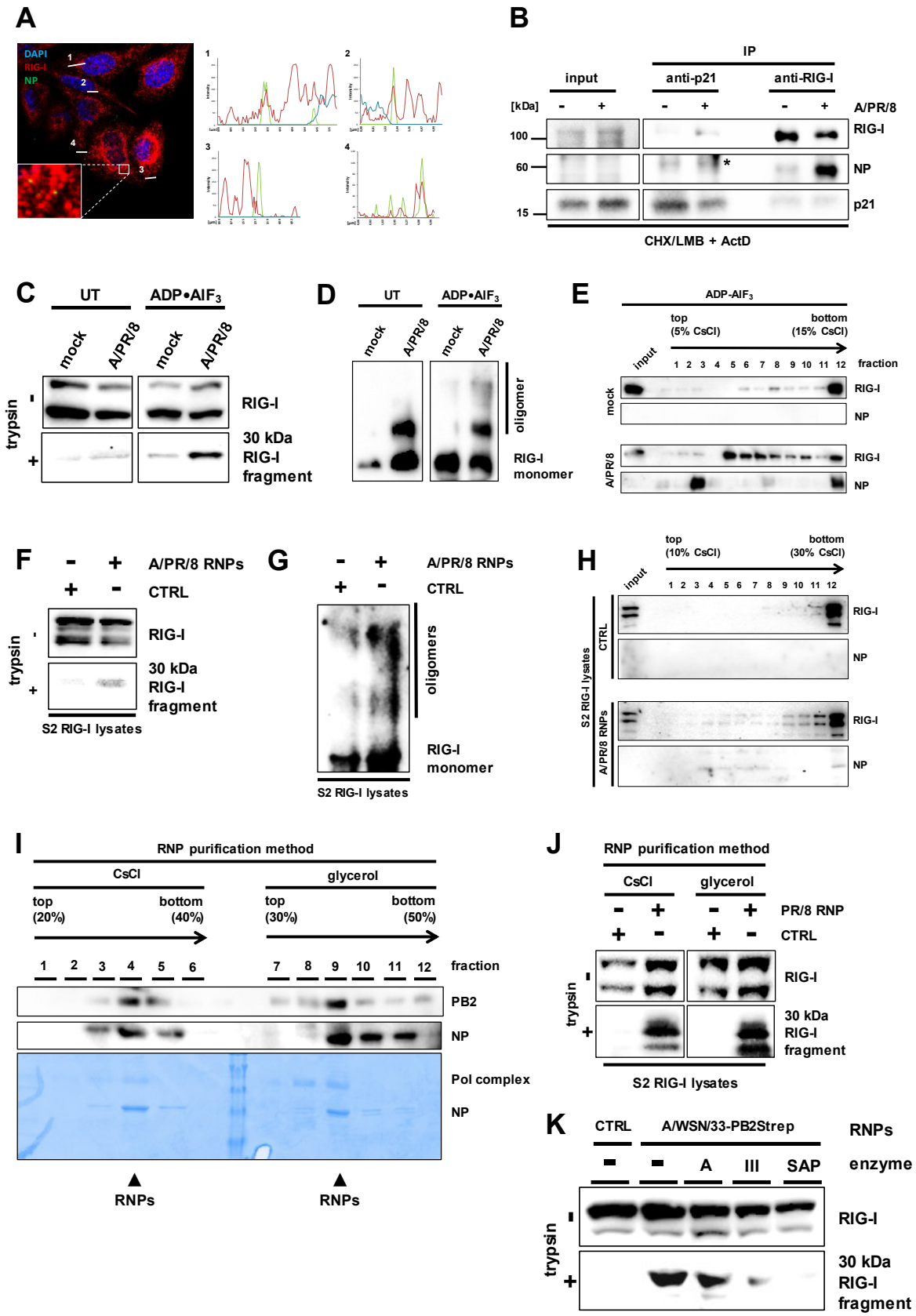
A
DAPI
RIG-I
NP
B
IP
input
anti-p21
anti-RIG-I
[kDa]
A/PR/8
RIG-I
NP
p21
CHX/LMB + ActD
C
UT
ADP•AlF3
mock
A/PR/8
trypsin
RIG-I
30 kDa RIG-I fragment
D
oligomer
RIG-I monomer
E
ADP-AlF3
top (5% CsCl)
bottom (15% CsCl)
fraction
F
A/PR/8 RNPs
CTRL
S2 RIG-I lysates
G
oligomers
RIG-I monomer
H
top (10% CsCl)
bottom (30% CsCl)
S2 RIG-I lysates
I
RNP purification method
CsCl
glycerol
top (20%)
bottom (40%)
top (30%)
bottom (50%)
PB2
Pol complex
RNPs
J
PR/8 RNP
K
CTRL
A/WSN/33-PB2Strep
RNPs
enzyme
A
III
SAP

Figure S2. Interaction of RIG-I with FLUAV nucleocapsids (related to Figure 2).

(A) Colocalization analysis. A549 cells were pretreated for 1 h with CHX and LMB, inoculated with strain A/PR/8/34 (MOI 1) for 1 h at 4°C, and incubated for another hour at 37°C under inhibitor treatment. Cells were fixed and stained for double immunofluorescence analysis using antisera against RIG-I (red channel) and FLUAV NP (green channel). Cell nuclei were counterstained with DAPI (blue channel). The marked square area is shown digitally magnified in the lower left corner. Four fluorescence intensity overlays are shown on right. **(B) Interaction of RIG-I with FLUAV nucleocapsids is independent of viral RNA synthesis.** Co-immunoprecipitation analysis as performed for figure 2B, but with 1 µg/ml ActD added to the inhibitor mix containing CHX and LMB. Lysates of inhibitor- pretreated and 1 h-infected A549 cells were subjected to immunoprecipitation (IP) using antibodies against cyclin-dependent kinase inhibitor p21 (negative control), RIG-I, or FLUAV NP, and analyzed by immunoblot. Input control: 2% of the lysate. Asterisks (*) indicate unspecific bands. **(C, D, E) Activation of RIG-I by nucleocapsids in the absence of RIG-I ATPase activity.** Lysates from cells infected as indicated for (A) were treated with ADP●AlF3 and tested for conformational switching (C), oligomerization (D), and fractionation in a discontinuous CsCl gradient (2% lysate as input control) (E). Analyses were performed as described for figures 1 and 2. **(F, G, H) FLUAV nucleocapsids directly activate RIG-I *in vitro*.** Cell lysates of RIG-I-expressing *Drosophila* S2 cells were dialyzed, mixed with purified nucleocapsids (A/PR/8 RNPs) or a control preparation (CTRL), supplemented with 1 mM ATP, and assayed by limited trypsin digestion (F), native PAGE (G), or CsCl fractionation (H), coupled to immunoblot analysis. **(I, J, K) RIG-I activation does not depend on the nucleocapsid preparation method**. (I) Nucleocapsids of strain A/PR/8/34 were prepared and purified using a CsCl gradient (left panel) or a glycerol gradient (right panel) , and their composition monitored by PB2 and NP immunoblotting (upper panels) and by Coomassie staining (lower panel). The fractions with the subsequently used nucleocapsids (RNPs) are indicated. (J) Nucleocapsids prepared using either CsCl or glycerol gradients were tested for their ability to activate RIG-I conformational switching in the insect cell / *in vitro* reconstitution system as described for (F). (K) Nucleocapsids of strain A/WSN/33 carrying a C-terminal strep-tag on the PB2 protein were (Rameix-Welti et al., 2009) were prepared by affinity purification and used to activate RIG-I conformational switching in the insect cell / *in vitro* reconstitution system. The nucleocapsids had either been pretreated with RNase A (A), RNase III (III), or Shrimp Alkaline Phosphatase (SAP), or left untreated (-) as described for Fig. 2D.

Figure S3

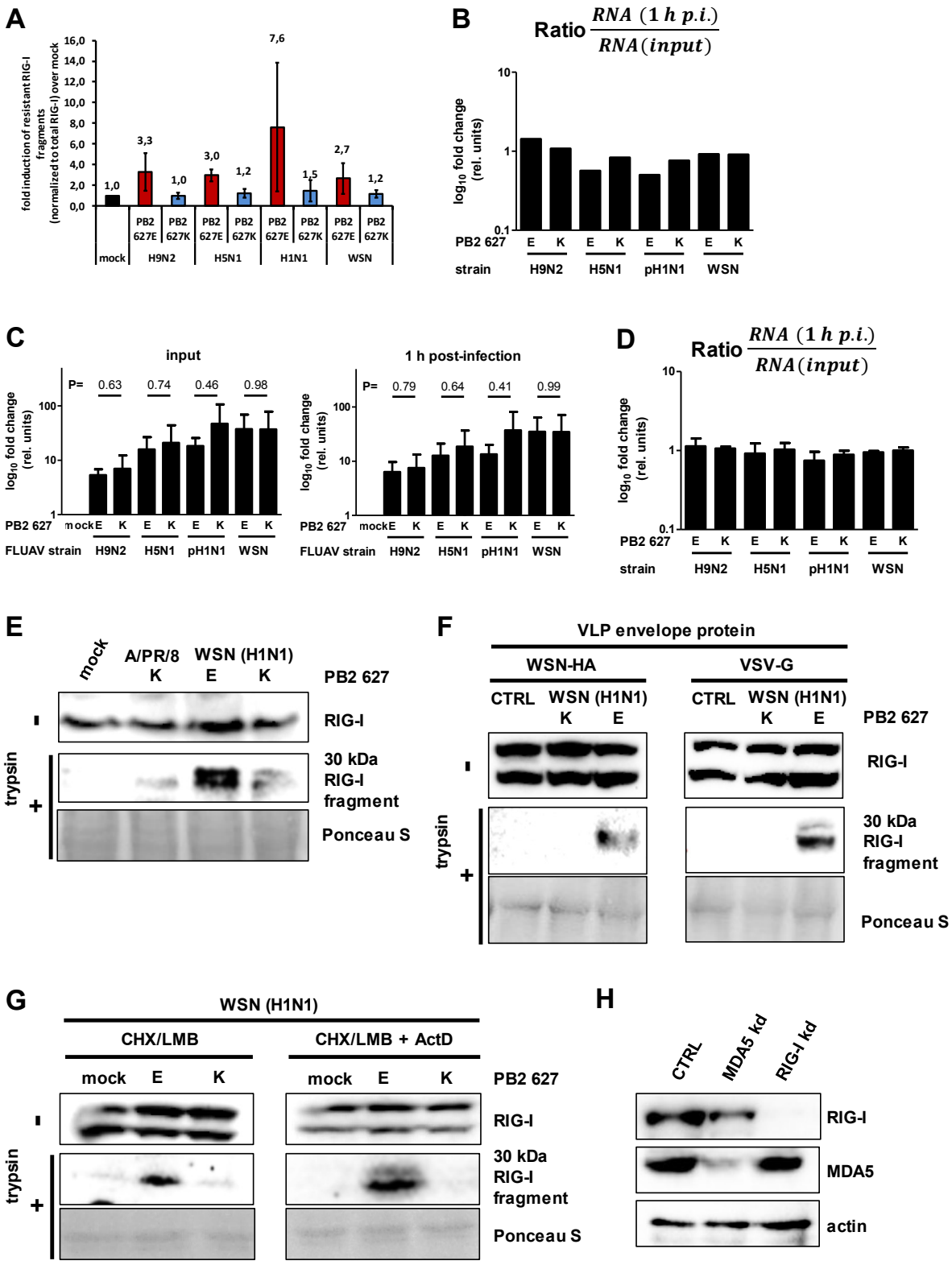
A
fold induction of resistant RIG-I fragments (normalized to total RIG-I) over mock
16,0
14,0
12,0
10,0
8,0
6,0
4,0
2,0
0,0
1,0
3,3
1,0
3,0
1,2
7,6
1,5
2,7
1,2
PB2 627E
PB2 627K
mock
H9N2
H5N1
H1N1
WSN
B
Ratio RNA (1 h p.i.) / RNA(input)
log10 fold change (rel. units)
10
1
0.1
PB2 627
E K E K E K E K
strain
H9N2 H5N1 pH1N1 WSN
C
input
1 h post-infection
P= 0.63 0.74 0.46 0.98
P= 0.79 0.64 0.41 0.99
log10 fold change (rel. units)
100
10
1
PB2 627
mock E K E K E K E K
FLUAV strain
H9N2 H5N1 pH1N1 WSN
D
Ratio RNA (1 h p.i.) / RNA(input)
log10 fold change (rel. units)
10
1
0.1
PB2 627
E K E K E K E K
strain
H9N2 H5N1 pH1N1 WSN
E
mock
A/PR/8 K
WSN (H1N1) E
WSN (H1N1) K
PB2 627
RIG-I
trypsin
-
+
30 kDa RIG-I fragment
Ponceau S
F
VLP envelope protein
WSN-HA
VSV-G
CTRL
WSN (H1N1) K
WSN (H1N1) E
PB2 627
RIG-I
trypsin
-
+
30 kDa RIG-I fragment
Ponceau S
G
WSN (H1N1)
CHX/LMB
CHX/LMB + ActD
mock E K
mock E K
PB2 627
RIG-I
trypsin
-
+
30 kDa RIG-I fragment
Ponceau S
H
CTRL
MDA5 kd
RIG-I kd
RIG-I
MDA5
actin

Figure S3. RIG-I activation by PB2-627E signature virus is mediated by nucleocapsids and independent of viral RNA synthesis (related to Figure 3).

(A) Quantification of RIG-I conformational switch provoked by different FLUAV strains. Cells were treated and infected as described for figure 3A. Signals for the trypsin resistant RIG-I fragment were quantified and normalized to the mock control. Data of the experiment shown in Figure 3A and of two other independent experiments were used to calculate values of mean and SD. **(B) Normalization of the RNA values shown in Figure 3B.** The quantification illustrates that nucleocapsids of avian and human strains contain similar amounts of RNA and that no RNA synthesis occurs during the 1 infection period. **(C and D) Systematic comparison of RNA amounts from input and 1 h-infections.** Mean values and standard deviations from 3 independent experiments are shown (C) and normalized (D). P values were determined by Student's t-test. **(E) RIG-I activation by nucleocapsids of strain A/PR8/34 is in the range expected for a virus with a PB2-627K signature.** Cells pretreated with CHX and LMB were infected for 1 h with the indicated viruses and tested for RIG-I conformational switching. **(F) RIG-I activation is independent of the viral envelope.** Cells pretreated with CHX and LMB were infected for 1 h with VLPs derived from strain A/WSN/33 (H1N1) that either contain the viral HA protein or that are pseudotyped with VSV-G, and tested for RIG-I conformational switching. **(G) RIG-I activation by PB2-627 variant viruses is independent of viral RNA synthesis.** RIG-I conformational switch assay for cells infected with A/WSN/33 (H1N1) which had been pretreated with CHX and LMB (left panel), or in addition with ActD (right panel). **(H) Control of siRNA treatment efficiency.** A549 cells were transfected with the indicated siRNAs or a negative control siRNA (CTRL). After two rounds of transfections, cells were tested for the presence of the target proteins by immunoblot.

Figure S4

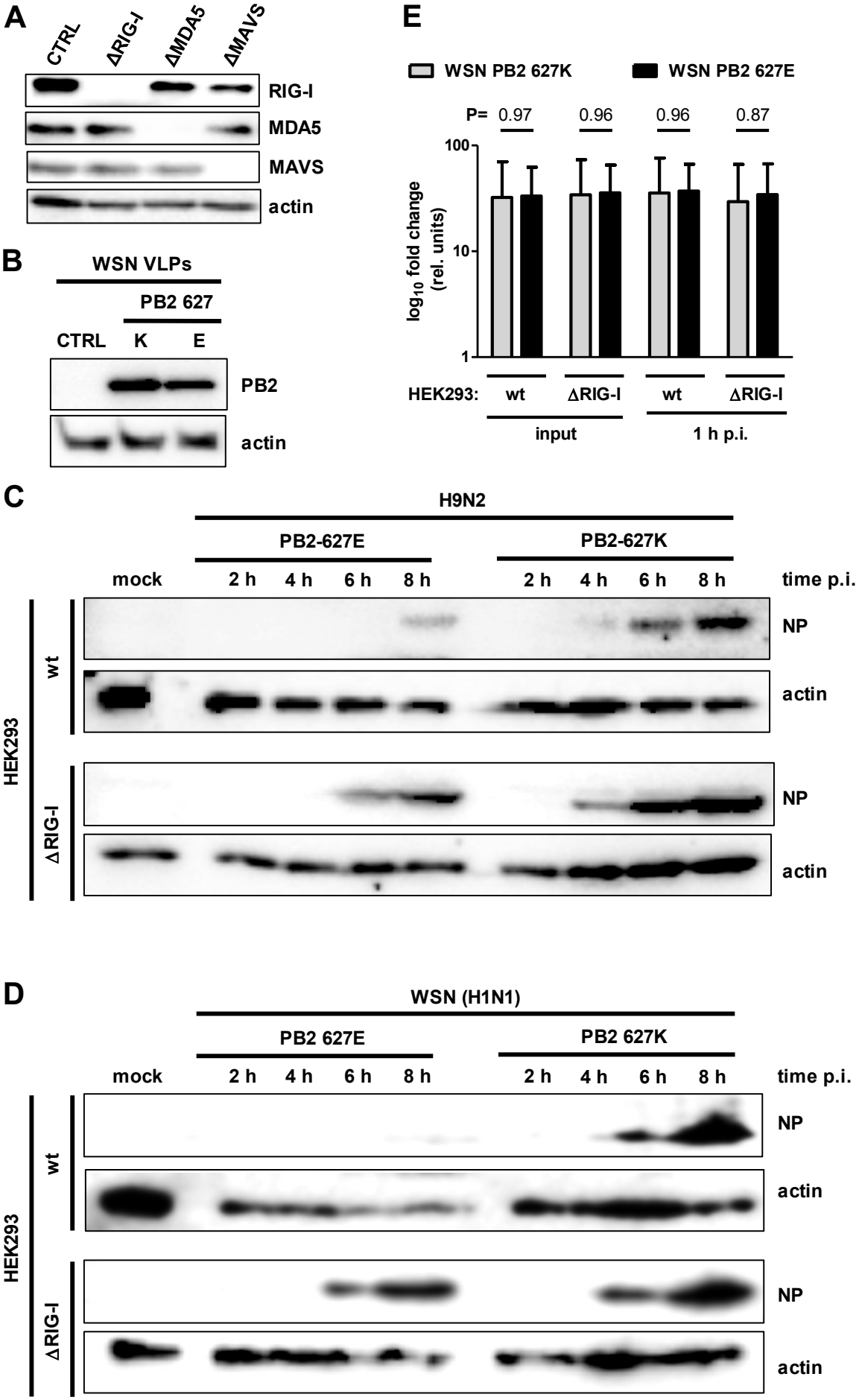
A
CTRL
ΔRIG-I
ΔMDA5
ΔMAVS
RIG-I
MDA5
MAVS
actin
B
WSN VLPs
PB2 627
CTRL
K
E
PB2
actin
E
WSN PB2 627K
WSN PB2 627E
P=
0.97
0.96
0.96
0.87
100
10
1
log10 fold change (rel. units)
HEK293:
wt
ΔRIG-I
wt
ΔRIG-I
input
1 h p.i.
C
H9N2
PB2-627E
PB2-627K
mock
2 h
4 h
6 h
8 h
2 h
4 h
6 h
8 h
time p.i.
HEK293
wt
ΔRIG-I
NP
actin
NP
actin
D
WSN (H1N1)
PB2 627E
PB2 627K
mock
2 h
4 h
6 h
8 h
2 h
4 h
6 h
8 h
time p.i.
HEK293
wt
ΔRIG-I
NP
actin
NP
actin

Figure S4. Onset of FLUAV infection in dependency of RIG-I (related to Figure 4).

(A) Characterization of knockout cells. Immunoblot analysis of HEK293 cells which had been engineered to disrupt the coding sequences of RIG-I, MDA5, and MAVS respectively (see Materials and Methods). **(B) PB2 of VLP-producing cells.** Immunoblot analysis of HEK293 wt cells transfected to produce VSV-G pseudotyped VLPs. **(C, D) Onset of infection kinetics.** HEK293 wt or *ΔRIG-I* cells were infected with PB2 variants of strain A/quail/Shantou/2061/2000 (H9N2) (C) or A/WSN/33 (H1N1) (D) at an MOI of 1, and tested by immunoblotting for the presence of NP at the indicated time points. **(E) Systematic comparison of RNA amounts from input and 1 h-infections of different PB2 signature viruses.** Mean values and standard deviations from 3 independent experiments are shown. P values were determined by Student's t-test.

Figure S5

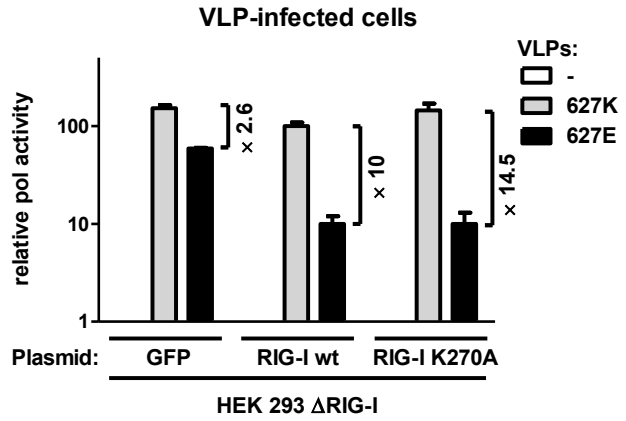

Figure S5. Signaling-independent RIG-I effect on infection with PB2-627E VLPs (related to Figure 5)

Activities of PB2 variant VLPs of strain A/WSN/33 (VSV-G pseudotyped) in *ΔRIG-I* cells transcomplemented with GFP, wt RIG-I, or RIG-I K270A as described for Figure 5. Cells had been additionally pretransfected with PB1, PA, NP, and matching PB2. Mean and SDs from 3 independent experiments are shown.

Figure S6

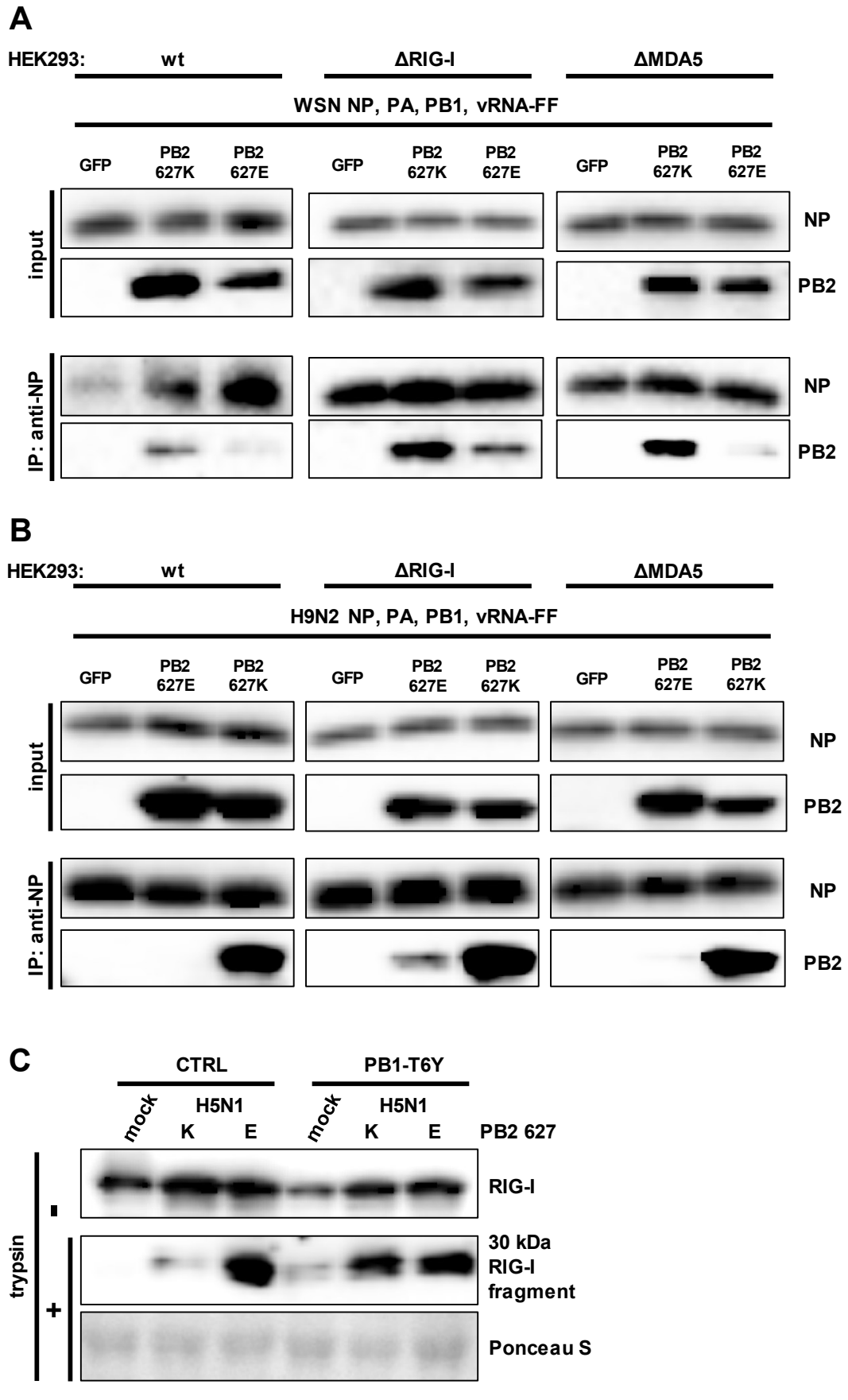
A
HEK293:
wt
ΔRIG-I
ΔMDA5
WSN NP, PA, PB1, vRNA-FF
GFP
PB2 627K
PB2 627E
input
IP: anti-NP
NP
PB2
B
HEK293:
wt
ΔRIG-I
ΔMDA5
H9N2 NP, PA, PB1, vRNA-FF
GFP
PB2 627E
PB2 627K
input
IP: anti-NP
NP
PB2
C
CTRL
PB1-T6Y
mock
H5N1
K
E
PB2 627
RIG-I
trypsin
-
+
30 kDa RIG-I fragment
Ponceau S

Figure S6. Protein-protein interactions in dependency of RIG-I (related to Figure 6). (A and B) NP-PB2 co-immunoprecipitation assay for strains WSN (H1N1) and H9N2. 293 wt, *ΔRIG-I* or *ΔMDA5* cells were transfected with plasmids for NP, PA, PB1, and a firefly luciferase minigenome (vRNA-FF) in combination with either GFP or PB2-627K or PB2-627E. The viral expression plasmids were either derived from strain A/WSN/33 (H1N1) (A) or strain A/quail/Shantou/2061/00 (H9N2) (B). At 24 h post-transfection, cell lysates were immunoprecipitated with a mouse monoclonal antibody recognizing NP and tested by Western blotting for the presence of NP and PB2. **(C) Influence of polymerase destabilization on RIG-I activation by strain H5N1**. A549 cells were pretreated with 10 ng/ml of peptides Borna-X-Tat (CTRL) or $PB1_{1\text{-}15}$ T6Y-Tat (PB1-T6Y) and infected with A/Thai/KAN-1/04 (H5N1) strains of the specified PB2 types. At 1 h post-infection, cells were lysed and subjected to limited trypsin digestion.

Supplemental Experimental Procedures

Inhibitor treatments

Brequinar (BRQ) and mycophenolic acid (MA) were purchased from Sigma Aldrich. Pyrazofurin (PYF, NSC-143095) and cyclopentenylcytosine (CPEC, NSC-375575) were kindly obtained from the Drug Synthesis and Chemistry Branch of the National Cancer Institute.

Cells were pretreated for 24 h before infection with CHX (see main text) combined with BRQ (10 µM, stocks dissolved in DMSO), MA (10 µM, stocks dissolved in methanol), PYF (10 µM, stocks dissolved in DMSO) or CPEC (5 µM, stocks dissolved in DMSO). Inhibitors were also included in the virus inoculum and the incubation medium.

Preparation and transfection of virus particle RNA

MDCK II cells grown in a T175 flask were infected with A/PR/8/34 (MOI 0,001). At 38 h post infection, supernatants were collected and centrifuged at 1,500 rpm for 7 min at 4°C in a JA-12 rotor (Beckman). The cleared supernatant was supplemented with 5 M NaCl and 30% PEG800 in NTE buffer (10 mM Tris-HCl pH 6.5, 1 mM EDTA, 100 mM NaCl) to a final concentration of 0.44 M NaCl and 15% PEG800 in NTE buffer, respectively. The suspension was incubated on ice for 30 min under constant shaking and centrifuged at 6,000 rpm for 1 h at 4°C. Subsequently, the pellet was resuspended in 1.5 ml peqGOLDTriFAST (Peqlab). After 5 min incubation at room temperature, 300 µl chloroform were added and the suspension was incubated for another 10 min at room temperature. After centrifugation at 4,600 rpm for 11 min at 4°C, the aqueous phase was collected and supplemented with 30 µg glycogen (Roche Diagnostics) and one volume of isopropanol. The RNA was precipitated for 16 h at -20°C and then pelleted at 4,600 rpm for 30 min at 4°C. The pellet was washed twice by adding 2 ml 70% ethanol followed by centrifugation at 12,000 × g for 10 min at 4°C. After the remaining ethanol had evaporated completely, the pellet was resuspended in TE buffer (10 mM Tris-HCl pH 8.0, 1 mM EDTA) and stored at -80°C.

For transfection, 500 ng virus particle RNA was incubated for 10 min at room temperature with 2 µl/µg RNA jetPRIME (PolyPlus Transfection) according to the manufacturer's instructions. The transfection mix was added dropwise onto human A549 cells grown in a T25 flask to 80% confluency and the cells incubated for 1 h at 37°C before lysis.

Immunofluorescence microscopy

For immunfluorescence analysis, human A549 cells were grown on coverslips and infected for 1 h as outlined above. Then, cells were fixed with 4% paraformaldehyde dissolved in PBS, permeabilized with 0.5% Triton X-100 dissolved in PBS for 15 min, and blocked with 2% bovine serum albumine (BSA), 5% glycerol, 0.2% Tween 20 dissolved in PBS for 1 h at room temperature. Primary antibodies, rabbit polyclonal recognizing A/quail/Shantou/2061/00 (H9N2) and mouse polyclonal anti-human RIG-I (1:200; Baum et al., 2010), were diluted in blocking solution and cells were stained for 1 h at room temperature. After three times washing with PBS, cells were incubated with Alexa Fluor 555 donkey anti-mouse (1:200) and Alexa Fluor 488 donkey anti-rabbit (1:200) secondary antibodies supplemented with 4,4-diamidino-2-phenylindole (DAPI, 1:10.000) for 45 min at room temperature. Cells were washed three times with PBS and coverslips were mounted using Fluorsave solution (Calbiochem). Stained cell samples were examined using a Leica SP5 confocal microscope.

Expression of RIG-I in S2 cells

D. mel. S2 cells were transfected with 1 µg of pRmHa3-RIG-I plasmid, induced with $CuSO_4$, lysed and extracts dialyzed as described (Weber et al., 2013).

Purification of recombinant viral nucleocapsids

For purification of recombinant nucleocapsids via Strep-affinity tag, MDCK II cells in a 10 cm dish were infected with A/WSN/33 carrying a C-terminal Strep-tag on the PB2 protein (Rameix-Welti et al., 2009) at an MOI of 1. After 16 h the cells were washed with PBS, scraped off in PBS, pelleted by centrifugation at 100 × g for 5 min at 4°C. Pellets were then resuspended in Strep-lysis buffer (50 mM Tris/HCl pH 7.5, 150 mM NaCl, 2 mM MgCl2, 2mM CaCl2, 1% PMSF, 1 mM DTT, 0.7% NP40 and 50 U/ml DNase I (Fermentas)) and incubated on ice for 20 min. Lysates were then centrifuged at 16.200 x g for 10 min at 4°C and the cleared lysates were incubated for 1 h at 4°C with Strep-Tactin beads (IBA Goettingen). Beads were then pelleted by centrifugation at 100 × g for 1 min at 4°C, supernatant was removed and the beads were resuspended with wash buffer (50 mM Tris/HCl pH 7.5, 150 mM NaCl, 2 mM MgCl2, 2mM CaCl2, 1% PMSF, 1 mM DTT). Washing was performed three times and nucleocapsids were eluted by incubating the beads for 15 min on ice with wash buffer supplemented with 2.5 mM desthiobiotin (IBA Goettingen) Suspension was centrifuged at 100 × g for 1 min at 4°C and the eluate was transferred in a fresh tube and nucleocapsids were dialyzed against PBS.

Co-immunoprecipitation assay of recombinant nucleocapsids

For immunoprecipitations of recombinant nucleocapsids produced in minireplicon systems of strains A/WSN/33 (Neumann et al., 2000) or H9N2 (Baron et al., 2013), cells were seeded in T25 flasks and transiently transfected with expression plasmids encoding GFP (1 µg) or strain-specific PB2-627K or 627E (1 µg) together with NP (1 µg) alone or additionally with strain-specific PB1 (1 µg), PA (100 ng) and the firefly luciferase reporter minigenome construct (1 µg). At 24 h post-transfection, cell lysates were prepared and subjected to co-immunoprecipitation assay. Thereby, beads were directly coupled with mouse monoclonal HB65 antibody recognizing NP (Wisskirchen et al., 2011) or RIG-I (ALME-1). Coupled beads were incubated with the lysates for 2 h at 4°C and eluted as described. Co-immunoprecipitations were validated by immunoblotting using rabbit polyclonal H9N2, mouse monoclonal anti-PB2 JG6 (Marazzi et al., 2012) and mouse monoclonal anti-RIG-I antibody ALME-1.

Supplemental Reference

Marazzi, I., Ho, J.S., Kim, J., Manicassamy, B., Dewell, S., Albrecht, R.A., Seibert, C.W., Schaefer, U., Jeffrey, K.L., Prinjha, R.K., et al. (2012). Suppression of the antiviral response by an influenza histone mimic. Nature 483, 428-433.

4.4. Intergenic region of incoming nucleocapsid activate PKR -Lassa virus nucleoprotein provides a PKR evasion strategy-

Own contribution:

I performed all experiments of the main figures. Samples of Suppl. Fig. 2 were prepared by Markus Kainulainen (group of Prof. Dr. Weber, Institute for Virology, Marburg), Sarah Katharina Fehling (group of Dr. Strecker, Institute for Virology, Marburg) and Svenja Wolff (group of Prof. Dr. Becker, Institute for Virology, Marburg) while I performed analysis of the samples. I contributed to writing of the manuscript.

Michaela Gerlach

Intergenic region of incoming nucleocapsid activate PKR -Lassa virus nucleoprotein provides a PKR evasion strategy-

Michaela Weber[1], Sarah Katharina Fehling[1], Ulrike Felgenhauer[1], Markus Henrikki Kainulainen[2], Svenja Wolff[1], Stephan Becker[1], Thomas Strecker[1], Friedemann Weber[1]

[1]Institute for Virology, Philipps-University Marburg, Marburg, Germany

[2]current address: Centers for Disease Control and Prevention, Atlanta, USA

Abstract

Surveillance of non-self RNA by receptors of the innate immune system is a crucial first line of defense against viral infection. A rapid detection is thereby required for initiating an antiviral response to ensure survival of the host. Protein kinase R (PKR) represent one immune sensor able to recognize dsRNA and specific RNA secondary structures. Despite recognizing viral replicative dsRNA intermediates, we identified in this study the hairpin-structured intergenic region (IGR) of viral ambisense genomes as natural PKR agonists. Thus, the IGR seems to be exposed from nucleoprotein protection within the nucleocapsid complex allowing PKR to interact. Upon IGR recognition, PKR undergoes conformational switching and phosphorylation, identifying IGRs of RVFV S segment, New World arenavirus Tacaribe (TCRV) and Junin virus (JUNV) and Old World arenavirus Lassa virus (LASV) nucleocapsids as natural PKR agonists. To antagonize antiviral activity of PKR, TCRV, JUNV and LASV induce proteasomal degradation of activated PKR. In case of LASV, the newly synthesized nucleoprotein interacts with PKR and promotes its degradation. Hence, we identified the IGR as part of the viral nucleocapsid as an immediate PKR agonist. Furthermore, we pin down LASV nucleoprotein as a PKR antagonist by promoting its proteasomal degradation. This highlights PKR as an immune sensor of immediate infection and that arenaviruses have adapted to rapidly and efficiently avert antiviral PKR activity. Furthermore, IGRs play an essential role in the control of viral protein synthesis indicating the necessity to conserve this structure despite the presence of antiviral defense mechanisms. This suggests targeting of the IGR to block virus replication a promising target for drug development.

Introduction

Virus infection is a constant threat to human mankind. Thus, to rapidly control virus infection an immediate recognition of the viral intruder is required. Several groups of innate immune receptors, including Toll-like receptors (TLR), RIG-I like receptors (RLR), NOD-like receptors (NLR), C-type lectin receptors (CLR), and other cytosolic RNA and DNA sensors are thereby crucial to distinguish between host cell (self) and pathogen associated structures (non-self) (Pandey et al., 2014).

RLR have a central role to detect RNA virus infection in the cytoplasm of the infected cell. The family of RLR is formed by retinoic acid inducible gene 1 (RIG-I), melanoma differentiation association factor 5 (MDA5) and laboratory of genetics and physiology 2 (LGP2). Studies have demonstrated that RIG-I and MDA5 recognize mostly distinct RNA structures. MDA5 is known to sense longer double-stranded RNA (dsRNA) molecules, ideally with higher order RNA structures (Pichlmair et al., 2009, Schlee, 2013). RIG-I mainly responds to 5' ppp blunt-ended dsRNA of a minimal length of 10 base pairs (Kohlway et al., 2013, Schmidt et al., 2009, Schlee et al., 2009). Recently, dsRNA stretches bearing a 5`diphosphate were identified to stimulate a RIG-I dependent response (Goubau et al., 2014). Interestingly, also in the encapsidated state, RIG-I can sense short 5`ppp dsRNA panhandle structures of incoming nucleocapsids (Weber et al., 2013). Ligand-mediated activation of RIG-I stimulates a signaling reaction that culminates in the induction of type I interferon (IFN-alpha/beta), proinflammatory cytokines and eventually numerous interferon stimulated genes (ISGs) (Goubau et al., 2013, Reikine et al., 2014, Ivashkiv and Donlin, 2014, Hertzog and Williams, 2013). ISG represent viral restriction factors that directly inhibit all steps of virus replication and furthermore co-stimulatory molecules, cytokines and chemokines which favor the initiation of adaptive immune responses (Schoggins, 2014, Schneider et al., 2014, Loo and Gale, 2011).

Viruses have evolved to impair or evade RIG-I recognition. Further immune sensors are thus required to ensure a rapid detection and response to the viral intruder. However, whether other immune sensors recognize like RIG-I incoming protein-associated viral RNA and stimulate an antiviral response remained elusive. Here, we addressed the question whether protein kinase R (PKR) contributes to an immediate immune recognition.

PKR represents an RNA sensor which is expressed at a low constitutive level mainly in the cytoplasm. Despite being upregulated upon virus induced IFN response, PKR expression can also be increased upon other cellular stress signals like disturbances of calcium homeostasis (Williams, 1999). PKR represents a multifunctional protein involved in the regulation of cap-dependent translation by phosphorylation of the alpha subunit of eukaryotic initiation factor 2 (eIF2α). Furthermore, PKR is crucial for the virus induced formation of stress granules required for IFN-signaling (Onomoto et al., 2012). To stimulate PKR activation there is a minimal dsRNA length requirement of approximately 33 base pairs, but also specific structural modalities like bulges and loops and nucleotide modifications

like a 5`ppp support PKR stimulation (Nallagatla et al., 2007, Dzananovic et al., 2013, Bevilacqua and Cech, 1996). Thereby, replicative intermediates of negative-strand RNA viruses can form PKR activating dsRNA stretches. PKR thus senses virus replication, but involvement of PKR as an immediate immune sensor and inducer of antiviral defense mechanisms remains to be resolved. An interaction of PKR with viral RNA secondary structures like the hepatitis C virus IRES or dimerized stem-loop structures of transactivation (TAR) RNA of human immunodeficiency virus 1 was previously reported (Shimoike et al., 2009, Heinicke et al., 2009). Whether PKR would however recognize viral RNA in the encapsidated state was not addressed so far.

In this study, we report the hairpin-structured intergenic region (IGR) of two distinct virus families as PKR agonists. Thereby, the IGR seems to be exposed from nucleoprotein protection within the nucleocapsid complex allowing PKR to interact. Upon IGR recognition, PKR undergoes conformational switching and phosphorylation identifying IGRs of RVFV S segment, New World arenavirus Tacaribe (TCRV) and Junin virus (JUNV) and Old World arenavirus Lassa virus (LASV) nucleocapsids as natural PKR activators. To antagonize antiviral activity of PKR, TCRV, JUNV and LASV induce proteasomal degradation of activated PKR. In case of LASV, the newly synthesized nucleoprotein interacts with PKR and promotes its degradation. Hence, we identified the IGR as part of the viral nucleocapsid as an immediate PKR agonist. LASV nucleoprotein counteracts antiviral PKR activity by promoting its proteasomal degradation. Furthermore, this seems to be a common mechanism within the arenavirus family although the responsible TCRV and JUNV protein could not be identified so far. This highlights PKR as an immune sensor of immediate infection and that arenaviruses have adapted to rapidly and efficiently avert antiviral PKR activity.

Experimental Procedures

Cells, Viruses and Transfection

Human A549 and HEK293T cells were cultivated in Dulbecco's modified Eagle's medium (DMEM) supplemented with 10% fetal calf serum (FCS) at 37°C and 5% CO_2. Recombinant La Crosse virus lacking the virulence factor NSs (LACV; (Blakqori and Weber, 2005)) and recombinant Rift Valley fever virus expressing Renilla luciferase instead of NSs (RVFV; (Habjan et al., 2009a)), Junin virus (JUNV), Tacaribe virus (TCRV) and Lassa virus (LASV) were propagated on Vero E6 cells. All work with LASV and JUNV was performed in the BSL-4 laboratories at the Philipps University Marburg, Germany.

For transient overexpression, HEK293T cells were transfected by standard calcium phosphate transfection method with either 0.25, 0.5, 1 or 2 µg of pCAGGS_GP-HA, pCAGGS_NP-HA, pCAGGS_Z-HA or pcDNA3.1_ΔMX combined with 1 µg of pcDNA5_PKR.

Rift Valley Fever virus like particle (RVF VLP) production

Generation of RVF VLPs was carried out as previously described (Habjan et al., 2009a), with minor alterations. Briefly, 1x10e6 HEK293T cells were transfected with 1 µg each of plasmid pI.18_RVFV_N, pI.18_RVFV_L, pI.18_RVFV_M, and a reporter minigenome using Nanofectin transfection reagent (PAA Laboratories). Therefore, a minigenome with Renilla luciferase in negative sense flanked by 5' and 3' untranslated regions (UTRs) from either RVFV middle (M) or small (S) segment was used (pHH21_RVFV_vM and pHH21_RVFV_vS, respectively). In case of the S segment, the minigenome contained the full-length RVFV S segment and the NSs replaced by Renilla luciferase. For production of empty VLPs (no minigenome), 1 µg each of plasmid pI.18_RVFV_N, pI.18_RVFV_M and for DNA amount normalization pcDNA3.1_ΔMX was used for transfection. At 4 h post-transfection, the medium was exchanged and 48 h later supernatants were collected and clarified from cell debris by centrifugation at 500xg for 5 min. Subsequentially, VLPs were treated with 25 U/ml benzonase (Novagen) for 3 h at 37°C and then stored at -80°C.

Infection and Inhibitor treatment

A549 cells were inoculated for 1 h with viruses or RVF VLPs. Infection medium was replaced with DMEM containing 2% FCS thereafter. If indicated, cells were pretreated with 50 µg/ml cycloheximide (CHX) dissolved in complete medium for 1 h. CHX was also added to the virus inoculum and to the medium added afterwards. MG132 dissolved in media at the final concentration of 20 µM was added immediately after the virus inoculum was removed. In case of transfected cells, 20 µM MG132 containing complete media was added 8 h post-transfection and cells were incubated for additional 16 h at 37°C with 5% CO_2. CHX and MG132 were purchased from Sigma-Aldrich. Cells were lysed or fixed at the indicated time points.

Limited protease digestion

Limited protease digestion to monitor RIG-I and PKR conformational switching was essentially performed as described elsewhere (Weber and Weber, 2014a). Briefly, cells of one well of a six well plate were lysed in 25 µl 0.5% Triton X-100 in PBS supplemented with Phosphatase Inhibitor Cocktail set II (Calbiochem). After an incubation on ice for 10 min, the samples were centrifuged for 10 min at 10,000×g at 4°C and 10 µl of the cleared lysate were kept as input and the other 10 µl were digested for 20 min with 0.2 µg/µl L-1-tosylamido-2-phenylethyl chloromethyl ketone (TPCK)-treated trypsin (Sigma-Aldrich) at 37°C. Reaction was stopped by adding 4-fold sample buffer (200 mM Tris-HCl pH 6.8, 8% SDS, 40% glycerol, 25% β-Mercaptoethanol, 0.4% Bromphenol Blue) and boiling for 10 min at 100°C according to BSL4 safety procedures. Samples were subjected to SDS-PAGE and Western Blot analysis using mouse monoclonal anti-RIG-I antibody (ALME-1, Enzo Life Sciences) at 1:1,000; mouse monoclonal anti-PKR B10 (Santa Cruz) at 1:500 and rabbit monoclonal against phosphorylated PKR at position threonine 446 (p-PKR Thr 446; Epitomics) at 1:500.

Co-immunoprecipitation

Cells grown in a T75 tissue culture flask (infection) or in two wells of a six well plate (transfection) were scraped off in PBS, centrifuged at low speed, and the pellets were lysed in 50 mM Tris-HCl pH 7.5, 150 mM NaCl and 1% NP40 supplemented with phosphatase inhibitor and Protease inhibitor cocktail Complete (Roche), incubated on ice for 10 min and centrifuged for 10 min at 10,000×g at 4°C. Cleared cell lysates were transferred to fresh tubes and 2% were kept as input control. The remaining lysate was subjected to immunoprecipitation (IP) using magnetic beads (Dynabeads, Invitrogen). The coupling of the beads with the corresponding antibody was performed according to the manufacturer's instructions with minor modifications. For each IP, 1.5 mg of beads were incubated with rabbit polyclonal anti-mouse antibody (DAKO) at a dilution of 1:200 for 16 h at 37°C. After the first antibody coupling, beads were washed three times with lysis buffer, and the anti-mouse antibody beads were further incubated with mouse monoclonal anti-p21 (Santa Cruz Biotechnology), mouse monoclonal anti-RIG-I or mouse monoclonal anti-PKR B10 at a 1:200 dilution in lysis buffer for 24 h at 4°C. Beads were washed three times with lysis buffer and then incubated with the lysates for 2 h at 4°C. The immunoprecipitates were washed three times with lysis buffer and eluted by adding 1-fold sample buffer (50 mM Tris-HCl pH 6.8, 2% SDS, 10% glycerol, 6.25% β-Mercaptoethanol, 0.1% Bromphenol Blue). Western blot analysis was performed with mouse monoclonal anti-RIG-I at 1:1000, mouse monoclonal anti-PKR B10 at 1:500, rabbit monoclonal anti-p-PKR Thr 446 at 1:500, mouse monoclonal anti-p21 (Santa Cruz) at 1:500, rabbit polyclonal anti-HA (abcam) at 1:1000, rabbit polyclonal anti-LACV N at 1:1000, mouse polyclonal anti-RVFV N serum (Habjan et al., 2009b) at 1:1000 and rabbit monoclonal anti LASV NP at 1:3000. As a secondary antibody protein A-horseradish

peroxidase (HRP) conjugate (Millipore) at a dilution of 1:10,000 was used to avoid detection of heavy and light antibody chains.

Co-sedimentation assay

For co-sedimentation assays, cell lysates were prepared as described for co-IP. The cleared lysate was loaded on top of a discontinuous 50% to 70% glycerol gradient in 50 mM Tris-HCl pH 7.5, 150 mM NaCl and centrifuged at 52.000 rpm for 2 h at 12°C in a SW60 rotor (Beckman). Twelve fractions were recovered from top to bottom and pelleted at 45,000 rpm for 1 h at 4°C in a TLA45 rotor (Beckman). Pellets were dissolved in 1-fold sample buffer, boiled for 5 min at 100°C and validated by SDS-PAGE followed by Western Blot analysis. Proteins were detected with mouse monoclonal anti-RIG-I antibody at 1:1000, mouse monoclonal anti-PKR B10 at 1:500, rabbit polyclonal anti-LACV N at 1:1000, and mouse polyclonal anti-RVFV N serum at 1:1000.

GSDIM

For immunfluorescence analysis via ground state depletion microscopy followed by individual molecule return (GSDIM), 4x10e5 A549 cells were grown on coverslips and infected for 1 h as outlined above. Then, cells were fixed with 4% paraformaldehyde dissolved in PBS for 20 min, permeabilized with 0.5% Triton X-100 in PBS for 15 min, and blocked with 2% bovine serum albumine, 5% glycerol, 0.2% Tween 20 in PBS for 1 h. Primary antibodies, rabbit anti-RVFV MP12 hyperimmune serum C2, mouse polyclonal anti-human RIG-I (Baum et al., 2010) and mouse monoclonal anti-PKR B10, were diluted 1:200 in blocking solution and cells were stained for 1 h. After three times washing with PBS, cells were incubated with secondary antibody Alexa Fluor 555 donkey anti-mouse at 1:200 and Alexa Fluor 647 donkey anti-rabbit at 1:200 supplemented with 4,4-diamidino-2-phenylindole (DAPI) at 1:10,000 for 45 min at room temperature. Cells were washed three times with PBS and samples were embedded in freshly prepared 100 mM β-mercaptoethylamine in PBS pH 7.4 directly before imaging. Analysis was performed with the Leica SR GSD microscope. Quantification was performed of three independent experiments. Student's T-test was carried out for statistical analysis.

Results

RIG-I and PKR differ in their agonist specificity

It was recently described by our group that the 5'ppp panhandle structure of incoming viral nucleocapsids serve as a natural RIG-I agonist to promote an immediate antiviral IFN response (Weber et al., 2013). To test whether other immune receptors would contribute to an immediate virus recognition, cells were infected with either La Crosse virus (LACV) or Rift valley fever virus (RVFV) (*Bunyaviridae*), both lacking the virulence marker NSs. Bunyavirus are peculiar since their transcription is dependent on an on-going translation (Elliott, 1990). Hence, treatment with the translation inhibitor cycloheximide (CHX) aborts viral transcription and allows analysis of immune receptor activation by incoming nucleocapsids in the physiological context of virus infection.

By performing limited protease digestion to monitor RIG-I activation status (Weber and Weber, 2014a), stimulated RIG-I undergoes conformational rearrangements leading to detection of trypsin resistant fragments. RIG-I activation is thereby independent whether viral replication occurs (Fig. 1A, left panel) or if only incoming nucleocapsids are present (Fig. 1A, right panel).

PKR is another well-known cytoplasmic pattern recognition receptor able to detect dsRNA stretches of at least 33 nucleotides or RNA secondary structures (Dabo and Meurs, 2012). PKR is composed of two amino-terminal dsRNA binding domains (dsRBD), a carboxy-terminal serine/threonine kinase domain and both domains are linked by a flexible linker (VanOudenhove et al., 2009). In absence of a stimulus, PKR is present as a monomer with an extended open conformation where the dsRBD are impeding kinase domain activity. Agonist recognition induces conformational rearrangements to a closed conformation allowing dimerization and auto-phosphorylation (Dabo and Meurs, 2012, Clemens, 1997, VanOudenhove et al., 2009, Lemaire et al., 2006). Like RIG-I, also PKR conformational changes can be measured by limited protease digestion (Weber and Weber, 2014a). Upon agonist recognition, PKR reorganizes its domains leading to partial protease resistance. Surprisingly, LACV and RVFV differ in their ability to promote PKR resistance to trypsin treatment and induction of PKR phosphorylation at threonine 446. LACV full viral replication only poorly and incoming LACV nucleocapsids even fail to induce these two markers of PKR activation (Fig. 1B). However, RVFV full infectious cycle and incoming nucleocapsids lead to a robust induction of PKR resistant fragments and detection of PKR phosphorylation. Since strongest differences between LACV and RVFV induced PKR activation were observed by stimulating with incoming nucleocapsids, we focused on the immediate pathogen recognition.

By performing co-sedimentation assay the migration pattern in a discontinuous glycerol gradient of RIG-I and PKR upon stimulation with LACV or RVFV nucleocapsids was analyzed. In mock infected cells, RIG-I was mainly distributed from fraction 6 to 8 (Fig. 1C, upper panel). LACV and RVFV nucleocapsids

induced a shift of RIG-I up to fraction 4 confirming the previous observation that RIG-I is able to recognize these two bunyaviruses (Fig. 1C, middle and lower panel). PKR distribution upon LACV nucleocapsid stimulation showed a comparable distribution pattern from fraction 7 to 10 as mock infection (Fig. 1C, upper and middle panel). In contrast, RVFV nucleocapsids induced a concentration of total PKR in fraction 7 (Fig. 1C, lower panel). The observed shift of nucleocapsids can hence be associated to recognition of LACV and RVFV nucleocapsids by RIG-I or RIG-I and PKR, respectively. Noteworthy, migration of RIG-I and PKR was dependent on RNA since overexpression of the nucleoprotein alone did not induce a change in the distribution pattern (Suppl. 1).

To further validate an interaction between PKR and incoming bunyavirus nucleocapsids co-immunoprecipitation (co-IP) assays were performed. As reported before, RIG-I interacted with LACV as well as RVFV nucleocapsids (Fig 1D). However, with a PKR specific co-IP only RVFV, but not LACV nucleocapsids could be co-precipitated.

In summary, these data indicate that LACV and RVFV nucleocapsids can be both recognized by RIG-I and mediate its activation. RVFV nucleocapsids, on the contrary, serve also as PKR agonist.

Presence of an intergenic region within viral nucleocapsids determines PKR recognition and activation

Since the observed differences of LACV and RVFV nucleocapsid recognition by PKR seemed to be dependent on viral RNA, we wondered whether this could be due to the different LACV and RVFV coding strategies. Bunyavirus particles comprise three genome segments with negative polarity which are named according to their size large (L), middle (M) and small (S). RVFV L and M segment contain only a single transcriptional unit in negativesense orientation, whereas the S segment uses ambisense coding strategy (Giorgi et al., 1991). Thereby, two open reading frames are separated by a highly conserved non-coding intergenic region (IGR). RVFV IGR forms a hairpin structure with a central dsRNA stem with internal loops and peculiar poly-C (viral sense) and poly-G (viral anti-sense) repeats (Fig. 2A) (Lara et al., 2011, Ikegami, 2012). Members of the Orthobunyavirus family like LACV do not use ambisense coding strategy (Elliott, 2014). During the replication cycle, each genome segment is transcribed into mRNA and then translated to allow genome replication and generation of progeny viruses (Fig. 2B). Amplification of the viral genome (vRNA) involves the synthesis of an exact copy of the vRNA, called complementary RNA (cRNA). In case of the RVFV S segment, the cRNA serves also as a template for mRNA synthesis (Ikegami, 2012, Walter and Barr, 2011). Since it was described that the RVFV IGR is accessible for other proteins (Moy et al., 2014) we wondered whether PKR would also use this structure to gain access to RVFV nucleocapsids.

To validate the importance of the IGR for PKR activation, virus like particles (VLPs) were generated containing nucleocapsids either with the RVFV M or S genome segment. PKR activation status was

monitored by detection of protease resistance. As a control we included RIG-I activation since 5`ppp panhandle structures of M and S segmented nucleocapsids should activate RIG-I to the same extend. Indeed, infection with RVF VLPs regardless which genome segment is packaged within the particle as well as nucleocapsids from RVFV infection stimulated RIG-I conformational rearrangements (Fig. 2C). Likewise, stimulation with RVF VLPs with S segmented nucleocapsids induce PKR resistant fragments whereas VLPs containing an encapsidated RVFV M genome segment failed to promote PKR activation. To visualize the interaction of RIG-I and PKR with the RVF VLP M or S nucleocapsids super-resolution microscopy was employed. As previously reported, RVFV nucleocapsids are displayed as pseudocircular structures with RIG-I attached via a single site (Fig 2D). Thereby, interaction of RIG-I with RVFV nucleocapsids was independent of which genome segment was packaged in the viral particle. Also PKR co-localized with nucleocapsids of RVFV infection presenting all genome segments. This interaction was significantly reduced if only M segmented nucleocapsids were present. In case of RVF VLPs enclosing S segmented nucleocapsids almost 80% of the viral nucleocapsids co-localized with PKR. Like RIG-I also PKR contacts the nucleocapsids only via a single position, most likely the IGR. This indicates that PKR recognizes the IGR of incoming RVFV nucleocapsids which promotes PKR activation.

Arenavirus nucleocapsids promote PKR activation in absence of translation

In comparison to RVFV, representatives of the *Arenaviridae* contain two genome segments and each uses ambisense coding strategy with an IGR separating the open reading frames (McLay et al., 2014). Arenavirus IGR represents like RVFV IGR a hairpin structure composed of a dsRNA stem with internal loops and sporadic mismatches (Fig. 3a). Therefore, we hypothesized that during arenavirus infection nucleocapsids would present strong stimulators of PKR activation. New World Junin virus (JUNV) and Tacaribe virus (TCRV) and Old World Lassa virus (LASV) were chosen as representatives of the arenavirus family to validate the potential of their nucleocapsids to promote PKR activation. Surprisingly, full infectious cycle of TCRV, JUNV and LASV did not stimulate PKR phosphorylation and conformational switching (Fig. 3b). An abort of the infectious cycle at primary transcription due to CHX treatment, however, partially rescued PKR activation. These results could be confirmed by a time-course experiment (Suppl. 2). LACV full replication cycle induced a robust PKR activation whereas LACV nucleocapsids did not stimulate a detectable amount of phosphorylated PKR. Furthermore, 24 h post-infection total PKR gets degraded indicating the induction of a negative feedback loop to control PKR signaling. In contrast, RVFV infection and incoming nucleocapsids induced phosphorylation of PKR. Therefore, only incoming nucleocapsids containing an IGR are able to promote PKR activation as observed in Fig. 1B. Full infectious cycle of TCRV, JUNV and LASV did not stimulate PKR phosphorylation though translation inhibition did partially rescue PKR activation. This indicates on the one hand, that arenavirus nucleocapsids are indeed able to stimulate PKR activation. On the other hand, PKR

activation by arenaviruses can only be detected in absence of protein synthesis. This raises the question whether newly synthesized arenavirus proteins prevents PKR activation during the full viral life cycle.

LASV nucleoprotein induces proteasomal degradation of phosphorylated PKR

To gain further insights into an arenavirus PKR antagonist, the focus was put on LASV. By performing co-IPs, an interaction of PKR with nucleocapsids which are just entering the cell (CHX), but also with nucleocapsids generated during viral replication (UT) could be observed (Fig. 4A). However, phosphorylated PKR could only be detected if translation was blocked. Furthermore, a weak interaction of RIG-I with LASV nucleocapsids could only be detected, when full viral replication was allowed. This is confirm with the observation that 5` overhangs of arenavirus nucleocapsids hinder RIG-I recognition (Marq et al., 2010) and that RIG-I might rather interact with arenavirus dsRNA replicative intermediates generated during virus replication.

To identify the responsible protein able to impair PKR activation, LASV nucleoprotein (NP), glycoprotein (GP) and matrix protein (Z) were overexpressed with increasing concentrations together with PKR at a constant concentration. PKR overexpression alone was able to promote PKR phosphorylation (Fig. 4B). Thus, in case of excessive PKR within the cytoplasm of the transfected cells two PKR molecules are able to promote each other's phosphorylation due to proximity. PKR activation status was further supported with increasing amounts of LASV GP and Z. However, overexpression of LASV NP results in a reduction of phosphorylated PKR in a dose-dependent manner, without having major effects on the total PKR amount. By performing co-IP, phosphorylated PKR is reduced in LASV NP expressing cells and also total PKR seems to be slightly decreased (Fig 4C). With a PKR specific co-IP, LASV NP, but not GP or Z, could be co-precipitated indicating an interaction between PKR and LASV NP.

As described above, RVFV and arenavirus nucleocapsids are likewise recognized by PKR. Due to this first similarity between the representatives of these two distinct virus families argues whether they would also share similar PKR antagonistic mechanisms. Hence, since RVFV NSs promotes the proteasomal degradation of PKR (Ikegami et al., 2009, Habjan et al., 2009b) we wondered whether the proteasome would also be involved in reduction of activated PKR during the course of arenavirus infection. Thus, cells were transfected with the individual LASV proteins together with PKR and analyzed for PKR phosphorylation status in absence or presence of the proteasomal inhibitor MG132. In untreated (UT) cells LASV NP overexpression reduces PKR phosphorylation in comparison to LASV GP and Z, and GFP control (Fig. 4D, left panel). However, if proteasomal degradation is blocked PKR phosphorylation is rescued in LASV NP transfected cells (Fig. 4D, right panel). However, LASV GP and Z do not affect PKR activation status in absence or presence of MG132. Also under infectious conditions,

in untreated cells (UT) TCRV, JUNV and also LASV infection failed to promote PKR activation which could be restored by MG132 treatment (Fig. 4E). This indicates that LASV NP specifically induces the proteasomal degradation of activated PKR. Additionally, since inhibition of the proteasomal pathway also rescues phosphorylated PKR in case of TCRV and JUNV suggests a similar mechanism to prevent antiviral PKR activity throughout the arenavirus family.

Taken together, after LASV entry the viral nucleocapsids are released into the cytoplasm of the infected cell for viral transcription and replication (Fig. 5). The IGR of the viral nucleocapsids is recognized by PKR, which leads to PKR conformational rearrangements and phosphorylation. Activated PKR initiates translation block via phosphorylation of eIF2α and type I IFN and proinflammatory cytokine response via NF-κB to impair LASV replication. Once inside the cytoplasm however transcription and viral protein synthesis is rapidly initiated. With an increasing concentration within the cell, LASV NP interacts with PKR and induces its proteasomal degradation. This identifies nucleocapsids bearing an IGR as natural PKR agonists and that arenaviruses have evolved to rapidly counteract immediate immune recognition.

Discussion

Surveillance of non-self RNA by receptors of the innate immune system is a crucial first line of defense against viral infection. A rapid detection is thereby required to efficiently control or even eliminate the viral intruder. Our group has recently shown, that RIG-I is able to recognize the 5`ppp dsRNA panhandle structure of incoming viral nucleocapsids to induce an immediate antiviral type I IFN response (Weber et al., 2013). However, whether other host receptors would likewise be able to recognize viral structures immediately after virus entry remained unresolved.

Thus, PKR activation by incoming nucleocapsids of two representatives of the *Bunyaviridae* was validated. Surprisingly, PKR recognizes and gets activated by RVFV but not LACV nucleocapsids. Considering the differences of PKR activation between the two related viruses let us conclude that the diverse coding strategies and hence different RNA structures play a role. All three genome segments of LACV and RVFV L and M segment are in negative polarity with only one transcriptional unit. RVFV S segment, however, uses ambisense coding strategy to direct synthesis of two proteins in an opposite direction, separated by a non-coding IGR (Giorgi et al., 1991, Elliott, 2014). By analyzing the predicted RVFV IGR, a hairpin structure can be observed with a central dsRNA stem with internal loops and peculiar poly-C/G repeats. These repeats were previously described as essential transcription termination signals (Albarino et al., 2007). As a minimal requirement for PKR activation serves a hairpin with a 16-base pair dsRNA stem flanked by 10 to 15 nucleotides of single-stranded tails (Zheng and Bevilacqua, 2004). The dsRNA stem thereby does not have to possess perfect base pairing since PKR can tolerate non-Watson-Crick structures and also internal loop structures within the dsRNA stem as long as the overall A-form geometry of the RNA is retained (Bevilacqua et al., 1998, Bevilacqua and Cech, 1996).

Thus, RVFV IGR presents all criteria of a potential PKR agonist. It was furthermore reported that PKR can interact with structured elements of viral RNA like HCV IRES or dimerized stem-loop structures of transactivation (TAR) RNA of HIV (Shimoike et al., 2009, Heinicke et al., 2009). However, whether PKR recognizes viral RNA packaged into nucleocapsids in infectious context remained elusive.

Moy *et al*. previously reported in this regard that human DDX17 or *Drosophila* Rm62 specifically interacts with RVFV S segment IGR (Moy et al., 2014) indicating that the IGR would also be exposed for PKR interaction. PKR contacts the dsRNA mainly via 2`hydroxyl groups of the ribose sugar and oxygen residues of the phosphate backbone in a sequence independent manner (Bevilacqua and Cech, 1996). Orthobunyavirus, like LACV, RNA is deeply sequestered within the nucleocapsids (Ariza et al., 2013) making the RNA highly inaccessible for PKR. RVFV nucleocapsids, however, are less symmetric and with few specific protein–protein interactions leaving the phosphate backbone partially exposed (Raymond et al., 2010, Raymond et al., 2012). Thus, oxygen groups of the phosphate backbone would be accessible for PKR interaction. Indeed, our data demonstrates that PKR is able to engage the IGR within

the viral nucleocapsid in the authentic context of virus infection. Interaction with the IGR promotes PKR conformational switching and phosphorylation identifying IGRs as natural PKR agonist. Partial exposure of the viral RNA alone, however, is not sufficient for PKR activation. This is indicated by the observation that RVFV M or S segmented nucleocapsids with the same packaging grade of the viral RNA only activate PKR if the IGR is present. As previously reported, influenza B virus nucleocapsids serve as PKR agonists at late stages of infection (Dauber et al., 2009). PKR, thereby, interacts with the 5`ppp dsRNA panhandle. Here, recognition of incoming nucleocapsids by PKR seems to be independent of the panhandle since RVFV M segmented nucleocapsids presenting a 5`ppp dsRNA panhandle failed to promote PKR activation. It can be postulated that at an early infectious stage, when low amounts of nucleocapsids are present RIG-I outcompetes PKR for 5`ppp panhandle interaction. It seems also plausible that PKR is only interacting with the 5`ppp promoter structure at later time-points of infection when misencapsidated side product of viral replication occur. Furthermore, PKR might not gain access to the panhandle of incoming nucleocapsids covered by the viral polymerase since PKR was not associated with the ability to remove proteins from RNA as it was postulated for RIG-I (Schmidt et al., 2011).

Interestingly, PKR interaction with the IGR of incoming nucleocapsids is independent on IFN induced upregulation of PKR as previously observed (Nallagatla et al., 2007). Already basal PKR levels are sufficient to recognize the IGR of viral nucleocapsids.

Despite RVFV, also representatives of the *Arenaviridae* use ambisense coding strategy, thus, bearing an IGR for transcriptional control. Arenavirus nucleoprotein sequesters the RNA bases like RVFV not completely leaving them partially exposed (Hastie et al., 2011b). The predicted IGR of TCRV, JUNV and LASV S and L segment represents a similar structure in comparison to RVFV with a hairpin composed of a dsRNA stem with internal loops and sporadic mismatches. Therefore, it was not surprising that like RVFV, also Old World Lassa virus and New World TCRV and JUNV nucleocapsids are able to promote PKR activation. This indicates, that the IGR presented in the nucleocapsids of two distinct virus families represent natural PKR agonist to promote an immediate antiviral response. Moy *et al.* postulated that interaction of a protein with the IGR of viral genomes has a negative impact on virus replication (Moy et al., 2014). We may, therefore, hypothesize that by interaction with bunyavirus RVFV and arenavirus TCRV, JUNV and LASSV IGR, PKR could also impair virus replication independent of its downstream signaling activity. However, this was beyond the scope of our study and requires further investigation.

PKR activation surprisingly could only be detected with incoming arenavirus nucleocapsids, but not if full infectious cycle was allowed. This raised the question whether arenaviruses encode for a PKR antagonist. By applying a diverse set of molecular biological assays LASV NP was identified as an inhibitor of PKR activation. Thereby, LASV NP interacts with PKR and induces its proteasomal degradation. It seems that the LASV NP encapsidating the viral genome does not affect the activation

status of PKR, which suggests that only free LASV NP acts as a PKR antagonist. LASV NP comprises dsRNA binding properties (Hastie et al., 2011a), hence, RNA could serve as a scaffold for PKR interaction. However, data supports rather a viral RNA independent interaction of LASV NP with PKR. Nevertheless, it cannot be excluded that LASV NP forms a complex with cellular RNA. It was reported in this regard that recombinant nucleoproteins of NSV can associate with cellular RNA into nucleocapsid like structures (Ruigrok et al., 2011).

Interestingly, LASV NP comprises the ability to oligomerize (Lennartz et al., 2013). It remains to be resolved, whether NP monomers or LASV oligomeric complexes promote PKR antagonism. It was previously demonstrated that interference with the IFN response is not strictly dependent on NP oligomerization (Lennartz et al., 2013). Besides, Hastie *et al.* reported that rather the dsRNA specific 3` to 5` exonuclease activity of LASV NP is essential for inhibiting IFN signaling (Hastie et al., 2011a). Since incoming nucleocapsids do not present long dsRNA stretches to the host immune system, degradation of dsRNA might play a distinct immune evasion strategy during later infectious stages.

Arenavirus NP is well conserved between Old and New World arenaviruses (Hastie et al., 2011b), suggesting that an IFN antagonistic activity may be a shared feature (Hastie et al., 2011a). Indeed, Old World arenavirus LCMV and New World arenaviruses Whitewater Arroyo virus, Pichinde virus, JUNV, Machupo virus and Latino virus, but not TCRV were able to impair IFN and proinflammatory response (Martinez-Sobrido et al., 2006, Martinez-Sobrido et al., 2007, Rodrigo et al., 2012). However, the underlying mechanism still needs to be clarified. Likewise, arenaviruses use proteasomal degradation as a common PKR antagonism. However, the responsible viral protein could not be identified so far. TCRV unable to impair IFN signaling (Martinez-Sobrido et al., 2007) was surprisingly able to inhibit PKR activation. This highlights the requirement to prevent early recognition by PKR to ensure efficient virus propagation even in the case of apathogenic viruses like TCRV.

Conclusively, we identified the hairpin-structured IGR of RVFV S segment, New World arenavirus TCRV and JUNV and Old World arenavirus LASV nucleocapsids as natural PKR agonists. To prevent the antiviral PKR activity, TCRV, JUNV and LASV induce proteasomal degradation of activated PKR. In case of LASV, the newly synthesized nucleoprotein interacts with PKR and promotes its degradation via the proteasomal pathway. Hence, we identified the IGR as part of the viral nucleocapsid as an immediate PKR agonist in the authentic context of virus infection. Addtionally, LASV NP was pinned down as a novel PKR antagonist. In addition to antagonizing immediate PKR recognition, arenavirus also impair early detection of viral nucleocapsids by RIG-I via an unpaired 5`ppp (Marq et al., 2010). Therefore, arenaviruses have evolved an efficient strategy to counteract immediate recognition and activation of antiviral defense mechanisms. Interestingly, IGRs play essential roles in the control of viral protein synthesis and hence virus replication (Lopez and Franze-Fernandez, 2007, Emery and Bishop, 1987, Geerts-Dimitriadou et al., 2012, Albarino et al., 2007), indicating the necessity to conserve this

structure despite the presence of antiviral defense mechanisms. This makes targeting of the IGR to block virus replication a promising target for drug development.

Acknowledgments

We thank Julia Wulle for excellent technical assistance. We also thank Alejandro Brun from CISA-INIA for providing anti-Rift Valley fever Virus sera. Work in our laboratories is supported by Deutsche Forschungsgemeinschaft grants We 2616/7-1, SFB 593 and SFB 1021, grant 47/2012MR from the Forschungsförderung (§2 Abs. 3) Kooperationsvertrag UKGM, and the Leibniz Graduate School for Emerging viral diseases (EIDIS).

Disclosures:

No conflicts of interest declared.

Figure Legend

Fig. 1: RIG-I and PKR differ in their agonist specificity

A549 cells were either left untreated (UT) or were treated with 50 µg/ml cycloheximide (CHX) and mock infected or infected with LACVΔNSs or RVFVΔNSs at an multiplicity of infection (MOI) of 5. After 5 h, cells were lysed and subjected to limited protease digestion (A and B), co-sedimentation (C) or co-immunoprecipitation assay (D). (A and B) Conformational switch. Cell lysates were treated with trypsin (+) and untreated cell lysates (-) served as input control. Western Blot analysis was performed with anti-RIG-I antibody (A) and with antibodies recognizing PKR and phosphorylated PKR (P-PKR) (B). (C) Co-sedimentation assay. Cell lysates were loaded on a 50-70% discontinuous glycerol gradient, centrifuged and collected fractions were concentrated. Samples were subjected to Western Blot analysis using antibodies directed against RIG-I, PKR and LACV or RVFV N as a marker for viral nucleocapsids. (D) Co-immunoprecipitation. Cell lysates were mixed with anti-p21 (negative control), anti-RIG-I or anti-PKR coupled magnetic beads and incubated for 2 h at 4°C. As input control 2% of the lysates were kept. Input and eluates were analyzed by Western Blotting using anti-RIG-I, anti-PKR, anti-LACV or RVFV N and anti-p21 antibodies.

Fig. 2: Intergenic region of incoming RVFV nucleocapsids serve as PKR agonists.

(A) RVFV intergenic region. Secondary structure prediction of RVFV S segment (data base entry EU312104.1) intergenic region via free energy minimization (mFold). (B) RVFV coding strategy. Viral particles contain three genome segments in negative polarity (vRNA) which are named large (L), middle (M) and small (S). L and M segment contain only a single transcriptional unit whereas the S segment uses ambisense coding strategy. Thereby, two open reading frames are separated by an intergenic region (IGR). During replication, each genome segment is first transcribed to allow protein synthesis of essential proteins for genome replication. Amplification of the viral genome (vRNA) involves the synthesis of an exact copy of the vRNA, called complementary RNA (cRNA). In case of the S segment, the cRNA serves also as a template for mRNA synthesis. (C) Conformational switch. A549 cells were treated with 50 µg/ml CHX and then infected for 5 h with RVF VLPs containing either M or S segmented nucleocapsids. Limited protease digestion and analysis of the samples was performed as for Fig. 1A and B. (D) Super-resolution Immunofluorescence Microscopy of RIG-I and PKR nucleocapsid complexes. Cells were treated and infected as described for C and then fixed and stained against RVFV N (green channel) and RIG-I (upper panel; red channel) or PKR (lower panel; red channel). Quantification was performed of three independent experiments. Student's T-test was carried out for statistical analysis. Significant differences are indicated by asterisks (** $p<0.01$).

Fig. 3: Arenavirus replication products prevent nucleocapsid promoted PKR activation.

(A) Secondary structure prediction of TCRV S segment (data base entry NC_004293.1), TCRV L segment (data base entry NC_004292.1), JUNV S segment (data base entry JF799984.1), JUNV L segment (data base entry JF799980.1), LASV S segment (data base entry HQ688673.1) and LASV L segment (data base entry HQ688674.1) intergenic region via free energy minimization (mFold). (B) PKR activation status. A549 cells were either left untreated (UT) or were treated with 50 µg/ml CHX and mock infected or infected with RVFVΔNSs, TCRV, JUNV or LASV at an MOI of 1. Infection was stopped 5 h post-infection and cell lysates were prepared with 0.5% Triton X-100 in PBS. Limited protease digestion and analysis of the samples was performed as for Fig. 1B.

Fig. 4: LASV nucleoprotein promotes proteasomal degradation of PKR.

(A) Interaction of RIG-I and PKR with LASV nucleocapsids. A549 cells were left untreated (UT) or were treated with 50 µg/ml CHX and either mock or LASV infected at an MOI of 5. After 5 h, cell lysates were prepared and co-immunoprecipitation was performed as described for Fig. 1D. For Western Blot analysis anti-RIG, anti-PKR, anti-P-PKR, anti-LASV NP and anti-p21 antibodies were used. (B) Overexpression analysis. HEK293T cells were transfected with either 0.25, 0.5, 1 or 2 µg of HA-tagged expression constructs for LASV NP, GP or Z together with 1 µg PKR plasmid. Normalization of transfected plasmid amount was done with ΔMx plasmid. Expression was allowed for 24 h and then cell lysates were prepared. Samples were analyzed by Western Blotting using anti-P-PKR, anti-PKR and anti-HA antibodies. (C) Co-immunoprecipitation. HEK293T cells were transfected with 1 µg of LASV NP, GP or Z together with 1 µg PKR plasmid. Lysates were prepared 24 h post-transfection and subjected to co-immunorprecipitation with anti-PKR coupled beads as described in Fig. 1D. Input samples and eluates were validated as described for B. (D and E) Influence of proteasomal degradation. (D) HEK293T cells were transfected like C and 8 h post-transfection either left untreated or treated with 20 µM MG132. After additional 16 h, cells were lysed and analyzed as described for B. (E) Conformational switch. A549 cells were infected with RVFVΔNSs, TCRV, JUNV or LASV at an MOI of 1 and after the inoculum was removed the cells were left either untreated (UT) or were treated with 20 µM MG132. After 5 h, cells were lysed and limited protease digestion and Western Blotting was performed as described for Fig. 1B.

Fig. 5: Mechanism of LASV NP mediated PKR antagonism

Arenavirus IGR exposed from the viral nucleocapsid can be recognized by PKR. Once activated, PKR blocks cap-dependent translation of viral and host cell proteins by phosphorylation of the alpha subunit of eukaryotic initiation factor 2 (eIF2α). Additionally, PKR induces an antiviral type I interferon

(IFN) and proinflammatory response. However, to circumvent PKR activation, LASV NP interacts with PKR and promotes its proteasomal degradation

Supplemental information

Supplemental Experimental Procedure

Co-sedimentation assay of recombinant LCV and RVFV nucleoprotein

For co-sedimentation assays, A549 cells grown in two wells of a 6 well plate were transiently transfected with 1 µg pI.18_RVFV N or pTM_LACV N using Nanofectin transfection reagent (PAA Laboratories). Cell lysates were prepared 24 h post-transfection and subjected to co-sedimentation assay as ascribed above. Western Blot analysis was performed with mouse monoclonal anti-RIG-I antibody at 1:1000, mouse monoclonal anti-PKR B10 at 1:500, rabbit polyclonal anti-LACV N at 1:1000, and mouse polyclonal anti-RVFV N serum at 1:1000.

Time-course experiment

A549 cells were infected with LACVΔNSs, RVFVΔNSs, TCRV, JUNV or LASV at an MOI of 1. If indicated, cells were treated with 50 µg/ml CHX 1 h prior, during infection and while the course of the experiment. After 2, 5 and 24 h cells were washed and lysed in 1-fold sample buffer. Samples were analyzed by SDS-PAGE and Western Blotting using mouse monoclonal anti-PKR B10 at 1:500, rabbit monoclonal anti-p-PKR Thr 446 at 1:500, rabbit polyclonal anti-LACV N at 1:1000, mouse polyclonal anti-RVFV N serum at 1:1000, rabbit monoclonal anti LASV NP at 1:3000, guinea pig polyclonal anti-JUNV NP at 1:500 and guinea pig polyclonal anti-TCRV NP at 1:500. Staining with mouse monoclonal anti-actin served as a loading control

Suppl. 1: RIG-I and PKR do not interact with LACV and RVFV nucleoprotein

Co-sedimentation assay. HEK293T cells were transfected with either LACV or RVFV N and 24 h post-transfection cell lysates were prepared. Samples were loaded on a 50-70% discontinuous glycerol gradient, centrifuged and collected fractions were concentrated. Samples were subjected to Western Blot analysis using antibodies directed against RIG-I, PKR and LACV or RVFV N as a marker for viral nucleocapsids.

Suppl. 2: PKR activation during bunyavirus and arenavirus infection

PKR activation status. A549 cells were either left untreated (UT) or were treated with 50 µg/ml CHX and mock infected or infected with LACVΔNSs, RVFVΔNSs, TCRV, JUNV or LASV at an MOI of 1. After 2, 5 and 24 h cell lysates were prepared with 1-fold sample buffer and samples were analyzed by Western blotting using antisera against phosphorylated PKR, PKR and LASV N, RVFV N, TCRV NP, JUNV NP or LASV NP, respectively. Staining against actin served as a loading control.

References

ALBARINO, C. G., BIRD, B. H. & NICHOL, S. T. 2007. A shared transcription termination signal on negative and ambisense RNA genome segments of Rift Valley fever, sandfly fever Sicilian, and Toscana viruses. *J Virol,* 81**,** 5246-56.

ARIZA, A., TANNER, S. J., WALTER, C. T., DENT, K. C., SHEPHERD, D. A., WU, W., MATTHEWS, S. V., HISCOX, J. A., GREEN, T. J., LUO, M., ELLIOTT, R. M., FOOKS, A. R., ASHCROFT, A. E., STONEHOUSE, N. J., RANSON, N. A., BARR, J. N. & EDWARDS, T. A. 2013. Nucleocapsid protein structures from orthobunyaviruses reveal insight into ribonucleoprotein architecture and RNA polymerization. *Nucleic Acids Res,* 41**,** 5912-26.

BAUM, A., SACHIDANANDAM, R. & GARCIA-SASTRE, A. 2010. Preference of RIG-I for short viral RNA molecules in infected cells revealed by next-generation sequencing. *Proc Natl Acad Sci U S A,* 107**,** 16303-8.

BEVILACQUA, P. C. & CECH, T. R. 1996. Minor-groove recognition of double-stranded RNA by the double-stranded RNA-binding domain from the RNA-activated protein kinase PKR. *Biochemistry,* 35**,** 9983-94.

BEVILACQUA, P. C., GEORGE, C. X., SAMUEL, C. E. & CECH, T. R. 1998. Binding of the protein kinase PKR to RNAs with secondary structure defects: role of the tandem A-G mismatch and noncontiguous helixes. *Biochemistry,* 37**,** 6303-16.

BLAKQORI, G. & WEBER, F. 2005. Efficient cDNA-based rescue of La Crosse bunyaviruses expressing or lacking the nonstructural protein NSs. *J Virol,* 79**,** 10420-8.

CARROLL, K., ELROY-STEIN, O., MOSS, B. & JAGUS, R. 1993. Recombinant vaccinia virus K3L gene product prevents activation of double-stranded RNA-dependent, initiation factor 2 alpha-specific protein kinase. *J Biol Chem,* 268**,** 12837-42.

CLEMENS, M. J. 1997. PKR--a protein kinase regulated by double-stranded RNA. *Int J Biochem Cell Biol,* 29**,** 945-9.

DABO, S. & MEURS, E. F. 2012. dsRNA-dependent protein kinase PKR and its role in stress, signaling and HCV infection. *Viruses,* 4**,** 2598-635.

DAUBER, B., MARTINEZ-SOBRIDO, L., SCHNEIDER, J., HAI, R., WAIBLER, Z., KALINKE, U., GARCIA-SASTRE, A. & WOLFF, T. 2009. Influenza B virus ribonucleoprotein is a potent activator of the antiviral kinase PKR. *PLoS Pathog,* 5**,** e1000473.

DZANANOVIC, E., PATEL, T. R., DEO, S., MCELENEY, K., STETEFELD, J. & MCKENNA, S. A. 2013. Recognition of viral RNA stem-loops by the tandem double-stranded RNA binding domains of PKR. *Rna,* 19**,** 333-44.

ELLIOTT, R. M. 1990. Molecular biology of the Bunyaviridae. *J Gen Virol,* 71 (Pt 3)**,** 501-22.

ELLIOTT, R. M. 2014. Orthobunyaviruses: recent genetic and structural insights. *Nat Rev Microbiol,* 12**,** 673-85.

EMERY, V. C. & BISHOP, D. H. 1987. Characterization of Punta Toro S mRNA species and identification of an inverted complementary sequence in the intergenic region of Punta Toro phlebovirus ambisense S RNA that is involved in mRNA transcription termination. *Virology,* 156**,** 1-11.

GEERTS-DIMITRIADOU, C., LU, Y. Y., GEERTSEMA, C., GOLDBACH, R. & KORMELINK, R. 2012. Analysis of the Tomato spotted wilt virus ambisense S RNA-encoded hairpin structure in translation. *PLoS One,* 7**,** e31013.

GIORGI, C., ACCARDI, L., NICOLETTI, L., GRO, M. C., TAKEHARA, K., HILDITCH, C., MORIKAWA, S. & BISHOP, D. H. 1991. Sequences and coding strategies of the S RNAs of Toscana and Rift Valley fever viruses compared to those of Punta Toro, Sicilian Sandfly fever, and Uukuniemi viruses. *Virology,* 180**,** 738-53.

GOUBAU, D., DEDDOUCHE, S. & REIS, E. S. C. 2013. Cytosolic sensing of viruses. *Immunity,* 38**,** 855-69.

GOUBAU, D., SCHLEE, M., DEDDOUCHE, S., PRUIJSSERS, A. J., ZILLINGER, T., GOLDECK, M., SCHUBERTH, C., VAN DER VEEN, A. G., FUJIMURA, T., REHWINKEL, J., ISKARPATYOTI, J. A., BARCHET, W., LUDWIG, J., DERMODY, T. S., HARTMANN, G. & REIS, E. S. C. 2014. Antiviral immunity via RIG-I-mediated recognition of RNA bearing 5'-diphosphates. *Nature*.

HABJAN, M., PENSKI, N., WAGNER, V., SPIEGEL, M., OVERBY, A. K., KOCHS, G., HUISKONEN, J. T. & WEBER, F. 2009a. Efficient production of Rift Valley fever virus-like particles: The antiviral protein MxA can inhibit primary transcription of bunyaviruses. *Virology,* 385**,** 400-8.

HABJAN, M., PICHLMAIR, A., ELLIOTT, R. M., OVERBY, A. K., GLATTER, T., GSTAIGER, M., SUPERTI-FURGA, G., UNGER, H. & WEBER, F. 2009b. NSs protein of rift valley fever virus induces the specific degradation of the double-stranded RNA-dependent protein kinase. *J Virol,* 83**,** 4365-75.

HASTIE, K. M., KIMBERLIN, C. R., ZANDONATTI, M. A., MACRAE, I. J. & SAPHIRE, E. O. 2011a. Structure of the Lassa virus nucleoprotein reveals a dsRNA-specific 3' to 5' exonuclease activity essential for immune suppression. *Proc Natl Acad Sci U S A,* 108**,** 2396-401.

HASTIE, K. M., LIU, T., LI, S., KING, L. B., NGO, N., ZANDONATTI, M. A., WOODS, V. L., JR., DE LA TORRE, J. C. & SAPHIRE, E. O. 2011b. Crystal structure of the Lassa virus nucleoprotein-RNA complex reveals a gating mechanism for RNA binding. *Proc Natl Acad Sci U S A,* 108**,** 19365-70.

HEINICKE, L. A., WONG, C. J., LARY, J., NALLAGATLA, S. R., DIEGELMAN-PARENTE, A., ZHENG, X., COLE, J. L. & BEVILACQUA, P. C. 2009. RNA dimerization promotes PKR dimerization and activation. *J Mol Biol,* 390**,** 319-38.

HERTZOG, P. J. & WILLIAMS, B. R. 2013. Fine tuning type I interferon responses. *Cytokine Growth Factor Rev,* 24**,** 217-25.

IKEGAMI, T. 2012. Molecular biology and genetic diversity of Rift Valley fever virus. *Antiviral Res,* 95**,** 293-310.

IKEGAMI, T., NARAYANAN, K., WON, S., KAMITANI, W., PETERS, C. J. & MAKINO, S. 2009. Rift Valley fever virus NSs protein promotes post-transcriptional downregulation of protein kinase PKR and inhibits eIF2alpha phosphorylation. *PLoS Pathog,* 5**,** e1000287.

IVASHKIV, L. B. & DONLIN, L. T. 2014. Regulation of type I interferon responses. *Nat Rev Immunol,* 14**,** 36-49.

KOHLWAY, A., LUO, D., RAWLING, D. C., DING, S. C. & PYLE, A. M. 2013. Defining the functional determinants for RNA surveillance by RIG-I. *EMBO Rep,* 14**,** 772-9.

LARA, E., BILLECOCQ, A., LEGER, P. & BOULOY, M. 2011. Characterization of wild-type and alternate transcription termination signals in the Rift Valley fever virus genome. *J Virol,* 85**,** 12134-45.

LEMAIRE, P. A., TESSMER, I., CRAIG, R., ERIE, D. A. & COLE, J. L. 2006. Unactivated PKR exists in an open conformation capable of binding nucleotides. *Biochemistry,* 45**,** 9074-84.

LOO, Y. M. & GALE, M., JR. 2011. Immune signaling by RIG-I-like receptors. *Immunity,* 34**,** 680-92.

LOPEZ, N. & FRANZE-FERNANDEZ, M. T. 2007. A single stem-loop structure in Tacaribe arenavirus intergenic region is essential for transcription termination but is not required for a correct initiation of transcription and replication. *Virus Res,* 124**,** 237-44.

MARQ, J. B., KOLAKOFSKY, D. & GARCIN, D. 2010. Unpaired 5' ppp-nucleotides, as found in arenavirus double-stranded RNA panhandles, are not recognized by RIG-I. *J Biol Chem,* 285**,** 18208-16.

MARTINEZ-SOBRIDO, L., GIANNAKAS, P., CUBITT, B., GARCIA-SASTRE, A. & DE LA TORRE, J. C. 2007. Differential inhibition of type I interferon induction by arenavirus nucleoproteins. *J Virol,* 81**,** 12696-703.

MARTINEZ-SOBRIDO, L., ZUNIGA, E. I., ROSARIO, D., GARCIA-SASTRE, A. & DE LA TORRE, J. C. 2006. Inhibition of the type I interferon response by the nucleoprotein of the prototypic arenavirus lymphocytic choriomeningitis virus. *J Virol,* 80**,** 9192-9.

MCLAY, L., LIANG, Y. & LY, H. 2014. Comparative analysis of disease pathogenesis and molecular mechanisms of New World and Old World arenavirus infections. *J Gen Virol,* 95**,** 1-15.

MOY, R. H., COLE, B. S., YASUNAGA, A., GOLD, B., SHANKARLING, G., VARBLE, A., MOLLESTON, J. M., TENOEVER, B. R., LYNCH, K. W. & CHERRY, S. 2014. Stem-loop recognition by DDX17 facilitates miRNA processing and antiviral defense. *Cell,* 158**,** 764-77.

NALLAGATLA, S. R., HWANG, J., TORONEY, R., ZHENG, X., CAMERON, C. E. & BEVILACQUA, P. C. 2007. 5'-triphosphate-dependent activation of PKR by RNAs with short stem-loops. *Science,* 318**,** 1455-8.

ONOMOTO, K., JOGI, M., YOO, J. S., NARITA, R., MORIMOTO, S., TAKEMURA, A., SAMBHARA, S., KAWAGUCHI, A., OSARI, S., NAGATA, K., MATSUMIYA, T., NAMIKI, H., YONEYAMA, M. & FUJITA, T. 2012. Critical role of an antiviral stress granule containing RIG-I and PKR in viral detection and innate immunity. *PLoS One,* 7**,** e43031.

PANDEY, S., KAWAI, T. & AKIRA, S. 2014. Microbial Sensing by Toll-Like Receptors and Intracellular Nucleic Acid Sensors. *Cold Spring Harb Perspect Biol*.

PICHLMAIR, A., SCHULZ, O., TAN, C. P., REHWINKEL, J., KATO, H., TAKEUCHI, O., AKIRA, S., WAY, M., SCHIAVO, G. & REIS E SOUSA, C. 2009. Activation of MDA5 requires higher-order RNA structures generated during virus infection. *J Virol,* 83**,** 10761-9.

RAYMOND, D. D., PIPER, M. E., GERRARD, S. R., SKINIOTIS, G. & SMITH, J. L. 2012. Phleboviruses encapsidate their genomes by sequestering RNA bases. *Proc Natl Acad Sci U S A,* 109**,** 19208-13.

RAYMOND, D. D., PIPER, M. E., GERRARD, S. R. & SMITH, J. L. 2010. Structure of the Rift Valley fever virus nucleocapsid protein reveals another architecture for RNA encapsidation. *Proc Natl Acad Sci U S A,* 107**,** 11769-74.

REIKINE, S., NGUYEN, J. B. & MODIS, Y. 2014. Pattern Recognition and Signaling Mechanisms of RIG-I and MDA5. *Front Immunol,* 5**,** 342.

RODRIGO, W. W., ORTIZ-RIANO, E., PYTHOUD, C., KUNZ, S., DE LA TORRE, J. C. & MARTINEZ-SOBRIDO, L. 2012. Arenavirus nucleoproteins prevent activation of nuclear factor kappa B. *J Virol,* 86**,** 8185-97.

ROMANO, P. R., ZHANG, F., TAN, S. L., GARCIA-BARRIO, M. T., KATZE, M. G., DEVER, T. E. & HINNEBUSCH, A. G. 1998. Inhibition of double-stranded RNA-dependent protein kinase PKR by vaccinia virus E3: role of complex formation and the E3 N-terminal domain. *Mol Cell Biol,* 18**,** 7304-16.

RUIGROK, R. W., CREPIN, T. & KOLAKOFSKY, D. 2011. Nucleoproteins and nucleocapsids of negative-strand RNA viruses. *Curr Opin Microbiol,* 14**,** 504-10.

SCHLEE, M. 2013. Master sensors of pathogenic RNA - RIG-I like receptors. *Immunobiology,* 218**,** 1322-35.

SCHLEE, M., ROTH, A., HORNUNG, V., HAGMANN, C. A., WIMMENAUER, V., BARCHET, W., COCH, C., JANKE, M., MIHAILOVIC, A., WARDLE, G., JURANEK, S., KATO, H., KAWAI, T., POECK, H., FITZGERALD, K. A., TAKEUCHI, O., AKIRA, S., TUSCHL, T., LATZ, E., LUDWIG, J. & HARTMANN, G. 2009. Recognition of 5' triphosphate by RIG-I helicase requires short blunt double-stranded RNA as contained in panhandle of negative-strand virus. *Immunity,* 31**,** 25-34.

SCHMIDT, A., SCHWERD, T., HAMM, W., HELLMUTH, J. C., CUI, S., WENZEL, M., HOFFMANN, F. S., MICHALLET, M. C., BESCH, R., HOPFNER, K. P., ENDRES, S. & ROTHENFUSSER, S. 2009. 5'-triphosphate RNA requires base-paired structures to activate antiviral signaling via RIG-I. *Proc Natl Acad Sci U S A,* 106**,** 12067-72.

SCHNEIDER, W. M., CHEVILLOTTE, M. D. & RICE, C. M. 2014. Interferon-stimulated genes: a complex web of host defenses. *Annu Rev Immunol,* 32**,** 513-45.

SCHOGGINS, J. W. 2014. Interferon-stimulated genes: roles in viral pathogenesis. *Curr Opin Virol,* 6**,** 40-6.

SHIMOIKE, T., MCKENNA, S. A., LINDHOUT, D. A. & PUGLISI, J. D. 2009. Translational insensitivity to potent activation of PKR by HCV IRES RNA. *Antiviral Res,* 83**,** 228-37.

TAYLOR, D. R., SHI, S. T., ROMANO, P. R., BARBER, G. N. & LAI, M. M. 1999. Inhibition of the interferon-inducible protein kinase PKR by HCV E2 protein. *Science,* 285**,** 107-10.

VANOUDENHOVE, J., ANDERSON, E., KRUEGER, S. & COLE, J. L. 2009. Analysis of PKR structure by small-angle scattering. *J Mol Biol,* 387**,** 910-20.

WALTER, C. T. & BARR, J. N. 2011. Recent advances in the molecular and cellular biology of bunyaviruses. *J Gen Virol.*

WEBER, M., GAWANBACHT, A., HABJAN, M., RANG, A., BORNER, C., SCHMIDT, A. M., VEITINGER, S., JACOB, R., DEVIGNOT, S., KOCHS, G., GARCIA-SASTRE, A. & WEBER, F. 2013. Incoming RNA virus

nucleocapsids containing a 5'-triphosphorylated genome activate RIG-I and antiviral signaling. *Cell Host Microbe,* 13**,** 336-46.

WEBER, M. & WEBER, F. 2014a. Monitoring Activation of the Antiviral Pattern Recognition Receptors RIG-I And PKR By Limited Protease Digestion and Native PAGE. *J Vis Exp*.

WEBER, M. & WEBER, F. 2014b. RIG-I-like receptors and negative-strand RNA viruses: RLRly bird catches some worms. *Cytokine Growth Factor Rev*.

WILLIAMS, B. R. 1999. PKR; a sentinel kinase for cellular stress. *Oncogene,* 18**,** 6112-20.

ZHENG, X. & BEVILACQUA, P. C. 2004. Activation of the protein kinase PKR by short double-stranded RNAs with single-stranded tails. *Rna,* 10**,** 1934-45.

1A

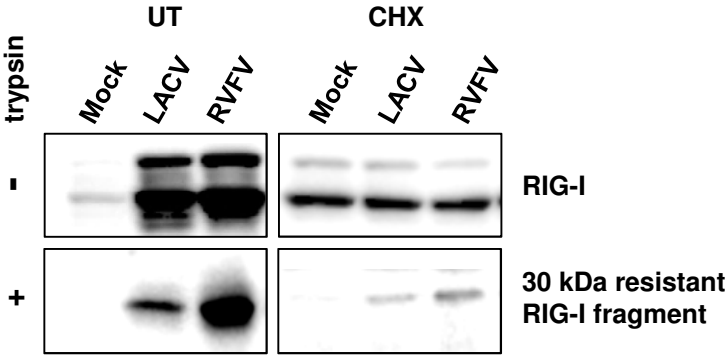
UT
CHX
trypsin
Mock
LACV
RVFV
Mock
LACV
RVFV
-
+
RIG-I
30 kDa resistant
RIG-I fragment

1B

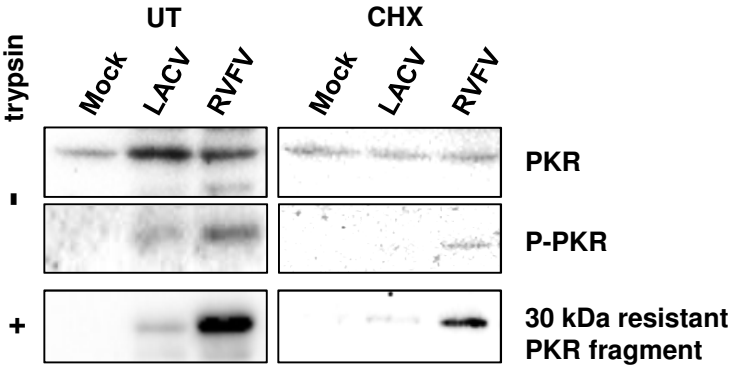
UT
CHX
trypsin
Mock
LACV
RVFV
Mock
LACV
RVFV
-
+
PKR
P-PKR
30 kDa resistant
PKR fragment

1C

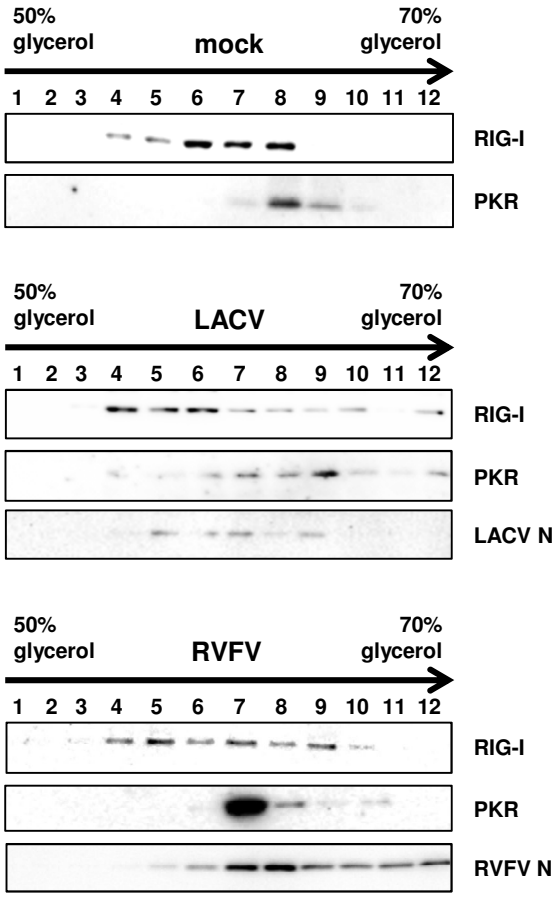
50%
glycerol
mock
70%
glycerol
1 2 3 4 5 6 7 8 9 10 11 12
RIG-I
PKR
50%
glycerol
LACV
70%
glycerol
1 2 3 4 5 6 7 8 9 10 11 12
RIG-I
PKR
LACV N
50%
glycerol
RVFV
70%
glycerol
1 2 3 4 5 6 7 8 9 10 11 12
RIG-I
PKR
RVFV N

1D

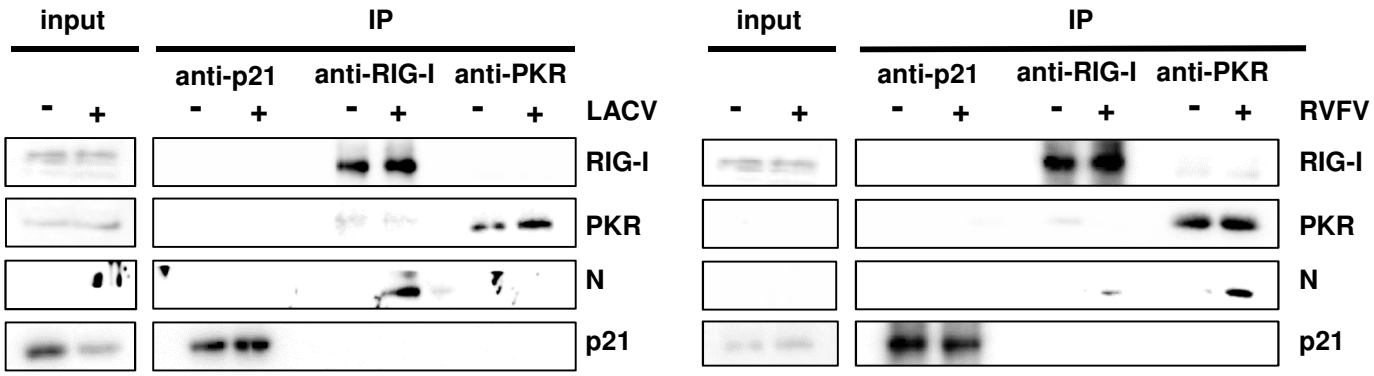
input
IP
anti-p21
anti-RIG-I
anti-PKR
- + - + - + - +
LACV
RIG-I
PKR
N
p21
input
IP
anti-p21
anti-RIG-I
anti-PKR
- + - + - + - +
RVFV
RIG-I
PKR
N
p21

2A

2B

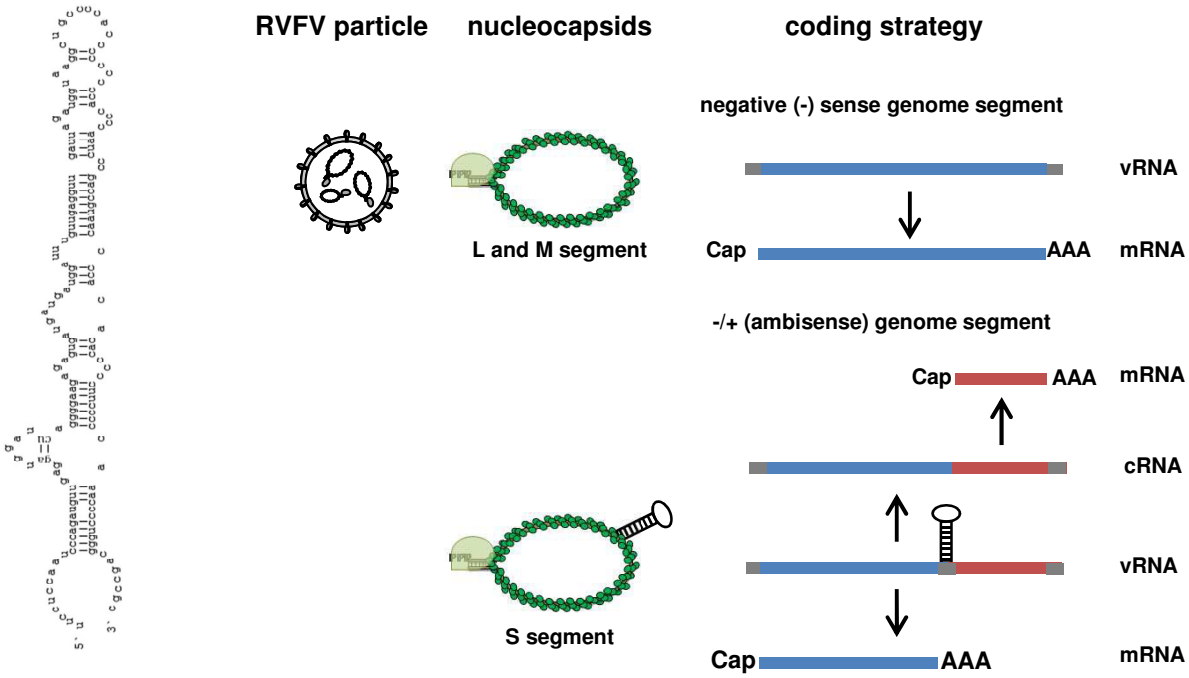
RVFV particle
nucleocapsids
coding strategy
negative (-) sense genome segment
vRNA
Cap
AAA
mRNA
L and M segment
-/+ (ambisense) genome segment
Cap
AAA
mRNA
cRNA
vRNA
Cap
AAA
mRNA
S segment

2C

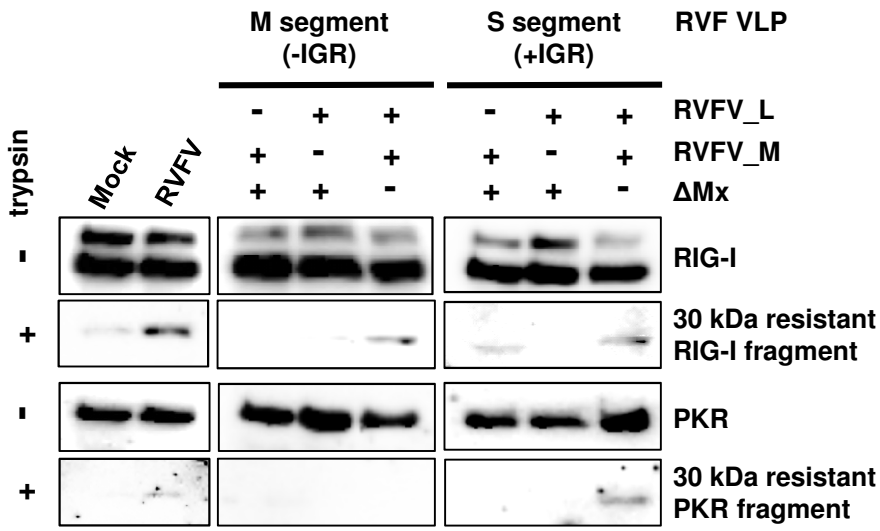
M segment (-IGR)
S segment (+IGR)
RVF VLP
RVFV_L
RVFV_M
ΔMx
trypsin
Mock
RVFV
RIG-I
30 kDa resistant RIG-I fragment
PKR
30 kDa resistant PKR fragment

2D

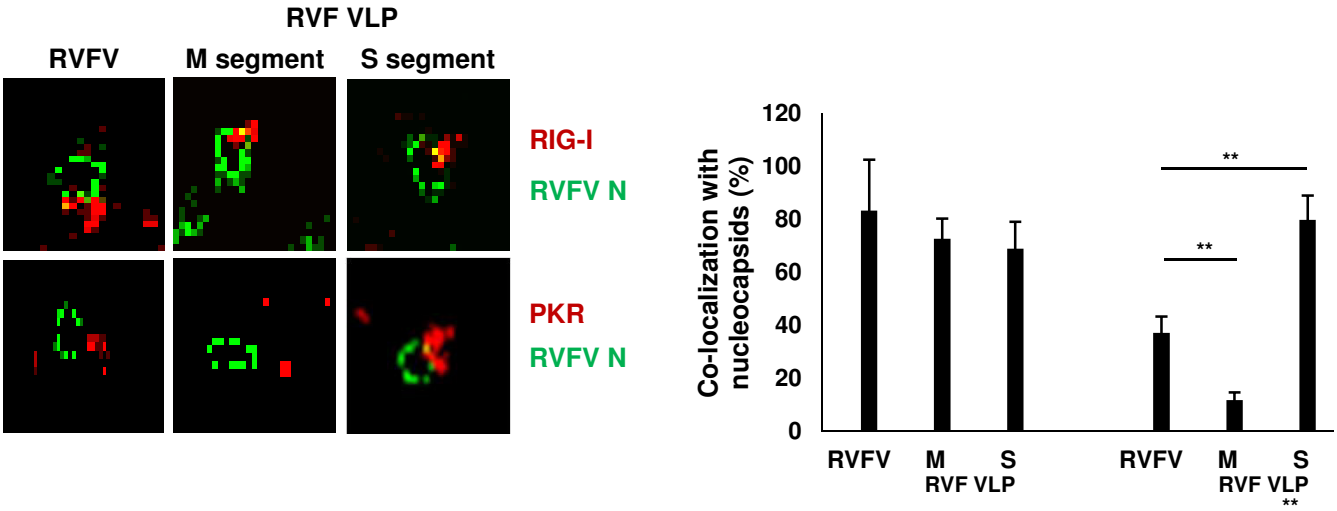
RVF VLP
RVFV
M segment
S segment
RIG-I
RVFV N
PKR
RVFV N
Co-localization with nucleocapsids (%)
120
100
80
60
40
20
0
**
**
RVFV
M
S
RVF VLP
RVFV
M
S
RVF VLP
**

3a

TCRV S segment

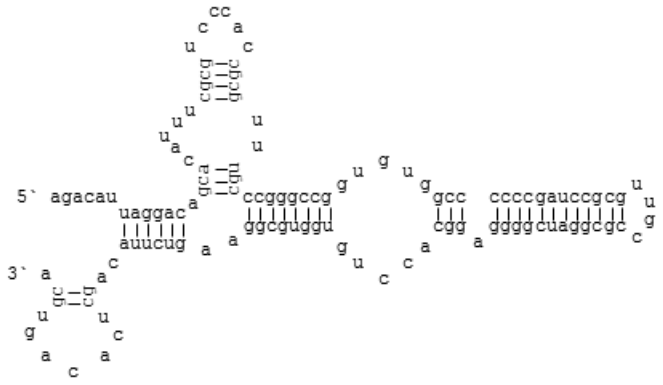

TCRV L segment

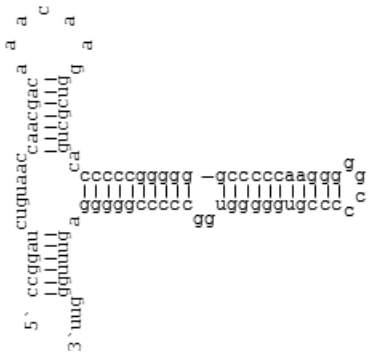

JUNV S segment

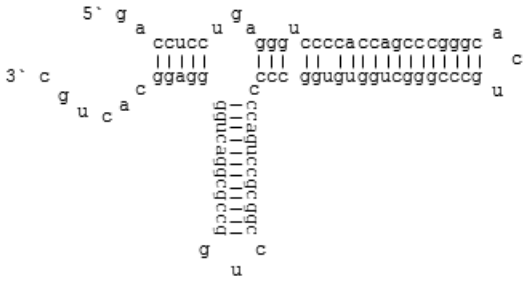

JUNV L segment

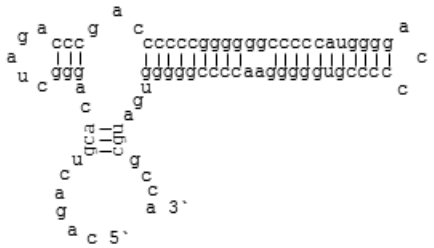

LASV S segment

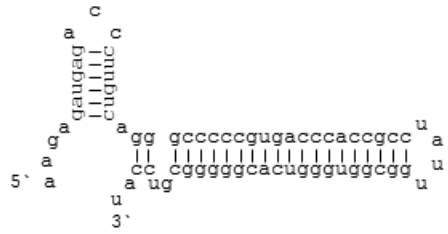

LASV L segment

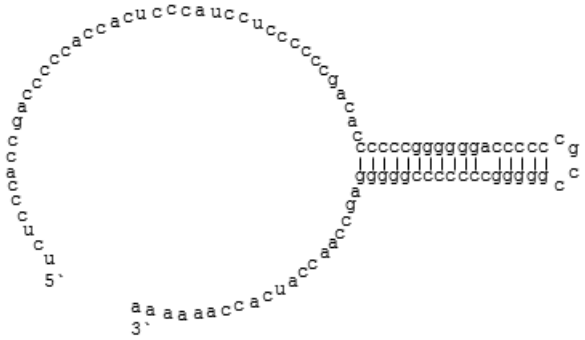

3b

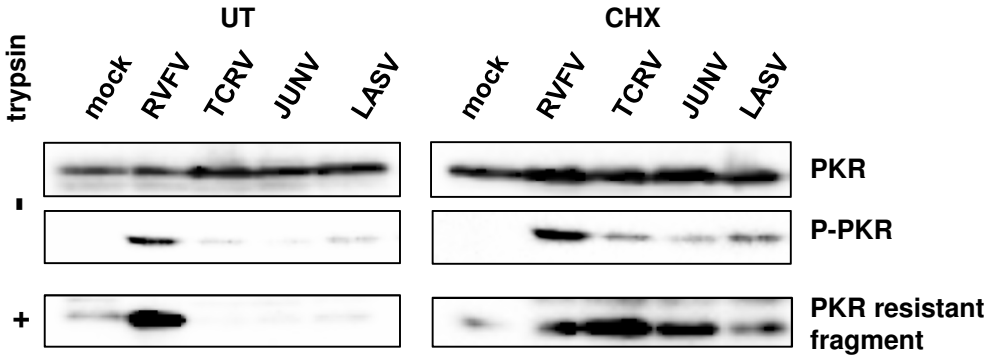

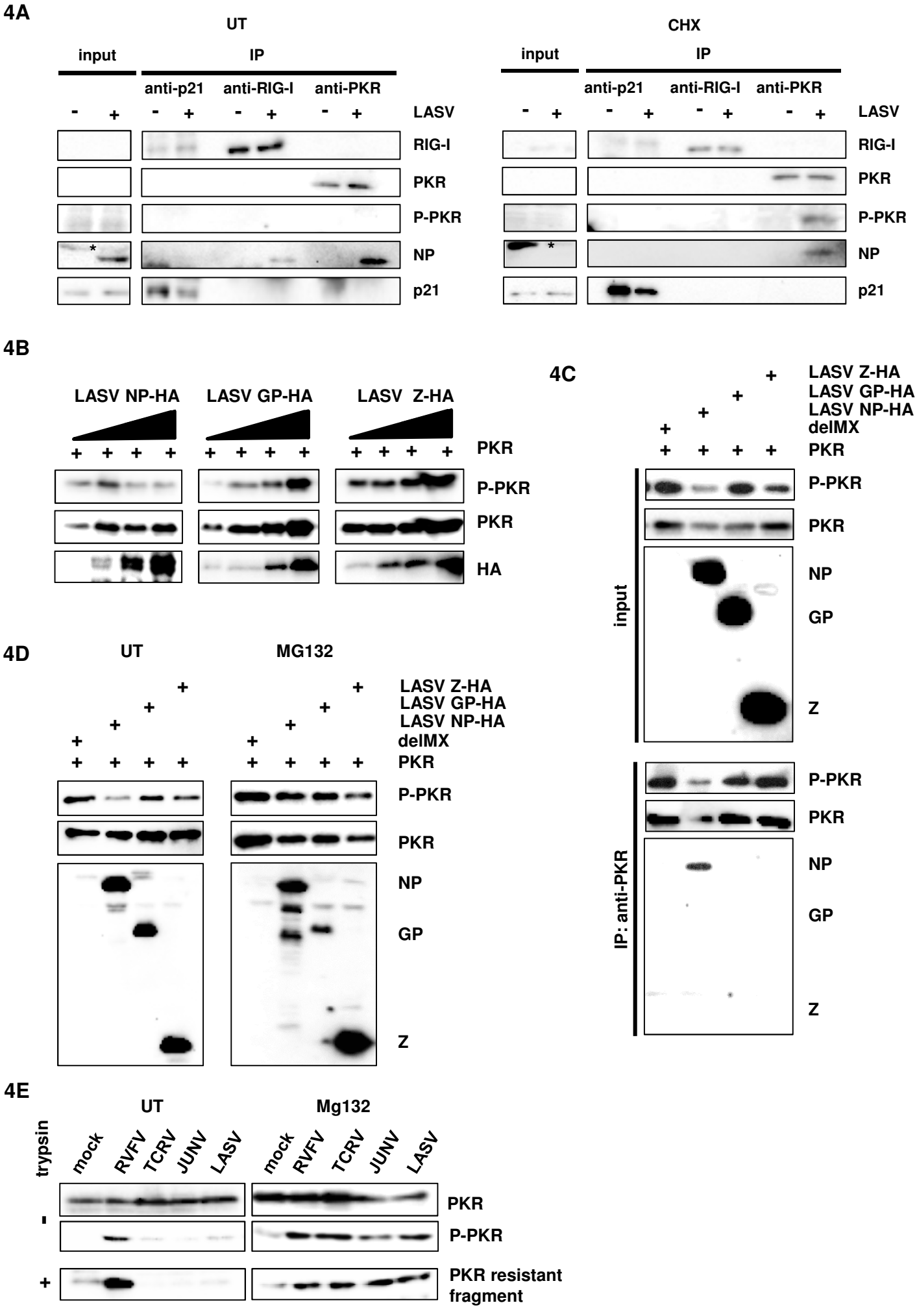
4A
UT
CHX
input
IP
anti-p21
anti-RIG-I
anti-PKR
LASV
RIG-I
PKR
P-PKR
NP
p21
4B
LASV NP-HA
LASV GP-HA
LASV Z-HA
PKR
P-PKR
PKR
HA
4C
LASV Z-HA
LASV GP-HA
LASV NP-HA
delMX
PKR
P-PKR
PKR
NP
GP
Z
input
IP: anti-PKR
4D
UT
MG132
LASV Z-HA
LASV GP-HA
LASV NP-HA
delMX
PKR
P-PKR
PKR
NP
GP
Z
4E
UT
Mg132
trypsin
mock
RVFV
TCRV
JUNV
LASV
PKR
P-PKR
PKR resistant fragment

5

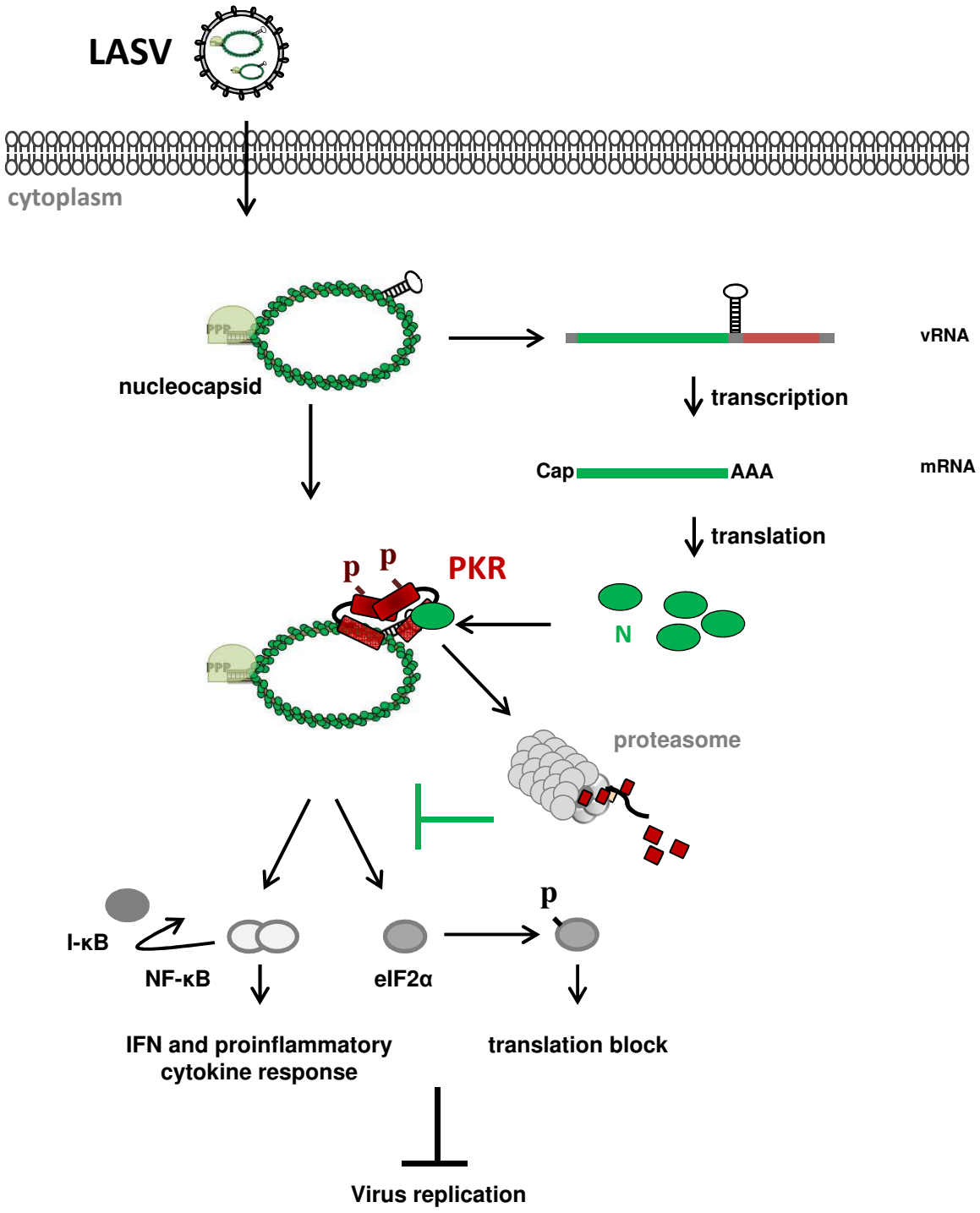
LASV
cytoplasm
nucleocapsid
vRNA
transcription
Cap
AAA
mRNA
translation
p
p
PKR
N
proteasome
I-κB
NF-κB
eIF2α
p
IFN and proinflammatory cytokine response
translation block
Virus replication

Suppl. 1

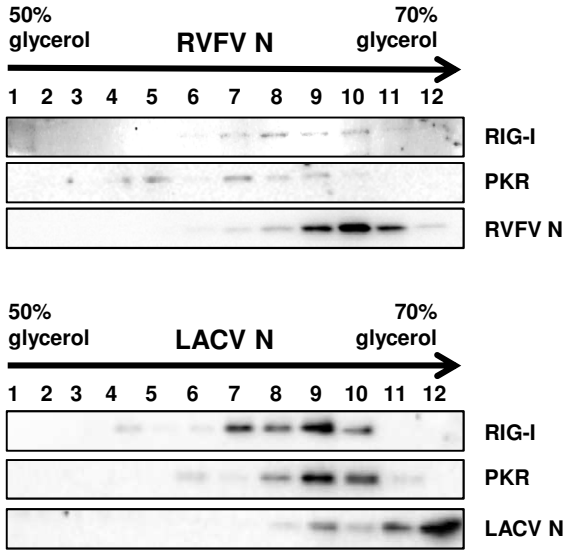
50%
glycerol
RVFV N
70%
glycerol
1 2 3 4 5 6 7 8 9 10 11 12
RIG-I
PKR
RVFV N
50%
glycerol
LACV N
70%
glycerol
1 2 3 4 5 6 7 8 9 10 11 12
RIG-I
PKR
LACV N

Suppl. 2

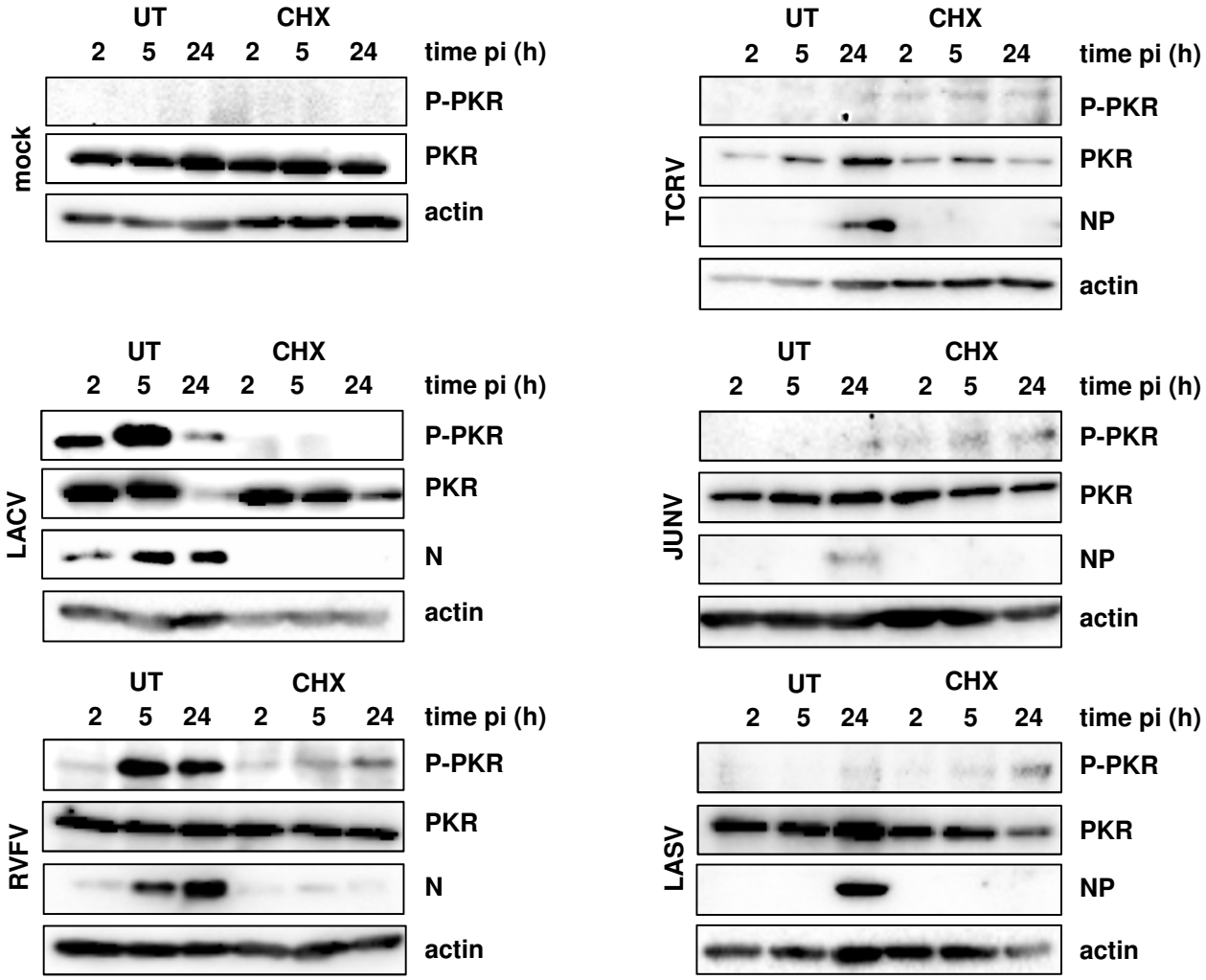
UT
CHX
2 5 24 2 5 24
time pi (h)
mock
P-PKR
PKR
actin
TCRV
NP
LACV
N
JUNV
RVFV
LASV

4.5. REVIEW: RIG-I-like receptors and negative-strand RNA viruses: RLRly bird catches some worms

Own contribution:

I contributed to writing of the manuscript.

Michaela Gerlach

Cytokine & Growth Factor Reviews 25 (2014) 621–628

Contents lists available at ScienceDirect

Cytokine & Growth Factor Reviews

journal homepage: www.elsevier.com/locate/cytogfr

Mini review

RIG-I-like receptors and negative-strand RNA viruses: RLRly bird catches some worms

Michaela Weber, Friedemann Weber *

Institute for Virology, Philipps-University Marburg, D-35043 Marburg, Germany

ARTICLE INFO

Article history:
Available online 20 May 2014

Keywords:
Negative-strand RNA virus
Genome segmentation
RIG-I-like receptors
Panhandle
Viral countermeasures

ABSTRACT

Negative strand RNA viruses with a nonsegmented genome (ns-NSVs) or a segmented genome (s-NSVs) are an important source of human and animal diseases. Survival of the host from those infections is critically dependent on rapidly reacting innate immune responses. Two cytoplasmic RNA helicases, RIG-I and MDA5 (collectively termed RIG-I-like receptors, RLRs), are essential for recognizing virus-specific RNA structures to initiate a signalling cascade, resulting in the production of the antiviral type I interferons. Here, we will review the current knowledge and views on RLR agonists, RLR signalling, and the wide variety of countermeasures ns-NSVs and s-NSVs have evolved. Specific aspects include the consequences of genome segmentation for RLR activation and a discussion on the physiological ligands of RLRs.

1. Introduction

Viruses with a single-stranded (ss) RNA genome of negative polarity (negative-strand RNA viruses, NSVs) are responsible for a wide range of diseases. Members of the NSV group cause respiratory problems (e.g. influenza, hantavirus pulmonary syndrome, respiratory syncytial virus), severe childhood diseases (measles, mumps), neuronal infection (La Crosse virus, Toscana virus, Borna disease virus), even with up to 100% mortality (Rabies), as well as multi-organ failure and haemorrhagic fevers (Rift Valley fever, Severe fever with Thrombocytopenia, Nipah, Ebola, Lassa, Hanta, Crimean Congo haemorrhagic fever).

NSVs encode highly active polymerases, producing in a typical case 100,000 RNA copies per cell within 10 h of infection [1]. Quite expectedly, such numbers of non-self RNAs in the cytoplasm are highly immunogenic and could trigger massive antiviral responses. To avoid being defeated by the innate immune system, NSVs have evolved strategies against recognition, antiviral signalling, and the launched antiviral mechanisms. In this review article, we will attempt to provide an update on the principles of cytoplasmic virus recognition and viral escape. For deeper insights into specific aspects and into the extracellular virus recognition which is not covered here, we refer to the wealth of recent, excellent reviews by others [2–14].

2. Negative-strand RNA viruses

Taxonomically, the group of NSVs is divided into those having one, continuous strand of genomic RNA (the *Mononegavirales*) and those whose genome is divided into several segments. The *Mononegavirales*, also called nonsegmented NSVs (ns-NSVs) have all genes lined up along the ssRNA genome, separated by regulatory intergenic regions acting as transcriptional promoters, and flanked by the regulatory leader and trailer sequences (Fig. 1A). For segmented NSVs (s-NSVs), by contrast, each RNA segment contains one promoter (formed by annealing of the 5′ and 3′ ends) driving expression of one gene (Fig. 1B). The number of segments differs between s-NSV families. Members of the *Orthomyxoviridae* possess mostly 8 segments, whereas *Bunyaviridae* have 3 and *Arenaviridae* have 2 segments (Table 1). Some bunyaviruses and all arenaviruses enlarge the genetic capacity of their segments by transcribing an additional gene from the copy of the genome RNA (the cRNA), the so-called ambisense strategy.

3. Intracellular virus recognition by RIG-I like receptors

A rapid and efficient antiviral response is essential to limit virus replication and ensure survival of the host. The cytoplasmic RIG-I-like receptors (RLRs) are able to detect viral RNA species and to trigger an intracellular signalling cascade that eventually results in the release of specific cytokines and chemokines [2,10]. Type I interferons (IFN-α/β) represent the most important antiviral cytokines, inducing expression of more than 300 IFN-stimulated

* Corresponding author. Tel.: +49 6421 2864525; fax: +49 6421 2868962.
E-mail address: friedemann.weber@staff.uni-marburg.de (F. Weber).

http://dx.doi.org/10.1016/j.cytogfr.2014.05.004
1359-6101/

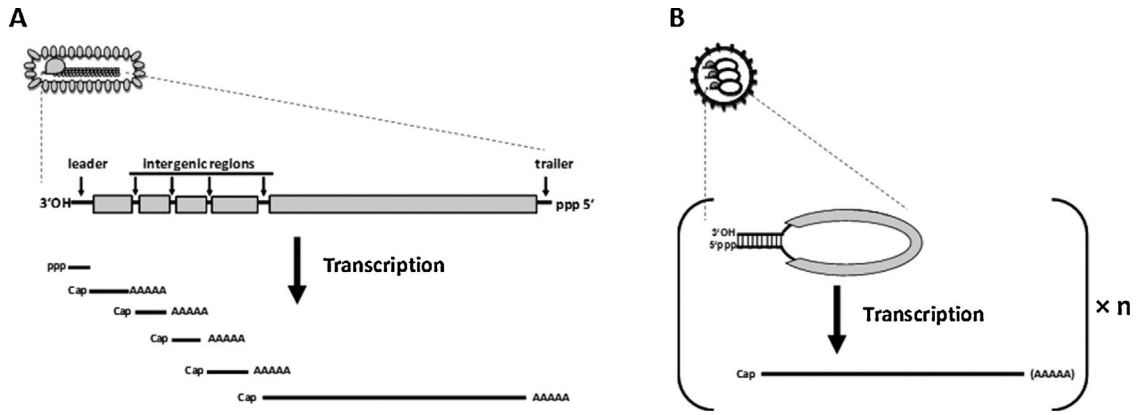

Fig. 1. Differing coding strategies of nonsegmented and segmented NSVs. Symbolized virus particles are shown on top, followed by a sketch of the unencapsidated viral genome with the individual genes as grey boxes. By convention the ssRNA genomes of NSVs are drawn from 3′–5′. (A) The genome of ns-NSVs consists of one continuous stretch of ssRNA from which all mRNAs are synthesized. Intergenic regions contain stop/start signals regulating termination and initiation of transcription. Note the uncapped 5′ppp RNA transcribed from the leader region. Basic set-up of a Rhabdovirus is shown as example. (B) s-NSVs transcribe mostly one mRNA per genome segment (with the exception of ambisense segments which express another gene transcribed from the opposite direction). *n* = number of segments. Not all s-NSVs have mRNAs with a polyA, which is therefore shown in brackets.

genes (ISGs) [12]. ISGs act in a variety of ways to inhibit virus replication, to elevate antiviral alertness in the infected and surrounding cells, and to modulate the adaptive immune system.

3.1. RLR structure

The group of RLRs consists of RIG-I (retinoic acid inducible gene 1), MDA5 (melanoma differentiation association factor 5) and LGP2 (laboratory of genetics and physiology 2) [10]. RLRs are members of the DExD/H box RNA helicase family and consist of a carboxy-terminal domain (CTD), a central DExD/H box RNA helicase domain (composed of Hel1, Hel2 with the insertion domain Hel2i in between) and, in the case of RIG-I and MDA5, two additional amino-terminal caspase recruitment domains (CARDs) (Fig. 2) [15,16]. For RIG-I, the CTD and the helicase domain are conducting ligand recognition, whereas in case of MDA5 this function seems to be performed by the helicase domain. The terminal CARDs are required for signal transduction. LGP2 does not signal by itself but can bind double-stranded RNA (dsRNA) and acts as a positive regulator of MDA5 [17,18].

Table 1
Negative-strand RNA viruses.

Family	Genome organization	Representative members[a]
Filoviridae	Nonsegmented	Ebola virus (EBOV), Marburg virus (MARV)
Paramyxoviridae	Nonsegmented	Nipah virus (NiV), measles virus (MeV), Parainfluenza virus (PIV), Respiratory syndrome virus (RSV), Sendai virus (SeV)
Rhabdoviridae	Nonsegmented	Rabies virus, vesicular stomatitis virus (VSV)
Bornaviridae	Nonsegmented	Borna disease virus (BDV)
Arenaviridae	2 Segments	Lassa virus (LASV)
Bunyaviridae	3 Segments	Bunyamwera virus (BUNV; Orthobunyavirus) La Crosse virus (LACV; Orthobunyavirus) Rift Valley fever virus (RVFV; Phlebovirus) Toscana virus (TOSV; Phlebovirus) Severe fever with thrombocytopenia virus (SFTSV; Phlebovirus) Hantaan virus (HTNV; Hantavirus) Crimean-Congo haemorrhagic fever virus (CCHFV; Nairovirus)
Orthomyxoviridae	6–8 Segments	Influenza A virus (FLUAV), Thogoto virus (THOV)

[a]Virus acronyms and genera shown in brackets

3.2. RLR signalling

RIG-I has in non-infected cells an auto-repressed conformation in which the CARDs are masking the RNA binding site of the helicase domain [16]. The CTD is exposed to the cytosol and connected by a flexible linker. When the CTD binds to a specific ligand, RIG-I switches its conformation to wrap around the RNA ligand (via CTD and helicase domain) and expose the CARDs instead of the CTD [9]. Stabilization of the active conformation and homo-oligomerization of RIG-I are facilitated by post-translational modifications like dephosphorylation, covalent K63 ubiquitinylation via TRIM25, and association of unanchored ubiquitin chains [4,19–23]. Activated RIG-I can form helical tetramers, but – similar to MDA5 – also longer oligomers along dsRNA [21,24,25].

The oligomers of RIG-I and MDA5 serve as platforms to recruit the adaptor protein MAVS (mitochondrial antiviral signalling) via multiple CARD-CARD interactions [2]. Activated MAVS associates with TRAF3/6 to promote activation of the kinases TBK1/IKKε which are responsible for the phosphorylation of the transcription factors IRF3 and IRF7 [2]. In parallel, the kinases IKKα and IKKβ can activate NF-κB. IRF3/7 and NF-κB translocate into the nucleus to initiate expression of IFN-α/β and proinflammatory cytokines. The basics of RLR signalling are outlined in Fig. 3 (middle panel).

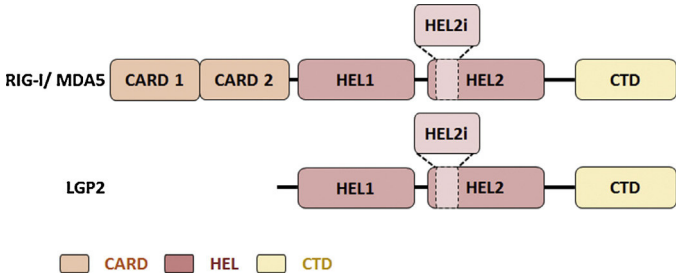

Fig. 2. RIG-I like receptors and their domains. Domain structure of RIG-I, MDA5 and LGP2. CARD, caspase activation recruitment domains; HEL, DExD/H-box helicase domain; HEL2i, insertion domain of helicase domain 2; CTD, carboxy-terminal domain.

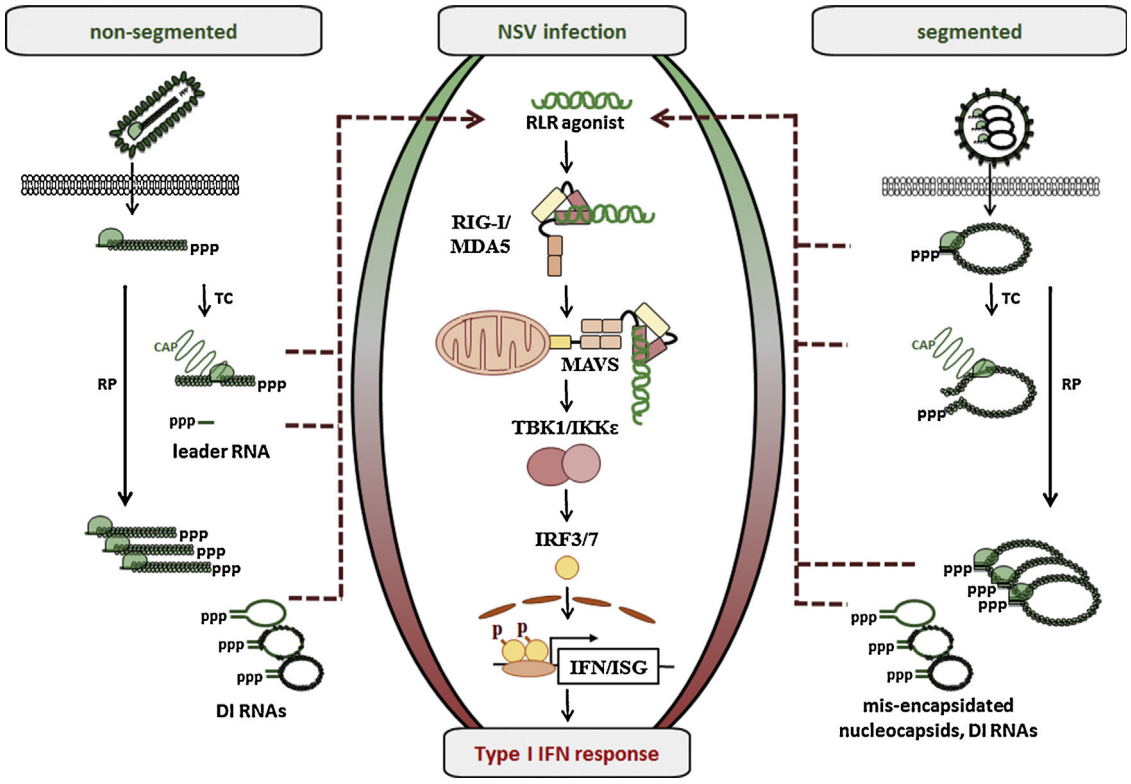

Fig. 3. Agonists of RIG-I like receptors produced by NSV infection. Left panel: Upon infection with ns-NSVs, RNAs and DI particles are produced which activate RIG-I and MDA5. Right panel: RNA synthesis by s-NSVs similarly generates regular and aberrant RLR agonists. In contrast to ns-NSVs, the incoming nucleocapsids of s-NSVs can directly activate RIG-I independent of RNA synthesis. Middle panel: Ligand-bound RLRs switch conformation and homo-oligomerize (not depicted) to recruit the signalling adapter MAVS on mitochondria. MAVS triggers antiviral type I IFN responses through a signalling cascade involving the kinases TBK1/IKKε and their substrates IRF3 and IRF7. TC, transcription; RP, replication.

3.3. *RLR agonists*

Despite their structural and functional similarity, RIG-I and MDA5 recognize different RNA ligands (see below), and are activated by distinct but overlapping subsets of viruses [13]. Ligand-wise, RIG-I is strongly activated by blunt-ended dsRNAs of at least 10 base pairs length bearing a 5′triphosphate (5′ppp) group [15,26,27], by long dsRNA molecules of more than 200 base pairs (irrespective of the 5′ end) [24,28], but also by 3′-monophosphorylated ssRNAs [29] and poly U/UC rich stretches of ssRNA [30]. MDA5 detects long dsRNA molecules, ideally with higher order RNA structures [31], and can be activated by particular stretches of NSV RNAs [32,33]. Both RLRs also show preference for AU-rich ssRNAs which seems independent of structure [33,34].

While these activating molecules had mostly been identified and characterized by transfections and manipulations of naked RNAs, they nonetheless allowed conclusions on the nature of the physiological RLR agonists present in infected cells (summarized in Fig. 3, left and right panels). NSVs encapsidate their ssRNA genome and its template (and copy), the antigenome, with nucleocapsid proteins [35]. Therefore, NSVs do not produce detectable amounts of RLR-critical dsRNA [36]. However, synthesis of the NSV genome is initiated with an unprimed nucleoside triphosphate, resulting in a 5′ppp terminus. For ns-NSVs, nucleocapsids are linear [35], suggesting that the 5′ppp ssRNA end does not meet the 3′ counterpart and hence cannot activate RIG-I [13]. For s-NSVs, by contrast, the promoter structure which is formed by annealing of the genome termini (“panhandle”, see Fig. 1B) bears hallmarks of a RIG-I agonist. Indeed, we recently showed that the 5′ppp dsRNA panhandle structures packaged into nucleocapsids of two members of the *Bunyaviridae* (La Crosse virus (LACV) and Rift Valley Fever virus (RVFV)) act as RIG-I agonists in the natural context of infection [37]. Therefore, RIG-I can recognize the nucleocapsids of s-NSVs directly after their entry into the cytoplasm. In the case of ns-NSVs, only RNA synthesis products (e.g. 5′ppp leader RNA) can act as triggers of RIG-I [6,20,33,38–41]. Moreover, particular stretches of viral mRNA can activate MDA5 [32,33]. During replication of the RNA genome, the viral polymerase occasionally jumps template, resulting in RNA products with internal deletions, the defective interfering (DI) RNAs, named so because they strongly compete with the full-length genomes for resources [42]. One particular class, the copy-back DI RNAs, contain complementary 5′ and 3′ ends. It is thought that a percentage of DI RNAs is incompletely encapsidated [43]. For the ns-NSV Sendai virus (SeV), it was shown that copyback DI RNAs form panhandle-like dsRNA structures which can accommodate RIG-I oligomers and activate IFN induction [20,43]. Also for s-NSVs, products of viral RNA synthesis (including internally deleted genomes) can activate RIG-I and innate immune signalling [34,44–46]. Thus, taken together, for s-NSVs incoming nucleocapsids can be detected by RIG-I, and also later RNA synthesis products trigger innate immunity. For ns-NSVs, by contrast, the RLRs have to await the appearance of regular and irregular products of viral RNA synthesis.

4. Pros and cons of genome segmentation

s-NSVs are schlepping a bundle of genome segments, each with a RIG-I-sensitive 5′ppp dsRNA promoter. This clearly represents a

disadvantage with respect of immune activation. Moreover, segmentation requires sophisticated packaging mechanisms to ensure each virion contains the full set of genes. On the other hand, the segments can easily be exchanged between different virus variants (reassortment), allowing rapid emergence of new viral strains with altered antigenic or replicatory properties [5,47]. Dividing the genome in separate units is also considered an insurance against sequence degeneration in systems with high error rates, such as RNA-dependent polymerases [48], and packaging several shorter segments instead of one large genome was recently shown to increase the physical stability of virus particles [49]. One evolutionary trade-off of genome segmentation, however, is the elevated number of RLR agonists presented to the innate immune system. It is therefore conceivable that s-NSVs have to express early-hitting IFN evasion strategies which may also be stronger than those of ns-NSVs.

5. RLR evasion strategies of NSVs

To our knowledge, all NSVs investigated so far have evolved countermechanisms of RLR signalling, acting to prevent recognition by RLRs, to interfere with RLR signalling, and/or to suppress

Table 2
Mechanisms of NSVs to counteract RLR signalling.

Interference with	Viral protein or function	Virus	Mechanism	References
RLR sensing	ssRNA encapsidation	all NSVs	Prevents dsRNA formation	[35,36]
	dsRNA unwinding by cellular helicases UAP56 and URH49	FLUAV, VSV	Prevents dsRNA formation	[50,51]
	Recruitment of La	ns-NSVs	Prevents RIG-I recognition of viral leader RNA	[39]
	Regulation of RNA synthesis by viral proteins or promoter sequences	ns-NSVs, FLUAV	Prevents formation of aberrant RNAs	[45,52–57]
	Nuclear replication	FLUAV	Hiding from cytoplasmic RLRs	[44]
	VP35	EBOV, MARV	dsRNA binding	[60,61]
	NS1	FLUAV	dsRNA binding	[59,62]
	Cleavage of the 5′ppp RNA end to 5′p	*Bornaviridae*, Hantaviruses, CCHFV	Prevents RIG-I activation	[67,68]
	Genome RNA 5′overhang	*Arenaviridae*	Disturbs RIG-I function	[71]
	dsRNA degradation by nucleocapsid protein	Lassa virus	Removes dsRNA	[72,73]
RLR signalling	NS2	RSV	Interacts with RIG-I to prevent association with MAVS	[75]
	Z	New World Arenaviruses	Interacts with RIG-I to prevent association with MAVS	[74]
	OTU domain	Nairoviruses (*Bunyaviridae*)	De-ubiquitinylates RIG-I	[76,77]
	V	Paramyxoviruses	Wedges into MDA5 structure to prevent formation of signalling-competent filaments	[78,79]
	VP35	EBOV	Sequesters the RIG-I cofactor PACT	[64]
	V	Paramyxoviruses	Assemble RIG-I and LGP2 into a refractory complex	[80]
	NS1	FLUAV	Interacts with TRIM25 to counteract ubiquitinylation of RIG-I	[63]
	Upregulation of Siglec-G by unknown mechanism	VSV, SeV (NSVs in general?)	Ubiquitin-mediated RIG-I degradation	[81]
	NSs	TOSV	Ubiquitin-mediated RIG-I degradation	[82]
	N and P	RSV	Recruitment of MDA5, MAVS, and RIG-I into inclusion bodies	[83]
	NSs	SFTSV	Relocalization of RIG-I, TRIM25, TBK1, IKKε and IRF3 into inclusion bodies	[84,85]
	NS1 and NS2	RSV	Formation of degradosome to destroy MAVS and IRFs	[86]
	PB1, PB2, PA, PB1-F2	FLUAV	Impairment of MAVS signalling	[87–91]
	Nucleocapsid protein	Arenaviruses, hantaviruses	Prevention of TBK1 or IKKε activation	[93,96]
	Gn	Hantaviruses	Prevention of TBK1 action	[95]
	P	BDV and Rabies	Prevention of TBK1 action	[92,97]
	V	Paramyxoviruses	Prevention of TBK1 activation	[94]
	VP35	EBOV	Prevents interactions of TBK1 and IKKε with IRFs	[66]
	VP35	EBOV	Inhibits IRF7 function by enhancing its SUMOylation via the cellular E3 ligase PIAS1	[98]
	ML	THOV	Blocks IRF3 and IRF7 dimerization and association with CBP, TRAF6 and the general transcription factor IIB	[99,100]
	V	Paramyxoviruses	Interact with IRF3 and impair nuclear translocation.	[101]
	W	NiV	Inhibits activation of the IFN-β promoter	[102]
	NSs	RVFV	Recruits repression factor SAP30 to inhibit IFN-β transcription	[103]
Host cell gene expression	Cap-snatching	s-NSVs	Destruction of host cell mRNAs by viral endonuclease function	[108]
	PA-X	FLUAV	Separate endonuclease domain, suppresses antiviral host cell responses	[109]
	NS1	FLUAV	Interferes with processing, nuclear export and translation of host mRNAs	[8]
	M	VSV	Interferes with nuclear export of host mRNAs	[110]
	NSs	RVFV	Disturbs assembly of TFIIH	[111]
	NSs	RVFV	Promotes degradation of the TFIIH subunit p62 via the E3 ubiquitin ligase FBXO3.	[112,113]
	NSs	BUNV	Inhibits phosphorylation of the RNA polymerase II subunit RPB1	[114]
	NSs	LACV	Drives proteasomal degradation of RPB1	[115]

induction of the type I IFN response. The molecular mechanisms involved range from a selective interference with key components of the IFN system to a broad shut-off of the host cell transcription. Since it has become virtually impossible to summarize all known mechanisms and factors of viral IFN antagonism, we can only describe prominent examples to highlight the underlying principles (Table 2).

5.1. Prevention of RLR sensing

An efficient way of innate immune escape is to avoid the initiation of RLR signalling directly at its root, i.e. at the level of detection. As mentioned, NSVs do normally not produce long dsRNAs [36], first of all because of the packaging of genome and antigenome RNAs into separate nucleocapsids [35]. For the s-NSV influenza A virus (FLUAV), depletion of the cellular helicases UAP56 and URH49, which are known to be involved in RNA encapsidation [50], resulted in the appearance of long dsRNA [51]. Also for an ns-NSV (vesicular stomatitis virus, VSV) UAP56 and URH49 are necessary for prevention of dsRNA formation, suggesting a general mechanism [51]. In addition, ns-NSVs are recruiting the cellular RNA binding protein La to shield the leader RNA from RIG-I recognition [39]. The generation of immuno-active RNAs products can also be avoided by tightly controlling the processivity of genome transcription and replication. For several paramyxoviruses (i.e. ns-NSVs) it was described that a loss of regulatory proteins (dependent on the virus either P, C, V) or a promoter mutation enhanced viral RNA synthesis but also facilitated appearance of innate immunity-inducing dsRNA, DI particles, or other aberrant RNAs [52–57]. A similar control of RNA synthesis and DI particle formation to avoid IFN induction was recently reported for FLUAV, suggesting that this is a general mechanism of NSVs [45].

RLR sensing could also be a reason why members of the *Orthomyxoviridae* are replicating in the nucleus. This virus family contain 6 (Thogoto virus, THOV) to 8 (FLUAV) genome segments, i.e. the virions contain at least 2 times as many RLR ligands as those of other s-NSVs. Since RLRs are localized in the cytoplasm, they are only transiently in contact with orthomyxoviral nucleocapsids, namely during the initial transport from the endosome to the nucleus, and during the late step of particle egress. Hiding in the nucleus could be thus a way by which heavily-segmented NSVs can minimize RLR sensing. Indeed, innate immunity activation by FLUAV requires RNA synthesis and RNA nuclear export [44,58]. Thus, the early cytoplasmic passage of nucleocapsids can occur largely unnoticed by the cell.

On top of the strategies to prevent production or exposure of RLR-relevant RNAs, both ns-NSVs and s-NSVs exhibit a range of active mechanisms. The proteins VP35 of Ebola (EBOV) and Marburg virus (MARV) and NS1 of FLUAV directly bind dsRNA [59–62], although it seems that additional host factor interactions are necessary to prevent IFN induction [63–66]. Moreover, members of the *Bornaviridae* (ns-NSVs) and *Bunyaviridae* (s-NSVs) remove the 5′ppp group from their genome to avoid RIG-I activation [67,68], although some residual activating potential seems to remain [37,69]. Similarly, for the *Arenaviridae* (s-NSVs) a fraction of genome ends [70] can exhibit a single 5′overhanging nucleotide with the potential to disturb RIG-I function [71]. Moreover, Lassa virus (LASV, family *Arenaviridae*) encodes a nucleoprotein with 3′–5′ exoribonuclease activity to degrade dsRNA [72,73].

5.2. Specific interference with RLR signalling

In addition to masking, processing or degrading RLR agonists, NSVs can interfere with key components of the RLR signalling pathway. Several factors of ns-NSVs and s-NSVs are known to act on the level of RLRs. NS2 of respiratory syncytial virus (RSV) and the Z protein of New World Arenaviruses directly interact with RIG-I to prevent the association with MAVS [74,75]. The ovarian tumour (OTU) domain of Nairoviruses (family *Bunyaviridae*) supresses IFN induction and de-ubiquitinylates RIG-I [76,77]. MDA5 was originally discovered as a host interactor and inhibitor of the paramyxovirus IFN antagonist V [78]. The V proteins are wedging into the MDA5 structure in a manner that prevents assembly into signalling-competent filaments [79]. VP35 of EBOV sequesters the RIG-I activating protein PACT to interfere with RIG-I activation [64], V proteins of paramyxoviruses assemble RIG-I and LGP2 into a complex which becomes refractory to activation by RIG-I ligands [80], and NS1 of FLUAV interacts with TRIM25 to counteract ubiquitinylation of RIG-I [63]. Interestingly, infections with VSV or SeV were shown to upregulate the lectin Siglec-G, resulting in RIG-I degradation via K48-linked ubiquitinylation [81]. A strategy of ubiquitin-dependent RIG-I degradation is also conducted by Toscana virus (TOSV) via its NSs protein [82].

Some viral factors also sequester key components of RLR signalling in cellular compartments. RSV N and P proteins recruit MDA5, MAVS, and less efficiently RIG-I, into virus induced inclusion bodies [83]. Also Severe fever with thrombocytopenia syndrome virus (SFTSV) NSs prevents RLR signalling by promoting relocalization of RIG-I, TRIM25, TBK1, IKKε and IRF3 into virus-induced cytoplasmic structures [84,85]. NS1 and NS2 of RSV induce the formation of the so-called degradosome to target MAVS and IRFs for degradation [86]. MAVS signalling is impaired by FLUAV polymerase subunits (PB1, PB2 and PA) [87,88] and the accessory protein PB1-F2 [89–91]. Further downstream, TBK1 activation or action are prevented by N of arenaviruses and hantaviruses, and Gn proteins of hantaviruses, P proteins of BDV and Rabies virus, V proteins of paramyxoviruses, and also by EBOV VP35 [66,92–97].

Finally, at the level of IFN transcription, several viral factors are known to interfere with IRF or NF-κB activity. EBOV VP35 (a multifunctional IFN antagonist like FLUAV NS1) enhances SUMOylation of IRF7 via the cellular E3 ligase PIAS1, thereby inhibiting its function as an IFN transcription factor [98]. ML of THOV (family *Orthomyxoviridae*), acts by blocking IRF3 and IRF7 dimerization and association with CBP, TRAF6 and the general transcription factor IIB [99,100]. V proteins of several (but not all) paramyxoviruses interact with IRF3 and impair its nuclear translocation [101]. In case of the highly pathogenic Nipah virus (NiV) (family *Paramyxoviridae*), the W protein translocates into the nucleus to inhibit activation of the IFN-β promoter [102]. Also the NSs protein of RVFV specifically inhibits IFN-β mRNA transcription by forming a promoter-bound complex with the repression factor SAP30 [103].

5.3. Unspecific interference with RLR signalling

In contrast to the above-described specific mechanisms aiming at antiviral signalling pathways, some representatives of the NSVs interfere with the cellular transcription machinery in total. It is thereby important to distinguish between a primary host cell shut-off imposed by specific viral mechanisms from the secondary shut-off caused by translation inhibition due to the dsRNA-activated host cell kinase PKR. While the primary, "intended" shut-off seems to be mostly (but not exclusively) the domain of s-NSVs, the secondary shut-off is in fact an efficient antiviral host reaction. PKR activation is thus avoided by both s-NSVs and sn-NSVs, either by tight regulation of RNA synthesis (see above), or by specific anti-PKR mechanisms [11,104].

A virus-induced, general block of gene expression provides an efficient mechanism to prevent synthesis of IFN and ISGs, but could

bear the disadvantage of cutting off from renewable resources. However, viruses undergoing rapid and lytic infection cycles seem to care little for such considerations. That the viral host shut-off, a long-known phenomenon, is often an IFN antagonism in disguise was revealed by genetic complementation studies showing that the particular viral shut-off factor is only necessary if the host organism possesses a functional IFN system [105–107]. In other words, in an IFN-free host environment the shut-off factors are dispensable for viral success. Interestingly, all s-NVs (but not ns-NSVs) commit cap-snatching, an endonuclease-mediated mechanism to degrade host mRNAs by depriving them of their 5′ cap structure. Cap-snatching spares the s-NSVs to encode their own mRNA capping enzyme, and could have the convenient side effect of reducing host cell gene expression, including that of upregulated components of the RLR and IFN signalling pathways [108]. FLUAV expresses its endonuclease even as a separate domain, called PA-X, which was actually shown to suppress antiviral host cell responses [109]. FLUAV impairs host gene expression also by other mechanisms. The multifunctional protein NS1 interferes with processing, nuclear export and translation of host mRNAs [8]. Inhibition of nuclear-cytoplasmic RNA transport is a strategy shared by the matrix protein M of VSV [110]. Broad disruption of RNA polymerase II activity is achieved by representatives of the *Bunyaviridae*. The NSs of RVFV disturbs assembly of the general transcriptional factor TFIIH [111] and promotes degradation of the TFIIH subunit p62 via the E3 ubiquitin ligase FBXO3 [112,113]. The NSs protein of Bunyamwera virus and LACV impact on the RNA polymerase II subunit RPB1, disturbing its phosphorylation (and hence processivity) or driving its proteasomal degradation [114,115].

6. Conclusions and outlook

NSV-infected cells are flooded with foreign RNAs which are – compared to the pool of host cell RNAs – rather homogeneous in sequence and structure. Unusual features like double-strandedness or triphosphorylated 5′ends are extremely efficient markers of infection. However, also structures with less prominent features are conceivable to act as triggers of antiviral responses if they appear in high enough amounts.

Since the discoveries of RIG-I and MDA5 [78,116], the research field of intracellular RNA recognition and viral countermechanisms has virtually exploded. There are ongoing discussions on the physiological ligands of RLRs and on major RLRs engaged during a particular infection, questions which are touching the very core of the immune reponse, the distinction between self and non-self. In our review, we wanted to highlight that NSVs are a quite heterogeneous taxonomic group, with different genome and nucleocapsid structures, subcellular localizations, replication strategies, tendencies to produce DI particles, and a multitude of IFN antagonists which can obscure RLR–ligand interactions. Moreover, different infection phases may produce different RLR triggers. To make things even more complicated, it is meanwhile established that RLRs can get help from accessory factors such as e.g. other RNA-binding proteins, helicases or RNases, further expanding the range of in vivo RLR triggers [17,32,39,117–119], which may not work as such in vitro. So, again, the question which RLR recognizes which virus and viral structure under physiological conditions may return different answers which depend on the infection phase, the DI particle content of virus stocks, the specific activity of virus regulators and IFN antagonists, and on host cell cofactors.

Conflict of interest

No conflicts of interest declared.

Acknowledgments

Work in our laboratories is supported by the Deutsche Forschungsgemeinschaft grants We 2616/7-1, SFB 593 and SFB 1021, by the Forschungsförderung gem. §2 Abs. 3 Kooperationsvertrag Universitätsklinikum Giessen und Marburg, and by the Leibniz Graduate School for Emerging viral diseases (EIDIS).

References

[1] Moya A, Elena SF, Bracho A, Miralles R, Barrio E. The evolution of RNA viruses: a population genetics view. Proc Natl Acad Sci U S A 2000;97:6967–73.
[2] Belgnaoui SM, Paz S, Hiscott J. Orchestrating the interferon antiviral response through the mitochondrial antiviral signaling (MAVS) adapter. Curr Opin Immunol 2011;23:564–72.
[3] Eifan S, Schnettler E, Dietrich I, Kohl A, Blomstrom AL. Non-structural proteins of arthropod-borne bunyaviruses: roles and functions. Viruses 2013;5:2447–68.
[4] Gack MU. Mechanisms of RIG-I-like receptor activation and manipulation by viral pathogens. J Virol 2014;88:5213–6.
[5] Garcia-Sastre A. Induction and evasion of type I interferon responses by influenza viruses. Virus Res 2011;162:12–8.
[6] Gerlier D, Lyles DS. Interplay between innate immunity and negative-strand RNA viruses: towards a rational model. Microbiol Mol Biol Rev MMBR 2011;75:468–90 [second page of table of contents].
[7] Goubau D, Deddouche S, Reis e Sousa C. Cytosolic sensing of viruses. Immunity 2013;38:855–69.
[8] Hale BG, Randall RE, Ortin J, Jackson D. The multifunctional NS1 protein of influenza A viruses. J Gen Virol 2008;89:2359–76.
[9] Kolakofsky D, Kowalinski E, Cusack S. A structure-based model of RIG-I activation. RNA 2012;18:2118–27.
[10] Ng CS, Kato H, Fujita T. Recognition of viruses in the cytoplasm by RLRs and other helicases – how conformational changes, mitochondrial dynamics and ubiquitination control innate immune responses. Int Immunol 2012;24:739–49.
[11] Parks GD, Alexander-Miller MA. Paramyxovirus activation and inhibition of innate immune responses. J Mol Biol 2013;425:4872–92.
[12] Schoggins JW, Rice CM. Interferon-stimulated genes and their antiviral effector functions. Curr Opin Virol 2011;1:519–25.
[13] Schlee M. Master sensors of pathogenic RNA – RIG-I like receptors. Immunobiology 2013;218:1322–35.
[14] Zinzula L, Tramontano E. Strategies of highly pathogenic RNA viruses to block dsRNA detection by RIG-I-like receptors: hide, mask, hit. Antiviral Res 2013;100:615–35.
[15] Kohlway A, Luo D, Rawling DC, Ding SC, Pyle AM. Defining the functional determinants for RNA surveillance by RIG-I. EMBO Rep 2013;14:772–9.
[16] Kowalinski E, Lunardi T, McCarthy AA, Louber J, Brunel J, Grigorov B, et al. Structural basis for the activation of innate immune pattern-recognition receptor RIG-I by viral RNA. Cell 2011;147:423–35.
[17] Childs KS, Randall RE, Goodbourn S. LGP2 plays a critical role in sensitizing MDA-5 to activation by double-stranded RNA. PLoS ONE 2013;8:e64202.
[18] Satoh T, Kato H, Kumagai Y, Yoneyama M, Sato S, Matsushita K, et al. LGP2 is a positive regulator of RIG-I- and MDA5-mediated antiviral responses. Proc Natl Acad Sci U S A 2010;107:1512–7.
[19] Gack MU, Shin YC, Joo CH, Urano T, Liang C, Sun L, et al. TRIM25 RING-finger E3 ubiquitin ligase is essential for RIG-I-mediated antiviral activity. Nature 2007;446:916–20.
[20] Patel JR, Jain A, Chou YY, Baum A, Ha T, Garcia-Sastre A. ATPase-driven oligomerization of RIG-I on RNA allows optimal activation of type-I interferon. EMBO Rep 2013;14:780–7.
[21] Peisley A, Wu B, Xu H, Chen ZJ, Hur S. Structural basis for ubiquitin-mediated antiviral signal activation by RIG-I. Nature 2014.
[22] Wies E, Wang MK, Maharaj NP, Chen K, Zhou S, Finberg RW, et al. Dephosphorylation of the RNA sensors RIG-I and MDA5 by the phosphatase PP1 is essential for innate immune signaling. Immunity 2013;38:437–49.
[23] Zeng WW, Sun LJ, Jiang XM, Chen X, Hou FJ, Adhikari A, et al. Reconstitution of the RIG-I pathway reveals a signaling role of unanchored polyubiquitin chains in innate immunity. Cell 2010;141:315–30.
[24] Binder M, Eberle F, Seitz S, Mucke N, Huber CM, Kiani N, et al. Molecular mechanism of signal perception and integration by the innate immune sensor retinoic acid-inducible Gene-I (RIG-I). J Biol Chem 2011;286:27278–87.
[25] Wu B, Peisley A, Richards C, Yao H, Zeng X, Lin C, et al. Structural basis for dsRNA recognition, filament formation, and antiviral signal activation by MDA5. Cell 2013;152:276–89.
[26] Schlee M, Roth A, Hornung V, Hagmann CA, Wimmenauer V, Barchet W, et al. Recognition of 5′ triphosphate by RIG-I helicase requires short blunt double-stranded RNA as contained in panhandle of negative-strand virus. Immunity 2009;31:25–34.
[27] Schmidt A, Schwerd T, Hamm W, Hellmuth JC, Cui S, Wenzel M, et al. 5′-Triphosphate RNA requires base-paired structures to activate antiviral signaling via RIG-I. Proc Natl Acad Sci U S A 2009;106:12067–72.

[28] Kato H, Takeuchi O, Mikamo-Satoh E, Hirai R, Kawai T, Matsushita K, et al. Length-dependent recognition of double-stranded ribonucleic acids by retinoic acid-inducible gene-I and melanoma differentiation-associated gene 5. J Exp Med 2008;205:1601–10.
[29] Malathi K, Saito T, Crochet N, Barton DJ, Gale Jr M, Silverman RH, Nase R. L releases a small RNA from HCV RNA that refolds into a potent PAMP. RNA 2010;16:2108–19.
[30] Saito T, Owen DM, Jiang F, Marcotrigiano J, Gale Jr M. Innate immunity induced by composition-dependent RIG-I recognition of hepatitis C virus RNA. Nature 2008;454:523–7.
[31] Pichlmair A, Schulz O, Tan CP, Rehwinkel J, Kato H, Takeuchi O, et al. Activation of MDA5 requires higher-order RNA structures generated during virus infection. J Virol 2009;83:10761–69.
[32] Luthra P, Sun D, Silverman RH, He B. Activation of IFN-beta expression by a viral mRNA through RNase L and MDA5. Proc Natl Acad Sci U S A 2011;108:2118–23.
[33] Runge S, Sparrer KM, Lassig C, Hembach K, Baum A, Garcia-Sastre A, et al. In vivo ligands of MDA5 and RIG-I in measles virus-infected cells. PLoS Pathogens 2014;10:e1004081.
[34] Davis WG, Bowzard JB, Sharma SD, Wiens ME, Ranjan P, Gangappa S, et al. The 3′ untranslated regions of influenza genomic sequences are 5′ppp-independent ligands for RIG-I. PLoS ONE 2012;7:e32661.
[35] Ruigrok RW, Crepin T, Kolakofsky D. Nucleoproteins and nucleocapsids of negative-strand RNA viruses. Curr Opin Microbiol 2011;14:504–10.
[36] Weber F, Wagner V, Rasmussen SB, Hartmann R, Paludan SR. Double-stranded RNA is produced by positive-strand RNA viruses and DNA viruses but not in detectable amounts by negative-strand RNA viruses. J Virol 2006;80:5059–64.
[37] Weber M, Gawanbacht A, Habjan M, Rang A, Borner C, Schmidt AM, et al. Incoming RNA virus nucleocapsids containing a 5′-triphosphorylated genome activate RIG-I and antiviral signaling. Cell Host Microbe 2013;13:336–46.
[38] Baum A, Sachidanandam R, Garcia-Sastre A. Preference of RIG-I for short viral RNA molecules in infected cells revealed by next-generation sequencing. Proc Natl Acad Sci U S AV 107 2010;16303–08.
[39] Bitko V, Musiyenko A, Bayfield MA, Maraia RJ, Barik S. Cellular La protein shields nonsegmented negative-strand RNA viral leader RNA from RIG-I and enhances virus growth by diverse mechanisms. J Virol 2008;82:7977–87.
[40] Ikegame S, Takeda M, Ohno S, Nakatsu Y, Nakanishi Y, Yanagi Y. Both RIG-I and MDA5 RNA helicases contribute to the induction of alpha/beta interferon in measles virus-infected human cells. J Virol 2010;84:372–9.
[41] Plumet S, Herschke F, Bourhis JM, Valentin H, Longhi S, Gerlier D. Cytosolic 5′-triphosphate ended viral leader transcript of measles virus as activator of the RIG I-mediated interferon response. PLoS ONE 2007;2:e279.
[42] Perrault J. Origin and replication of defective interfering particles. Curr Top Microbiol Immunol 1981;93:151–207.
[43] Strahle L, Garcin D, Kolakofsky D. Sendai virus defective-interfering genomes and the activation of interferon-beta. Virology 2006;351:101–11.
[44] Killip MJ, Smith M, Jackson D, Randall RE. Activation of the interferon induction cascade by influenza a viruses requires viral RNA synthesis and nuclear export. J Virol 2014;88:3942–52.
[45] Perez-Cidoncha M, Killip MJ, Oliveros JC, Asensio VJ, Fernandez Y, Bengoechea JA, et al. An unbiased genetic screen reveals the polygenic nature of the influenza virus anti-interferon response. J Virol 2014;88:4632–46.
[46] Rehwinkel J, Tan CP, Goubau D, Schulz O, Pichlmair A, Bier K, et al. RIG-I detects viral genomic RNA during negative-strand RNA virus infection. Cell 2010;140:397–408.
[47] Briese T, Calisher CH, Higgs S. Viruses of the family Bunyaviridae: are all available isolates reassortants? Virology 2013;446:207–16.
[48] Pressing J, Reanney DC. Divided genomes and intrinsic noise. J Mol Evolution 1984;20:135–46.
[49] Ojosnegros S, Garcia-Arriaza J, Escarmis C, Manrubia SC, Perales C, Arias A, et al. Viral genome segmentation can result from a trade-off between genetic content and particle stability. PLoS Genetics 2011;7:e1001344.
[50] Kawaguchi A, Momose F, Nagata K. Replication-coupled and host factor-mediated encapsidation of the influenza virus genome by viral nucleoprotein. J Virol 2011;85:6197–204.
[51] Wisskirchen C, Ludersdorfer TH, Muller DA, Moritz E, Pavlovic J. The cellular RNA helicase UAP56 is required for prevention of double-stranded RNA formation during influenza A virus infection. J Virol 2011;85:8646–55.
[52] Boonyaratanakornkit J, Bartlett E, Schomacker H, Surman S, Akira S, Bae YS, et al. The C proteins of human parainfluenza virus type 1 limit double-stranded RNA accumulation that would otherwise trigger activation of MDA5 and protein kinase R. J Virol 2011;85:1495–506.
[53] Dillon PJ, Parks GD. Role for the phosphoprotein P subunit of the paramyxovirus polymerase in limiting induction of host cell antiviral responses. J Virol 2007;81:11116–27.
[54] Manuse MJ, Parks GD. Role for the paramyxovirus genomic promoter in limiting host cell antiviral responses and cell killing. J Virol 2009;83:9057–67.
[55] Nakatsu Y, Takeda M, Ohno S, Koga R, Yanagi Y. Translational inhibition and increased interferon induction in cells infected with C protein-deficient measles virus. J Virol 2006;80:11861–67.
[56] Pfaller CK, Radeke MJ, Cattaneo R, Samuel CE. Measles virus C protein impairs production of defective copyback double-stranded viral RNA and activation of protein kinase R. J Virol 2014;88:456–68.
[57] Takeuchi K, Komatsu T, Kitagawa Y, Sada K, Gotoh B. Sendai virus C protein plays a role in restricting PKR activation by limiting the generation of intracellular double-stranded RNA. J Virol 2008;82:10102–10.
[58] Osterlund P, Strengell M, Sarin LP, Poranen MM, Fagerlund R, Melen K, et al. Incoming influenza A virus evades early host recognition, while influenza B virus induces interferon expression directly upon entry. J Virol 2012;86:11183–93.
[59] Hatada E, Fukuda R. Binding of influenza A virus NS1 protein to dsRNA in vitro. J Gen Virol 1992;73(Pt 12):3325–9.
[60] Ramanan P, Edwards MR, Shabman RS, Leung DW, Endlich-Frazier AC, Borek DM, et al. Structural basis for Marburg virus VP35-mediated immune evasion mechanisms. Proc Natl Acad Sci U S A 2012;109:20661–66.
[61] Kimberlin CR, Bornholdt ZA, Li S, Woods Jr VL, MacRae IJ, Saphire EO. Ebolavirus VP35 uses a bimodal strategy to bind dsRNA for innate immune suppression. Proc Natl Acad Sci U S A 2010;107:314–9.
[62] Qian XY, Chien CY, Lu Y, Montelione GT, Krug RM. An amino-terminal polypeptide fragment of the influenza virus NS1 protein possesses specific RNA-binding activity and largely helical backbone structure. RNA 1995;1:948–56.
[63] Gack MU, Albrecht RA, Urano T, Inn KS, Huang IC, Carnero E, et al. Influenza A virus NS1 targets the ubiquitin ligase TRIM25 to evade recognition by the host viral RNA sensor RIG-I. Cell Host Microbe 2009;5:439–49.
[64] Luthra P, Ramanan P, Mire CE, Weisend C, Tsuda Y, Yen B, et al. Mutual antagonism between the Ebola virus VP35 protein and the RIG-I activator PACT determines infection outcome. Cell Host Microbe 2013;14:74–84.
[65] Noah DL, Twu KY, Krug RM. Cellular antiviral responses against influenza A virus are countered at the posttranscriptional level by the viral NS1A protein via its binding to a cellular protein required for the 3′ end processing of cellular pre-mRNAS. Virology 2003;307:386–95.
[66] Prins KC, Cardenas WB, Basler CF. Ebola virus protein VP35 impairs the function of interferon regulatory factor-activating kinases IKKepsilon and TBK-1. J Virol 2009;83:3069–77.
[67] Habjan M, Andersson I, Klingstrom J, Schumann M, Martin A, Zimmermann P, et al. Processing of genome 5′ termini as a strategy of negative-strand RNA viruses to avoid RIG-I-dependent interferon induction. PLoS ONE 2008;3:e2032.
[68] Wang H, Vaheri A, Weber F, Plyusnin A. Old world hantaviruses do not produce detectable amounts of dsRNA in infected cells and the 5′ termini of their genomic RNAs are monophosphorylated. J Gen Virol 2011;92:1199–204.
[69] Lee MH, Lalwani P, Raftery MJ, Matthaei M, Lutteke N, Kirsanovs S, et al. RNA helicase retinoic acid-inducible gene I as a sensor of Hantaan virus replication. J Gen Virol 2011;92:2191–200.
[70] Albarino CG, Bergeron E, Erickson BR, Khristova ML, Rollin PE, Nichol ST. Efficient reverse genetics generation of infectious junin viruses differing in glycoprotein processing. J Virol 2009;83:5606–14.
[71] Marq JB, Hausmann S, Veillard N, Kolakofsky D, Garcin D. Short double-stranded RNAs with an overhanging 5′ppp-nucleotide, as found in arenavirus genomes, act as RIG-I decoys. J Biol Chem 2011;286:6108–16.
[72] Hastie KM, Kimberlin CR, Zandonatti MA, MacRae IJ, Saphire EO. Structure of the Lassa virus nucleoprotein reveals a dsRNA-specific 3′ to 5′ exonuclease activity essential for immune suppression. Proc Natl Acad Sci U S A 2011;108:2396–401.
[73] Qi X, Lan S, Wang W, Schelde LM, Dong H, Wallat GD, et al. Cap binding and immune evasion revealed by Lassa nucleoprotein structure. Nature 2010;468:779–83.
[74] Fan L, Briese T, Lipkin WI. Z proteins of New World arenaviruses bind RIG-I and interfere with type I interferon induction. J Virol 2010;84:1785–91.
[75] Ling Z, Tran KC, Teng MN. Human respiratory syncytial virus nonstructural protein NS2 antagonizes the activation of beta interferon transcription by interacting with RIG-I. J Virol 2009;83:3734–42.
[76] Frias-Staheli N, Giannakopoulos NV, Kikkert M, Taylor SL, Bridgen A, Paragas J, et al. Ovarian tumor domain-containing viral proteases evade ubiquitin- and ISG15-dependent innate immune responses. Cell Host Microbe 2007;2:404–16.
[77] van Kasteren PB, Beugeling C, Ninaber DK, Frias-Staheli N, van Boheemen S, Garcia-Sastre A, et al. Arterivirus and nairovirus ovarian tumor domain-containing Deubiquitinases target activated RIG-I to control innate immune signaling. J Virol 2012;86:773–85.
[78] Andrejeva J, Childs KS, Young DF, Carlos TS, Stock N, Goodbourn S, et al. The V proteins of paramyxoviruses bind the IFN-inducible RNA helicase, mda-5, and inhibit its activation of the IFN-beta promoter. Proc Natl Acad Sci U S A 2004;101:17264–69.
[79] Motz C, Schuhmann KM, Kirchhofer A, Moldt M, Witte G, Conzelmann KK, et al. Paramyxovirus V proteins disrupt the fold of the RNA sensor MDA5 to inhibit antiviral signaling. Science 2013;339:690–3.
[80] Childs K, Randall R, Goodbourn S, Paramyxovirus V. proteins interact with the RNA helicase LGP2 to inhibit RIG-I-dependent interferon induction. J Virol 2012;86:3411–21.
[81] Chen W, Han C, Xie B, Hu X, Yu Q, Shi L, et al. Induction of Siglec-G by RNA viruses inhibits the innate immune response by promoting RIG-I degradation. Cell 2013;152:467–78.
[82] Gori-Savellini G, Valentini M, Cusi MG. Toscana virus NSs protein inhibits the induction of type I interferon by interacting with RIG-I. J Virol 2013;87:6660–7.
[83] Lifland AW, Jung J, Alonas E, Zurla C, Crowe Jr JE, Santangelo PJ. Human respiratory syncytial virus nucleoprotein and inclusion bodies antagonize the innate immune response mediated by MDA5 and MAVS. J Virol 2012;86:8245–58.

[84] Santiago FW, Covaleda LM, Sanchez-Aparicio MT, Silvas JA, Diaz-Vizarreta AC, Patel JR, et al. Hijacking of RIG-I signaling proteins into virus-induced cytoplasmic structures correlates with the inhibition of Type I interferon responses. J Virol 2014;88:4572–85.
[85] Wu X, Qi X, Qu B, Zhang Z, Liang M, Li C, et al. Evasion of antiviral immunity through sequestering of TBK1/IKKepsilon/IRF3 into viral inclusion bodies. J Virol 2014;88:3067–76.
[86] Goswami R, Majumdar T, Dhar J, Chattopadhyay S, Bandyopadhyay SK, Verbovetskaya V, et al. Viral degradasome hijacks mitochondria to suppress innate immunity. Cell Res 2013;23:1025–42.
[87] Graef KM, Vreede FT, Lau YF, McCall AW, Carr SM, Subbarao K, et al. The PB2 subunit of the influenza virus RNA polymerase affects virulence by interacting with the mitochondrial antiviral signaling protein and inhibiting expression of beta interferon. J Virol 2010;84:8433–45.
[88] Iwai A, Shiozaki T, Kawai T, Akira S, Kawaoka Y, Takada A, et al. Influenza A virus polymerase inhibits type I interferon induction by binding to interferon beta promoter stimulator 1. J Biol Chem 2010;285:32064–74.
[89] Dudek SE, Wixler L, Nordhoff C, Nordmann A, Anhlan D, Wixler V, et al. The influenza virus PB1-F2 protein has interferon antagonistic activity. Biol Chem 2011;392:1135–44.
[90] Reis AL, McCauley JW. The influenza virus protein PB1-F2 interacts with IKKbeta and modulates NF-kappaB signalling. PLoS ONE 2013;8:e63852.
[91] Varga ZT, Ramos I, Hai R, Schmolke M, Garcia-Sastre A, Fernandez-Sesma A, et al. The influenza virus protein PB1-F2 inhibits the induction of type I interferon at the level of the MAVS adaptor protein. PLoS Pathogens 2011;7:e1002067.
[92] Brzozka K, Finke S, Conzelmann KK. Identification of the rabies virus alpha/beta interferon antagonist: phosphoprotein P interferes with phosphorylation of interferon regulatory factor 3. J Virol 2005;79:7673–81.
[93] Cimica V, Dalrymple NA, Roth E, Nasonov A, Mackow ER. An innate immunity-regulating virulence determinant is uniquely encoded by the Andes virus nucleocapsid protein. mBio 2014;5.
[94] Lu LL, Puri M, Horvath CM, Sen GC. Select paramyxoviral V proteins inhibit IRF3 activation by acting as alternative substrates for inhibitor of kappaB kinase epsilon (IKKe)/TBK1. J Biol Chem 2008;283:14269–76.
[95] Matthys VS, Cimica V, Dalrymple NA, Glennon NB, Bianco C, Mackow ER. Hantavirus GnT elements mediate TRAF3 binding and inhibit RIG-I/TBK1-directed beta interferon transcription by blocking IRF3 phosphorylation. J Virol 2014;88:2246–59.
[96] Pythoud C, Rodrigo WW, Pasqual G, Rothenberger S, Martinez-Sobrido L, de la Torre JC, et al. Arenavirus nucleoprotein targets interferon regulatory factor-activating kinase IKKepsilon. J Virol 2012;86:7728–38.
[97] Unterstab G, Ludwig S, Anton A, Planz O, Dauber B, Krappmann D, et al. Viral targeting of the interferon-{beta}-inducing Traf family member-associated NF-{kappa}B activator (TANK)-binding kinase-1. Proc Natl Acad Sci U S A 2005;102:13640–45.
[98] Chang TH, Kubota T, Matsuoka M, Jones S, Bradfute SB, Bray M, et al. Ebola Zaire virus blocks type I interferon production by exploiting the host SUMO modification machinery. PLoS Pathogens 2009;5:e1000493.
[99] Buettner N, Vogt C, Martinez-Sobrido L, Weber F, Waibler Z, Kochs G. Thogoto virus ML protein is a potent inhibitor of the interferon regulatory factor-7 transcription factor. J Gen Virol 2010;91:220–7.
[100] Vogt C, Preuss E, Mayer D, Weber F, Schwemmle M, Kochs G. The interferon antagonist ML protein of thogoto virus targets general transcription factor IIB. J Virol 2008;82:11446–53.
[101] Irie T, Kiyotani K, Igarashi T, Yoshida A, Sakaguchi T. Inhibition of interferon regulatory factor 3 activation by paramyxovirus V protein. J Virol 2012;86:7136–45.
[102] Shaw ML, Cardenas WB, Zamarin D, Palese P, Basler CF. Nuclear localization of the Nipah virus W protein allows for inhibition of both virus- and toll-like receptor 3-triggered signaling pathways. J Virol 2005;79:6078–88.
[103] Le May N, Mansuroglu Z, Leger P, Josse T, Blot G, Billecocq A, et al. A SAP30 complex inhibits IFN-beta expression in Rift Valley fever virus infected cells. PLoS Pathogens 2008;4:e13.
[104] Langland JO, Cameron JM, Heck MC, Jancovich JK, Jacobs BL. Inhibition of PKR by RNA and DNA viruses. Virus Res 2006;119:100–10.
[105] Blakqori G, Delhaye S, Habjan M, Blair CD, Sanchez-Vargas I, Olson KE, et al. La Crosse bunyavirus nonstructural protein NSs serves to suppress the type I interferon system of mammalian hosts. J Virol 2007;81:4991–9.
[106] Bouloy M, Janzen C, Vialat P, Khun H, Pavlovic J, Huerre M, et al. Genetic evidence for an interferon-antagonistic function of rift valley fever virus nonstructural protein NSs. J Virol 2001;75:1371–7.
[107] Stojdl DF, Lichty BD, tenOever BR, Paterson JM, Power AT, Knowles S, et al. VSV strains with defects in their ability to shutdown innate immunity are potent systemic anti-cancer agents. Cancer Cell 2003;4:263–75.
[108] Marcus PI, Rojek JM, Sekellick MJ. Interferon induction and/or production and its suppression by influenza A viruses. J Virol 2005;79:2880–90.
[109] Jagger BW, Wise HM, Kash JC, Walters KA, Wills NM, Xiao YL, et al. An overlapping protein-coding region in influenza A virus segment 3 modulates the host response. Science 2012;337:199–204.
[110] Rajani KR, Pettit Kneller EL, McKenzie MO, Horita DA, Chou JW, Lyles DS. Complexes of vesicular stomatitis virus matrix protein with host Rae1 and Nup98 involved in inhibition of host transcription. PLoS Pathogens 2012;8:e1002929.
[111] Le May N, Dubaele S, De Santis LP, Billecocq A, Bouloy M, Egly JM. TFIIH transcription factor, a target for the Rift Valley hemorrhagic fever virus. Cell 2004;116:541–50.
[112] Kainulainen M, Habjan M, Hubel P, Busch L, Lau S, Colinge J, et al. Virulence factor NSs of rift valley fever virus recruits the F-box protein FBXO3 to degrade subunit p62 of general transcription factor TFIIH. J Virol 2014;88:3464–73.
[113] Kalveram B, Lihoradova O, Ikegami T. NSs protein of rift valley fever virus promotes posttranslational downregulation of the TFIIH subunit p62. J Virol 2011;85:6234–43.
[114] Thomas D, Blakqori G, Wagner V, Banholzer M, Kessler N, Elliott RM, et al. Inhibition of RNA polymerase II phosphorylation by a viral interferon antagonist. J Biol Chem 2004;279:31471–77.
[115] Verbruggen P, Ruf M, Blakqori G, Overby AK, Heidemann M, Eick D, et al. Interferon antagonist NSs of La Crosse virus triggers a DNA damage response-like degradation of transcribing RNA polymerase II. J Biol Chem 2011;286:3681–92.
[116] Yoneyama M, Kikuchi M, Natsukawa T, Shinobu N, Imaizumi T, Miyagishi M, et al. The RNA helicase RIG-I has an essential function in double-stranded RNA-induced innate antiviral responses. Nat Immunol 2004;5:730–7.
[117] Kok KH, Lui PY, Ng MH, Siu KL, Au SW, Jin DY. The double-stranded RNA-binding protein PACT functions as a cellular activator of RIG-I to facilitate innate antiviral response. Cell Host Microbe 2011;9:299–309.
[118] Malathi K, Dong B, Gale Jr M, Silverman RH. Small self-RNA generated by RNase L amplifies antiviral innate immunity. Nature 2007;448:816–9.
[119] Yoo JS, Takahasi K, Ng CS, Ouda R, Onomoto K, Yoneyama M, et al. DHX36 enhances RIG-I signaling by facilitating PKR-mediated antiviral stress granule formation. PLoS Pathogens 2014;10:e1004012.

Michaela Weber did her diploma thesis in the group of Friedemann Weber at the Philipps-University in Marburg, Germany. In 2012, she graduated her studies of human biology and continued her work as a Ph.D. student. Her research focuses on the physiological agonists of pattern recognition receptors during RNA virus infection.

Friedemann Weber received his M.Sc. in 1993 from the Department of Microbiology and his Ph.D. in 1997 from the Department of Virology at the University of Freiburg, Germany. He was an EMBO Long Term Postdoctoral Fellow at the Institute of Virology in Glasgow, UK, and a research group leader in the Department of Virology, Freiburg, Germany. Since 2010, he holds a professorship at the Institute for Virology, Philipps-University Marburg, Germany. He has received several prestigious awards including the Milstein Young Investigator Award from the International Society for Interferon and Cytokine Research (ISICR) and the "Löffler-Frosch-Preis" of the Gesellschaft für Virologie. He is interested in the innate immune responses to highly pathogenic RNA viruses such as SARS-Coronavirus and bunyaviruses. The particular focus is on interferon-inducing viral structures, their intracellular receptors, and the viral escape strategies. He has published over 90 research papers, review articles and book chapters.

4.6. REVIEW: Segmented negative-strand RNA viruses and RIG-I: divide (your genome) and rule

Own contribution:

I contributed to writing of the manuscript.

Michaela Gerlach

Available online at www.sciencedirect.com

ScienceDirect

Current Opinion in Microbiology

Segmented negative-strand RNA viruses and RIG-I: divide (your genome) and rule

Michaela Weber and Friedemann Weber

The group of negative-stranded RNA viruses (NSVs) with a segmented genome comprises pathogens like influenza virus (eight segments), Rift Valley fever virus and Hantavirus (three segments), or Lassa virus (two segments). Partitioning the genome allows rapid evolution of new strains by reassortment. Each segment carries a short double-stranded (ds) 'panhandle' structure which serves as promoter. Similar dsRNA structures, however, represent the optimal ligand for RIG-I, a cytoplasmic pathogen sensor of the antiviral interferon response. Thus, segmenting a virus genome can entail an increased RIG-I sensitivity. Here, we outline the astonishingly diverse and efficient strategies by which segmented NSVs are compensating for the elevated number of RIG-I ligands in their genome.

Addresses
Institute for Virology, Philipps-University Marburg, D-35043 Marburg, Germany

Corresponding author: Weber, Friedemann (friedemann.weber@staff.uni-marburg.de)

Current Opinion in Microbiology 2014, **20**:96–102

This review comes from a themed issue on **Host-microbe interactions: viruses**

Edited by **Maria-Carla Saleh**

For a complete overview see the Issue and the Editorial

Available online 13th June 2014

http://dx.doi.org/10.1016/j.mib.2014.05.002

Introduction

Like eukaryotes, some negative-strand RNA viruses (NSVs) feature a genome which is divided into semi-autonomous pieces. The evolutionary advantage is an extra degree of freedom for recombination, facilitating the rapid admixture of genome segments to create hybrid offspring. The success of this strategy is obvious from the constant flow of new influenza strains afflicting mankind with epidemics or even pandemics [1]. Besides influenza viruses (belonging to the family *Orthomyxoviridae*) which have up to eight segments to offer for genetic mixing, there are two other families with a more modest set-up, namely the *Bunyaviridae* (three segments) and the *Arenaviridae* (two segments). Together these viruses are responsible for an impressive array of diseases ranging from severe pulmonary, hepatic or renal ailments (influenza, Rift Valley fever, Hantavirus) up to deadly hemorrhagic fevers (Lassa fever, Junin, Crimean Congo hemorrhagic fever, Hantavirus, Rift Valley fever).

Host organisms (e.g. us) are however not defenceless. Adaptive immunity would be too slow to protect from a first infectious encounter, but mammals can execute an immediate innate immune response enabled by germline-encoded factors specialized to rapid virus detection. A well-established example is given by the cytoplasmic pathogen recognition receptor RIG-I, an RNA helicase of the DExD/H type [2]. One of the best ligands for RIG-I is short doubled-stranded RNA (dsRNA) containing a blunt 5′ end with a triphosphate group, 5′ ppp dsRNA [3] (Figure 1a). Ligand-activated RIG-I is rapidly triggering a signalling chain which upregulates an antiviral innate immune response. 5′ ppp dsRNA structures similar to the ideal RIG-I ligand are formed by the genome ends of segmented NSVs (Figure 1b), but are not found on cellular RNA [3]. Thus, RIG-I seems well adapted to the genome of segmented NSVs, ensuring a specific and rapid immune reaction to this class of viruses.

In this opinion article, we will briefly outline how RIG-I-dependent ligand recognition and antiviral signalling work, how segmented NSVs are activating it, and share our thoughts on how these viruses are trying to escape detection and signalling by RIG-I.

RIG-I-mediated antiviral response

RIG-I is composed of an amino-terminal tandem of CARDs (caspase recruitment domains), a central RNA helicase domain, and a carboxy-terminal CTD (C-terminal domain) [4]. Ligand-mediated activation of RIG-I results in the binding of the adaptor protein MAVS (mitochondrial antiviral signalling) via polyubiquitin-mediated CARD–CARD interactions. After recruitment of further cofactors, the complex activates the transcription factors IRF-3/7 and NF-κB, which, in turn, initiate transcriptional activation of type I interferons (IFN-alpha/beta) and other proinflammatory cytokines [5]. Once secreted, IFNs bind to their cognate receptor on the cell surface to activate numerous ISGs (IFN-stimulated genes). Many ISGs encode antiviral restriction factors inhibiting different steps of virus replication such as entry, transcription, replication, translation, assembly or release from infected cells, thus slowing down or entirely blocking further viral spread [1,4–6].

Figure 1

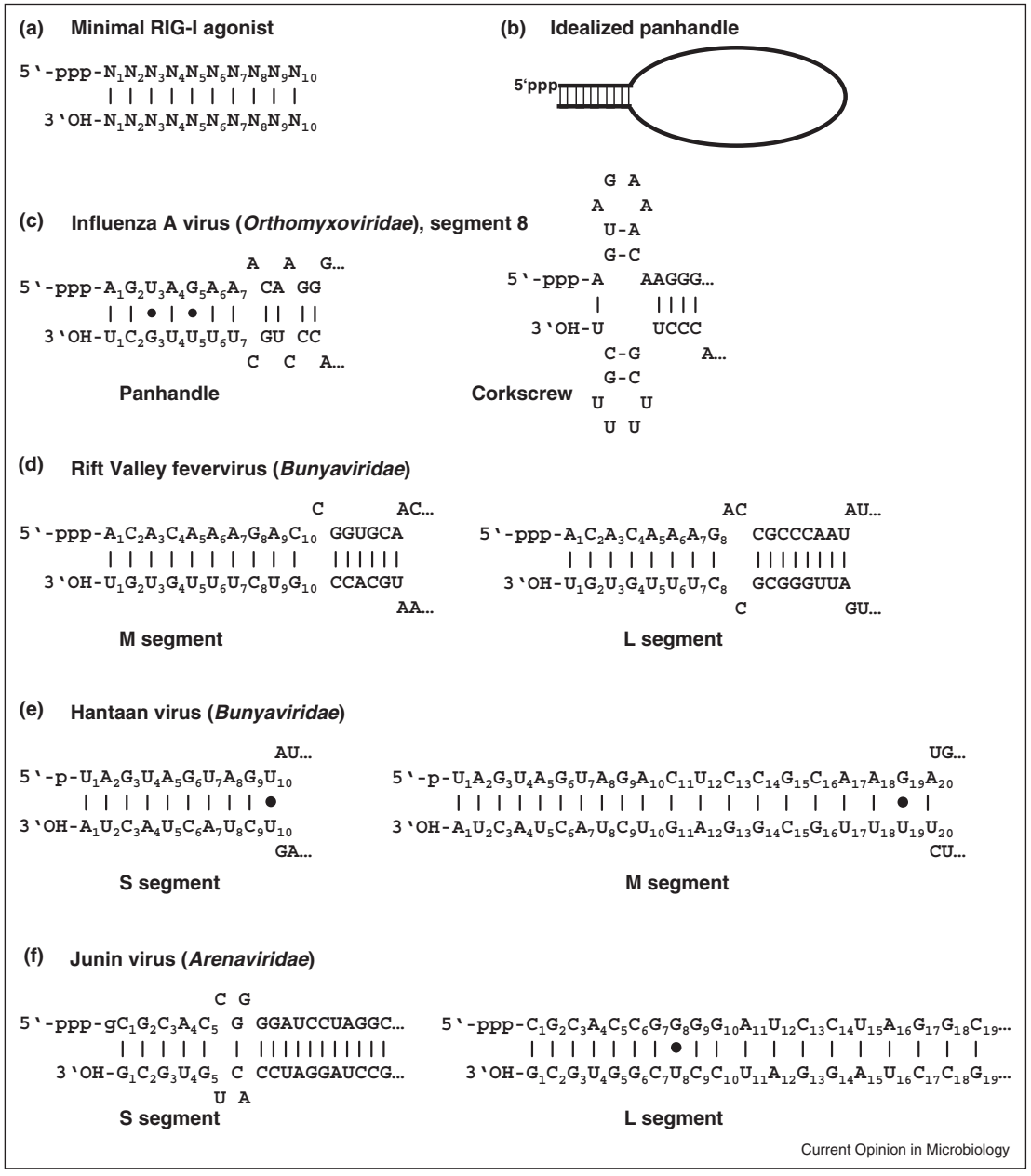

Synthetic and natural RNA structures relevant for RIG-I signalling. **(a)** Minimal RIG-I agonist as determined by RNA transfection experiments [7,10]. **(b)** Idealized structure of segmented negative-sense RNA genomes, with a large single-stranded coding region pseudocircularized by a double-stranded 'panhandle' promoter. (c)–(f) Predicted structures of viral panhandle regions. **(c)** Influenza A virus (H9N2) segment 8 (database entry AY790309), drawn as panhandle (left panel) or 'corkscrew' (right panel) [16,22]. **(d)** Rift Valley fever virus segments M (database entry DQ380206) and L (database entry DQ375403). **(e)** Hantaan virus segments S (database entry AF288644) and M (database entry KC344261). Note the monophosphate at the 5′ end. **(f)** Junin virus segments S (database entry NC_005081) and L (database entry NC_005080), both as corrected by Albariño *et al*. [24]. The unpaired nucleotide at the 5′ end found in a fraction of the S segment RNAs [24] is shown in lower case. In all subfigures, Watson-Crick basepairs are indicated by lines, and non-Watson-Crick basepairs [50] are indicated by dots. Sequences are in the viral sense orientation and nucleotides are numbered up to the first interruption of base pairing.

Activation of RIG-I by viral structures

In uninfected cells, RIG-I is present in an auto-inhibited conformation stabilized by internal interactions between the inner CARD (CARD2) and a part of the helicase domain, the Hel2i region [7,8,9••]. The CTD is flexibly exposed and thus available for scanning the cytosol for viral RNAs. Binding of 5′ ppp dsRNA to the CTD induces a massive conformational switch by disrupting

the Hel2i–CARD2 interaction, thereby clamping RIG-I around the RNA ligand and liberating the CARDs to interact with polyubiquitin and MAVS [4,6].

Besides 5′ ppp dsRNA of a minimal length of 10 bp [7,10], RIG-I responds to long dsRNA molecules of more than 200 bp (irrespective of the 5′ ends), to 3′-phosphorylated cleavage products of RNase L, and to poly-U/UC-rich ssRNA stretches [3,11–13]. Long dsRNA is not produced in a detectable amount during the course of NSV infection [14]. However, as outlined above, segmented NSVs form a RIG-I-critical 5′ ppp dsRNA region by base-pairing the terminal 5′ and 3′ non-translated regions of their genome (Figure 1c–f). This so-called 'panhandle' structure pseudo-circularizes the otherwise single-stranded RNA genome and serves as promoter for transcription and replication [15–17]. Moreover, at least for influenza viruses a 3′ untranslated ssRNA region of the genome activates RIG-I in a 5′ ppp independent fashion [18•].

In most of the RIG-I studies mentioned above, the structural characteristics of the ligands had been determined *in vitro* or by transfection of naked RNA into cells. Hence, the question was raised which of those structures are actually representing the natural ligands of RIG-I. Rehwinkel *et al.* [19] and Baum *et al.* [20] showed that full-length virus genomes and defective shortened RNAs arising during the course of the infection are indeed serving as RIG-I activators. Moreover, our group recently demonstrated that viral 5′ ppp dsRNA structures (i.e. the panhandle) can bind and activate RIG-I even when encapsidated by nucleoprotein [21••]. Thus, apparently, RIG-I is capable of recognizing RNAs at all stages of infection. It is activated by the panhandle on viral nucleocapsids in the immediate early phase, that is directly after they entered the cytoplasm [21••], but also by newly synthesized viral RNAs later in infection [19,20].

Inhibition of RIG-I by segmented NSVs

For all the evolutionary advantages of having a segmented genome, these viruses face a particular problem: with every additional piece of RNA they increase their load of RIG-I ligands. The extreme is represented by influenza viruses, which expose no less than eight 5′ ppp dsRNAs per infectious particle. Thus, strong and efficient anti-RIG-I measures are essential for these viruses to survive. The viral escape mechanisms act on many different levels (Figure 2). First of all, it might be no coincidence that influenza viruses and other orthomyxoviruses have evolved the unusual lifestyle of replicating in the nucleus. By this, they avoid constant exposure to cytoplasmic RIG-I, only passing the cytoplasm at the beginning and at the end of the replication cycle. Avoiding detection, in fact, represents an efficient way of RIG-I escape, since it is expected to demand less effort than blocking the amplified and diversified antiviral signalling events occurring further downstream. Influenza viruses exhibit also other features which could be interpreted as RIG-I escape. Firstly, the panhandle is not a perfect RIG-I ligand, but possesses mismatches and non-canonical base-pairs which weaken the dsRNA structure (see Figure 1c, left panel). Also, the nucleotide sequence of the orthomyxoviral panhandle enables the dsRNA panhandle to convert into a so-called 'hook' or 'corkscrew' by folding back the individual strands onto themselves [16,22] (see Figure 1c, right panel). The dsRNA-disrupting nucleotides and structural switches are known to regulate viral promoter activity, but it can be speculated they are disturbing RIG-I binding as well.

The panhandles of the less-segmented *Bunyaviridae* and *Arenaviridae* families often contain larger continuous double-stranded regions (see Figure 1d–f). However, some bunyavirus genera (Hantavirus and Nairovirus) are cleaving off the gamma and beta phosphates of the RIG-I-critical 5′ ppp group [23] (see Figure 1e), and some arenavirus genome ends can exhibit a single 5′ overhanging nucleotide [24] with the potential to disturb RIG-I function [17] (see Figure 1f).

It must be noted, however, that most of the viral panhandle modifications are apparently insufficient for a complete innate immune escape. While genomic RNAs isolated from particles of those bunyaviruses which cleave off the 5′ ppp do not activate RIG-I or antiviral signalling [23], the genomic RNAs of other bunyaviruses, influenza viruses, but also arenaviruses clearly activate RIG-I-dependent IFN induction if transfected into cells [23,25]. In the case of arenaviruses, this might be due to the fact that only a fraction of the RNAs actually seems to contain the unpaired 5′ nucleotide [24]. Moreover, RIG-I is most likely more flexible in its ligand requirements in vivo, a view which is supported by the observations that (i) not all nucleotides of the dsRNA helix are bound by amino acids of RIG-I [7,9••], (ii) bulges and 5′ overhangs of the 5′ ppp dsRNA can be tolerated by RIG-I to some extent [10,13], and (iii) RNAs other than 5′ ppp dsRNA can activate RIG-I [11,12,18•].

Independent of the 5′ end, dsRNA from a certain length on is a prototypical hallmark of virus infection and a strong inducer of innate immune responses. In the cytoplasm, not only RIG-I but also the sister helicase MDA5 and the RNA-binding antiviral kinase PKR are activated by dsRNA [4,6]. NSVs avoid formation of dsRNA hybrids between the viral genome and its complementary RNA species (antigenome and mRNA) [14], most probably due to the separate packaging of genome and antigenome into nucleocapsids. Moreover, influenza viruses use the cellular helicases UAP56 and URH49 to unwind any such dsRNA replication intermediates [26•].

Figure 2

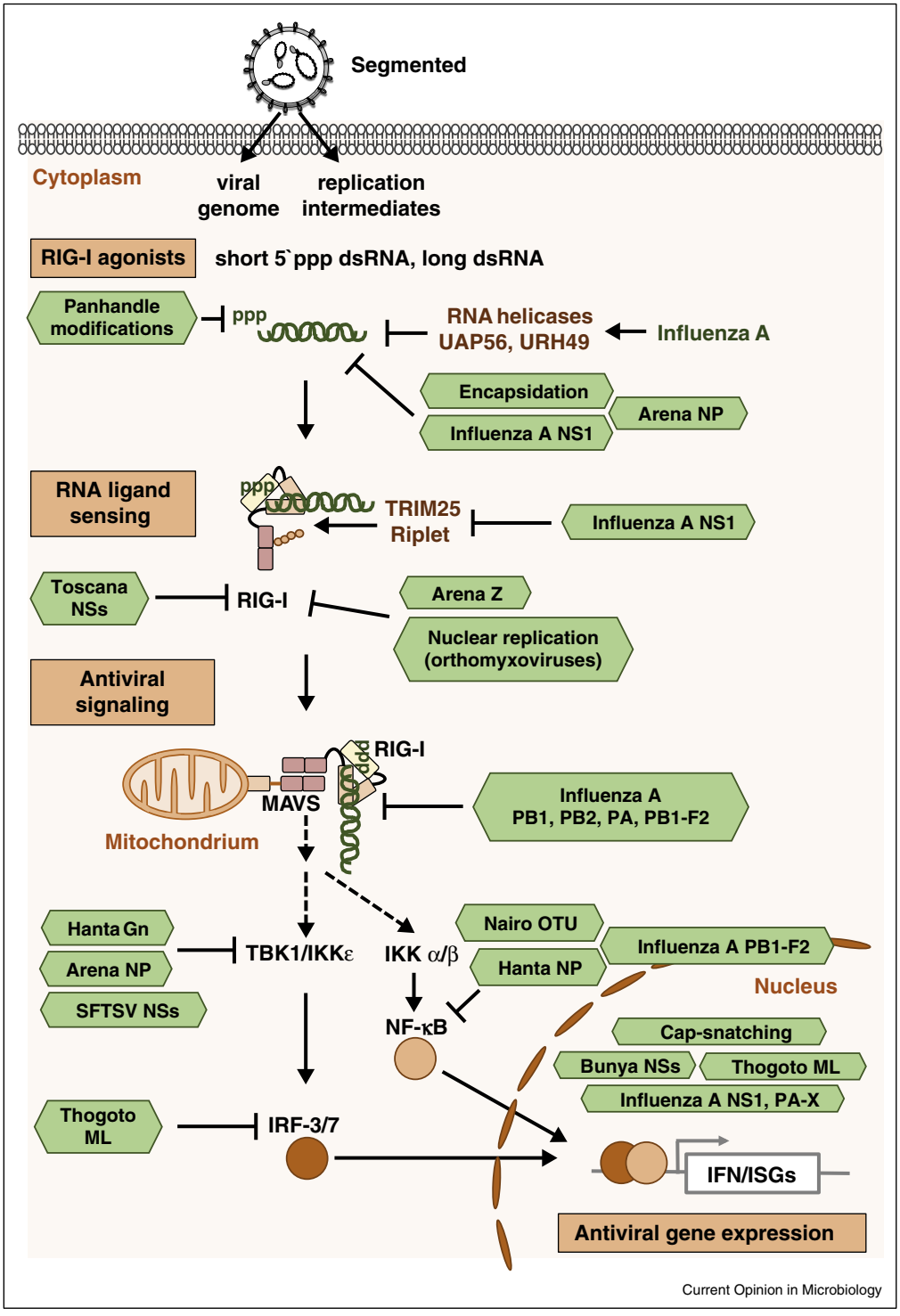

RIG-I antagonism by segmented negative-strand RNA viruses. Infection with segmented NSVs generates structures with the potential to act as agonists of RIG-I. The viruses have therefore evolved escape strategies (shown in green) which act on all levels of RIG-I signalling (shown in light red). For details see text. Abbreviations: Gn: glycoprotein (N-terminal), IFN: type I interferon, IKKε: Inhibitor of nuclear factor kappa-B kinase subunit epsilon, IRF-3/7: interferon regulatory factors 3/7, ISG: interferon stimulated gene, MAVS: mitochondrial antiviral signalling protein, ML: matrix protein long, NP: nucleoprotein, NS1: non-structural protein 1, NSs: non-structural protein encoded on the S segment, NSV: negative-strand RNA virus, OTU: ovarian tumour domain, PA: polymerase acidic, PB: polymerase basic, RIG-I: retinoic acid–inducible gene I, SFTSV: severe fever with thrombocytopenia syndrome virus (a bunyavirus), TBK1: TANK-binding kinase 1, 5′ ppp dsRNA: 5′ triphosphorylated double-stranded RNA, TRIM: tripartite motif, Z: Zink finger protein. Dotted arrows symbolize signalling factors which have been left out for the sake of simplicity.

The above-described strategies of disrupting RIG-I-critical panhandle features and of preventing formation of large dsRNA stretches could be considered as basic, 'passive' abilities of segmented NSVs against the antiviral IFN system. On top of this, there are several active mechanisms in place. First of all, it is interesting to note that all segmented NSV families (but not the non-segmented ones) are performing 'cap-snatching', that is, they cleave capped oligonucleotides from host cell mRNAs and use them as primers for viral transcription. The responsible endonuclease domain is embedded in the viral polymerase and likely contributes to the downmodulation of antiviral cell responses [1]. In fact, it was recently discovered that influenza viruses can express the endonuclease domain alone, by ribosomal frameshift, and that this protein (PA-X) strongly suppresses host cell gene expression [27••]. The influenza virus polymerase subunits (PB1, PB2 and PA) can also block IFN upregulation independent of cap-snatching, by binding to MAVS [28,29]. Prime example of a separate influenza virus factor dedicated to IFN antagonism is the nonstructural protein NS1, a truly multifunctional protein known to bind dsRNA, RIG-I and its regulatory ubiquitin ligases TRIM 25 and Riplet, and PKR, but also to inhibit host cell mRNA processing, transport, and translation in a strain-specific manner [1,30••]. Some influenza A virus strains express an additional protein, PB1-F2, which also downmodulates innate immune reactions [31–33]. A related orthomyxovirus, Thogoto virus, has evolved a different strategy. It encodes a splice variant of the viral matrix protein, ML, which blocks IFN induction by associating with IRF-7 and the general transcription factor IIB [34,35]. The three-segmented Bunyaviruses similarly express IFN antagonists, most prominently the nonstructural protein NSs. NSs proteins of different bunyavirus genera either bind and degrade RIG-I [36], degrade PKR [37,38], sequester TBK1 [39], or — in most cases — suppress host cell mRNA synthesis by dysregulating, sequestering, or degrading key factors of RNA polymerase II transcription [15,40,41]. Moreover for some Hantaviruses it was shown that the cytoplasmic tail of the glycoprotein Gn downregulates IFN induction by inhibiting the IRF-3 kinase TBK1 [42], and that the nucleoprotein inhibits the nuclear import of NF-κB [43]. Likewise, for the bunyavirus genus Nairovirus the ovarian tumour (OTU) domain of polymerase interferes with NF-κB activation by a de-ubiquitinylation/de-ISGylation activity [44]. Also in the case of arenaviruses several IFN antagonists were described, first of all the nucleoprotein which degrades viral dsRNA [45,46], and inhibits NF-kB and the IRF-3 kinase IKKε [47,48]. Moreover, the Z protein of several arenaviruses directly binds and inhibits RIG-I [49].

Thus, the evolutionary advantage of dividing a viral RNA genome into several, genetically semi-autonomous pieces comes at some costs. It has to be counterbalanced by strong and efficient anti-RIG-I strategies acting on all possible levels. Nonetheless, at late stages of infection the viral counter mechanisms can be overrun by accumulating erroneous replication products, eventually tipping the balance towards activation of antiviral and inflammatory responses. In the extreme case, a cytokine storm develops causing the severe symptoms typical for so many of these viruses.

Conflicts of interest

No conflicts of interest declared.

Acknowledgements

Work in our laboratories is supported by the Deutsche Forschungsgemeinschaft grants We 2616/7-1, SFB 593 and SFB 1021, by the Forschungsförderung gem. §2 Abs. 3 Kooperationsvertrag Universitätsklinikum Giessen und Marburg, and by the Leibniz Graduate School for Emerging Viral Diseases (EIDIS).

References and recommended reading

Papers of particular interest, published within the period of review, have been highlighted as:

- • of special interest
- •• of outstanding interest

1. Garcia-Sastre A: **Induction and evasion of type I interferon responses by influenza viruses**. *Virus Res* 2011, **162**:12-18.

2. Yoneyama M, Kikuchi M, Natsukawa T, Shinobu N, Imaizumi T, Miyagishi M, Taira K, Akira S, Fujita T: **The RNA helicase RIG-I has an essential function in double-stranded RNA-induced innate antiviral responses**. *Nat Immunol* 2004, **5**:730-737.

3. Schlee M: **Master sensors of pathogenic RNA — RIG-I like receptors**. *Immunobiology* 2013, **218**:1322-1335.

4. Ng CS, Kato H, Fujita T: **Recognition of viruses in the cytoplasm by RLRs and other helicases — how conformational changes, mitochondrial dynamics and ubiquitination control innate immune responses**. *Int Immunol* 2012, **24**:739-749.

5. Belgnaoui SM, Paz S, Hiscott J: **Orchestrating the interferon antiviral response through the mitochondrial antiviral signaling (MAVS) adapter**. *Curr Opin Immunol* 2011, **23**:564-572.

6. Goubau D, Deddouche S, Reis ESC: **Cytosolic sensing of viruses**. *Immunity* 2013, **38**:855-869.

7. Kohlway A, Luo D, Rawling DC, Ding SC, Pyle AM: **Defining the functional determinants for RNA surveillance by RIG-I**. *EMBO Rep* 2013, **14**:772-779.

8. Kolakofsky D, Kowalinski E, Cusack S: **A structure-based model of RIG-I activation**. *RNA* 2012, **18**:2118-2127.

9. •• Kowalinski E, Lunardi T, McCarthy AA, Louber J, Brunel J, Grigorov B, Gerlier D, Cusack S: **Structural basis for the activation of innate immune pattern-recognition receptor RIG-I by viral RNA**. *Cell* 2011, **147**:423-435.

References [7,8,9••] have solved the atomic structure of RIG-I and its 5′ ppp dsRNA ligand, and set up a model of RIG-I activation involving massive conformational rearrangements.

10. Schmidt A, Schwerd T, Hamm W, Hellmuth JC, Cui S, Wenzel M, Hoffmann FS, Michallet MC, Besch R, Hopfner KP *et al.*: **5′-Triphosphate RNA requires base-paired structures to activate antiviral signaling via RIG-I**. *Proc Natl Acad Sci U S A* 2009, **106**:12067-12072.

11. Malathi K, Saito T, Crochet N, Barton DJ, Gale M Jr, Silverman RH: **RNase L releases a small RNA from HCV RNA that refolds into a potent PAMP**. *RNA* 2010, **16**:2108-2119.

12. Saito T, Owen DM, Jiang F, Marcotrigiano J, Gale M Jr: **Innate immunity induced by composition-dependent RIG-I recognition of hepatitis C virus RNA**. *Nature* 2008, **454**:523-527.

13. Schlee M, Roth A, Hornung V, Hagmann CA, Wimmenauer V, Barchet W, Coch C, Janke M, Mihailovic A, Wardle G *et al.*: **Recognition of 5′ triphosphate by RIG-I helicase requires short blunt double-stranded RNA as contained in panhandle of negative-strand virus**. *Immunity* 2009, **31**:25-34.

14. Weber F, Wagner V, Rasmussen SB, Hartmann R, Paludan SR: **Double-stranded RNA is produced by positive-strand RNA viruses and DNA viruses but not in detectable amounts by negative-strand RNA viruses**. *J Virol* 2006, **80**:5059-5064.

15. Elliott RM, Weber F: **Bunyaviruses and the type I interferon system**. *Viruses* 2009, **1**:1003-1021.

16. Flick R, Neumann G, Hoffmann E, Neumeier E, Hobom G: **Promoter elements in the influenza vRNA terminal structure**. *RNA* 1996, **2**:1046-1057.

17. Marq JB, Hausmann S, Veillard N, Kolakofsky D, Garcin D: **Short double-stranded RNAs with an overhanging 5′ ppp-nucleotide, as found in arenavirus genomes, act as RIG-I decoys**. *J Biol Chem* 2011, **286**:6108-6116.

18. • Davis WG, Bowzard JB, Sharma SD, Wiens ME, Ranjan P, Gangappa S, Stuchlik O, Pohl J, Donis RO, Katz JM *et al.*: **The 3′ untranslated regions of influenza genomic sequences are 5′ PPP-independent ligands for RIG-I**. *PLoS One* 2012, **7**:e32661.

These authors identified influenza virus RNA structures other than the 5′-ppp dsRNA panhandle that can activate RIG-I.

19. Rehwinkel J, Tan CP, Goubau D, Schulz O, Pichlmair A, Bier K, Robb N, Vreede F, Barclay W, Fodor E *et al.*: **RIG-I detects viral genomic RNA during negative-strand RNA virus infection**. *Cell* 2010, **140**:397-408.

20. Baum A, Sachidanandam R, Garcia-Sastre A: **Preference of RIG-I for short viral RNA molecules in infected cells revealed by next-generation sequencing**. *Proc Natl Acad Sci U S A* 2010, **107**:16303-16308.

21. •• Weber M, Gawanbacht A, Habjan M, Rang A, Borner C, Schmidt AM, Veitinger S, Jacob R, Devignot S, Kochs G *et al.*: **Incoming RNA virus nucleocapsids containing a 5′-triphosphorylated genome activate RIG-I and antiviral signaling**. *Cell Host Microbe* 2013, **13**:336-346.

RIG-I is able to recognize 5′ ppp panhandle dsRNA even if packaged in nucleocapsids.

22. Weber F, Haller O, Kochs G: **Conserved vRNA end sequences of Thogoto-orthomyxovirus suggest a new panhandle structure**. *Arch Virol* 1997, **142**:1029-1033.

23. Habjan M, Andersson I, Klingstrom J, Schumann M, Martin A, Zimmermann P, Wagner V, Pichlmair A, Schneider U, Muhlberger E *et al.*: **Processing of genome 5′ termini as a strategy of negative-strand RNA viruses to avoid RIG-I-dependent interferon induction**. *PLoS One* 2008, **3**:e2032.

24. Albarino CG, Bergeron E, Erickson BR, Khristova ML, Rollin PE, Nichol ST: **Efficient reverse genetics generation of infectious Junin viruses differing in glycoprotein processing**. *J Virol* 2009, **83**:5606-5614.

25. Pichlmair A, Schulz O, Tan CP, Naslund TI, Liljestrom P, Weber F, Reis e Sousa C: **RIG-I-mediated antiviral responses to single-stranded RNA bearing 5′-phosphates**. *Science* 2006, **314**:997-1001.

26. • Wisskirchen C, Ludersdorfer TH, Muller DA, Moritz E, Pavlovic J: **The cellular RNA helicase UAP56 is required for prevention of double-stranded RNA formation during influenza A virus infection**. *J Virol* 2011, **85**:8646-8655.

Influenza virus recruits cellular helicases to unwind dsRNA structures arising during genome replication.

27. •• Jagger BW, Wise HM, Kash JC, Walters KA, Wills NM, Xiao YL, Dunfee RL, Schwartzman LM, Ozinsky A, Bell GL *et al.*: **An overlapping protein-coding region in influenza A virus segment 3 modulates the host response**. *Science* 2012, **337**:199-204.

The authors have discovered that influenza A virus expresses the endonuclease domain independent of the polymerase context to suppress host cell gene expression.

28. Graef KM, Vreede FT, Lau YF, McCall AW, Carr SM, Subbarao K, Fodor E: **The PB2 subunit of the influenza virus RNA polymerase affects virulence by interacting with the mitochondrial antiviral signaling protein and inhibiting expression of beta interferon**. *J Virol* 2010, **84**:8433-8445.

29. Iwai A, Shiozaki T, Kawai T, Akira S, Kawaoka Y, Takada A, Kida H, Miyazaki T: **Influenza A virus polymerase inhibits type I interferon induction by binding to interferon beta promoter stimulator 1**. *J Biol Chem* 2010, **285**:32064-32074.

30. •• Rajsbaum R, Albrecht RA, Wang MK, Maharaj NP, Versteeg GA, Nistal-Villan E, Garcia-Sastre A, Gack MU: **Species-specific inhibition of RIG-I ubiquitination and IFN induction by the influenza A virus NS1 protein**. *PLoS Pathog* 2012, **8**:e1003059.

This paper illustrates the astonishing flexibility by which influenza virus NS1 manages to inhibit activatory RIG-I ubiquitination in various host species.

31. Dudek SE, Wixler L, Nordhoff C, Nordmann A, Anhlan D, Wixler V, Ludwig S: **The influenza virus PB1-F2 protein has interferon antagonistic activity**. *Biol Chem* 2011, **392**:1135-1144.

32. Reis AL, McCauley JW: **The influenza virus protein PB1-F2 interacts with IKKbeta and modulates NF-kappaB signalling**. *PLoS One* 2013, **8**:e63852.

33. Varga ZT, Ramos I, Hai R, Schmolke M, Garcia-Sastre A, Fernandez-Sesma A, Palese P: **The influenza virus protein PB1-F2 inhibits the induction of type I interferon at the level of the MAVS adaptor protein**. *PLoS Pathog* 2011, **7**:e1002067.

34. Buettner N, Vogt C, Martinez-Sobrido L, Weber F, Waibler Z, Kochs G: **Thogoto virus ML protein is a potent inhibitor of the interferon regulatory factor-7 transcription factor**. *J Gen Virol* 2010, **91**:220-227.

35. Vogt C, Preuss E, Mayer D, Weber F, Schwemmle M, Kochs G: **The interferon antagonist ML protein of Thogoto virus targets general transcription factor IIB**. *J Virol* 2008, **82**:11446-11453.

36. Gori-Savellini G, Valentini M, Cusi MG: **Toscana virus NSs protein inhibits the induction of type I interferon by interacting with RIG-I**. *J Virol* 2013, **87**:6660-6667.

37. Ikegami T, Narayanan K, Won S, Kamitani W, Peters CJ, Makino S: **Rift Valley fever virus NSs protein promotes post-transcriptional downregulation of protein kinase PKR and inhibits eIF2alpha phosphorylation**. *PLoS Pathog* 2009, **5**:e1000287.

38. Habjan M, Pichlmair A, Elliott RM, Overby AK, Glatter T, Gstaiger M, Superti-Furga G, Unger H, Weber F: **NSs protein of rift valley fever virus induces the specific degradation of the double-stranded RNA-dependent protein kinase**. *J Virol* 2009, **83**:4365-4375.

39. Qu B, Qi X, Wu X, Liang M, Li C, Cardona CJ, Xu W, Tang F, Li Z, Wu B *et al.*: **Suppression of the interferon and NF-kappaB responses by severe fever with thrombocytopenia syndrome virus**. *J Virol* 2012, **86**:8388-8401.

40. Kainulainen M, Habjan M, Hubel P, Busch L, Lau S, Colinge J, Superti-Furga G, Pichlmair A, Weber F: **Virulence factor NSs of rift valley fever virus recruits the F-box protein FBXO3 to degrade subunit p62 of general transcription factor TFIIH**. *J Virol* 2014, **88**:3464-3473.

41. Verbruggen P, Ruf M, Blakqori G, Overby AK, Heidemann M, Eick D, Weber F: **Interferon antagonist NSs of La Crosse virus triggers a DNA damage response-like degradation of transcribing RNA polymerase II**. *J Biol Chem* 2011, **286**:3681-3692.

42. Matthys VS, Cimica V, Dalrymple NA, Glennon NB, Bianco C, Mackow ER: **Hantavirus GnT elements mediate TRAF3 binding and inhibit RIG-I/TBK1-directed beta interferon transcription by blocking IRF3 phosphorylation**. *J Virol* 2014, **88**:2246-2259.

43. Taylor SL, Frias-Staheli N, Garcia-Sastre A, Schmaljohn CS: **Hantaan virus nucleocapsid protein binds to importin alpha proteins and inhibits tumor necrosis factor alpha-induced activation of nuclear factor kappa B**. *J Virol* 2009, **83**:1271-1279.

44. Frias-Staheli N, Giannakopoulos NV, Kikkert M, Taylor SL, Bridgen A, Paragas J, Richt JA, Rowland RR, Schmaljohn CS, Lenschow DJ *et al.*: **Ovarian tumor domain-containing viral**

proteases evade ubiquitin-dependent and ISG15-dependent innate immune responses. *Cell Host Microbe* 2007, **2**:404-416.

45. Hastie KM, Kimberlin CR, Zandonatti MA, MacRae IJ, Saphire EO: **Structure of the Lassa virus nucleoprotein reveals a dsRNA-specific 3′ to 5′ exonuclease activity essential for immune suppression**. *Proc Natl Acad Sci U S A* 2011, **108**:2396-2401.

46. Qi X, Lan S, Wang W, Schelde LM, Dong H, Wallat GD, Ly H, Liang Y, Dong C: **Cap binding and immune evasion revealed by Lassa nucleoprotein structure**. *Nature* 2010, **468**:779-783.

47. Pythoud C, Rodrigo WW, Pasqual G, Rothenberger S, Martinez-Sobrido L, de la Torre JC, Kunz S: **Arenavirus nucleoprotein targets interferon regulatory factor-activating kinase IKKepsilon**. *J Virol* 2012, **86**:7728-7738.

48. Rodrigo WW, Ortiz-Riano E, Pythoud C, Kunz S, de la Torre JC, Martinez-Sobrido L: **Arenavirus nucleoproteins prevent activation of nuclear factor kappa B**. *J Virol* 2012, **86**:8185-8197.

49. Fan L, Briese T, Lipkin WI: **Z proteins of New World arenaviruses bind RIG-I and interfere with type I interferon induction**. *J Virol* 2010, **84**:1785-1791.

50. Baeyens KJ, De Bondt HL, Holbrook SR: **Structure of an RNA double helix including uracil-uracil base pairs in an internal loop**. *Nat Struct Biol* 1995, **2**:56-62.

5. References

1. Albarino CG, Bird BH, Nichol ST (2007) A shared transcription termination signal on negative and ambisense RNA genome segments of Rift Valley fever, sandfly fever Sicilian, and Toscana viruses. J Virol 81:5246-5256
2. Anderson E, Cole JL (2008) Domain stabilities in protein kinase R (PKR): evidence for weak interdomain interactions. Biochemistry 47:4887-4897
3. Ariza A, Tanner SJ, Walter CT, Dent KC, Shepherd DA, Wu W, Matthews SV, Hiscox JA, Green TJ, Luo M, Elliott RM, Fooks AR, Ashcroft AE, Stonehouse NJ, Ranson NA, Barr JN, Edwards TA (2013) Nucleocapsid protein structures from orthobunyaviruses reveal insight into ribonucleoprotein architecture and RNA polymerization. Nucleic Acids Res 41:5912-5926
4. Barber MR, Aldridge JR, Jr., Webster RG, Magor KE (2010) Association of RIG-I with innate immunity of ducks to influenza. Proc Natl Acad Sci U S A 107:5913-5918
5. Baum A, Sachidanandam R, Garcia-Sastre A (2010) Preference of RIG-I for short viral RNA molecules in infected cells revealed by next-generation sequencing. Proceedings of the National Academy of Sciences of the United States of America 107:16303-16308
6. Bente DA, Forrester NL, Watts DM, McAuley AJ, Whitehouse CA, Bray M (2013) Crimean-Congo hemorrhagic fever: history, epidemiology, pathogenesis, clinical syndrome and genetic diversity. Antiviral Res 100:159-189
7. Bevilacqua PC, Cech TR (1996) Minor-groove recognition of double-stranded RNA by the double-stranded RNA-binding domain from the RNA-activated protein kinase PKR. Biochemistry 35:9983-9994
8. Bevilacqua PC, George CX, Samuel CE, Cech TR (1998) Binding of the protein kinase PKR to RNAs with secondary structure defects: role of the tandem A-G mismatch and noncontiguous helixes. Biochemistry 37:6303-6316
9. Binder M, Eberle F, Seitz S, Mucke N, Huber CM, Kiani N, Kaderali L, Lohmann V, Dalpke A, Bartenschlager R (2011) Molecular mechanism of signal perception and integration by the innate immune sensor retinoic acid-inducible gene-I (RIG-I). J Biol Chem 286:27278-27287
10. Bortz E, Westera L, Maamary J, Steel J, Albrecht RA, Manicassamy B, Chase G, Martinez-Sobrido L, Schwemmle M, Garcia-Sastre A (2011) Host- and strain-specific regulation of influenza virus polymerase activity by interacting cellular proteins. mBio 2
11. Bouloy M (1991) Bunyaviridae: genome organization and replication strategies. Adv Virus Res 40:235-275
12. Bowie AG, Unterholzner L (2008) Viral evasion and subversion of pattern-recognition receptor signalling. Nat Rev Immunol 8:911-922
13. Carroll K, Elroy-Stein O, Moss B, Jagus R (1993) Recombinant vaccinia virus K3L gene product prevents activation of double-stranded RNA-dependent, initiation factor 2 alpha-specific protein kinase. J Biol Chem 268:12837-12842
14. Cauldwell AV, Moncorge O, Barclay WS (2013) Unstable polymerase-nucleoprotein interaction is not responsible for avian influenza virus polymerase restriction in human cells. J Virol 87:1278-1284
15. Cauldwell AV, Long JS, Moncorge O, Barclay WS (2014) Viral determinants of influenza A virus host range. J Gen Virol 95:1193-1210
16. Clemens MJ (1997) PKR--a protein kinase regulated by double-stranded RNA. Int J Biochem Cell Biol 29:945-949
17. Cole JL (2007) Activation of PKR: an open and shut case? Trends Biochem Sci 32:57-62
18. Dabo S, Meurs EF (2012) dsRNA-dependent protein kinase PKR and its role in stress, signaling and HCV infection. Viruses 4:2598-2635
19. Dauber B, Martinez-Sobrido L, Schneider J, Hai R, Waibler Z, Kalinke U, Garcia-Sastre A, Wolff T (2009) Influenza B virus ribonucleoprotein is a potent activator of the antiviral kinase PKR. PLoS Pathog 5:e1000473
20. Dauber B, Wolff T (2009) Activation of the Antiviral Kinase PKR and Viral Countermeasures. Viruses 1:523-544

21. Davis WG, Bowzard JB, Sharma SD, Wiens ME, Ranjan P, Gangappa S, Stuchlik O, Pohl J, Donis RO, Katz JM, Cameron CE, Fujita T, Sambhara S (2012) The 3' untranslated regions of influenza genomic sequences are 5'PPP-independent ligands for RIG-I. PLoS One 7:e32661
22. Dey M, Cao C, Dar AC, Tamura T, Ozato K, Sicheri F, Dever TE (2005) Mechanistic link between PKR dimerization, autophosphorylation, and eIF2alpha substrate recognition. Cell 122:901-913
23. Dixit E, Boulant S, Zhang Y, Lee AS, Odendall C, Shum B, Hacohen N, Chen ZJ, Whelan SP, Fransen M, Nibert ML, Superti-Furga G, Kagan JC (2010) Peroxisomes are signaling platforms for antiviral innate immunity. Cell. 2010 Elsevier Inc, United States, pp 668-681
24. Dudek SE, Wixler L, Nordhoff C, Nordmann A, Anhlan D, Wixler V, Ludwig S (2011) The influenza virus PB1-F2 protein has interferon antagonistic activity. Biol Chem 392:1135-1144
25. Dzananovic E, Patel TR, Deo S, McEleney K, Stetefeld J, McKenna SA (2013) Recognition of viral RNA stem-loops by the tandem double-stranded RNA binding domains of PKR. Rna 19:333-344
26. Elliott RM, Weber F (2009) Bunyaviruses and the type I interferon system. Viruses 1:1003-1021
27. Flick R, Neumann G, Hoffmann E, Neumeier E, Hobom G (1996) Promoter elements in the influenza vRNA terminal structure. Rna 2:1046-1057
28. Foeglein A, Loucaides EM, Mura M, Wise HM, Barclay WS, Digard P (2011) Influence of PB2 host-range determinants on the intranuclear mobility of the influenza A virus polymerase. J Gen Virol 92:1650-1661
29. Gack MU, Shin YC, Joo CH, Urano T, Liang C, Sun L, Takeuchi O, Akira S, Chen Z, Inoue S, Jung JU (2007) TRIM25 RING-finger E3 ubiquitin ligase is essential for RIG-I-mediated antiviral activity. Nature 446:916-920
30. Garcia-Sastre A (2011) Induction and evasion of type I interferon responses by influenza viruses. Virus research 162:12-18
31. Garcin D, Lezzi M, Dobbs M, Elliott RM, Schmaljohn C, Kang CY, Kolakofsky D (1995) The 5' ends of Hantaan virus (Bunyaviridae) RNAs suggest a prime-and-realign mechanism for the initiation of RNA synthesis. J Virol 69:5754-5762
32. Goubau D, Deddouche S, Reis ESC (2013) Cytosolic sensing of viruses. Immunity 38:855-869
33. Goubau D, Schlee M, Deddouche S, Pruijssers AJ, Zillinger T, Goldeck M, Schuberth C, Van der Veen AG, Fujimura T, Rehwinkel J, Iskarpatyoti JA, Barchet W, Ludwig J, Dermody TS, Hartmann G, Reis ESC (2014) Antiviral immunity via RIG-I-mediated recognition of RNA bearing 5'-diphosphates. Nature
34. Graef KM, Vreede FT, Lau YF, McCall AW, Carr SM, Subbarao K, Fodor E (2010) The PB2 subunit of the influenza virus RNA polymerase affects virulence by interacting with the mitochondrial antiviral signaling protein and inhibiting expression of beta interferon. J Virol 84:8433-8445
35. Grant A, Seregin A, Huang C, Kolokoltsova O, Brasier A, Peters C, Paessler S (2012) Junin virus pathogenesis and virus replication. Viruses 4:2317-2339
36. Habjan M, Andersson I, Klingstrom J, Schumann M, Martin A, Zimmermann P, Wagner V, Pichlmair A, Schneider U, Muhlberger E, Mirazimi A, Weber F (2008) Processing of genome 5' termini as a strategy of negative-strand RNA viruses to avoid RIG-I-dependent interferon induction. PloS one 3:e2032
37. Habjan M, Pichlmair A, Elliott RM, Overby AK, Glatter T, Gstaiger M, Superti-Furga G, Unger H, Weber F (2009) NSs protein of rift valley fever virus induces the specific degradation of the double-stranded RNA-dependent protein kinase. J Virol 83:4365-4375
38. Hare D, Mossman KL (2013) Novel paradigms of innate immune sensing of viral infections. Cytokine 63:219-224
39. Hastie KM, Kimberlin CR, Zandonatti MA, MacRae IJ, Saphire EO (2011) Structure of the Lassa virus nucleoprotein reveals a dsRNA-specific 3' to 5' exonuclease activity essential for immune suppression. Proc Natl Acad Sci U S A 108:2396-2401
40. Hastie KM, Liu T, Li S, King LB, Ngo N, Zandonatti MA, Woods VL, Jr., de la Torre JC, Saphire EO (2011) Crystal structure of the Lassa virus nucleoprotein-RNA complex reveals a gating mechanism for RNA binding. Proc Natl Acad Sci U S A 108:19365-19370

41. Hastie KM, Bale S, Kimberlin CR, Saphire EO (2012) Hiding the evidence: two strategies for innate immune evasion by hemorrhagic fever viruses. Current opinion in virology 2:151-156
42. Hatada E, Fukuda R (1992) Binding of influenza A virus NS1 protein to dsRNA in vitro. J Gen Virol 73 (Pt 12):3325-3329
43. Heinicke LA, Wong CJ, Lary J, Nallagatla SR, Diegelman-Parente A, Zheng X, Cole JL, Bevilacqua PC (2009) RNA dimerization promotes PKR dimerization and activation. J Mol Biol 390:319-338
44. Hertzog PJ, Williams BR (2013) Fine tuning type I interferon responses. Cytokine Growth Factor Rev 24:217-225
45. Horner SM, Liu HM, Park HS, Briley J, Gale M, Jr. (2011) Mitochondrial-associated endoplasmic reticulum membranes (MAM) form innate immune synapses and are targeted by hepatitis C virus. Proc Natl Acad Sci U S A 108:14590-14595
46. Hornung V, Ellegast J, Kim S, Brzozka K, Jung A, Kato H, Poeck H, Akira S, Conzelmann KK, Schlee M, Endres S, Hartmann G (2006) 5'-Triphosphate RNA is the ligand for RIG-I. Science 314:994-997
47. Hou F, Sun L, Zheng H, Skaug B, Jiang QX, Chen ZJ (2011) MAVS forms functional prion-like aggregates to activate and propagate antiviral innate immune response. Cell 146:448-461
48. Hsu MT, Parvin JD, Gupta S, Krystal M, Palese P (1987) Genomic RNAs of influenza viruses are held in a circular conformation in virions and in infected cells by a terminal panhandle. Proc Natl Acad Sci U S A 84:8140-8144
49. Hutchinson EC, Charles PD, Hester SS, Thomas B, Trudgian D, Martinez-Alonso M, Fodor E (2014) Conserved and host-specific features of influenza virion architecture. Nat Commun 5:4816
50. Ikegami T, Narayanan K, Won S, Kamitani W, Peters CJ, Makino S (2009) Rift Valley fever virus NSs protein promotes post-transcriptional downregulation of protein kinase PKR and inhibits eIF2alpha phosphorylation. PLoS Pathog 5:e1000287
51. Ikegami T, Makino S (2011) The pathogenesis of Rift Valley fever. Viruses 3:493-519
52. Ivashkiv LB, Donlin LT (2014) Regulation of type I interferon responses. Nat Rev Immunol 14:36-49
53. Iwai A, Shiozaki T, Kawai T, Akira S, Kawaoka Y, Takada A, Kida H, Miyazaki T (2010) Influenza A virus polymerase inhibits type I interferon induction by binding to interferon beta promoter stimulator 1. J Biol Chem 285:32064-32074
54. Iwamura T, Yoneyama M, Yamaguchi K, Suhara W, Mori W, Shiota K, Okabe Y, Namiki H, Fujita T (2001) Induction of IRF-3/-7 kinase and NF-kappaB in response to double-stranded RNA and virus infection: common and unique pathways. Genes Cells 6:375-388
55. Jacobs JL, Coyne CB (2013) Mechanisms of MAVS regulation at the mitochondrial membrane. J Mol Biol 425:5009-5019
56. Jiang X, Kinch LN, Brautigam CA, Chen X, Du F, Grishin NV, Chen ZJ (2012) Ubiquitin-induced oligomerization of the RNA sensors RIG-I and MDA5 activates antiviral innate immune response. Immunity 36:959-973
57. Kageyama M, Takahasi K, Narita R, Hirai R, Yoneyama M, Kato H, Fujita T (2011) 55 Amino acid linker between helicase and carboxyl terminal domains of RIG-I functions as a critical repression domain and determines inter-domain conformation. Biochem Biophys Res Commun 415:75-81
58. Kato H, Takeuchi O, Mikamo-Satoh E, Hirai R, Kawai T, Matsushita K, Hiiragi A, Dermody TS, Fujita T, Akira S (2008) Length-dependent recognition of double-stranded ribonucleic acids by retinoic acid-inducible gene-I and melanoma differentiation-associated gene 5. J Exp Med 205:1601-1610
59. Killip MJ, Smith M, Jackson D, Randall RE (2014) Activation of the interferon induction cascade by influenza a viruses requires viral RNA synthesis and nuclear export. J Virol 88:3942-3952
60. Kohlway A, Luo D, Rawling DC, Ding SC, Pyle AM (2013) Defining the functional determinants for RNA surveillance by RIG-I. EMBO reports 14:772-779
61. Kok KH, Lui PY, Ng MH, Siu KL, Au SW, Jin DY (2011) The double-stranded RNA-binding protein PACT functions as a cellular activator of RIG-I to facilitate innate antiviral response. Cell Host Microbe 9:299-309

62. Kolakofsky D, Kowalinski E, Cusack S (2012) A structure-based model of RIG-I activation. RNA 18:2118-2127
63. Koma T, Huang C, Kolokoltsova OA, Brasier AR, Paessler S (2013) Innate immune response to arenaviral infection: a focus on the highly pathogenic New World hemorrhagic arenaviruses. J Mol Biol 425:4893-4903
64. Kowalinski E, Lunardi T, McCarthy AA, Louber J, Brunel J, Grigorov B, Gerlier D, Cusack S (2011) Structural basis for the activation of innate immune pattern-recognition receptor RIG-I by viral RNA. Cell 147:423-435
65. Kowalinski E, Lunardi T, McCarthy AA, Louber J, Brunel J, Grigorov B, Gerlier D, Cusack S (2011) Structural Basis for the Activation of Innate Immune Pattern-Recognition Receptor RIG-I by Viral RNA. Cell. 2011 Elsevier Inc, United States, pp 423-435
66. Labadie K, Dos Santos Afonso E, Rameix-Welti MA, van der Werf S, Naffakh N (2007) Host-range determinants on the PB2 protein of influenza A viruses control the interaction between the viral polymerase and nucleoprotein in human cells. Virology 362:271-282
67. Lemaire PA, Tessmer I, Craig R, Erie DA, Cole JL (2006) Unactivated PKR exists in an open conformation capable of binding nucleotides. Biochemistry 45:9074-9084
68. Lennartz F, Hoenen T, Lehmann M, Groseth A, Garten W (2013) The role of oligomerization for the biological functions of the arenavirus nucleoprotein. Arch Virol 158:1895-1905
69. Li W, Chen H, Sutton T, Obadan A, Perez DR (2014) Interactions between the influenza A virus RNA polymerase components and retinoic acid-inducible gene I. J Virol 88:10432-10447
70. Loo YM, Gale M, Jr. (2011) Immune signaling by RIG-I-like receptors. Immunity 34:680-692
71. Luo D, Ding SC, Vela A, Kohlway A, Lindenbach BD, Pyle AM (2011) Structural Insights into RNA Recognition by RIG-I. Cell. 2011 Elsevier Inc, United States, pp 409-422
72. Luo D, Ding SC, Vela A, Kohlway A, Lindenbach BD, Pyle AM (2011) Structural insights into RNA recognition by RIG-I. Cell 147:409-422
73. Malathi K, Dong B, Gale M, Jr., Silverman RH (2007) Small self-RNA generated by RNase L amplifies antiviral innate immunity. Nature, England, pp 816-819
74. Manz B, Schwemmle M, Brunotte L (2013) Adaptation of avian influenza A virus polymerase in mammals to overcome the host species barrier. Journal of virology 87:7200-7209
75. Marq JB, Kolakofsky D, Garcin D (2010) Unpaired 5' ppp-nucleotides, as found in arenavirus double-stranded RNA panhandles, are not recognized by RIG-I. J Biol Chem 285:18208-18216
76. Marq JB, Hausmann S, Veillard N, Kolakofsky D, Garcin D (2011) Short double-stranded RNAs with an overhanging 5' ppp-nucleotide, as found in arenavirus genomes, act as RIG-I decoys. J Biol Chem 286:6108-6116
77. Martinez-Sobrido L, Zuniga EI, Rosario D, Garcia-Sastre A, de la Torre JC (2006) Inhibition of the type I interferon response by the nucleoprotein of the prototypic arenavirus lymphocytic choriomeningitis virus. J Virol 80:9192-9199
78. Martinez-Sobrido L, Giannakas P, Cubitt B, Garcia-Sastre A, de la Torre JC (2007) Differential inhibition of type I interferon induction by arenavirus nucleoproteins. J Virol 81:12696-12703
79. McCormick JB, King IJ, Webb PA, Johnson KM, O'Sullivan R, Smith ES, Trippel S, Tong TC (1987) A case-control study of the clinical diagnosis and course of Lassa fever. J Infect Dis 155:445-455
80. Mehle A, Doudna JA (2008) An inhibitory activity in human cells restricts the function of an avian-like influenza virus polymerase. Cell host & microbe 4:111-122
81. Miyashita M, Oshiumi H, Matsumoto M, Seya T (2011) DDX60, a DEXD/H box helicase, is a novel antiviral factor promoting RIG-I-like receptor-mediated signaling. Mol Cell Biol 31:3802-3819
82. Moeller A, Kirchdoerfer RN, Potter CS, Carragher B, Wilson IA (2012) Organization of the influenza virus replication machinery. Science (New York, NY) 338:1631-1634
83. Moy RH, Cole BS, Yasunaga A, Gold B, Shankarling G, Varble A, Molleston JM, tenOever BR, Lynch KW, Cherry S (2014) Stem-loop recognition by DDX17 facilitates miRNA processing and antiviral defense. Cell 158:764-777

84. Nallagatla SR, Hwang J, Toroney R, Zheng X, Cameron CE, Bevilacqua PC (2007) 5'-triphosphate-dependent activation of PKR by RNAs with short stem-loops. Science 318:1455-1458
85. Onomoto K, Jogi M, Yoo JS, Narita R, Morimoto S, Takemura A, Sambhara S, Kawaguchi A, Osari S, Nagata K, Matsumiya T, Namiki H, Yoneyama M, Fujita T (2012) Critical role of an antiviral stress granule containing RIG-I and PKR in viral detection and innate immunity. PLoS One 7:e43031
86. Osterlund P, Strengell M, Sarin LP, Poranen MM, Fagerlund R, Melen K, Julkunen I (2012) Incoming influenza A virus evades early host recognition, while influenza B virus induces interferon expression directly upon entry. J Virol 86:11183-11193
87. Patel JR, Garcia-Sastre A (2014) Activation and regulation of pathogen sensor RIG-I. Cytokine Growth Factor Rev
88. Patel RC, Sen GC (1998) PACT, a protein activator of the interferon-induced protein kinase, PKR. Embo j 17:4379-4390
89. Peisley A, Wu B, Xu H, Chen ZJ, Hur S (2014) Structural basis for ubiquitin-mediated antiviral signal activation by RIG-I. Nature
90. Pflug A, Guilligay D, Reich S, Cusack S (2014) Structure of influenza A polymerase bound to the viral RNA promoter. Nature
91. Pichlmair A, Schulz O, Tan CP, Naslund TI, Liljestrom P, Weber F, Reis e Sousa C (2006) RIG-I-mediated antiviral responses to single-stranded RNA bearing 5'-phosphates. Science 314:997-1001
92. Pichlmair A, Schulz O, Tan CP, Rehwinkel J, Kato H, Takeuchi O, Akira S, Way M, Schiavo G, Reis e Sousa C (2009) Activation of MDA5 requires higher-order RNA structures generated during virus infection. J Virol 83:10761-10769
93. Qi X, Lan S, Wang W, Schelde LM, Dong H, Wallat GD, Ly H, Liang Y, Dong C (2010) Cap binding and immune evasion revealed by Lassa nucleoprotein structure. Nature 468:779-783
94. Raju R, Raju L, Kolakofsky D (1989) The translational requirement for complete La Crosse virus mRNA synthesis is cell-type dependent. J Virol 63:5159-5165
95. Ramanan P, Shabman RS, Brown CS, Amarasinghe GK, Basler CF, Leung DW (2011) Filoviral immune evasion mechanisms. Viruses 3:1634-1649
96. Rameix-Welti MA, Tomoiu A, Dos Santos Afonso E, van der Werf S, Naffakh N (2009) Avian Influenza A virus polymerase association with nucleoprotein, but not polymerase assembly, is impaired in human cells during the course of infection. Journal of virology 83:1320-1331
97. Rawling DC, Pyle AM (2014) Parts, assembly and operation of the RIG-I family of motors. Curr Opin Struct Biol 25:25-33
98. Rawling DC, Kohlway AS, Luo D, Ding SC, Pyle AM (2015) The RIG-I ATPase core has evolved a functional requirement for allosteric stabilization by the Pincer domain. Nucleic Acids Res 42:11601-11611
99. Raymond DD, Piper ME, Gerrard SR, Smith JL (2010) Structure of the Rift Valley fever virus nucleocapsid protein reveals another architecture for RNA encapsidation. Proc Natl Acad Sci U S A 107:11769-11774
100. Raymond DD, Piper ME, Gerrard SR, Skiniotis G, Smith JL (2012) Phleboviruses encapsidate their genomes by sequestering RNA bases. Proc Natl Acad Sci U S A 109:19208-19213
101. Rehwinkel J, Tan CP, Goubau D, Schulz O, Pichlmair A, Bier K, Robb N, Vreede F, Barclay W, Fodor E, Reis e Sousa C (2010) RIG-I detects viral genomic RNA during negative-strand RNA virus infection. Cell 140:397-408
102. Reich S, Guilligay D, Pflug A, Malet H, Berger I, Crepin T, Hart D, Lunardi T, Nanao M, Ruigrok RW, Cusack S (2014) Structural insight into cap-snatching and RNA synthesis by influenza polymerase. Nature
103. Reikine S, Nguyen JB, Modis Y (2014) Pattern Recognition and Signaling Mechanisms of RIG-I and MDA5. Front Immunol 5:342
104. Rodrigo WW, Ortiz-Riano E, Pythoud C, Kunz S, de la Torre JC, Martinez-Sobrido L (2012) Arenavirus nucleoproteins prevent activation of nuclear factor kappa B. Journal of virology 86:8185-8197

105. Romano PR, Zhang F, Tan SL, Garcia-Barrio MT, Katze MG, Dever TE, Hinnebusch AG (1998) Inhibition of double-stranded RNA-dependent protein kinase PKR by vaccinia virus E3: role of complex formation and the E3 N-terminal domain. Mol Cell Biol 18:7304-7316
106. Ruigrok RW, Crepin T, Kolakofsky D (2011) Nucleoproteins and nucleocapsids of negative-strand RNA viruses. Curr Opin Microbiol 14:504-510
107. Saito T, Hirai R, Loo YM, Owen D, Johnson CL, Sinha SC, Akira S, Fujita T, Gale M, Jr. (2007) Regulation of innate antiviral defenses through a shared repressor domain in RIG-I and LGP2. Proc Natl Acad Sci U S A 104:582-587
108. Saito T, Owen DM, Jiang F, Marcotrigiano J, Gale M, Jr. (2008) Innate immunity induced by composition-dependent RIG-I recognition of hepatitis C virus RNA. Nature 454:523-527
109. Satoh T, Kato H, Kumagai Y, Yoneyama M, Sato S, Matsushita K, Tsujimura T, Fujita T, Akira S, Takeuchi O (2010) LGP2 is a positive regulator of RIG-I- and MDA5-mediated antiviral responses. Proc Natl Acad Sci U S A 107:1512-1517
110. Schlee M, Barchet W, Hornung V, Hartmann G (2007) Beyond double-stranded RNA-type I IFN induction by 3pRNA and other viral nucleic acids. Curr Top Microbiol Immunol 316:207-230
111. Schlee M, Roth A, Hornung V, Hagmann CA, Wimmenauer V, Barchet W, Coch C, Janke M, Mihailovic A, Wardle G, Juranek S, Kato H, Kawai T, Poeck H, Fitzgerald KA, Takeuchi O, Akira S, Tuschl T, Latz E, Ludwig J, Hartmann G (2009) Recognition of 5' triphosphate by RIG-I helicase requires short blunt double-stranded RNA as contained in panhandle of negative-strand virus. Immunity 31:25-34
112. Schlee M (2013) Master sensors of pathogenic RNA - RIG-I like receptors. Immunobiology 218:1322-1335
113. Schmidt A, Schwerd T, Hamm W, Hellmuth JC, Cui S, Wenzel M, Hoffmann FS, Michallet MC, Besch R, Hopfner KP, Endres S, Rothenfusser S (2009) 5'-triphosphate RNA requires base-paired structures to activate antiviral signaling via RIG-I. Proc Natl Acad Sci U S A 106:12067-12072
114. Schmidt A, Rothenfusser S, Hopfner KP (2011) Sensing of viral nucleic acids by RIG-I: From translocation to translation. Eur J Cell Biol
115. Schneider WM, Chevillotte MD, Rice CM (2014) Interferon-stimulated genes: a complex web of host defenses. Annu Rev Immunol 32:513-545
116. Schoggins JW, Rice CM (2011) Interferon-stimulated genes and their antiviral effector functions. Current opinion in virology 1:519-525
117. Schoggins JW (2014) Interferon-stimulated genes: roles in viral pathogenesis. Curr Opin Virol 6:40-46
118. Schrauwen EJ, de Graaf M, Herfst S, Rimmelzwaan GF, Osterhaus AD, Fouchier RA (2014) Determinants of virulence of influenza A virus. Eur J Clin Microbiol Infect Dis 33:479-490
119. Shimoike T, McKenna SA, Lindhout DA, Puglisi JD (2009) Translational insensitivity to potent activation of PKR by HCV IRES RNA. Antiviral Res 83:228-237
120. Subbarao EK, London W, Murphy BR (1993) A single amino acid in the PB2 gene of influenza A virus is a determinant of host range. J Virol 67:1761-1764
121. Takahasi K, Yoneyama M, Nishihori T, Hirai R, Kumeta H, Narita R, Gale M, Jr., Inagaki F, Fujita T (2008) Nonself RNA-sensing mechanism of RIG-I helicase and activation of antiviral immune responses. Mol Cell, United States, pp 428-440
122. Tarendeau F, Crepin T, Guilligay D, Ruigrok RW, Cusack S, Hart DJ (2008) Host determinant residue lysine 627 lies on the surface of a discrete, folded domain of influenza virus polymerase PB2 subunit. PLoS pathogens 4:e1000136
123. Taylor DR, Shi ST, Romano PR, Barber GN, Lai MM (1999) Inhibition of the interferon-inducible protein kinase PKR by HCV E2 protein. Science 285:107-110
124. tenOever BR, Servant MJ, Grandvaux N, Lin R, Hiscott J (2002) Recognition of the measles virus nucleocapsid as a mechanism of IRF-3 activation. J Virol 76:3659-3669
125. tenOever BR, Sharma S, Zou W, Sun Q, Grandvaux N, Julkunen I, Hemmi H, Yamamoto M, Akira S, Yeh WC, Lin R, Hiscott J (2004) Activation of TBK1 and IKKvarepsilon kinases by vesicular stomatitis virus infection and the role of viral ribonucleoprotein in the development of interferon antiviral immunity. J Virol 78:10636-10649

126. VanOudenhove J, Anderson E, Krueger S, Cole JL (2009) Analysis of PKR structure by small-angle scattering. J Mol Biol 387:910-920
127. Varga ZT, Grant A, Manicassamy B, Palese P (2012) Influenza virus protein PB1-F2 inhibits the induction of type I interferon by binding to MAVS and decreasing mitochondrial membrane potential. J Virol 86:8359-8366
128. Vela A, Fedorova O, Ding SC, Pyle AM (2012) The thermodynamic basis for viral RNA detection by the RIG-I innate immune sensor. J Biol Chem 287:42564-42573
129. Versteeg GA, Garcia-Sastre A (2010) Viral tricks to grid-lock the type I interferon system. Current opinion in microbiology 13:508-516
130. Wagstaff KM, Sivakumaran H, Heaton SM, Harrich D, Jans DA (2012) Ivermectin is a specific inhibitor of importin alpha/beta-mediated nuclear import able to inhibit replication of HIV-1 and dengue virus. Biochem J 443:851-856
131. Weber F, Wagner V, Rasmussen SB, Hartmann R, Paludan SR (2006) Double-stranded RNA is produced by positive-strand RNA viruses and DNA viruses but not in detectable amounts by negative-strand RNA viruses. Journal of virology 80:5059-5064
132. Weber M, Gawanbacht A, Habjan M, Rang A, Borner C, Schmidt AM, Veitinger S, Jacob R, Devignot S, Kochs G, Garcia-Sastre A, Weber F (2013) Incoming RNA virus nucleocapsids containing a 5'-triphosphorylated genome activate RIG-I and antiviral signaling. Cell host & microbe 13:336-346
133. Weber M, Weber F (2014) Monitoring Activation of the Antiviral Pattern Recognition Receptors RIG-I And PKR By Limited Protease Digestion and Native PAGE. J Vis Exp
134. Weber M, Weber F (2014) Segmented negative-strand RNA viruses and RIG-I: divide (your genome) and rule. Current opinion in microbiology 20c:96-102
135. Weber M, Weber F (2014) RIG-I-like receptors and negative-strand RNA viruses: RLRly bird catches some worms. Cytokine & growth factor reviews
136. Wisskirchen C, Ludersdorfer TH, Muller DA, Moritz E, Pavlovic J (2011) Interferon-induced antiviral protein MxA interacts with the cellular RNA helicases UAP56 and URH49. J Biol Chem 286:34743-34751
137. Wisskirchen C, Ludersdorfer TH, Muller DA, Moritz E, Pavlovic J (2011) The cellular RNA helicase UAP56 is required for prevention of double-stranded RNA formation during influenza A virus infection. J Virol 85:8646-8655
138. Wittig I, Schagger H (2005) Advantages and limitations of clear-native PAGE. Proteomics 5:4338-4346
139. Wu B, Peisley A, Richards C, Yao H, Zeng X, Lin C, Chu F, Walz T, Hur S (2013) Structural basis for dsRNA recognition, filament formation, and antiviral signal activation by MDA5. Cell 152:276-289
140. Wu B, Peisley A, Tetrault D, Li Z, Egelman EH, Magor KE, Walz T, Penczek PA, Hur S (2014) Molecular imprinting as a signal-activation mechanism of the viral RNA sensor RIG-I. Mol Cell 55:511-523
141. Wunderlich K, Juozapaitis M, Ranadheera C, Kessler U, Martin A, Eisel J, Beutling U, Frank R, Schwemmle M (2011) Identification of high-affinity PB1-derived peptides with enhanced affinity to the PA protein of influenza A virus polymerase. Antimicrob Agents Chemother 55:696-702
142. Xu H, He X, Zheng H, Huang LJ, Hou F, Yu Z, de la Cruz MJ, Borkowski B, Zhang X, Chen ZJ, Jiang QX (2014) Structural basis for the prion-like MAVS filaments in antiviral innate immunity. Elife 3:e01489
143. Yoneyama M, Suhara W, Fujita T (2002) Control of IRF-3 activation by phosphorylation. J Interferon Cytokine Res 22:73-76
144. Yoneyama M, Kikuchi M, Natsukawa T, Shinobu N, Imaizumi T, Miyagishi M, Taira K, Akira S, Fujita T (2004) The RNA helicase RIG-I has an essential function in double-stranded RNA-induced innate antiviral responses. Nature immunology 5:730-737
145. Yoo JS, Kato H, Fujita T (2014) Sensing viral invasion by RIG-I like receptors. Curr Opin Microbiol 20:131-138
146. Yoo JS, Takahasi K, Ng CS, Ouda R, Onomoto K, Yoneyama M, Lai JC, Lattmann S, Nagamine Y, Matsui T, Iwabuchi K, Kato H, Fujita T (2014) DHX36 enhances RIG-I

signaling by facilitating PKR-mediated antiviral stress granule formation. PLoS Pathog 10:e1004012
147. Yun NE, Walker DH (2012) Pathogenesis of Lassa fever. Viruses 4:2031-2048
148. Zamanian-Daryoush M, Mogensen TH, DiDonato JA, Williams BR (2000) NF-kappaB activation by double-stranded-RNA-activated protein kinase (PKR) is mediated through NF-kappaB-inducing kinase and IkappaB kinase. Mol Cell Biol 20:1278-1290
149. Zeng W, Sun L, Jiang X, Chen X, Hou F, Adhikari A, Xu M, Chen ZJ (2010) Reconstitution of the RIG-I pathway reveals a signaling role of unanchored polyubiquitin chains in innate immunity. Cell 141:315-330
150. Zheng X, Bevilacqua PC (2004) Activation of the protein kinase PKR by short double-stranded RNAs with single-stranded tails. Rna 10:1934-1945
151. Zhu Z, Zhang X, Wang G, Zheng H (2014) The laboratory of genetics and physiology 2: emerging insights into the controversial functions of this RIG-I-like receptor. Biomed Res Int 2014:960190
152. Zinzula L, Tramontano E (2013) Strategies of highly pathogenic RNA viruses to block dsRNA detection by RIG-I-like receptors: Hide, mask, hit. Antiviral Res 100:615-635

Appendix

I. Zusätzliche Publikationen

Siegfried A, Berchtold S, Manncke B, Deuschle E, Reber J, Ott T, **Weber M**, Kalinke U, Hofer MJ, Hatesuer B, Schughart K, Gailus-Durner V, Fuchs H, Hrabe de Angelis M, Weber F, Hornef MW, Autenrieth IB, Bohn E. IFIT2 is an effector protein of type I IFN-mediated amplification of lipopolysaccharide (LPS)-induced TNF-alpha secretion and LPS-induced endotoxin shock. Journal of immunology (Baltimore, Md. : 1950) 191:3913-3921. October, 2013.

Zielecki F, **Weber M**, Eickmann M, Spiegelberg L, Zaki AM, Matrosovich M, Becker S, Weber F. Human cell tropism and innate immune system interactions of human respiratory coronavirus EMC compared to those of severe acute respiratory syndrome coronavirus. Journal of virology 87:5300-5304. May, 2013.

Hoenen T, Shabman RS, Groseth A, Herwig A, **Weber M**, Schudt G, Dolnik O, Basler CF, Becker S, Feldmann H. Inclusion bodies are a site of ebolavirus replication. Journal of virology 86:11779-11788. November, 2012.

Groseth A, Hoenen T, **Weber M**, Wolff S, Herwig A, Kaufmann A, Becker S. Tacaribe virus but not junin virus infection induces cytokine release from primary human monocytes and macrophages. PLoS neglected tropical diseases 5:e1137. May, 2011.

II. Kongressbeiträge

Mündliche Präsentationen

24. Treffen der Gesellschaft für Virologie, Alpach/ Österreich (2014)
Human-adaptive influenza virus mutation PB2 627K contributes to evasion of nucleocapsid recognition by RIG-I

23. Treffen der Gesellschaft für Virologie, Kiel (2013)
Activation of RIG-I by incoming RNA virus nucleocapsids containing a 5'-triphosphorylated genome

5. Europäischer Kongress für Virologie (ECV; European congress of Virology), Lyon/ Frankreich (2013)
Activation of RIG-I by incoming RNA virus nucleocapsids containing a 5'-triphosphorylated genome

EMBO Konferenz, „Helikasen and Nukleinsäuretranslokasen“ Cambridge/ England (2013)

Activation of RIG-I by incoming RNA virus nucleocapsids containing a 5'-triphosphorylated genome

6. Internationales Seminar „Interferon und Infektion", Braunschweig (2013)
Activation of RIG-I by incoming RNA virus nucleocapsids containing a 5'-triphosphorylated genome

22. Treffen der Gesellschaft für Virologie, Essen (2012)
Activation of RIG-I by incoming RNA virus nucleocapsids containing a 5'-triphosphorylated genome

11. Seminar der Gesellschaft für Virologie „Pathogenitätsmechanismen und Immunkontrolle viraler Erreger", Deidesheim (2012)
Activation of RIG-I by incoming RNA virus nucleocapsids containing a 5'-triphosphorylated genome

Posterpräsentation

4. Internationales Influenza-Treffen, Münster (2014)
Human-adaptive influenza virus mutation PB2 627K contributes to evasion of nucleocapsid recognition by RIG-I

5. Treffen der italienischen Proteom Gesellschaft, Florenz/ Italien (2010)
Protein expression profile of plasmepsin IV knock-out Plasmodium berghei parasite and immunoreactive proteins identification

4. Treffen der internationalen Gesellschaft für Neurochemie, Italien (2010)
Recruitment of plasma membrane beta-hexosaminidase in lipid rafts upon T-cell activation

III. Verzeichnis der akademischen Lehrer

Bauer U., Bauer S., Becker, Brehm, Daut, Del Rey, Eilers, Elsässer, Feuser, Frenking, Garten, Glorius, Hasilik, Hassel, Huber, Jacob, Jänsch, Jungclas, Klenk, Koolman, Lill, Löffler M., Löffler G., Lohoff, Lüers, Maisner, Matrosovich, Müller, Müller-Brüsselbach, Petz, Röhm, Schäfer, Schwarz, Seitz, Suske, Voigt, Weber, Weihe, Westermann.

IV. Danksagung

Nach aufregenden Jahren des Studiums, einer intensiven Phase der Diplomarbeit und den ereignisreichen Jahren der Doktorarbeit an der Philipps-Universität Marburg, neigt sich nun auch diese Zeit dem Ende. Ich wurde auf meinem Weg von zahlreichen Personen begleitet, die mich unterstützt, geprägt, motiviert, gelehrt und glücklich gemacht haben. Sie haben es mir erst ermöglicht diesen Punkt in meinem Leben erreicht zu haben und dafür bin ich ihnen unendlich dankbar.

Einem besonderen Dank gilt zunächst Prof. Dr. Friedemann Weber. Ich habe viel von Ihm gelernt, er hat mir Chancen geboten, die mir niemand anderes hätte bieten können und meiner Kreativität (auch wenn sie noch so verrückt war) freien Lauf gelassen. Ich bin zudem zutiefst dankbar, dass er mir mit der Post-Doc-Stelle bei Prof. Takashi Fujita in Kyoto/Japan geholfen hat. Vielen Dank auch an das Labor Weber für die tolle Arbeitsatmosphäre und die tolle Zeit zwischen und nach den Experimenten. Besonderen Dank gilt dabei Andreas, Markus, Julia und Stèph. Zudem möchte ich mich auch bei Mitgliedern anderer Arbeitsgruppen, wie Hanna, Jan, Thomas, Alex und Julià bedanken. Euch als Freunde zu haben ist unaufwiegbar. Bei meinen Studenten Ulrike Felgenhauer, Ina Binzen, Sarah Doll und Ana Rita Ferreira (Universität Aveiro, Portugal) möchte ich mich ebenfalls bedanken. Ich hoffe sie haben so viel von mir gelernt, wie ich von Ihnen. Einem Dank gilt auch den zahlreichen Kollaborationspartner für die wissenschaftliche Kompetenz, stete Diskussionsbereitschaft und die geteilten Materialen. Ich danke diesbezüglich Ina Fehling und Thomas Strecker (AG Strecker, Philipps-Universität Marburg), Svenja Wolff (AG Becker, Philipps-Universität Marburg), Prof. Dr. Klenk (AG Klenk, Philipps-Universität Marburg), Sophie Veitinger und Sebastian Bänfer (AG Jacob, Philipps-Universität Marburg), Linda Brunotte und Martin Schwemmle (AG Schwemmle, Universität Freiburg), Georg Kochs (AG Kochs, Universität Freiburg), Veit Hornung (AG Hornung, Universität Bonn) und García-Sastre (Icahn School of Medicine at Mount Sinai, New York, USA).

Meinen Freunden Anna, Anne, Silvana, Cathi, Johannes, Kathi, und Evelyn. Schon die Studienzeit war mit Eurer Unterstützung eine wunderbare Zeit. Trotz der weiten Entfernungen haben wir uns nicht aus den Augen verloren und Ihr wart und werdet für mich immer die Besten sein.

Ein großer Dank gilt auch meiner Familie, insbesondere meinen Großeltern. Danke für ihr reges Interesse an meiner Arbeit, die aufmunternden Worte und einfach dafür, dass es sie gibt. Meinen geliebten Schwestern Claudi und Heidi, meinem fantastischem Schwager Sven und meinen Neffen Luis und Rafael. Es ist schön Euch zu haben! Meinem Ehemann Alex. Du bist die beste Entdeckung, die ich während meiner Doktorarbeit machen konnte. Du hast viel Geduld gezeigt, Stunden investiert um mein Doktorthema zu verstehen, gemeinsam mit mir über leere Puffer geflucht, mich Nachts vom Labor abgeholt, wenn ich mich gegruselt habe, für mein leibliches Wohl gesorgt und mit deiner Liebe mein Leben bereichert. Vielen Dank!

„Leider läßt sich eine wahrhafte Dankbarkeit mit Worten nicht ausdrücken."

Johann Wolfgang von Goethe (1749 - 1832)